BEILSTEIN JOURNAL OF ORGANIC CHEMISTRY

Electrosynthesis

Edited by Siegfried R. Waldvogel

Imprint

Beilstein Journal of Organic Chemistry
www.bjoc.org
ISSN 1860-5397
Email: journals-support@beilstein-institut.de

The *Beilstein Journal of Organic Chemistry* is published by the Beilstein-Institut zur Förderung der Chemischen Wissenschaften.

Beilstein-Institut zur Förderung der Chemischen Wissenschaften
Trakehner Straße 7–9
60487 Frankfurt am Main
Germany
www.beilstein-institut.de

BEILSTEIN JOURNAL OF ORGANIC CHEMISTRY

Electrosynthesis and electrochemistry

Siegfried R. Waldvogel

Editorial

Open Access

Address:
Institute for Organic Chemistry, Johannes Gutenberg University Mainz, Duesbergweg 10–14, 55128 Mainz, Germany

Email:
Siegfried R. Waldvogel - waldvogel@uni-mainz.de

Keywords:
chemical method; electrochemistry; electrosynthesis; sustainability

Beilstein J. Org. Chem. **2015,** *11,* 949–950.
doi:10.3762/bjoc.11.105

Received: 24 April 2015
Accepted: 08 May 2015
Published: 02 June 2015

This article is part of the Thematic Series "Electrosynthesis".

Guest Editor: S. R. Waldvogel

Since the pioneering work of Kolbe, electrochemistry and electrosynthetic methods have been a part of the repertoire of the organic synthesis toolbox [1,2]. In general, only electrons are employed as reagents or the reagents are electrochemically regenerated. Consequently, waste can be avoided, and limited resources can be used in a careful and economic manner. Because alternative reaction pathways are employed by electrosynthetic methods, scarce and toxic elements can be replaced or are not required at all [3]. Moreover, in the foreseeable future regenerative sources of electricity, for example, photovoltaics and wind power, will provide a surplus of electricity as the current unsteady supply does not match the demand. Thus, the use of abundant electric power in electrosynthetic processes seems to be rational because high valorisation can be expected. Therefore, electrosynthesis fulfils all requirements for "green chemistry" [4]. When changing feed stocks and natural resources begin to play a more crucial role, electrosynthetic methodologies will not only be of ecological interest but also of economic significance. Unfortunately, the research in the past two decades was understated and considered as a niche methodology by the synthetic community. In addition, electrochemistry is mostly taught by physical chemists, which seems to create a natural barrier to preparative organic applications. However, the systematic use of cationic species as intermediates to avoid over-oxidation establishes new ways for functionalization of substrates and paves the way to novel synthetic tools [5-8].

Recently, a renaissance of electro-organic methods occurred in several fields, including the construction of rather complex molecules (e.g., natural products) [9]. Not only is the construction of biologically active molecules of interest but also the anodic degradation of drug-like molecules. Such electro-oxidative treatment generates potential metabolites that can be then biologically studied [10]. The combination of electrosynthesis with other powerful techniques, such as ultrasonic treatment and flow microcells, will push the electrosynthetic applications beyond current limits [11].

In addition, remarkable breakthroughs have been achieved regarding electrodes and electrolytes, which allow for expansion of the electrochemical window and/or novel reaction pathways. This leads to new electro-organic concepts and further applications for a sustainable synthetic methodology. The contributions within this Thematic Series demonstrate the broad use of electrosynthesis and represent a snapshot of this current

and vividly developing field. I am convinced that electro-organic synthesis is an emerging field and that this issue will stimulate the reader to employ electrochemical methods in their own field.

Siegfried R. Waldvogel

Mainz, April 2015

References

1. Kolbe, H. *Justus Liebigs Ann. Chem.* **1849,** *69,* 257–294. doi:10.1002/jlac.18490690302
2. Schäfer, H.-J. *Top. Curr. Chem.* **1990,** *152,* 91–151. doi:10.1007/BFb0034365
3. Elsler, B.; Schollmeyer, D.; Dyballa, K. M.; Franke, R.; Waldvogel, S. R. *Angew. Chem., Int. Ed.* **2014,** *53,* 5210–5213. doi:10.1002/anie.201400627
4. Steckhan, E.; Arns, T.; Heineman, W. R.; Hilt, G.; Hoormann, D.; Jörissen, J.; Kröner, L.; Lewall, B.; Pütter, H. *Chemosphere* **2001,** *43,* 63–73. doi:10.1016/S0045-6535(00)00325-8
5. Waldvogel, S. R.; Möhle, S. *Angew. Chem., Int. Ed.* **2015,** *54.* doi:10.1002/anie.201502638
6. Morofuji, T.; Shimizu, A.; Yoshida, J.-i. *J. Am. Chem. Soc.* **2013,** *135,* 5000–5003. doi:10.1021/ja402083e
7. Morofuji, T.; Shimizu, A.; Yoshida, J.-i. *J. Am. Chem. Soc.* **2014,** *136,* 4496–4499. doi:10.1021/ja501093m
8. Morofuji, T.; Shimizu, A.; Yoshida, J.-i. *Chem. – Eur. J.* **2015,** *21,* 3211–3214. doi:10.1002/chem.201406398
9. Waldvogel, S. R.; Janza, B. *Angew. Chem., Int. Ed.* **2014,** *53,* 7122–7123. doi:10.1002/anie.201405082
10. Torres, S.; Brown, R.; Szucs, R.; Hawkins, J. M.; Scrivens, G.; Pettman, A.; Kraus, D.; Taylor, M. R. *Org. Process Res. Dev.* **2015,** *19.* doi:10.1021/op500312e
11. Watts, K.; Baker, A.; Wirth, T. *J. Flow Chem.* **2014,** *4,* 2–11. doi:10.1556/JFC-D-13-00030

License and Terms

BEILSTEIN JOURNAL OF ORGANIC CHEMISTRY

Recent advances in the electrochemical construction of heterocycles

Robert Francke

Review

Open Access

Address:
Department of Chemistry, University of Rostock, Albert-Einstein-Str. 3a, 18059 Rostock, Germany

Email:
Robert Francke - robert.francke@uni-rostock.de

Keywords:
anodic cyclization; electrosynthesis; heterocycle; olefin coupling; organic electrochemistry; radical cyclization

Beilstein J. Org. Chem. **2014,** *10,* 2858–2873.
doi:10.3762/bjoc.10.303

Received: 05 October 2014
Accepted: 18 November 2014
Published: 03 December 2014

This article is part of the Thematic Series "Electrosynthesis".

Guest Editor: S. R. Waldvogel

Abstract

Due to the fact that the major portion of pharmaceuticals and agrochemicals contains heterocyclic units and since the overall number of commercially used heterocyclic compounds is steadily growing, heterocyclic chemistry remains in the focus of the synthetic community. Enormous efforts have been made in the last decades in order to render the production of such compounds more selective and efficient. However, most of the conventional methods for the construction of heterocyclic cores still involve the use of strong acids or bases, the operation at elevated temperatures and/or the use of expensive catalysts and reagents. In this regard, electrosynthesis can provide a milder and more environmentally benign alternative. In fact, numerous examples for the electrochemical construction of heterocycles have been reported in recent years. These cases demonstrate that ring formation can be achieved efficiently under ambient conditions without the use of additional reagents. In order to account for the recent developments in this field, a selection of representative reactions is presented and discussed in this review.

Introduction

The construction of heterocyclic cores undoubtedly represents a highly important discipline of organic synthesis. The large interest in this field is attributable to the occurrence of heterocyclic units in numerous natural products and biologically active compounds such as hormones, antibiotics and vitamins [1]. Considering the fact that more than 70% of all active ingredients in pharmaceutical and agrochemical products contain at least one heterocyclic unit, the particular importance of heterocyclic compounds becomes clear [2].

Most of the classical methods for heterocycle synthesis are based on the use of acids or bases at elevated temperatures, conditions which are often not compatible with the presence of certain functional groups [3,4]. In the last decades, research in this field has therefore been focused on the development of more efficient and selective strategies. In the current focus of heterocycle synthesis are C,H-activation with transition metal catalysts [5-8], oxidative cyclization using hypervalent iodine reagents [9-12], and homogeneously or heterogeneously

catalyzed multicomponent reactions [13,14]. Moreover, radical cyclizations predominantly conducted using Bu_3SnH in the presence of azobisisobutyronitrile (AIBN) play a crucial role [15,16]. However, all these methods require the use of an expensive catalyst and/or toxic and hazardous reagents. In order to meet increasing environmental and economic constraints, further efforts should be directed towards the development of mild and reagent-free methods [17,18]. In this context, electroorganic synthesis can provide an interesting and practical alternative to conventional methods for heterocycle synthesis [19,20]. Since toxic and hazardous redox reagents are either replaced by electric current (direct electrolysis) or generated in situ from stable and non-hazardous precursors (indirect electrolysis), electrosynthesis is considered to be a safe and environmentally friendly methodology [21-25]. A further interesting feature is that electrochemical reactions are feasible under very mild conditions; since the reaction rate is determined by the electrode potential, reactions with high activation energies can be conducted at low temperatures.

The electrochemical synthesis of heterocyclic compounds can be considered as a mature discipline. The last comprehensive review dealing with electrochemical heterocycle generation has been published in 1997 by Tabaković [26]. Earlier reviews on different aspects of the electrochemistry of heterocyclic compounds are also available [27-29]. However, recent innovations in electrosynthesis such as the cation pool method or the development of novel electron transfer mediators also have a significant impact on heterocyclic chemistry [30,31]. This review focuses upon both anodic and cathodic processes that lead to the formation of heterocyclic structures in view of these recent developments. Its scope is to highlight advances since the appearance of Tabacovićs review in 1997. The intention is rather to provide the reader with a general insight than to give an exhaustive overview.

Review

Numerous mechanistic pathways to the formation of heterocycles have been described and for a detailed treatment, interested readers are referred to earlier reviews by Lund and Tabaković [26-28]. The electrochemical heterocycle synthesis can principally proceed through C–Het-, C–C- and Het–Het-bond formation, whereby the former two represent the predominant case in recent literature (Figure 1). Furthermore, one can distinguish between intramolecular and intermolecular cyclization. The intramolecular version typically involves two functional groups linked by a tether. The electrochemical reaction leads to an Umpolung of the functional group with the lower redox potential, triggering the ring-closure reaction between a nucleophilic and an electrophilic site. Another possibility for an intramolecular ring closure is represented by electrochemically induced radical cyclization. Intermolecular cyclizations generally fall into two further categories. In the first scenario, an anodically generated nucleophile (cathodically generated electrophile) reacts with an electrophile (nucleophile) present in solution. Consequently, an intermediate is formed, which undergoes ring-closure reaction. The second scenario involves the electrochemical formation of a reactive species followed by cycloaddition in a concerted mechanism.

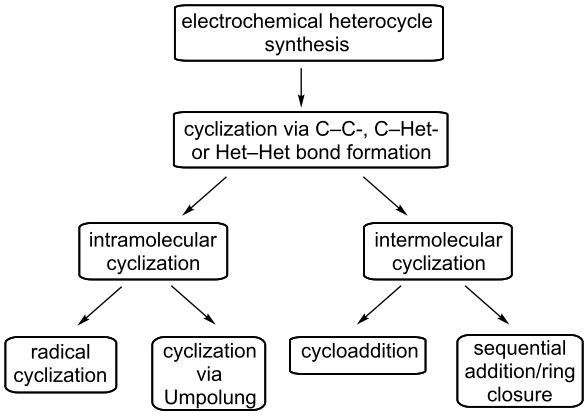

Figure 1: Common types of electrochemically induced cyclization reactions.

The examples presented hereafter are classified according to the reaction type rather than to the resulting type of heterocycle. Among the intramolecular reactions, recent efforts in electrochemical heterocycle synthesis can mostly be differentiated into anodic olefin coupling (section 1.1), radical cyclization (section 1.2), and trapping of anodically generated iminium/alkoxycarbenium ions (section 1.3). On the other hand, cycloadditions (section 2.1), sequential Michael addition/ring closure with in situ generated quinones (section 2.2) and sequential cyclizations involving acyliminium species and alkoxycarbenium ions (section 2.3) represent the majority of recently reported intermolecular electrochemical cyclizations. Cases which do not fall into any of these categories are discussed in sections 1.4 and 2.4.

A further important aspect is the type of electron transfer involved in the reaction. With regard to heterocycle synthesis, both direct electrolysis involving heterogeneous electron transfer between electrode and substrate as well as indirect electrolysis using electron transfer mediators (Scheme 1) play an important role. With regard to selectivity, the direct method is often complementary to typical chemical oxidations and reductions, since electrochemical oxidation or reduction proceeds via discrete electron transfer steps rather than atom transfer. In contrast, the indirect process can either be initiated

with a discrete electron transfer (outer-sphere mechanism) or proceed via bond formation (inner-sphere mechanism), depending on the type of mediator [31]. In both cases, the electrode reaction proceeds at such a low potential that the substrate is electrochemically inactive. In many cases, undesired side-reactions can be avoided by using redox mediators, since reactive intermediates do not accumulate on the electrode surface. Moreover, the indirect approach is often used in order to inhibit electrode passivation caused by formation of polymer films. In the context of heterocycle synthesis, a number of mediators based on organic molecules, inorganic salts and metal complexes have been used recently and their use will be discussed later on the basis of the relevant examples.

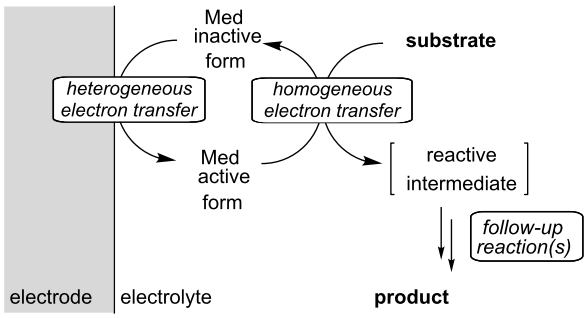

Scheme 1: Principle of indirect electrolysis.

1 Intramolecular cyclizations

1.1 Anodic olefin coupling

The anodic oxidation of electron-rich olefins such as enol ethers **1** in methanolic solution generates radical cation **2** which can be used for a number of cyclization reactions (Scheme 2) [32,33]. Moeller et al. demonstrated that by intramolecular trapping of this highly reactive intermediate with a tethered alcohol nucleophile, a variety of tetrahydrofuran, tetrahydropyran and oxepane structures **4** can be synthesized (Scheme 2, X = O) [34]. The reaction is initiated by single electron oxidation to generate intermediate **2**, which after cyclization and deprotonation gives radical **3**. Further oxidation results in the formation of a cationic species which is trapped by methanol to yield product **4**.

This cyclization method is not restricted to hydroxy groups as trapping agents. More recently, Moeller and Xu reported that *N*-nucleophiles such as the tosylamine group can efficiently trap **2**-type radical cations, resulting in *N*-tosylated pyrrolidine products (Scheme 2, X = NHTs) [35,36].

The reactions can be carried out under galvanostatic conditions (C.C.E. = constant current electrolysis) at room temperature in an undivided cell using a vitreous carbon anode. The presence of a proton scavenger is necessary in order to obtain reasonable

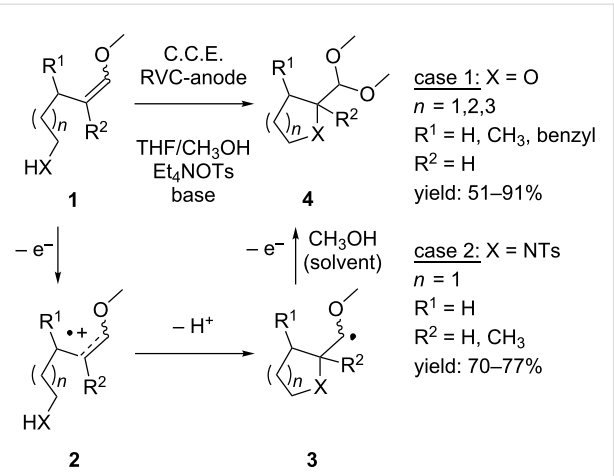

Scheme 2: Anodic intramolecular cyclization of olefines in methanol.

reaction rates. When the radical cation is trapped with a hydroxy group, the use of 2,6-lutidine is sufficient. However, a stronger base such as NaOMe is needed when tosylamines are converted in order to facilitate the cyclization reaction and to suppress intermolecular coupling. In addition to enol ethers **1**, vinyl sulfides and ketene acetals have successfully been cyclized according to Scheme 2 [34-36].

An interesting modification of this anodic coupling method was achieved by Yoshida, Nokami and co-workers using the "cation pool" concept [37-39]. In this approach, the anodic oxidation of olefins was combined with a sequential chemical oxidation in a one-pot fashion (Scheme 3) [39]. By using DMSO instead of methanol as nucleophilic co-solvent for electrolysis, a pool of alkoxysulfonium ions **7** is generated from tosylamine **5**. The generation of the cation pool has to be carried out at 0 °C in order to stabilize the reactive alkoxysulfonium species. Analogously to Swern- and Moffat-type reactions, this key intermediate is then converted to ketone **8** by quenching with NEt_3 at slightly elevated temperatures under elimination of dimethyl sulfide.

Alternatively, a tethered carboxy group can be used as the nucleophilic component, leading to the formation of lactone rings [39]. A further option is the hydrolysis of alkoxysulfonium species **7** with aqueous NaOH under formation of the corresponding secondary alcohol [40].

The idea of integrating a chemical oxidation into the anodic cyclization of olefins was extended to intramolecular coupling of 1,6-dienes **9** (Scheme 4) [39]. In this version of the combined cyclization/oxidation, the second carbon–carbon double bond acts as the nucleophile after anodic oxidation, leading to bisalkoxysulfonium species **10**. When the reaction conditions

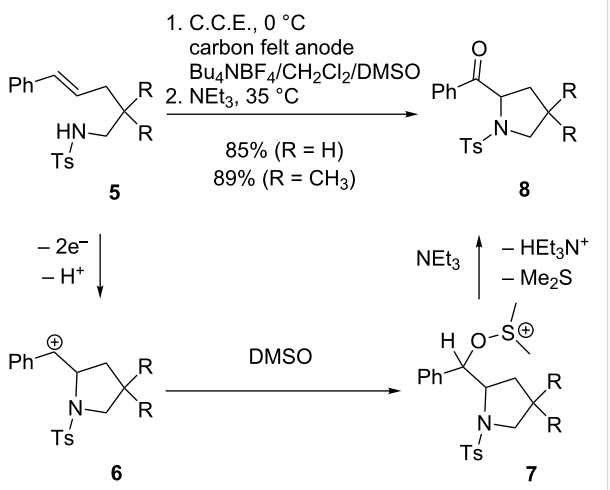

Scheme 3: Anodic cyclization of olefines in CH_2Cl_2/DMSO.

depicted in Scheme 3 are applied, including quenching with NEt_3, *exo–exo*-cyclization product **11** is obtained in 63% yield with 100% *trans*-selectivity. The yield can be increased to 72% when $Bu_4NB(C_6F_5)_4$ is used as supporting electrolyte.

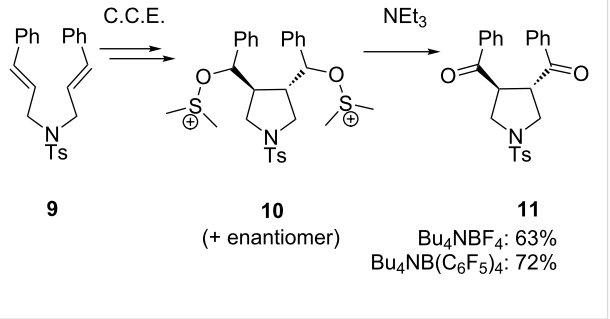

Scheme 4: Intramolecular coupling of 1,6-dienes in CH_2Cl_2/DMSO.

1.2 Electrochemically induced radical cyclizations

Among the numerous existing radical cyclization methods, the conversion of unsaturated alkyl halogenides represents one of the key-reactions for the synthesis of natural products containing aliphatic heterocycles. Such ring-closing reactions are frequently carried out using toxic tri-*n*-butyltin hydride in combination with a radical initiator such as AIBN. Peters and co-workers described an electrochemical alternative using cathodically generated nickel(I) complexes as mediators [41,42]. Under potentiostatic conditions (C.P.E. = controlled potential electrolysis) in a divided cell, bromopropargyloxy ester **12** was converted using $[Ni(tmc)]Br_2$ (tmc = 1,4,8,11-tetramethylcyclam) as catalyst, leading to cyclization products **13** and **14** (Scheme 5). When **12** was electrolyzed in absence of mediator, significantly lower yields were obtained [42].

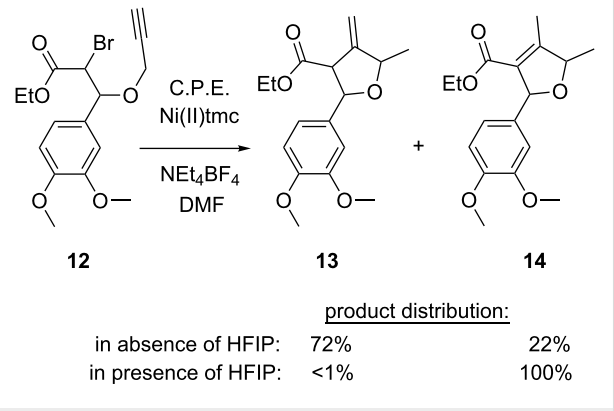

Scheme 5: Cyclization of bromopropargyloxy ester **12**.

The acidity of the reaction medium strongly influences the product distribution. Under aprotic conditions, the formation of **13** is favored, whereas in presence of HFIP (1,1,1,3,3,3-hexafluoroisopropanol) as a proton donor, product **14** is formed exclusively. On the basis of faradaic yields, cyclic voltammetry data and product distribution, the authors proposed the mechanism shown in Scheme 6. The sequence starts with electron transfer from cathodically generated $[Ni(tmc)]^+$ to **12**, triggering the cleavage of the C–Br bond in the rate-determining step and resulting in radical species **15**. After rapid intramolecular cyclization, followed by hydrogen atom abstraction from the solvent, product **13** is afforded, which equilibrates in the presence of a proton donor to form the more stable α,β-unsaturated product **14**.

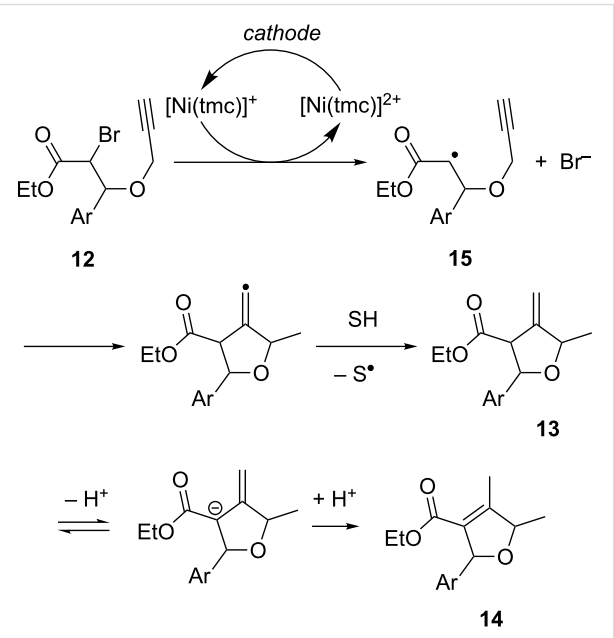

Scheme 6: Proposed mechanism for the radical cyclization of bromopropargyloxy ester **12**.

A different radical cyclization method for the synthesis of tetrahydrofurans and pyrrolidines was developed earlier by Schäfer and co-workers [43-45]. In their approach, unsaturated and saturated carboxylic acids were simultaneously subjected to a mixed Kolbe-type oxidation in a KOH/methanol electrolyte using an undivided cell under galvanostatic conditions (Scheme 7). The cyclization reaction is initiated with the generation of radical **17** upon anodic oxidation of the potassium salt of **16**. Rapid cyclization gives **18**, which recombines with the alkyl radical $R^{4\bullet}$ under formation of product **19**. A synthetic challenge is represented by the competing recombination of intermediate **17** with $R^{4\bullet}$, resulting in an open structure which was also isolated in some cases. With unsubstituted substrate **16** ($R^1 = R^2 = R^3 = H$) this side reaction leads to the formation of a significant amount of the undesired byproduct. However, increasing alkyl substitution leads to improved yields of the cyclization product; apparently, the cyclization rate is significantly enhanced in this case due to the Thorpe–Ingold effect [46].

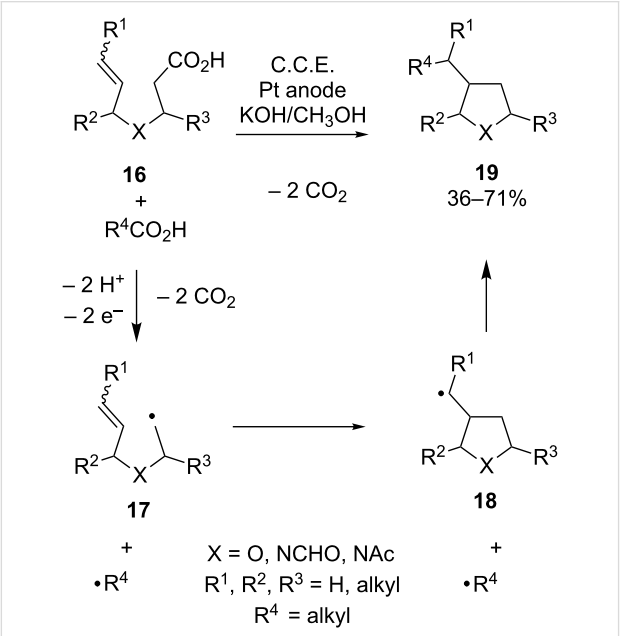

Scheme 7: Preparation of pyrrolidines and tetrahydrofurans via Kolbe-type electrolysis of unsaturated carboxylic acids **16**.

Recently, Zeng, Little and co-workers reported a new electrochemical method for the preparation of 3,5-disubstituted isoxazoles from chalcone oximes **20** (Scheme 8) [47]. The electrolysis of **20** is carried out in an undivided cell under galvanostatic conditions using a $NaClO_4/CH_3OH$ electrolyte. The cyclization is proposed to proceed via iminoxyl intermediate **22**, which is generated through deprotonation by cathodically generated methanolate and subsequent anodic oxidation. Cyclization of radical **22** is followed by further oxidation and proton abstraction to afford isoxazol **21**. The reported method features a simple setup, mild conditions (room temperature, low concentration of base) and a broad scope.

1.3 Cyclization of alkoxycarbenium and iminium intermediates

A well-studied method for generation of aliphatic *N*- and *O*-heterocycles is the intramolecular nucleophilic trapping of anodically formed iminium (**23**) or alkoxycarbenium species (**24**). The reactive intermediates can be generated directly from ethers or carboxylic acid amides (Scheme 9) [32]. However, aliphatic ethers and amides generally exhibit high oxidation potentials, and a large number of functional groups are therefore not compatible with direct oxidation [48]. A milder and more selective approach is represented by the installation of an electroauxiliary (EA), a functional group which lowers the oxidation potential of the compound, in α-position to the oxygen/nitrogen

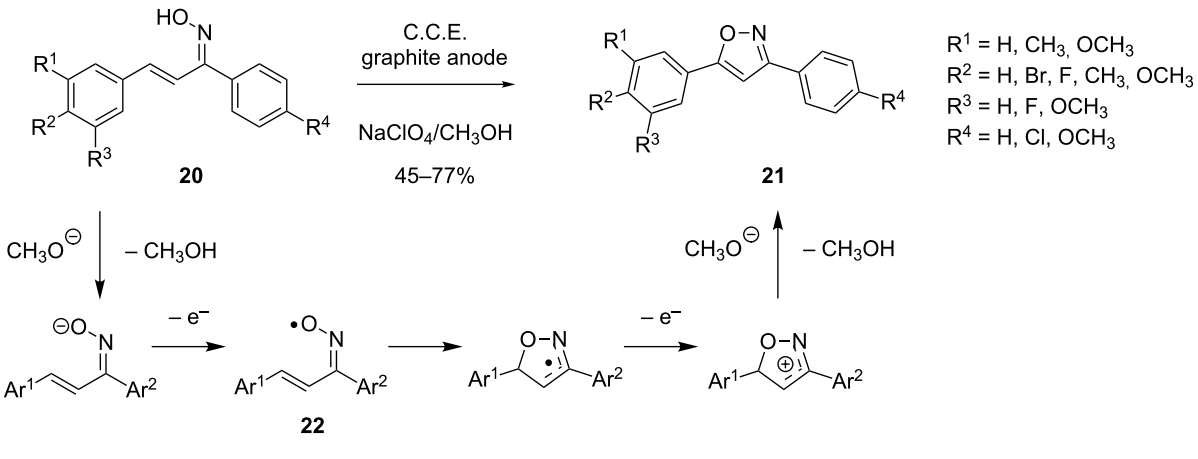

Scheme 8: Anodic cyclization of chalcone oximes **19**.

[30,49]. In this context, the use of silyl, stannyl and thioether groups is generally preferred, since these groups are typically cleaved off upon anodic oxidation. A number of intramolecular cyclizations of **23**- and **24**-type intermediates have been reported both in presence and absence of electroauxiliaries.

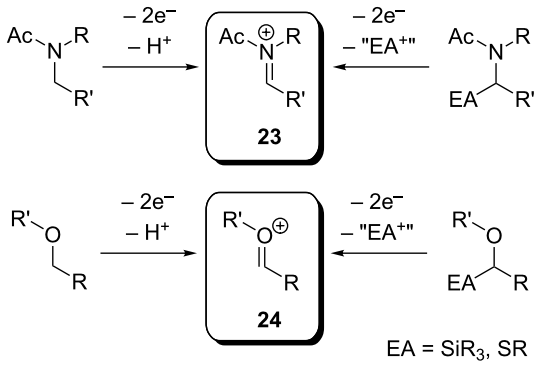

Scheme 9: Generation of *N*-acyliminium (**23**) and alkoxycarbenium species (**24**) from amides and ethers with and without the use of electroauxiliaries.

In the course of their research on functionalized peptidomimetics, Moeller and co-workers found that the amide unit provides an excellent opportunity for oxidative modification of the peptide framework [50,51]. In order to construct constrained peptidomimetics, several electrochemical protocols for generation and cyclization of *N*-acyliminium species have been developed, resulting in the synthesis of a number of lactams and lactam-derived heterocycles [52]. One representative example is depicted in Scheme 10, where dipeptide **25** cyclizes via intramolecular nucleophilic attack of the hydroxy group on the anodically generated *N*-acyliminium unit [53].

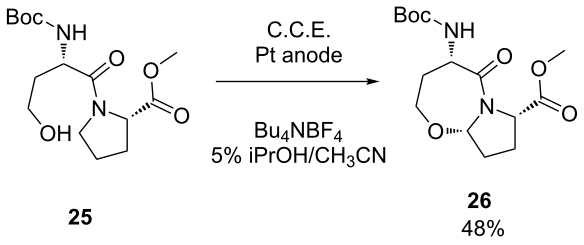

Scheme 10: Anodic cyclization of dipeptide **25**.

While this reaction proved to be very useful for the cyclization of simple amino acid derivatives, major limitations were encountered when more complicated systems were oxidized [52]. As outlined before, amide groups exhibit rather high oxidation potentials in the order of 1.95–2.10 V vs. Ag/AgCl, and their oxidation becomes therefore less selective with increasing electron-donating character of functional groups attached to the peptide. In this context, the introduction of electroauxiliaries to the peptidomimetic structures and their use for site-selective oxidation was explored [52]. The cyclization of dipeptide **27** as a model reaction is shown exemplarily in Scheme 11. Since the tethered olefin group is easier to oxidize than the amide unit, a dimethylphenylsilyl group was introduced in α-position to the amide and served as electroauxiliary. The cyclization was then accomplished in two steps, starting with the anodic oxidation of **27** in methanolic solution under galvanostatic conditions. In the second step, the resulting α-methoxy substituted intermediate was treated with $TiCl_4$ in CH_2Cl_2 at −78 °C to give cyclized product **28**.

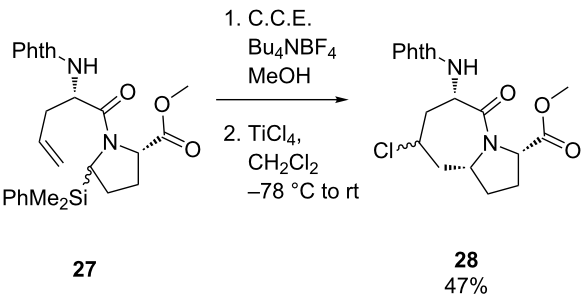

Scheme 11: Anodic cyclization of a dipeptide using an electroauxiliary.

Generally, the anodic oxidation of aliphatic amines leads to the formation of radical anions which can undergo multiple reaction pathways, typically leading to complex product mixtures [54]. The anodic generation of iminium species from amines for a nucleophilic α-substitution analogously to acyliminium intermediates **23** is therefore a rare case. However, Okimoto et al. could recently demonstrate that iminium species can be generated selectively and used for a cyclization reaction when a stabilizing benzyl group is attached to the nitrogen (Scheme 12, compound **29**) [55]. The hydroxy group tethered to the substrate serves for nucleophilic trapping of the iminium species under formation of oxazolidine or 1,3-oxazinane species **30**. According to their protocol, **29** is electrolyzed under galvanostatic conditions in a divided cell, using a NaOMe/MeOH electrolyte and potassium iodide as electron transfer mediator. The method provides access to a number of 2-aryl-1,3-oxazolidines and 2-aryl-1,3-oxazinanes.

An intriguing example for the intramolecular cyclization of alkoxycarbenium species has been reported recently by Suga, Yoshida et al. [56]. Unsaturated thioacetals **31** were converted anodically to 2,4-substituted tetrahydropyrans **32** using a mediating system that is based on the $ArS(ArSSAr)^+$ species, an equivalent of ArS^+ (Scheme 13). $ArS(ArSSAr)^+$ is formed upon anodic oxidation of ArSSAr at low temperatures and can be

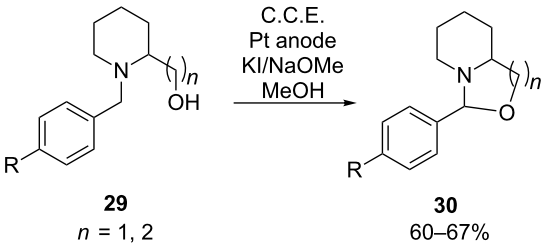

Scheme 12: Anodic cyclization of hydroxyamino compound **29**.

employed for the generation of cationic intermediates (indirect cation pool method) [57]. In the presence of a substrate with a thioaryl group (**31**), "ArS^+" is continuously regenerated (cation chain mechanism) and therefore, both ArSSAr and electric current can be employed in catalytic amounts. After formation of alkoxycarbenium ion **33**, cyclization proceeds and the resulting carbenium ion **34** is trapped by ArSSAr to give **32**.

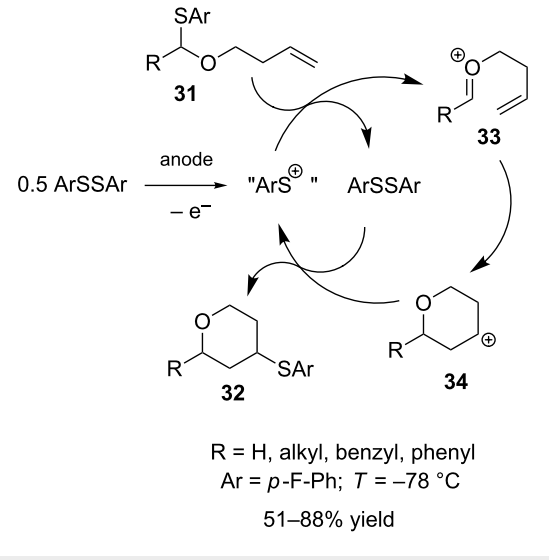

Scheme 13: Cyclization of unsaturated thioacetals using the $ArS(ArSSAr)^+$ mediator.

The $ArS(ArSSAr)^+$ species can either be generated prior to addition of **31** or in presence of the substrates. The use of tetrafluoroborate salts is associated with low yields due to fluorination of intermediate **34** and therefore has to be avoided. In contrast, good results are obtained when the reaction is carried out using $Bu_4NB(C_6F_5)_4$ as supporting electrolyte.

1.4 Further intramolecular cyclization reactions

As a part of their efforts in the total synthesis of several natural products, Nishiyama and co-workers developed an electrochemical method for the construction of *N*-heterocyclic cores (see examples depicted in Scheme 14 and Scheme 15) [58-60]. $PhI(OCH_2CF_3)_2$ was generated anodically from iodobenzene in a solution of $LiClO_4$ in 2,2,2-trifluoroethanol and served as reagent for the oxidative intramolecular coupling of phenyl rings with amide or carbamate groups. With control experiments the authors demonstrated that this in situ generated reagent works more efficiently in such cyclizations than the more frequently used PIFA reagent. For instance, cyclization of biaryl **35** to carbazole **36** was achieved using this indirect electrochemical approach (Scheme 14) [59,60]. The transformation represents the key-step of the synthesis of glycozoline **37**, an antifungal and antibacterial agent. Analogously, **38** was converted to **39** as a part of the multistep synthesis of two different tetrahydropyrroloiminoquinone alkaloids **40** and **41** (Scheme 15) [58,60].

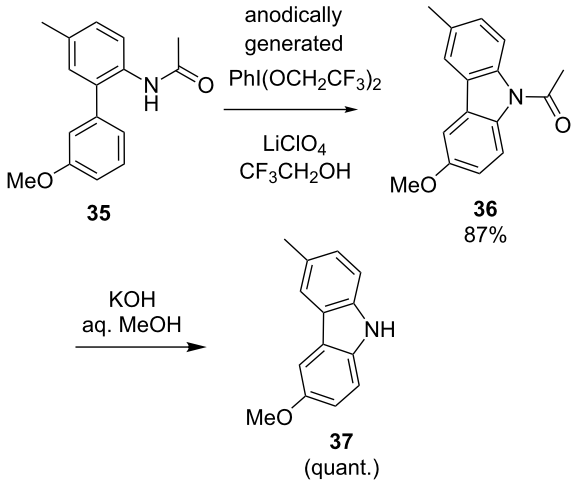

Scheme 14: Cyclization of biaryl **35** to carbazol **36** as key-step of the synthesis of glycozoline (**37**).

Tanaka et al. could achieve the electrochemical construction of 2,3-dihydrobenzofuran structures **43** via double-mediatory Wacker-type cyclization of alkenyl phenols **42** [61]. $Pd(OAc)_2$ was used to catalyze the cyclization while TEMPO served as redox mediator for the electrochemical regeneration of the catalytically active Pd(II) species. In contrast to conventional Wacker-type cyclizations, where stoichiometric amounts of co-oxidant are employed at elevated temperatures, the electrochemical version proceeds smoothly at room temperature. In the case depicted in Scheme 16, the electrolysis was carried out in a divided cell under galvanostatic conditions using platinum electrodes. Among several electrolyte compositions, $NaClO_4$ in a 7:1 mixture of dioxane/water proved to be the most efficient one. Halogen substituents on the phenol unit are tolerated under the described reaction conditions. In contrast, electron rich substrates (R = OMe) render unsatisfactory results.

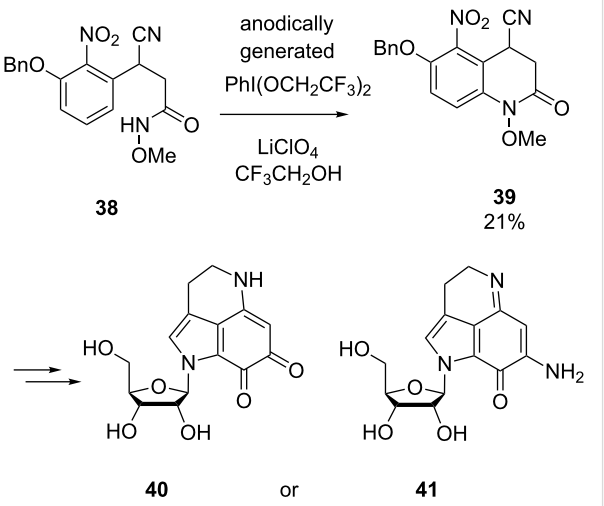

Scheme 15: Electrosynthesis of **39** as part of the total synthesis of alkaloids **40** and **41**.

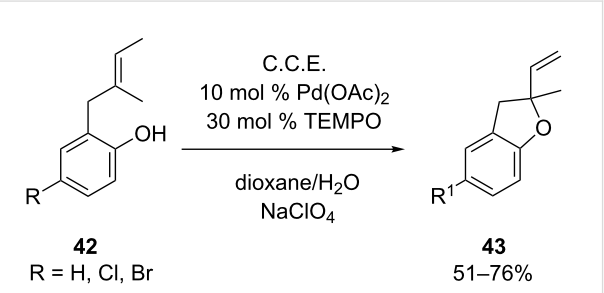

Scheme 16: Wacker-type cyclization of alkenyl phenols **42**.

In view of the fact that the indole unit is present in a variety of natural products and biologically active compounds, Arcadi, Rossi et al. reported a clean and mild electrochemical method for the construction of this heterocycle (Scheme 17) [62]. The procedure is initiated with the electrolysis of the Et_4NBF_4/CH_3CN electrolyte at 0 °C in a divided cell, followed by addition of **44** to the cathodic chamber after completed electrolysis (Q = 2.5F/mol). The cyanomethyl anion, a cathodically generated base which is formed upon reduction of the solvent CH_3CN, triggers the cyclization reaction via deprotonation of the amide group. According to the authors, the deprotonation is followed by ring closure on the C–C-triple bond, generating a carbanion intermediate which is then protonated by the solvent. For sufficient cyclization rates, the reaction mixture has to be heated to 80 °C. Various alkynylanilines with different substituents on the aromatic ring and on the alkynyl group were cyclized in good to excellent yields. When *N*-ethoxycarbonyl-substituted anilines are converted under the conditions described above, the carbamate group is cleaved and unprotected indoles are obtained.

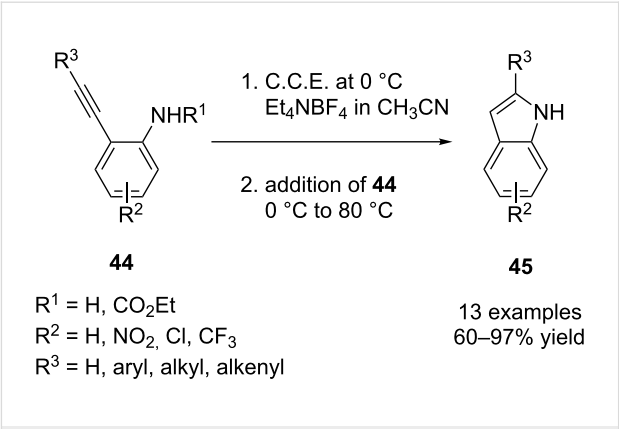

Scheme 17: Cathodic synthesis of indol derivatives.

An electrochemical method for the synthesis of oxindoles and 3-oxotetrahydroisoquinolines **47** via intramolecular cyclization under C–C-bond formation was reported by Atobe, Fuchigami et al. (Scheme 18) [63]. The protocol is based on the anodic oxidation of α-(phenylthio)acetamides **46** in the presence of $Et_3N{\cdot}3HF$. The latter serves as supporting electrolyte and as fluoride source for mediation of the reaction. In absence of fluoride, the formation of the cyclization product was not observed. The authors proposed a mechanism, in which after initial one-electron oxidation the resulting radical cation **48** is attacked by a fluoride ion under formation of an S–F bond. Radical **49** is then further oxidized to the corresponding cationic species **50**,

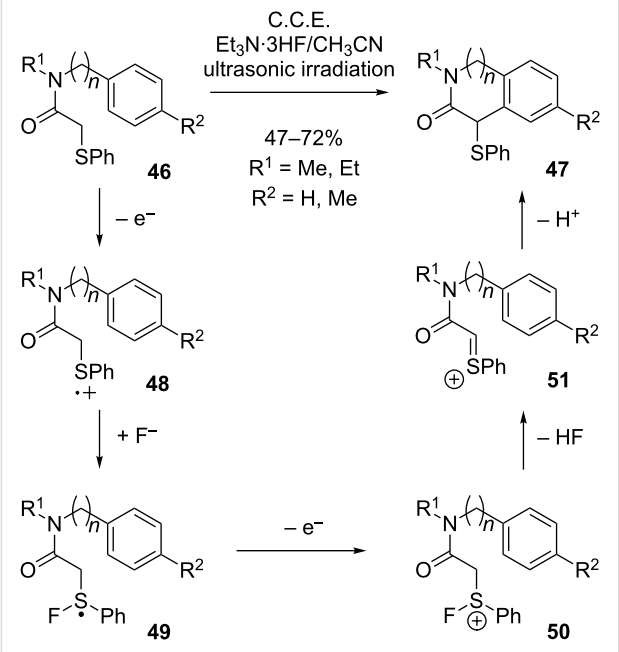

Scheme 18: Fluoride mediated anodic cyclization of α-(phenylthio)acetamides.

which undergoes elimination of HF under formation of cationic intermediate **51**. Finally, intramolecular trapping by the aromatic ring in a Friedel–Crafts type reaction leads to cyclization and formation of product **47**. A selectivity problem is caused by concurrent nucleophilic attack of fluoride ions on intermediate **51**. However, this undesired side reaction is suppressed when ultrasonic irradiation is applied during electrolysis. The authors studied the product distribution under variation of stirring speed and temperature in order to determine whether improved mass transport or strong local heating is responsible for the improved selectivity. Whereas an increase of the stirring speed did not significantly affect the ratio between desired cyclization product **47** and fluorinated byproduct, higher temperatures lead to preferential formation of the desired cyclization product. In the reported case, the use of ultrasonic radiation leads to significantly better results compared to conventional heating. These results suggest that the effect of ultrasound on the selectivity is attributable to strong local heating at the electrode surface, which increases the temperature sufficiently for cyclization. In contrast, such high temperatures are not available by conventional heating, where the reaction temperature is limited by the boiling point of the solvent.

Zeng, Little et al. described an indirect electrochemical method for the generation of 2-substituted benzoxazoles from Schiff bases (Scheme 19) [64]. Using 20 mol % NaI as redox mediator, the electrolysis is conducted under galvanostatic conditions in an undivided cell. A two-phase system composed of a sodium carbonate buffer solution and dichloromethane is employed as electrolyte. The method features attractive yields (70–95%) and a broad scope with regard to substitution on the phenylene moiety (R^1 and R^2) and on the oxazole unit (R^3).

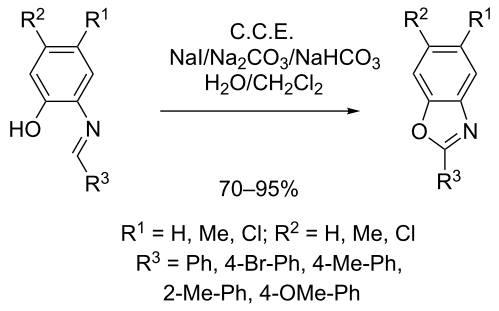

Scheme 19: Synthesis of 2-substituted benzoxazoles from Schiff bases.

2 Intermolecular cyclizations

2.1 Cycloadditions with anodically generated intermediates

A well-established strategy for the construction of certain six-membered heterocycles is the electrochemical generation of heterodienes for Diels–Alder cycloadditions [65,66]. In this context, electrosynthesis provides a significant advantage over conventional methods: Instable diene precursors which are difficult to synthesize by conventional means, can be conveniently generated in situ at low temperatures. The electrogenerated intermediate is subjected to cycloaddition either by in situ trapping with the dienophile or by using the cation pool approach.

Chiba et al. reported an interesting example for the use of such an electrochemically induced cycloaddition in natural product synthesis. The cyclization method was used for the generation of structures **54**–**56** (Scheme 20), which represent model com-

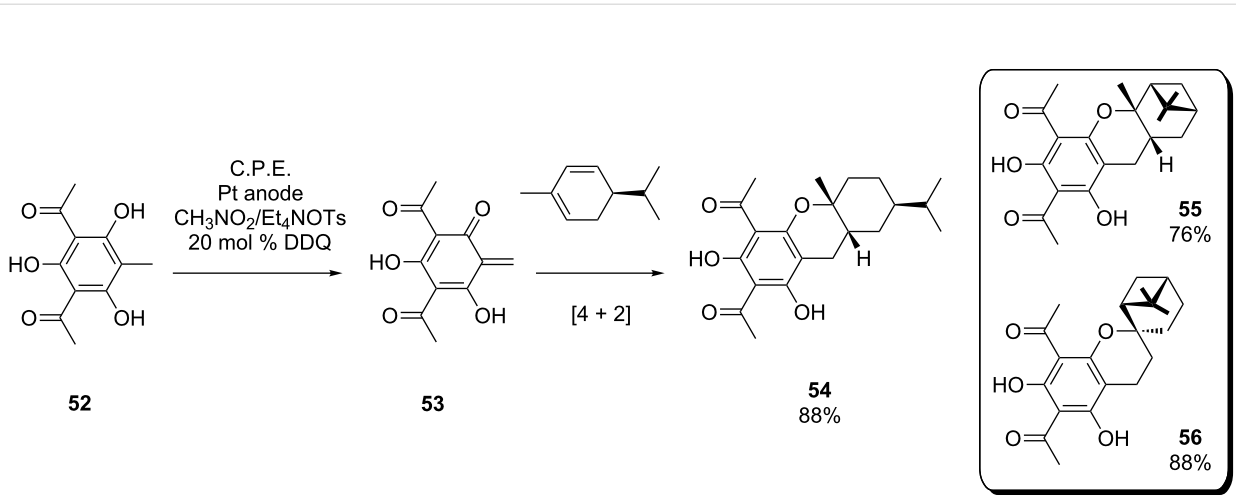

Scheme 20: Synthesis of euglobal model compounds via electrochemically induced Diels–Alder cycloaddition.

pounds for euglobals, natural products which can be obtained by extraction of eucalyptus leaves [65]. These structures consist of a terpene element and a benzodihydropyran unit and feature antiviral activity. First, quinomethane intermediate **53** is formed upon indirect anodic oxidation of **52**, which reacts with α-phellandrene at room temperature to give compound **54**. Alternatively, **53** can be converted with α- and β-pinene to form euglobal model compounds **55** and **56**.

The electrolysis was carried out in an undivided cell under potentiostatic conditions with a CH_3NO_2/Et_4NOTs electrolyte. DDQ was employed as a redox mediator, allowing for operation at a relatively low electrode potential of 0.45 V vs. SCE. Furthermore, the use of PTFE-coated platinum as working electrode proved to be beneficial. Presumably, the reaction sequence proceeds within the hydrophobic electrode coating, where the highly reactive intermediate **53** is protected from side-reactions and the reaction with the hydrophobic dienophile is facilitated.

Yoshida, Suga and co-workers reported on the use of electrogenerated *N*-acyliminium ions as heterodienes in [4 + 2] cycloadditions [66]. It was found that these highly reactive species, generated from silylated carbamate **57** at −78 °C (cation pool method), undergo cycloaddition at 0 °C with a variety of electron-rich alkenes and alkynes (Scheme 21) to afford 1,3-oxazinan-2-ones **59** and 3,4-dihydro-1,3-oxazin-2-ones **60**, respectively. The product yields strongly depend on the electronic character of the substituents on the dienophile. While monoalkyl- and monophenyl-substituted dienophiles generally render moderate to good yields, excellent results can be obtained either with silylated or acetoxylated alkenes/alkynes or with dienophiles containing two phenyl moieties. The conversion of alkyl-substituted olefins proceeds stereospecifically with respect to *E*- and *Z*-configuration, yielding either the *cis*- or *trans*-cycloadduct exclusively. Consistent with the results of computational studies conducted by the authors, this stereospecifity points towards a concerted reaction mechanism. In contrast, cycloaddition of phenyl-substituted olefins seems to proceed via a stepwise mechanism involving a cationic intermediate, since partial loss of the stereospecifity was observed.

Furthermore, the method for mixing of the cation pool with a solution of dienophile plays an important role. Best results were obtained by using a micromixer at 0 °C. While simultaneous pouring of the solutions into a flask at −78 °C still renders attractive results, addition of dienophile to **58** and vice versa leads to significantly lower yields.

Due to the synthetic usefulness of aziridines, the aziridination of olefins is of particular interest for organic chemists [3]. The three-membered aziridine ring exhibits an enormous strain and is therefore susceptible to ring-opening reactions with a variety of nucleophiles [3,4]. Such transformations lead to 1,2-heteroatom structures which are often found in pharmaceuticals and natural products. Yudin et al. described an electrochemical aziridination process where an anodically generated nitrene equivalent was transferred to a broad range of olefins using readily available *N*-aminophthalimide (Scheme 22) [67,68]. In contrast to conventional olefin aziridation, which is typically accomplished via metal-catalyzed nitrene transfer to the C–C-double bond, the electrochemical approach proceeds reagent- and catalyst-free. Both electron-rich and electron-deficient olefins can be efficiently converted. The electrolysis is carried out under potentiostatic conditions in a divided cell at room temperature using a platinum working electrode. A mixture of triethylamine and glacial acetic acid (1:1 molar ratio) in acetonitrile serves as electrolyte. The presence of acetate turned out to be crucial for aziridine formation, since with the use of other supporting electrolytes such as Bu_4NBF_4 the formation of the desired product could not be observed. Apparently, acetate ions

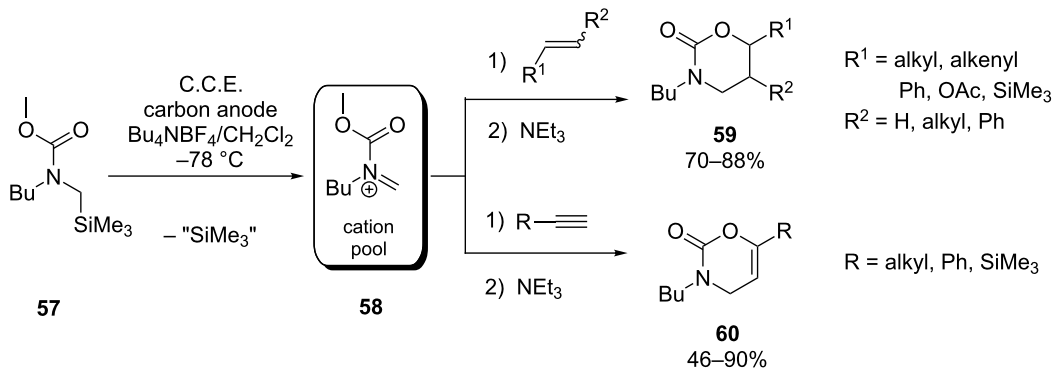

Scheme 21: Cycloaddition of anodically generated *N*-acyliminium species **58** with olefins and alkynes.

are stabilizing the anodically generated nitrene species via formation of adduct **61** (Scheme 23), which then undergoes concerted addition to the olefin. The fact that upon anodic oxidation in absence of olefins, *N*-aminophthalimide dimerizes readily to the corresponding tetrazene compounds, supports the postulated intermediate **61**. Furthermore, *N*-acetoxyamino species **61** can be observed by NMR at temperatures below 5 °C. Finally, the stereospecifity of the reaction with respect to *Z*- and *E*-configuration of the olefins is a further indication for a concerted mechanism involving intermediate **61**.

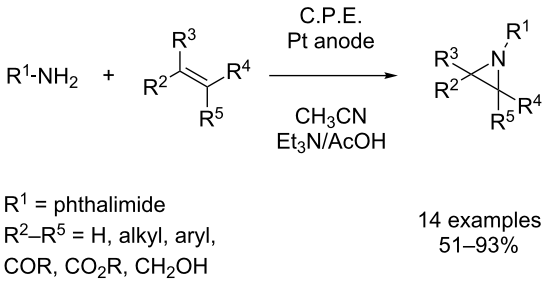

Scheme 22: Electrochemical aziridination of olefins.

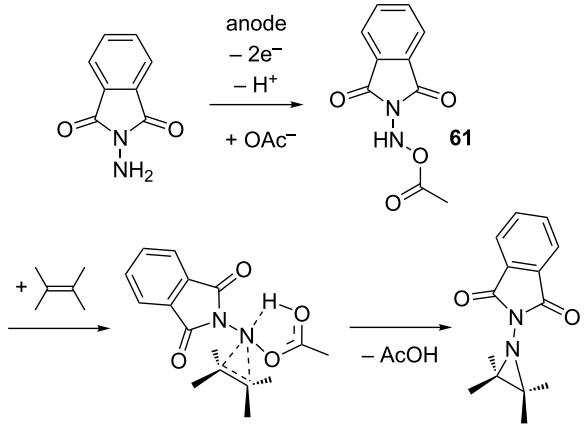

Scheme 23: Proposed mechanism for the aziridination reaction.

2.2 Anellation of in situ generated 1,2-benzoquinones via sequential Michael addition/ring closure

An electrochemical method for the synthesis of benzofuran and indol derivatives is based on the oxidation of catechol in presence of 1,3-dicarbonyl compounds or analogous C,H-acidic compounds **62** (Scheme 24) [69-72]. The anodically generated 1,2-benzoquinone undergoes a Michael reaction with **62** under formation of adduct **63**, which is further oxidized to give benzoquinone **64**. Finally, anellation proceeds in a second Michael addition step under formation of heterocyclic compound **65**. In the reported cases, both the generation of 1,2-benzoquinone and the anellation reaction proceed smoothly at room temperature. In addition to the fact that the reaction is carried out without the use of oxidation agents, a further advantage of this method is the possibility for operation in an aqueous electrolyte. Typically, aqueous sodium acetate or phosphate buffer solutions are used for this type of reaction [69-72]. In many cases, the product can be obtained in high purity by simple filtration of the precipitate after completed reaction and thorough washing with water.

The synthesis of 11,12-dihydroxycoumestan **67** by anodic oxidation of catechol in the presence of 4-hydroxycoumarin was reported by Tabaković et al. (Scheme 25, left) [69]. Using an undivided cell, an aqueous sodium acetate electrolyte and a graphite anode, the product was obtained in 95% yield. In a similar fashion, benzofurans of type **68** and **69** were synthesized by Nematollahi and co-workers from 3-substituted catechols **66** (Scheme 25, right) [70,71]. Interestingly, the formation of **68** and **69** proceeds under very high regioselectivity.

Zeng et al. developed a method for the synthesis of 1,2-fused indoles **71** (Scheme 26) based on the reaction depicted in Scheme 24 [72]. In this example, 1,2-benzoquinone derivatives are generated in the presence of ketene *N*,*O*-acetals **70**. Out of four possible regioisomers, **71a** and **71b** are exclusively formed (in ratios **71a**/**71b** between 1:1 and 1:2). In a follow-up study, unreacted α-arylated ketene *N*,*O*-acetal intermediates (**63**, Scheme 24) have been identified as byproducts [73,74].

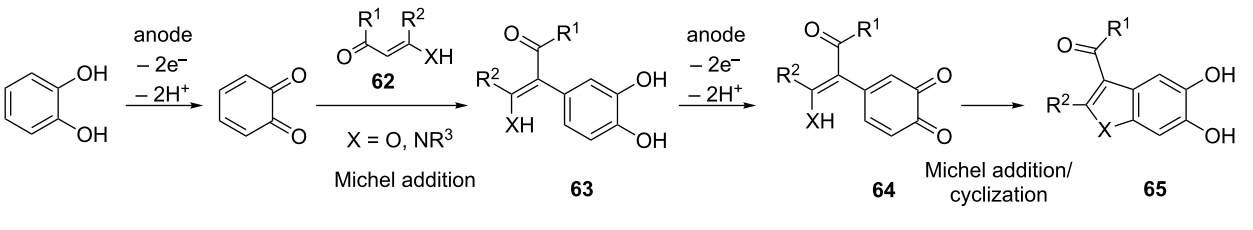

Scheme 24: Electrochemical synthesis of benzofuran and indole derivatives.

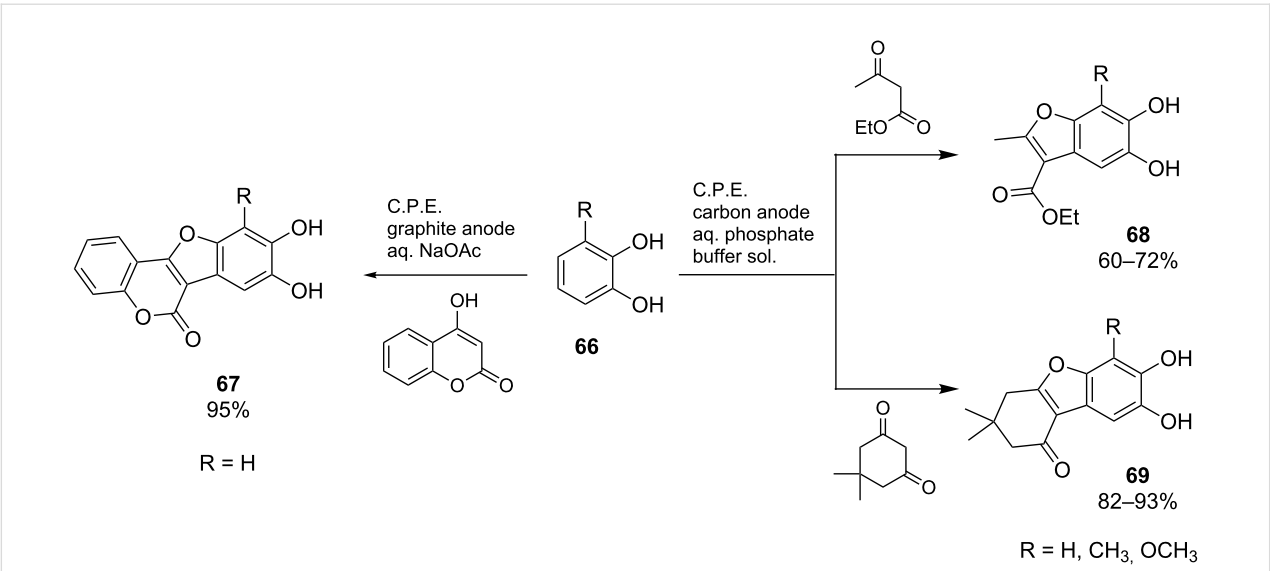

Scheme 25: Anodic anellation of catechol derivatives **66** with different 1,3-dicarbonyl compounds.

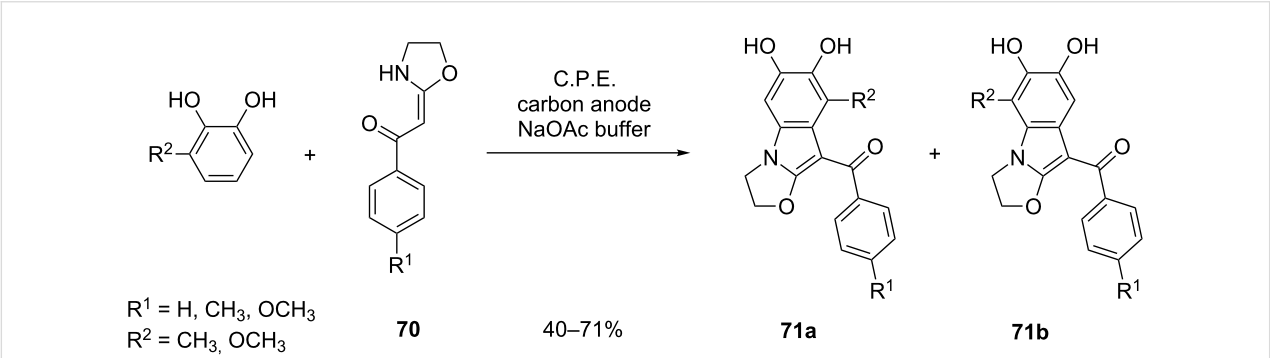

Scheme 26: Electrosynthesis of 1,2-fused indoles from catechol and ketene *N*,*O*-acetals.

Furthermore, it was demonstrated that ketene *N*,*S*-acetals can also be employed for indole synthesis, although the use of these substrates is associated with lower yields compared to *N*,*O*-acetals [75].

2.3 Acyl iminium ions and alkoxycarbenium ions in intermolecular cyclizations

Yoshida, Suga and co-workers investigated the electrochemical synthesis of five-membered heterocycles by integration of an intermolecular and an intramolecular step in one sequence. For this purpose, acyl iminium ions, electrogenerated as a cation pool at −78 °C, were converted at −23 °C with olefins bearing a nucleophilic group (Scheme 27) [76]. The cyclization is initiated by nucleophilic attack of the alkene on the acyl iminium species under C,C-bond formation. The resulting cationic intermediate is then trapped by the tethered nucleophile in an exo cyclization step under formation of a C,O-bond and generation of the five-membered heterocycle. Hydroxy, carboxy and oxime moieties were tested as nucleophiles for this reaction, leading to the corresponding tetrahydrofurans, γ-lactones and isoxazolines, respectively.

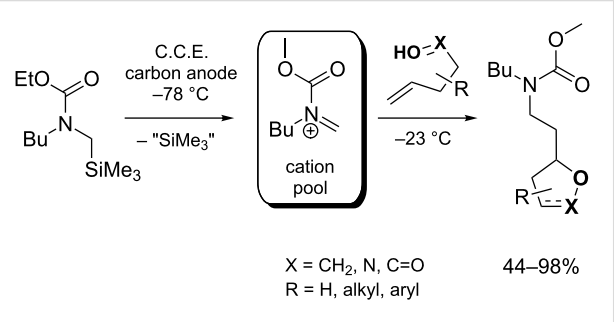

Scheme 27: Reaction of *N*-acyliminium pools with olefins having a nucleophilic substituent.

The chemistry depicted in Scheme 13 was also used for the construction of thiochroman frameworks in a sequential intermolecular cyclization reaction (Scheme 28) [77]. A cation pool of methoxycarbenium ions is generated at −78 °C from the corresponding thioacetal using anodically formed $ArS(ArSSAr)^+$, and converted at 0 °C with 4,4'-disubstituted stilbenes and ArSSAr to give the desired thiochroman. Both aliphatic (R = alkyl) and benzylic (R = Ar) thioacetals can be used, rendering the corresponding thiochroman in moderate to good yields. The reaction does not proceed stereospecifically with respect to *E*- and *Z*-configuration of the olefin. Out of four possible diastereomers, only two are obtained.

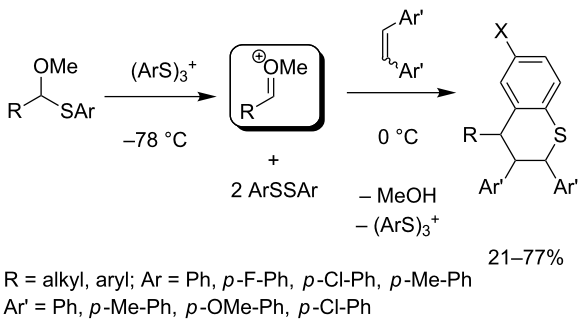

Scheme 28: Synthesis of thiochromans using the cation-pool method.

2.4 Anodic oxidation of 2,4-dimethylphenol

An interesting electrochemical route to complex scaffolds containing five membered *O*-heterocycles was found by Waldvogel and co-workers. In the course of their studies on the synthesis of 2,2'-biphenols via anodic coupling of phenols [78,79], they could observe the formation of spiropentacyclic scaffold **76** (Scheme 29) as byproduct of the electrolysis of 2,4-dimethylphenol (**72**) [80]. Later it turned out that compound **73** (a dehydrotetramer of **72**) is the actual electrolysis product, which reacted to **76** via thermal rearrangement under loss of a phenol unit during purification of the crude product by sublimation [81]. The authors proposed a mechanism where the formation of **73** starts with the anodic generation of a derivative of Pummerer's ketone (**74**) from two phenol units. After a second oxidation step and condensation with **72**, intermediate **75** is formed. Trapping by a further phenol unit results in product **73**.

Since spiropentacycle **76** resembles the core moieties of several natural products and therefore seemed to be a useful starting point for further investigations [81], the authors decided to optimize the reaction conditions in favor of the formation of **73**. As optimum reaction conditions, the use of a $Ba(OH)_2$/MeOH elec-

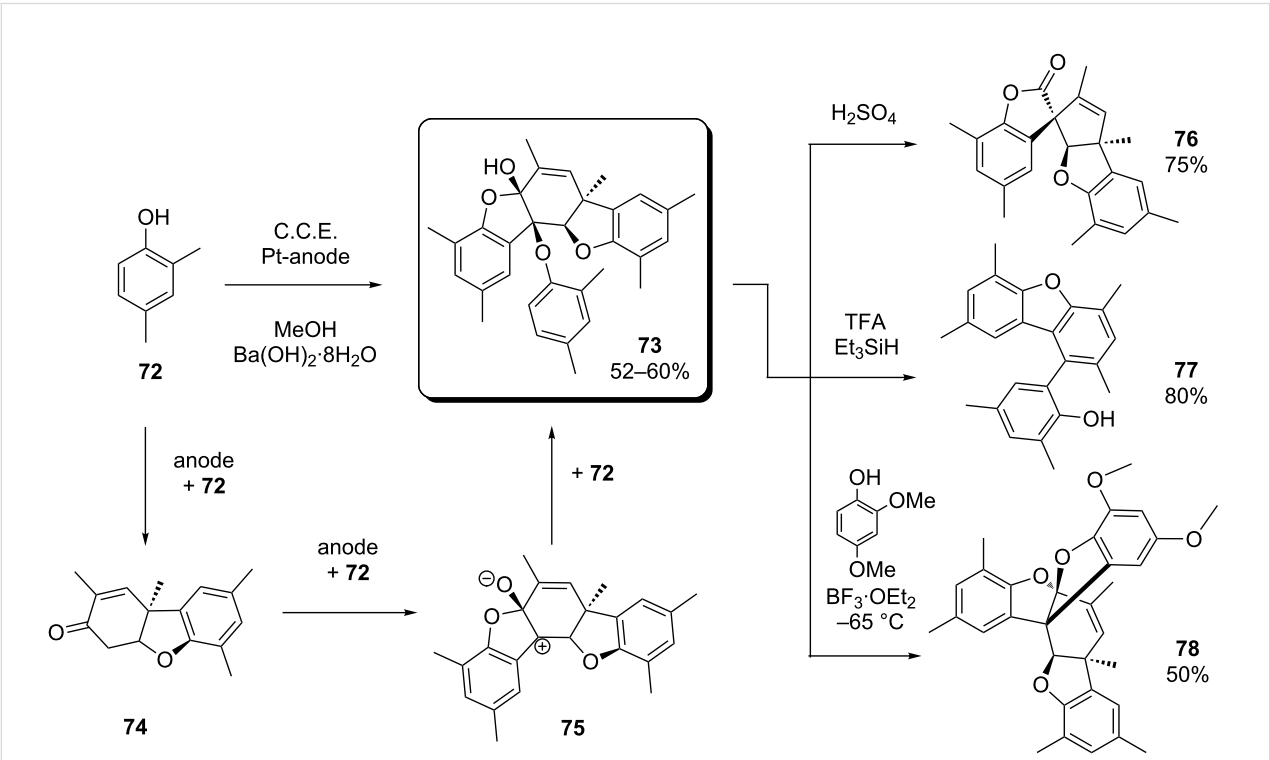

Scheme 29: Electrochemical synthesis and diversity-oriented modification of **73**.

trolyte in combination with platinum electrodes and a current density of 12.5 mA/cm^2 was identified. Under these conditions, **73** precipitates in the course of the electrolysis and can be obtained in high purity by simple filtration and washing. It was also found that compared to thermal treatment, the rearrangement of **73** to **76** proceeds by far more efficiently in the presence of sulfuric acid (Scheme 29, top right).

In a follow-up study, the elaborated electrolysis protocol served as a key-step for the generation of a variety of polycyclic structures containing typical structural elements of bioactive compounds [82]. Since **73** provides manifold possibilities for structural modifications, the generation of complex and structurally diverse scaffolds could be achieved in very few steps (diversity-oriented approach) [83]. In addition to the synthesis of **76**, two more examples for such diversity-oriented transformations are depicted in Scheme 29 (middle right and bottom right): Structures **77** and **78** were obtained upon treatment with TFA/Et_3SiH and $BF_3{\cdot}OEt_2$/2,4-dimethoxyphenol, respectively.

Conclusion

Undoubtedly, much progress has been made in the electrochemical synthesis of heterocyclic compounds since Tabaković's review appeared in 1997. Advances in anodic olefin coupling or electrochemically induced radical cyclization have made important contributions to this field. Moreover, the emergence of the cation-pool method has significantly expanded the toolbox of the electrochemist with regard to the synthesis of heterocyclic compounds. In many cases, the unique selectivity of electrochemical transformations could successfully be utilized for the construction of heterocyclic cores within natural products. It was also demonstrated that electrosynthesis can be a useful method for the generation of complex heterocyclic scaffolds from very simple precursors in a single step.

Obviously, electrosynthesis provides a number of possibilities for the construction of heterocyclic cores. In many cases, electrochemistry represents a complementary method to conventional synthesis, due to unique selectivity and the possibility for electrochemical Umpolung. However, considering the fact that heterocycle-containing compounds represent the major part of active ingredients in pharmaceutics and crop protection, a lack of efficient protocols for the electrosynthesis of such compounds becomes evident. In particular, the electrochemical construction of aromatic heterocycles deserves more attention, since they represent the larger portion of drugs [1]. Moreover, most of the electrochemical heterocycle syntheses reported so far were achieved by anodic oxidation, whereas cathodic heterocycle generation seems to represent a rare case. Of course this means that there are unexplored territories and numerous opportunities for research in this field.

Table 1: List of abbreviations.

Abbreviation	Explanation
C.C.E.	constant current electrolysis
C.P.E.	constant potential electrolysis
AIBN	azobisisobutyronitrile
tmc	1,4,8,11-tetramethylcyclam
DMSO	dimethyl sulfoxide
HFIP	1,1,1,3,3,3-hexafluoroisopropanol
EA	electroauxiliary
DDQ	2,3-dichloro-5,6-dicyano-1,4-benzoquinone
SCE	saturated calomel electrode
PTFE	polytetrafluoroethylene
PIFA	[bis(trifluoroacetoxy)iodo]benzene
TFA	2,2,2-trifluoroacetic acid
TEMPO	2,2,6,6-tetramethylpiperidine-1-oxyl

Acknowledgements

Financial support by the German Federal Ministry of Education and Research (BMBF – Bundesministerium für Bildung und Forschung, project number: 031A123) is highly appreciated.

References

1. Li, J. J., Ed. *Heterocyclic Chemistry in Drug Discovery;* John Wiley & Sons: Hoboken, 2013.
2. Lamberth, C.; Dinges, J., Eds. *Bioactive Heterocyclic Compound Classes: Agrochemicals;* Wiley-VCH: Weinheim, 2012.
3. Alvarez-Builla, J.; Vaquero, J. J.; Barluenga, J., Eds. *Modern Heterocyclic Chemistry;* Wiley-VCH: Weinheim, 2011.
4. Joule, J. A.; Mills, K. *Heterocyclic Chemistry;* Wiley-Blackwell: Hoboken, 2010.
5. Shi, Z.; Suri, M.; Glorius, F. *Angew. Chem., Int. Ed.* **2013,** *52,* 4892–4896. doi:10.1002/anie.201300477
6. Gulevich, A. V.; Dudnik, A. S.; Chernyak, N.; Gevorgyan, V. *Chem. Rev.* **2013,** *113,* 3084–3213. doi:10.1021/cr300333u
7. Thansandote, P.; Lautens, M. *Chem. – Eur. J.* **2009,** *15,* 5874–5883. doi:10.1002/chem.200900281
8. Mei, T.-S.; Kou, L.; Ma, S.; Engle, K. M.; Yu, J.-Q. *Synthesis* **2012,** 1778–1791. doi:10.1055/s-0031-1289766
9. Moriarty, R. M. *J. Org. Chem.* **2005,** *70,* 2893–2903. doi:10.1021/jo050117b
10. Zhdankin, V. V.; Stang, P. J. *Chem. Rev.* **2008,** *108,* 5299–5358. doi:10.1021/cr800332c
11. Wirth, T. *Angew. Chem., Int. Ed.* **2005,** *44,* 3656–3665. doi:10.1002/anie.200500115
12. Wirth, T.; Hirt, U. H. *Synthesis* **1999,** 1271–1287. doi:10.1055/s-1999-3540
13. Orru, R. V. A.; de Greef, M. *Synthesis* **2003,** 1471–1499. doi:10.1055/s-2003-40507
14. Dhakshinamoorthy, A.; Garcia, H. *Chem. Soc. Rev.* **2014,** *43,* 5750–5765. doi:10.1039/c3cs60442j
15. Ishibashi, H.; Sato, T.; Ikeda, M. *Synthesis* **2002,** 695–713. doi:10.1055/s-2002-25759

16. Bowman, W. R.; Cloonan, M. O.; Krintel, S. L. *J. Chem. Soc., Perkin Trans. 1* **2001,** 2885–2902. doi:10.1039/a909340k
17. Poliakoff, M.; Fitzpatrick, J. M.; Farren, T. R.; Anastas, P. T. *Science* **2002,** *297,* 807–810. doi:10.1126/science.297.5582.807
18. Clark, J. H. *Green Chem.* **1999,** *1,* 1–8. doi:10.1039/a807961g
19. Lund, H.; Hammerich, O., Eds. *Organic Electrochemistry;* Marcel Dekker: New York, 2001.
20. Fry, A. J. *Synthetic Organic Electrochemistry;* Wiley: New York, 1989.
21. Schäfer, H. J.; Harenbrock, M.; Klocke, E.; Plate, M.; Weiper-Idelmann, A. *Pure Appl. Chem.* **2007,** *79,* 2047–2057. doi:10.1351/pac200779112047
22. Frontana-Uribe, B. A.; Little, R. D.; Ibanez, J. G.; Palma, A.; Vasquez-Medrano, R. *Green Chem.* **2010,** *12,* 2099–2119. doi:10.1039/c0gc00382d
23. Sperry, J. B.; Wright, D. L. *Chem. Soc. Rev.* **2006,** *35,* 605–621. doi:10.1039/b512308a
24. Simonet, J.; Pilard, J. F. In *Organic Electrochemistry;* Lund, H.; Hammerich, O., Eds.; Marcel Dekker: New York, 2001; pp 1163–1226.
25. Utley, J. H. P.; Nielsen, M. F. In *Organic Electrochemistry;* Lund, H.; Hammerich, O., Eds.; Marcel Dekker: New York, 2001; pp 1227–1258.
26. Tabaković, I. *Top. Curr. Chem.* **1997,** *185,* 87–139.
27. Lund, H. *Adv. Heterocycl. Chem.* **1970,** *12,* 213–316. doi:10.1016/S0065-2725(08)60975-7
28. Lund, H.; Tabakovic, I. *Adv. Heterocycl. Chem.* **1984,** *36,* 235–341. doi:10.1016/S0065-2725(08)60116-6
29. Toomey, J. E., Jr. *Adv. Heterocycl. Chem.* **1984,** *37,* 167–215. doi:10.1016/S0065-2725(08)60242-1
30. Yoshida, J.; Kataoka, K.; Horcajada, R.; Nagaki, A. *Chem. Rev.* **2008,** *108,* 2265–2299. doi:10.1021/cr0680843
31. Francke, R.; Little, R. D. *Chem. Soc. Rev.* **2014,** *43,* 2492–2521. doi:10.1039/c3cs60464k
32. Moeller, K. D. *Tetrahedron* **2000,** *56,* 9527–9554. doi:10.1016/s0040-4020(00)00840-1
33. Little, R. D. In *Organic Electrochemistry;* Bard, A. J.; Stratmann, J., Eds.; Wiley-VCH: Weinheim, 2004; Vol. 8, pp 313–337.
34. Sutterer, A.; Moeller, K. D. *J. Am. Chem. Soc.* **2000,** *122,* 5636–5637. doi:10.1021/ja001063k
35. Xu, H.-C.; Moeller, K. D. *J. Am. Chem. Soc.* **2008,** *130,* 13542–13543. doi:10.1021/ja806259z
36. Xu, H.-C.; Moeller, K. D. *J. Am. Chem. Soc.* **2010,** *132,* 2839–2844. doi:10.1021/ja910586v
37. Yoshida, J.; Suga, S. *Chem. – Eur. J.* **2002,** *8,* 2650–2658. doi:10.1002/1521-3765(20020617)8:12<2650::AID-CHEM2650>3.0.CO;2-S
38. Yoshida, J.; Ashikari, Y.; Matsumoto, K.; Nokami, T. *J. Synth. Org. Chem., Jpn.* **2013,** *71,* 1136–1144. doi:10.5059/yukigoseikyokaishi.71.1136
39. Ashikari, Y.; Nokami, T.; Yoshida, J. *Org. Biomol. Chem.* **2013,** *11,* 3322–3331. doi:10.1039/c3ob40315g
40. Ashikari, Y.; Nokami, T.; Yoshida, J. *Org. Lett.* **2012,** *14,* 938–941. doi:10.1021/ol203467v
41. Esteves, A. P.; Goken, D. M.; Klein, L. J.; Lemos, M. A.; Medeiros, M. J.; Peters, D. G. *J. Org. Chem.* **2003,** *68,* 1024–1029. doi:10.1021/jo026102k
42. Esteves, A. P.; Goken, D. M.; Klein, L. J.; Medeiros, M. J.; Peters, D. G. *J. Electroanal. Chem.* **2003,** *560,* 161–168. doi:10.1016/j.jelechem.2003.07.011
43. Huhtasaari, M.; Schäfer, H. J.; Becking, L. *Angew. Chem., Int. Ed. Engl.* **1984,** *23,* 980–981. doi:10.1002/anie.198409801
44. Becking, L.; Schäfer, H. J. *Tetrahedron Lett.* **1988,** *29,* 2797–2800. doi:10.1016/0040-4039(88)85212-2
45. Weiguny, J.; Schäfer, H. J. *Liebigs Ann. Chem.* **1994,** 235–242. doi:10.1002/jlac.199419940303
46. Beesley, R. M.; Ingold, C. K.; Thorpe, J. F. *J. Chem. Soc., Trans.* **1915,** *107,* 1080–1106. doi:10.1039/ct9150701080
47. Xiao, H.-L.; Zeng, C.-C.; Tian, H.-Y.; Hu, L.-M.; Little, R. D. *J. Electroanal. Chem.* **2014,** *727,* 120–124. doi:10.1016/j.jelechem.2014.06.008
48. Weinberg, N. L.; Weinberg, H. R. *Chem. Rev.* **1968,** *68,* 449–523. doi:10.1021/cr60254a003
49. Yoshida, J.; Nishiwaki, K. *J. Chem. Soc., Dalton Trans.* **1998,** 2589–2596. doi:10.1039/A803343I
50. Beal, L. M.; Liu, B.; Chu, W.; Moeller, K. D. *Tetrahedron* **2000,** *56,* 10113–10125. doi:10.1016/S0040-4020(00)00856-5
51. Tong, Y.; Fobian, Y. M.; Wu, M.; Boyd, N. D.; Moeller, K. D. *J. Org. Chem.* **2000,** *65,* 2484–2493. doi:10.1021/jo991649t
52. Sun, H.; Martin, C.; Kesselring, D.; Keller, R.; Moeller, K. D. *J. Am. Chem. Soc.* **2006,** *128,* 13761–13771. doi:10.1021/ja064737l
53. Cornille, F.; Slomczynska, U.; Smythe, M. L.; Beusen, D. D.; Moeller, K. D.; Marshall, G. R. *J. Am. Chem. Soc.* **1995,** *117,* 909–917. doi:10.1021/ja00108a007
54. Steckhan, E. In *Organic Electrochemistry;* Lund, H.; Hammerich, O., Eds.; Marcel Dekker: New York, 2001; pp 545–588.
55. Okimoto, M.; Ohashi, K.; Yamamori, H.; Nishikawa, S.; Hoshi, M.; Yoshida, T. *Synthesis* **2012,** *44,* 1315–1322. doi:10.1055/s-0031-1290755
56. Matsumoto, K.; Fujie, S.; Ueoka, K.; Suga, S.; Yoshida, J. *Angew. Chem., Int. Ed.* **2008,** *47,* 2506–2508. doi:10.1002/anie.200705748
57. Suga, S.; Matsumoto, K.; Ueoka, K.; Yoshida, J. *J. Am. Chem. Soc.* **2006,** *128,* 7710–7711. doi:10.1021/ja0625778
58. Inoue, K.; Ishikawa, Y.; Nishiyama, S. *Org. Lett.* **2009,** *12,* 436–439. doi:10.1021/ol902566p
59. Kajiyama, D.; Inoue, K.; Ishikawa, Y.; Nishiyama, S. *Tetrahedron* **2010,** *66,* 9779–9784. doi:10.1016/j.tet.2010.11.015
60. Kajiyama, D.; Saitoh, T.; Nishiyama, S. *Electrochemistry* **2013,** *81,* 319–324. doi:10.5796/electrochemistry.81.319
61. Mitsudo, K.; Ishi, T.; Tanaka, H. *Electrochemistry* **2008,** *76,* 859–861. doi:10.5796/electrochemistry.76.859
62. Arcadi, A.; Bianchi, G.; Inesi, A.; Marinelli, F.; Rossi, L. *Eur. J. Org. Chem.* **2008,** 783–787. doi:10.1002/ejoc.200701011
63. Shen, Y.; Atobe, M.; Fuchigami, T. *Org. Lett.* **2004,** *6,* 2441–2444. doi:10.1021/ol049152f
64. Li, W.-C.; Zeng, C.-C.; Hu, L.-M.; Tian, H.-Y.; Little, R. D. *Adv. Synth. Catal.* **2013,** *355,* 2884–2890. doi:10.1002/adsc.201300502
65. Chiba, K.; Arakawa, T.; Tada, M. *J. Chem. Soc., Perkin Trans. 1* **1998,** 2939–2942. doi:10.1039/a802306i
66. Suga, S.; Nagaki, A.; Tsutsui, Y.; Yoshida, J. *Org. Lett.* **2003,** *5,* 945–947. doi:10.1021/ol0341243
67. Siu, T.; Picard, C. J.; Yudin, A. K. *J. Org. Chem.* **2005,** *70,* 932–937. doi:10.1021/jo048591p
68. Siu, T.; Yudin, A. K. *J. Am. Chem. Soc.* **2002,** *124,* 530–531. doi:10.1021/ja0172215
69. Grujić, Z.; Tabaković, I.; Trkovnik, M. *Tetrahedron Lett.* **1976,** *17,* 4823–4824. doi:10.1016/S0040-4039(00)78920-9

70. Fakhari, A. R.; Nematollahi, D.; Shamsipur, M.; Makarem, S.; Davarani, S. S. H.; Alizadeh, A.; Khavasi, H. R. *Tetrahedron* **2007,** *63,* 3894–3898. doi:10.1016/j.tet.2007.02.023
71. Nematollahi, D.; Habibi, D.; Rahmati, M.; Rafiee, M. *J. Org. Chem.* **2004,** *69,* 2637–2640. doi:10.1021/jo035304t
72. Zeng, C.-C.; Liu, F.-J.; Ping, D.-W.; Hu, L.-M.; Cai, Y.-L.; Zhong, R.-G. *J. Org. Chem.* **2009,** *74,* 6386–6389. doi:10.1021/jo901091s
73. Bai, Y.-X.; Ping, D.-W.; Little, R. D.; Tian, H.-Y.; Hu, L.-M.; Zeng, C.-C. *Tetrahedron* **2011,** *67,* 9334–9341. doi:10.1016/j.tet.2011.09.126
74. Zhang, N.-T.; Gao, X.-G.; Zeng, C.-C.; Hu, L.-M.; Tian, H.-Y.; She, Y.-B. *RSC Adv.* **2012,** *2,* 298–306. doi:10.1039/c1ra00683e
75. Gao, X.-G.; Zhang, N.-T.; Zeng, C.-C.; Liu, Y.-D.; Hu, L.-M.; Tian, H.-Y. *Curr. Org. Synth.* **2014,** *11,* 141–148. doi:10.2174/15701794111999140304143341
76. Ashikari, Y.; Kiuchi, Y.; Takeuchi, T.; Ueoka, K.; Suga, S.; Yoshida, J. *Chem. Lett.* **2014,** *43,* 210–212. doi:10.1246/cl.130947
77. Matsumoto, K.; Ueoka, K.; Fujie, S.; Suga, S.; Yoshida, J. *Heterocycles* **2008,** *76,* 1103–1119. doi:10.3987/COM-08-S(N)64
78. Malkowsky, I. M.; Rommel, C. E.; Fröhlich, R.; Griesbach, U.; Pütter, H.; Waldvogel, S. R. *Chem. – Eur. J.* **2006,** *12,* 7482–7488. doi:10.1002/chem.200600375
79. Malkowsky, I. M.; Griesbach, U.; Pütter, H.; Waldvogel, S. R. *Eur. J. Org. Chem.* **2006,** 4569–4572. doi:10.1002/ejoc.200600466
80. Malkowsky, I. M.; Rommel, C. E.; Wedeking, K.; Fröhlich, R.; Bergander, K.; Nieger, M.; Quaiser, C.; Griesbach, U.; Pütter, H.; Waldvogel, S. R. *Eur. J. Org. Chem.* **2006,** 241–245. doi:10.1002/ejoc.200500517
81. Barjau, J.; Königs, P.; Kataeva, O.; Waldvogel, S. R. *Synlett* **2008,** 2309–2312. doi:10.1055/s-2008-1078276
82. Barjau, J.; Schnakenburg, G.; Waldvogel, S. R. *Angew. Chem., Int. Ed.* **2011,** *50,* 1415–1419. doi:10.1002/anie.201006637
83. Schreiber, S. L. *Science* **2000,** *287,* 1964–1969. doi:10.1126/science.287.5460.1964

License and Terms

BEILSTEIN JOURNAL OF ORGANIC CHEMISTRY

The Shono-type electroorganic oxidation of unfunctionalised amides. Carbon–carbon bond formation via electrogenerated *N*-acyliminium ions

Alan M. Jones*§ and Craig E. Banks*¶

Review

Open Access

Address:
Manchester Metropolitan University, Faculty of Science and Engineering, School of Science and the Environment, Division of Chemistry and Environmental Science, John Dalton Building, Chester Street, Manchester, M1 5GD, UK

Email:
Alan M. Jones* - A.M.Jones@mmu.ac.uk; Craig E. Banks* - C.Banks@mmu.ac.uk

* Corresponding author
§ Tel: +44 (0) 161 247 6195; web: http://www.jonesgroupresearch.wordpress.com
¶ Tel: +44 (0) 161 247 1196; web: http://www.craigbanksresearch.com

Keywords:
anodic oxidation; electrochemistry; electroorganic, electrosynthesis, *N*-acyliminium ions; natural products; non-Kolbe oxidation; peptidomimetics; Shono oxidation; synthesis

Beilstein J. Org. Chem. **2014,** *10,* 3056–3072.
doi:10.3762/bjoc.10.323

Received: 06 November 2014
Accepted: 05 December 2014
Published: 18 December 2014

This article is part of the Thematic Series "Electrosynthesis".

Guest Editor: S. R. Waldvogel

Abstract

N-acyliminium ions are useful reactive synthetic intermediates in a variety of important carbon–carbon bond forming and cyclisation strategies in organic chemistry. The advent of an electrochemical anodic oxidation of unfunctionalised amides, more commonly known as the Shono oxidation, has provided a complementary route to the C–H activation of low reactivity intermediates. In this article, containing over 100 references, we highlight the development of the Shono-type oxidations from the original direct electrolysis methods, to the use of electroauxiliaries before arriving at indirect electrolysis methodologies. We also highlight new technologies and techniques applied to this area of electrosynthesis. We conclude with the use of this electrosynthetic approach to challenging syntheses of natural products and other complex structures for biological evaluation discussing recent technological developments in electroorganic techniques and future directions.

Review

N-Acyliminium ions are synthetically versatile

N-Acyliminium ions [1,2] have a long and distinguished history in organic chemistry being important components in carbon–carbon bond forming reactions and in the generation of cyclic and heterocyclic ring systems through such classic named reactions as the Pictet–Spengler and Diels–Alder [3,4]. There have been many excellent and comprehensive reviews on the art

of electroorganic synthesis and the reader is directed to these articles for a thorough background and insight into the many facets of electrosynthesis [5-10]. In this review, we focus upon the development and application of the Shono-type electrochemical oxidation of unfunctionalised amides (last comprehensively reviewed in 1984 by Prof. T. Shono) [10] to *N*-acyliminium ion intermediates and their application to synthetic challenges.

The Shono electrooxidation route to *N*-acyliminium intermediates

Shono and colleagues reported the first direct electrochemical anodic oxidation of an α-methylene group to an amide (or carbamate) to generate a new carbon–carbon bond via an anodic methoxylation step and Lewis acid mediated generation of an *N*-acyliminium ion reactive intermediate; Scheme 1 overviews such a process [11].

Although the anodic oxidation/alkoxylation of amides pre-dates this work [12,13], Shono showed the synthetic utility of combining an electroorganic step with key carbon–carbon bond forming reactions required in synthetic organic chemistry. The key anodic methoxylation is operationally straightforward with a standard electrochemical set-up using carbon electrodes and is well documented [14,15]. The anodic methoxylation of unsymmetrical amides raises a key question regarding the regioselectivity of the products formed. Onomura and colleagues have detailed the influence of the protecting group on nitrogen on a series of cyclic amines on the product formed. It was argued the protecting group would influence and stabilise the *N*-acyliminium ion formed, therefore altering the regioselectivity of the product obtained. It was found that in all cases (e.g., carbonyl or sulfonyl-based protecting groups and ring size, $n = 1$ or 2) the kinetic-type product was exclusively formed except when the protecting group (PG) was changed to a cyano group the thermodynamic-type product was the dominant product formed (see Scheme 2) [16]. Looking more closely at these examples (PG = CN), it was found that increasing the size of the R group had little effect in adjusting the kinetic/thermodynamic ratio when the ring size was $n = 1$. The kinetic/thermodynamic ratio became more pronounced when $n = 2$ and the thermodynamic product was formed exclusively when large R groups were used (for example, phenyl).

The conventional two-step electrochemical procedure for the generation of the *N*-acyliminium ion and trapping with solvent (e.g., methanol), regenerating the *N*-acyliminium ion through treatment with a Lewis acid (quenching with the nucleophile) can be overridden by the "cation pool" method [17]. The cation pool methodology relies on the low temperature electrolysis of carbamates to accumulate the *N*-acyliminium ion reactive intermediate then under non-oxidative conditions the nucleophile is introduced. Importantly, the nucleophile cannot be present when the *N*-acyliminium ion is being formed under electrochemical conditions, as in most cases it is easier to oxidise the nucleophile than the amide precursor. This circumvents the need to prepare, trap and release the *N*-acyliminium cation under more favourable conditions, allowing the direct α-alkylation or arylation of carbamates (Scheme 3); the cation pool method has been extensively studied [17-31].

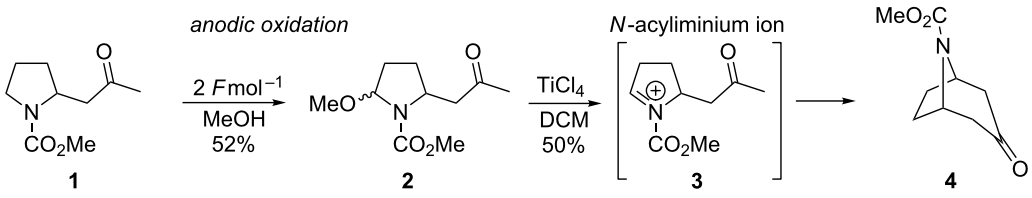

Scheme 1: Application of anodic oxidation to the generation of new carbon-carbon bonds [11].

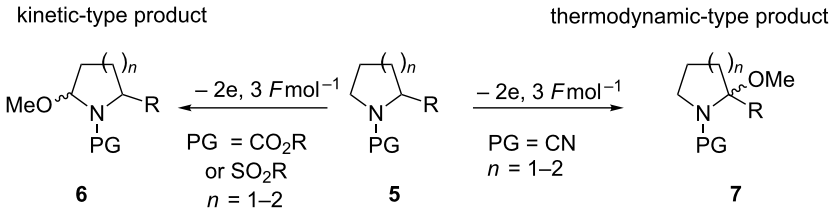

Scheme 2: The influence of the amino protecting group on the "kinetic" and "thermodynamic" anodic methoxylation [16].

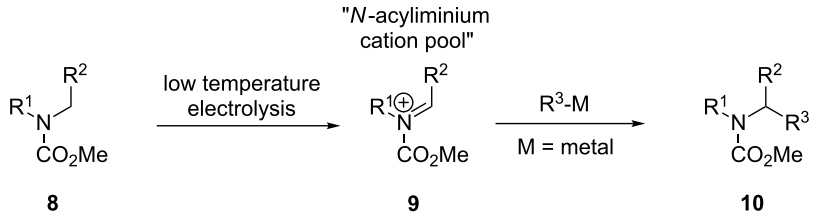

Scheme 3: Example of the application of the cation pool method [17].

The use of electroauxiliaries

The concept of electroauxiliaries has proven useful for developing and expanding the scope of the Shono-type oxidation of carbamates; electroauxiliaries activate organic compounds towards electron transfer controlling the fate of the generated reactive intermediates and assist in the formation of the desired products. Tin, silicon or sulfur-based electroauxiliaries have proved useful in this endeavour. Yoshida and co-workers developed an organothio electroauxiliary that is selectively cleaved under anodic oxidation conditions [32,33]. Although the introduction of an electroauxiliary requires an additional synthetic step to prepare, the resulting carbon–tin, carbon–silicon or carbon–sulfur bond has a less positive oxidation potential than an unfunctionalised carbamate. Therefore, exquisite control can be exerted on the introduction of the nucleophile to the C–X bond that contains the electroauxiliary (Scheme 4).

Similarly, α-silyl-carbamates undergo low potential anodic oxidation reactions with complete regiocontrol and in special cases diastereoselectivity [34,35]. Interestingly, a porous graphite felt anode and a stainless steel cathode were utilised in a flow cell set-up [35]. An important example of the scope and synthetic potential of the silyl electroauxiliary approach was reported by Yoshida (Scheme 5) in combination with a chiral auxiliary a highly diastereoselective cationic carbohydroxylation occurred [18]. The proposed formation of a bicyclic intermediate **18** resulting from a cycloaddition reaction would enhance the diastereoselectivity of the hydration step compared to an acyclic intermediate that would be formed in the step-wise mechanism to **18**. The authors' suggest the step-wise mechanism does play a role in reducing the diastereoselectivity of the reaction when the alkene is aryl- or alkyl-substituted. The hydration step can occur via pathway *a* or *b* to afford **17** (dr ca. 3:2).

The *N*-acyliminium ions formed during an anodic oxidation of a silyl auxiliary can be coupled to a radical pathway using a radical initiating agent such as distannane (Scheme 6). This allows the *N*-acyliminium ion to react with an alkyl halide to generate the typical carbon–carbon products of the Shono oxidation [19,27,28] Examples of reactions with activated olefins have been reported using the generation of carbon free radicals from the cation pool method [24,25].

Indirect electrolysis methods

The only indirect anodic oxidation method to perform the Shono-oxidation with a thiophenyl electroauxiliary has been reported by Fuchigami and co-workers [36]. Using a catalytic triarylamine redox mediator, anodic fluorodesulfurization occurred (Scheme 7). Direct Shono-type fluorination of an α-carbon to an amide has also been reported [37].

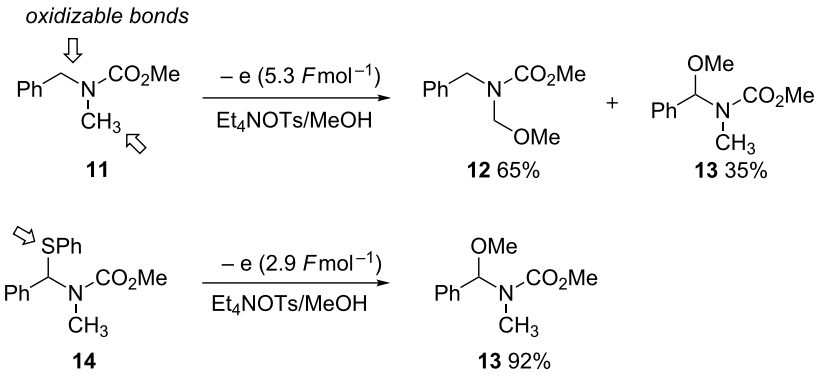

Scheme 4: A thiophenyl electroauxiliary allows for regioselective anodic oxidation [32].

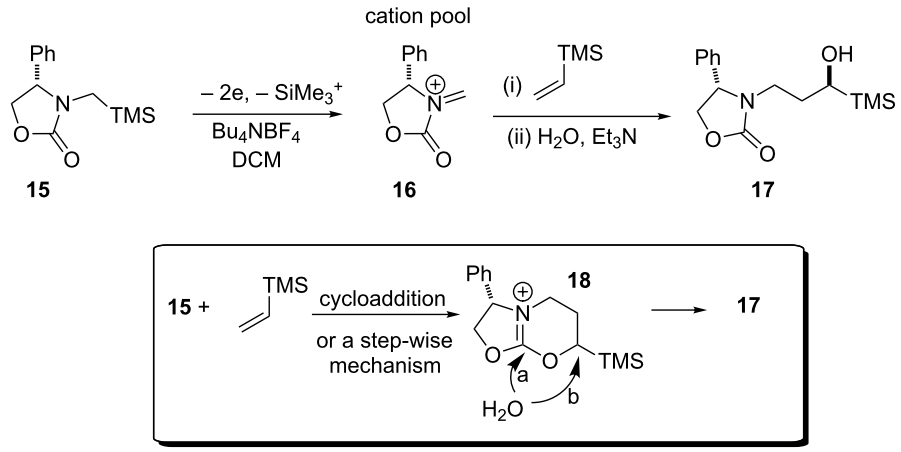

Scheme 5: A diastereoselective cation carbohydroxylation reaction and postulated intermediate **18** [18].

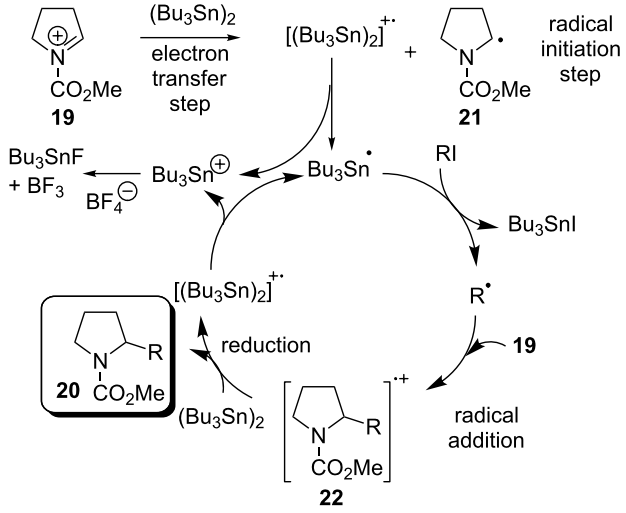

Scheme 6: A radical addition and electron transfer reaction of *N*-acyliminium ions generated electrosynthetically [19].

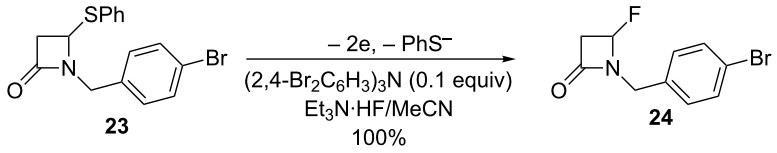

Scheme 7: Catalytic indirect anodic fluorodesulfurization reaction [37].

Technical advances in the Shono electroxidation reaction

The "cation-pool" method for the generation of *N*-acyliminium ions [17-31] has been adapted to efficiently generate novel small molecules in an electrochemical microflow system [26,30]. Combining the advantages of the cation-pool method with microflow technologies has enabled the concept of "cation flow" systems (Figure 1). In this arrangement a porous carbon felt is used as an anode and a platinum wire coil is used as the cathode; the flow cell is placed into a dry ice bath to maintain the −78 °C temperature required. Cation flow systems can be used to prepare individual molecules and combined with the concept of combinatorial chemistry to generate libraries of compounds.

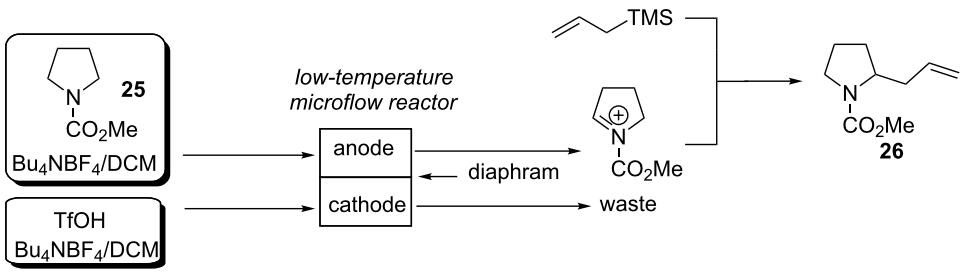

Figure 1: Schematic of a cation flow system and also shown is the electrochemical microflow reactor reported by Suga et al. Figure redrawn from reference [30].

A further advance to the micro-flow reactor strategy is to use a parallel laminar flow set-up (Figure 2 overviews such an experimental design) [38,39]. Due to the small size of the flow channel when two liquids are injected the liquid–liquid contact area will remain stable and laminar, where only contact between anodically generated carbocations occurs by mass transfer diffusion across the liquid–liquid contact area. Therefore, one liquid can be oxidized and the other liquid containing the nucleophile can intercept the *N*-acyliminium ion formed in the microflow reactor (when the two sides of the channel are anode and cathode) (viz. Figure 2).

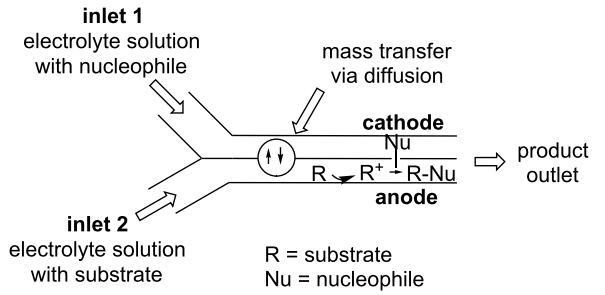

Figure 2: Example of a parallel laminar flow set-up. Figure redrawn from reference [38].

This technique of microflow mixing can also be applied to the synthesis of polymers [29]. A single channel miniaturised microfluidic electrolysis cell that is modular with other microfluidic techniques has now been developed to perform anodic methoxylation reactions [40]. Microflow mixing can confer other advantages such as increase electrode surface to reactant volume and reduced distance between electrodes. It has also been shown that electroorganic synthesis can be performed without supporting electrolyte in a microflow system [41]. If the cation pool method is unsuitable, for instance due to the instability of the cation formed, Chiba and co-workers have proposed a reversible capture method [42]. Using liquefiable micelle-like microparticles containing a thiomaleimide unit, *N*-acyliminium ions generated electroorganically can be intercepted and tagged in situ. The tagged and now stable "reactive intermediate" can then be removed from the electrolyte solution. Warming the tagged "reactive intermediate" converts the micelle (eicosane, a thermosensitive alkane) from solid to liquid and releases the thiomaleimide tagged *N*-acyliminium ion. Further warming breaks the C–S bond and allowed the regeneration of the *N*-acyliminium ion in a new solution containing the desired nucleophile interceptor to immediately react with the *N*-acyliminium ion as it is released from its thiomaleimide tag (Figure 3).

A micromixer has been used to generate an *N*-acyliminium ion pool and under Friedel–Crafts conditions mono-alkylation products are formed (Scheme 8) [43,44]. A problem with conventional Friedel–Crafts alkylation is the mono-alkylated product is more reactive than the starting material making di- and tri-alkylation products more likely. Improved yields and ratios of up to 96:4 mono-alkylated to dialkylated were observed using the cation pool micromixing strategy.

Acoustic emulsification can be used when the desired nucleophile for an anodic methoxylation reaction which is insoluble in the electrolyte [45,46]. Figure 4 depicts the experimental set-up where the nucleophile is insoluble in an electrolytic medium and is dispersed as sub-micrometre sized droplets by the application of power ultrasound; such an approach results in a high interfacial liquid–liquid area of the sono-emulsion and trapping of the product.

Power ultrasound (20 kHz) induced a "temporarily soluble" droplet of the nucleophile that can then intercept the *N*-acyliminium ion. Electrosynthesis have been adapted to use solid-supported bases [47-51], performing the electrosynthesis on compounds directly attached to a catch and release solid-support [52], or having the nucleophile solid-supported [53]. The use of ionic liquids as a green electrolyte/solvent [54] and using solar power to provide the electrical current [55] are some

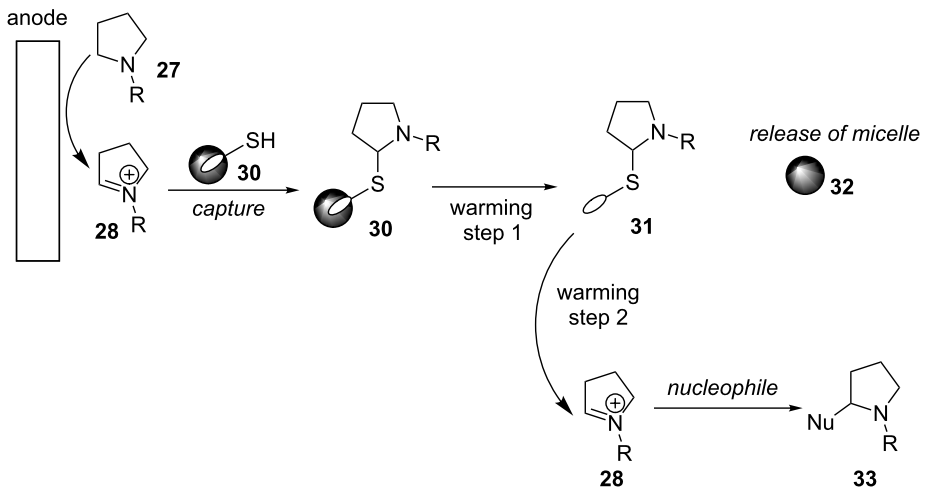

Figure 3: A catch and release cation pool method [42].

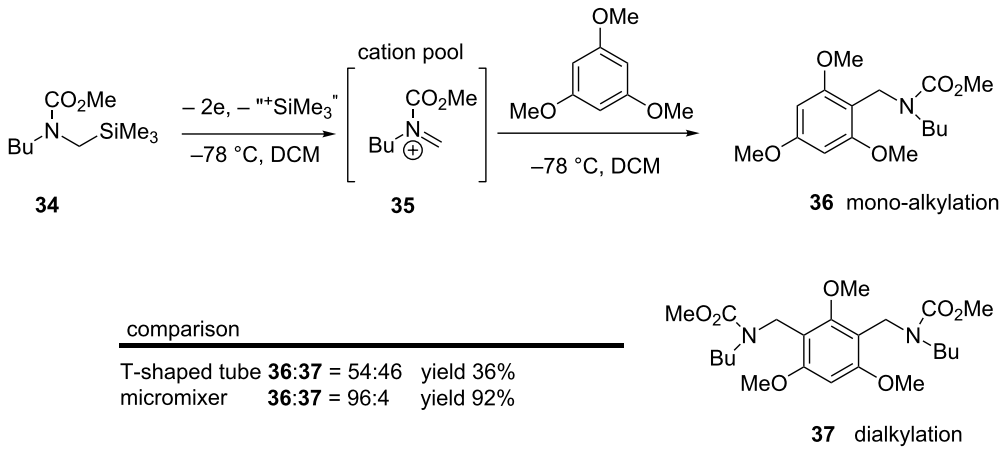

Scheme 8: Micromixing effects on yield 92% vs 36% and ratio of alkylation products [43].

of the recent additions to make electrosynthesis even more environmentally friendly. Further advances have been made using spatially addressable electrolysis platform's (SAEP) [56]. This technique has been used to prepare both parallel and combinatorial libraries using Shono-type oxidation on a microarray. Some technical aspects of anodic alkoxylation have been patented [57].

The use of the Shono-type electrooxidation in multiple branches of synthetic organic chemistry

The enantioselective electrooxidation of *sec*-alcohols mediated by azabicyclo-*N*-oxyls has been reported by Onomura and colleagues [58,59]. The azabicyclo-*N*-oxyl oxidation mediators were themselves prepared by anodic methoxylation. A chiral example of the azabicylco-*N*-oxyl was employed to kinetically resolve racemic *sec*-alcohols (Scheme 9).

The preparation of 1-(*N*-acylamino)alkyl sulfones from the anodic electrooxidation of non-Kolbe or Shono-type precursors affords the expected α-methoxyl products. Treatment with triphenylphosphonium salts and sodium aryl sulfinates afforded stable crystalline precursors of *N*-acyliminium ions that are activated by base [60]. The anodic methoxylation products of unfunctionalised amides can be converted to carbonyl compounds (aldehydes or esters) by treatment with cobaltacene [61] or be used as starting materials for the Morita–Baylis–Hillman-type reaction [62]. Anodic methoxylation can be combined with biocatalytic approaches to prepare stereodivergent 4-hydroxypiperidines [63]. 3-Hydroxy-6-substituted piperidines inacces-

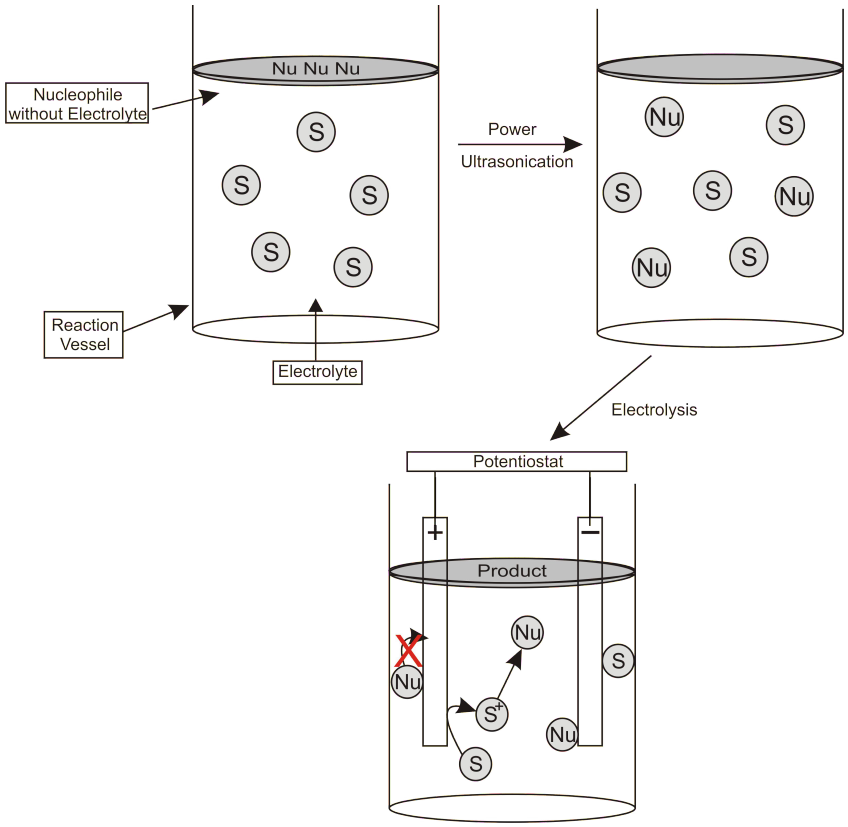

Figure 4: Schematic illustration of the anodic substitution reaction system using acoustic emulsification. Figure redrawn from reference [45].

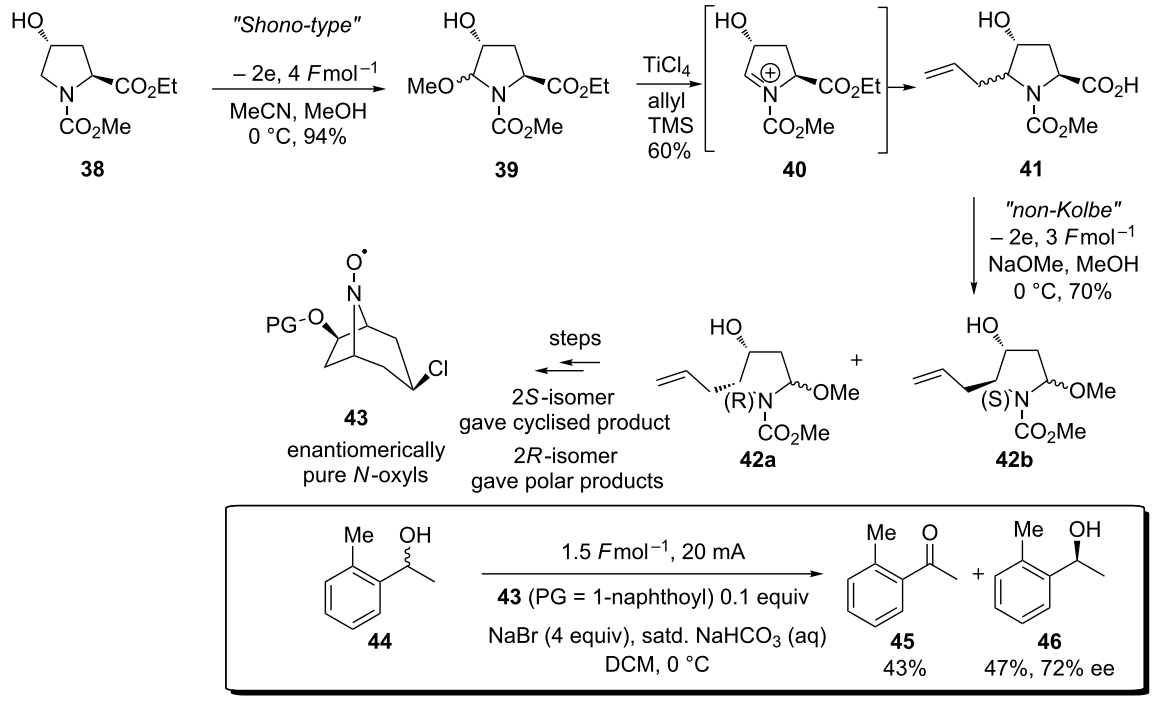

Scheme 9: Electrooxidation to prepare a chiral oxidation mediator and application to the kinetic resolution of *sec*-alcohols [58].

sible by conventional synthesis approaches can also be effectively synthesised by anodic methoxylation [64].

The scope of the anodic methoxylation has so far been limited to either acyclic or 4–6-membered ring sizes, the use of electrosynthetic approaches can also be applied to larger 7-membered ring systems, albeit less frequently [65,66]. β-Lactams (4-membered rings) undergo anodic oxidation of the carbon–silicon bond (when an electroauxiliary is present) or direct carbon–hydrogen bond fission to afford the α-methoxylated product (Scheme 10) [67,68].

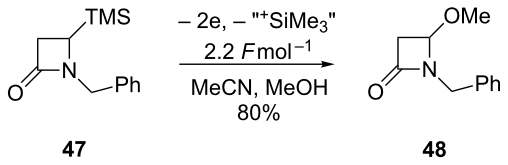

Scheme 10: Electrooxidation reactions on 4-membered ring systems [68].

The direct anodic oxidation reaction to afford the *N*-acyliminium ion can be intercepted with a carbon nucleophile enantioselectively when a chiral auxiliary is attached either to the carbamate or amide (Figure 5) [69-71] (using a platinum anode and tungsten cathode electrochemical set-up) [69] or the use of Cu-PyBox chiral ligand systems [72].

The cation pool method can be adapted to a multicomponent reaction (MCR) when an *N*-acyliminium ion is intercepted by an enamine [22]. Although the electrochemically generated *N*-acyliminium ion has reacted, the enamine generated a second

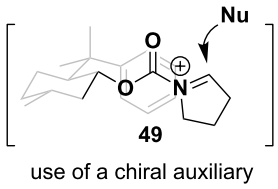

Figure 5: Example of a chiral auxiliary Shono-oxidation intermediate [69].

N-acyliminium which in turn can be intercepted by another carbon nucleophile (Scheme 11). It was postulated that intermediate **52a** could cyclise to the bicyclic system **52b**. It proved difficult to determine the *cis/trans* relationship in many examples due to the presence of rotameric forms, however the products of phenyl magnesiumbromide were identified to be *trans* presumably due to opposite face attack of intermediate **52b**.

Bicyclic lactams [73] and tricyclic systems [74] have also been prepared using the anodic oxidation route. Possibly, one of the most important uses of the Shono oxidation has been in the development of the [4 + 2] cycloaddition, more commonly known as the Diels–Alder reaction for the controlled preparation of *N*-acyliminium ions to react with dienophiles (Scheme 12) [21,23]. Another facet of this reaction was the controlled application of micro-mixing resulted in a significant improvement in isolated yield of the desired cycloadduct compared to batch synthesis (79% vs 20–57%).

The electrochemical version of the Diels–Alder reaction is gaining in popularity with an elegant synthesis of the natural product, kingianin A, recently published by the Moses group, albeit not through a Shono or non-Kolbe mechanism [75].

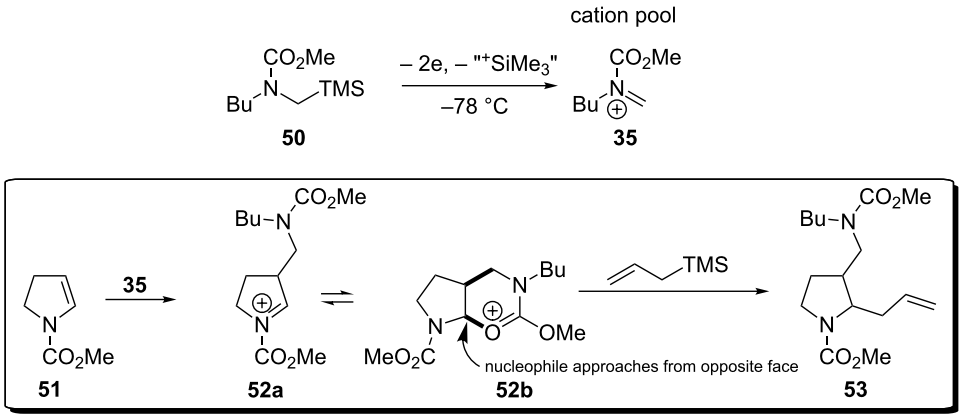

Scheme 11: An electrochemical multicomponent reaction where a carbon felt anode and platinum cathode were utilised and carried out at −78 °C [22].

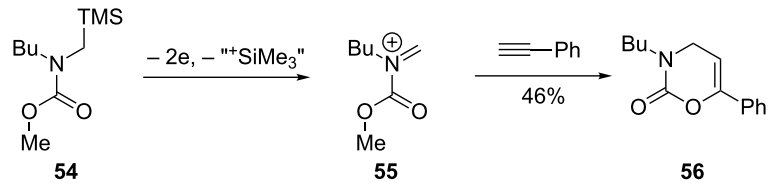

Scheme 12: Preparation of dienes using the Shono oxidation [23].

The Shono-type electrooxidation has been used to prepare spirocyclic compounds using a double silyl electroauxiliary approach (Scheme 13) [76,77]. The ability to introduce two carbon–carbon bonds on to the same α-carbon to prepare spirocyclic systems is a challenge, yet the application of electrochemistry in tandem with ring closing metathesis (RCM) readily achieved this feat.

The use of the Shono-type electrooxidation in natural product synthesis

The synthesis of natural products is considered a good test of the synthetic potential of a new reaction. The Shono-type oxidation has proved itself in the following syntheses. Hurvois and colleagues have reported an electrochemical asymmetric synthesis of (+)-myrtine (**66**) as shown in Scheme 14 [78]. (+)-

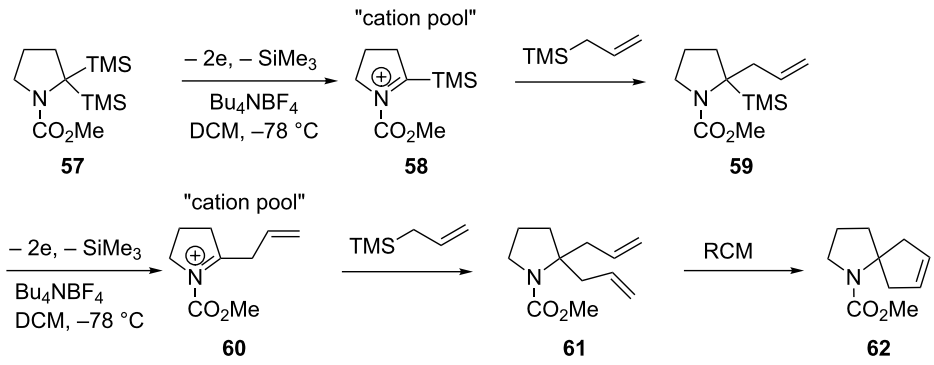

Scheme 13: Combination of an electroauxiliary mediated anodic oxidation and RCM to afford *spiro*cyclic compounds [76].

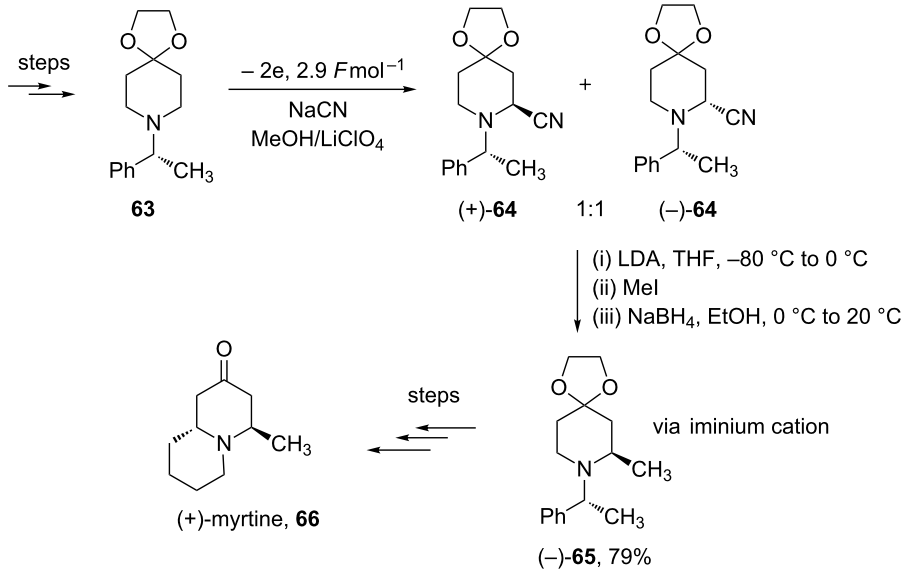

Scheme 14: Total synthesis of (+)-myrtine (**66**) using an electrochemical approach [78].

Myrtine (**66**) is a member of the *trans*-4,9a-quinolizidin-2-one family, originally isolated from *Vaccinium myrtillis* (Ericaceae). The synthesis relied on the introduction of a cyano group followed by α-deprotonation by LDA and installation of a methyl group. Reductive decyanation of the α-amino nitrile, reinstalled the *N*-acyliminium ion. Reduction of the *N*-acyliminium afforded the major diastereoisomer as shown in Scheme 14 in 79% after column chromatography. Further synthetic modification of this key intermediate afforded the total synthesis of (+)-myrtine (**66**) in a further 5 steps in an overall yield of 30%.

The Moeller research group has used an anodic amide oxidation for the total synthesis of the angiotensin-converting enzyme inhibitors, (−)-A58365A (**70**) and (±)-A58365B (**71**) (Scheme 15) [79]. This synthesis highlighted the power of the anodic amide oxidation-*N*-acyliminium ion cyclisation strategy in the presence of a disubstituted acetylene nucleophile. Anodic oxidation proceeded in high yield and a smooth cyclisation of the pendant acetylene nucleophile was triggered by treatment with titanium tetrachloride. Ozonolysis of the chloromethyl alkene intermediate afforded the carbonyl compound and the 5,6 and 6,6-ring systems of the target compounds.

Toyooka and co-workers have designed a route to both enantiomers of the quinolizidine poison frog alkaloid 195C. Key to the success of their synthetic endeavour was the preparation via direct anodic oxidation of intermediate **73** (Scheme 16) [80]. 195C had never before been prepared enantioselectively and the first total synthesis of 195C utilised a key asymmetric Shono oxidation step.

Electrosynthesis using anodic oxidation has also been applied to the α-methylene of an amide for the preparation of iminosugars [81,82]. Iminosugars have shown a variety of biological effects

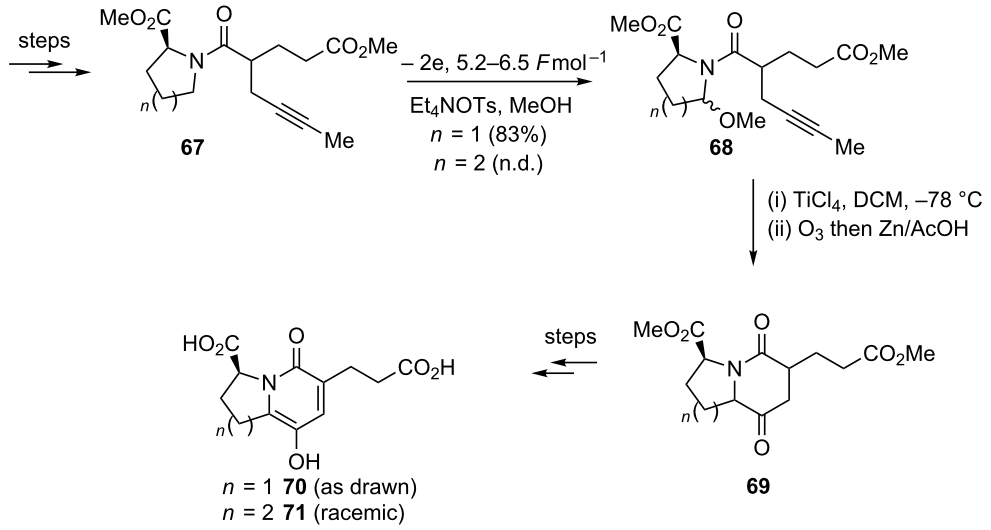

Scheme 15: Total synthesis of (−)-A58365A (**70**) and (±)-A58365B (**71**) [79].

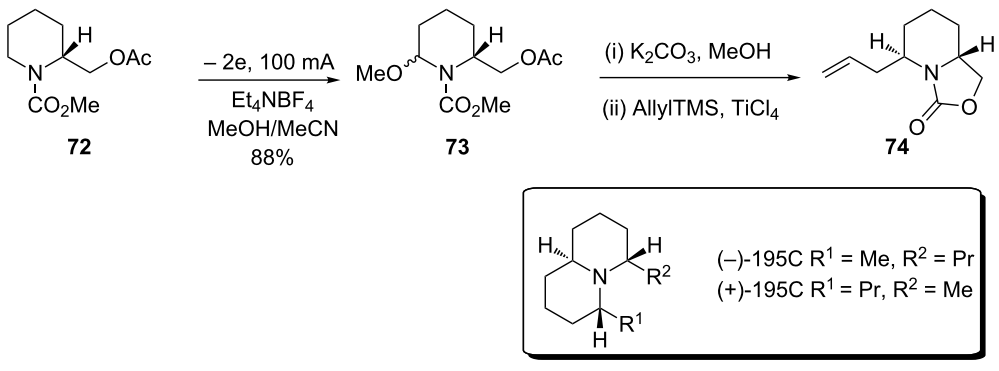

Scheme 16: Anodic oxidation used in the preparation of the poison frog alkaloid 195C [80].

including inhibiting glycosidases and glycoprotein-processing enzymes. Onomura and Matsumura and colleagues have used the anodic methoxylation and mild acid treatment strategy to prepare the initial starting materials in the synthetic campaign (Scheme 17).

The Shono-type oxidation of unfunctionalised amides has been applied to the synthesis of inhibitors of a variety of biological targets [83], in particular α-L-fucosidase [84,85]. Toyooka and co-workers also applied anodic methoxylation to prepare iminosugars as potent inhibitors of α-L-fucosidase, an important target in the inflammation response (Scheme 18). The α-methoxy group introduced could then be intercepted via an *N*-acyliminium ion intermediate with a variety of C–C bond forming reagents. The compounds prepared were interrogated for bioactivity against α-L-fucosidase and related targets and IC_{50}'s of as low as 1 nM were reported for α-L-fucosidase with limited off-target activity.

The total synthesis of the anaesthetic ropivacaine (**85**) was accomplished enantioselectively using as its key step a direct anodic oxidation to prepare at low temperatures a cation pool of *N*-acyliminium ions that were intercepted with cyanide [71]. The enantioselectivity induced in this step was as a result of using a chiral auxiliary, 8-phenylmenthyl attached to the carbamate (Scheme 19).

Other natural product syntheses have used the anodic oxidation approach, often as the first step in a synthesis campaign to functionalise a pyrrolidine or piperidine carbamate [86,87].

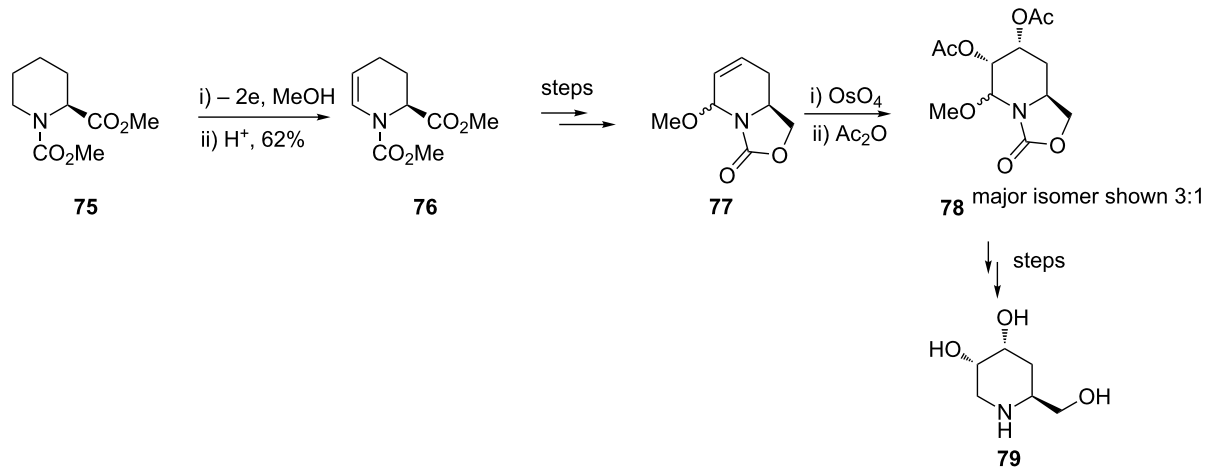

Scheme 17: Preparation of iminosugars using an electrochemical approach [81].

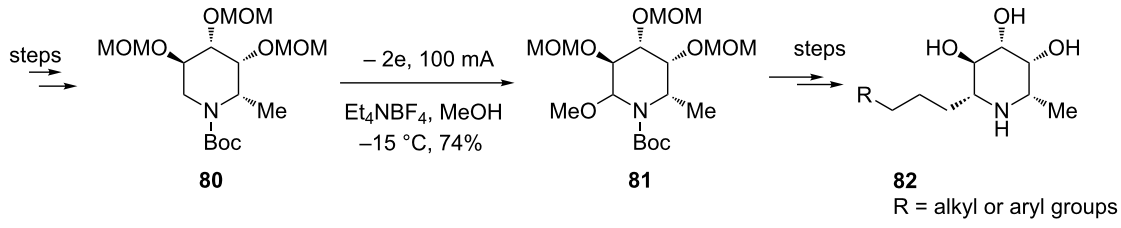

Scheme 18: The electrosynthetic preparation of α-L-fucosidase inhibitors [84,85].

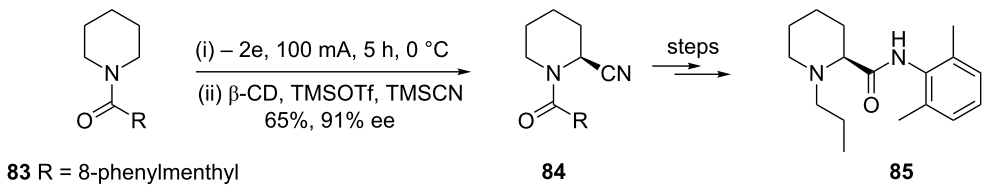

Scheme 19: Enantioselective synthesis of the anaesthetic ropivacaine **85** [71].

A lithium perchlorate–nitromethane system was used to prepare electrochemically azanucleoside derivatives [88]. Unactivated prolinol derivatives underwent anodic oxidation to generate *N*-acyliminium ions that were intercepted by nucleophilic bases such as the nucleobases: protected cytosine, guanine **87**, adenine, and thymine to afford azanucleoside products such as **88** (Scheme 20).

The use of the Shono-type electrooxidation in peptide and peptidomimetic chemistry

The preparation of a bridged tricyclic analogue to induce an α-helix conformation in a linear peptide sequence was accomplished using an anodic oxidation step (Scheme 21). The stabilisation of linear peptides via inducing a stabilised secondary structure is of importance in mimicking protein–protein interactions (PPI) for diseases such as cancer and HIV [89,90]. The methoxylated intermediate **90** was treated with a Lewis acid and vinylmagnesium bromide to afford the *trans*-diastereomer after column chromatography. Coupling of **91** and **92** (prepared using conventional chemistry) resulted in the peptide-turn inducing compound **93**.

The Moeller research group has carried out extensive research into the synthesis of functionalised peptides and peptidomimetics using the anode oxidation strategy [91-95]. The anodic oxidation of pyrrolidine derivatives and silylated peptides afforded a variety of bicyclic lactam peptidomimetics and functionalised peptides (Scheme 22) [91,92,94]. Constrained amino acid mimics such as **95** are important molecules as they display their functional group in a highly ordered way and can be used to mimic, for example, a proline residue of a natural peptide.

The Moeller research group has also employed an electrosynthetic approach to the synthesis of a peptidomimetic of substance P [93]. Substance P is an 11 amino acid peptide that contains a phenylalanine^7–phenylalanine^8 linkage (Phe^7–Phe^8) and a member of the mammalian tachykinin family of peptides implicated in diseases such as arthritis, asthma, inflammatory bowel disease and depression. Electrosynthesis of 3-phenylproline, mono- or bicyclic piperazinone derived cores (conformationally constrained mimics of the Phe^7–Phe^8 linkage) afforded the non-natural peptides. These compounds displayed their amino acid residues in similar conformations to the receptor bound conformation of substance P. The three analogues prepared (Scheme 23; **98**–**100**) showed competitive binding of the native ligand with IC_{50}'s = 32, 80, 5 μM using a radioiodinated peptide binding to the NK1 receptor in Chinese Hamster Ovary (CHO) cells (native ligand IC_{50} = 0.3 nM).

The preparation of arginine mimetics is an ongoing challenge for chemical biology and epigenetics. Dhimane and co-workers

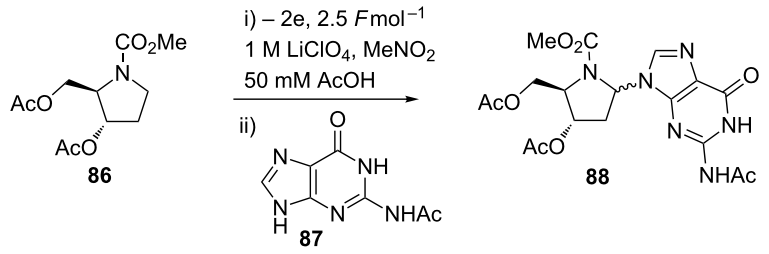

Scheme 20: The preparation of synthetically challenging aza-nucleosides employing an electrochemical step [88].

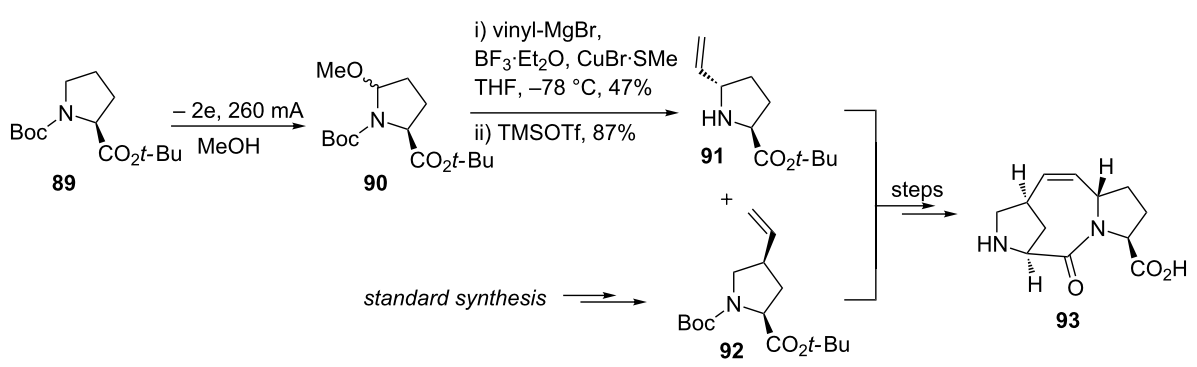

Scheme 21: Synthesis of a bridged tricyclic diproline analogue **93** that induces α-helix conformation into linear peptides [90].

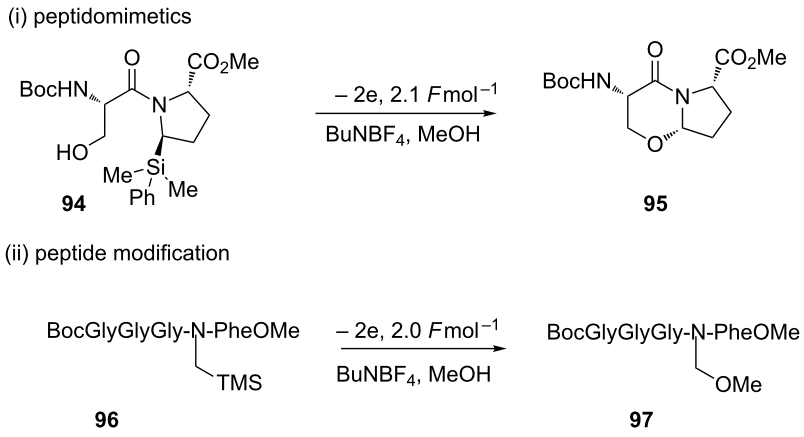

Scheme 22: Synthesis of (i) a peptidomimetic and (ii) a functionalised peptide from silyl electroauxiliary precursors [91].

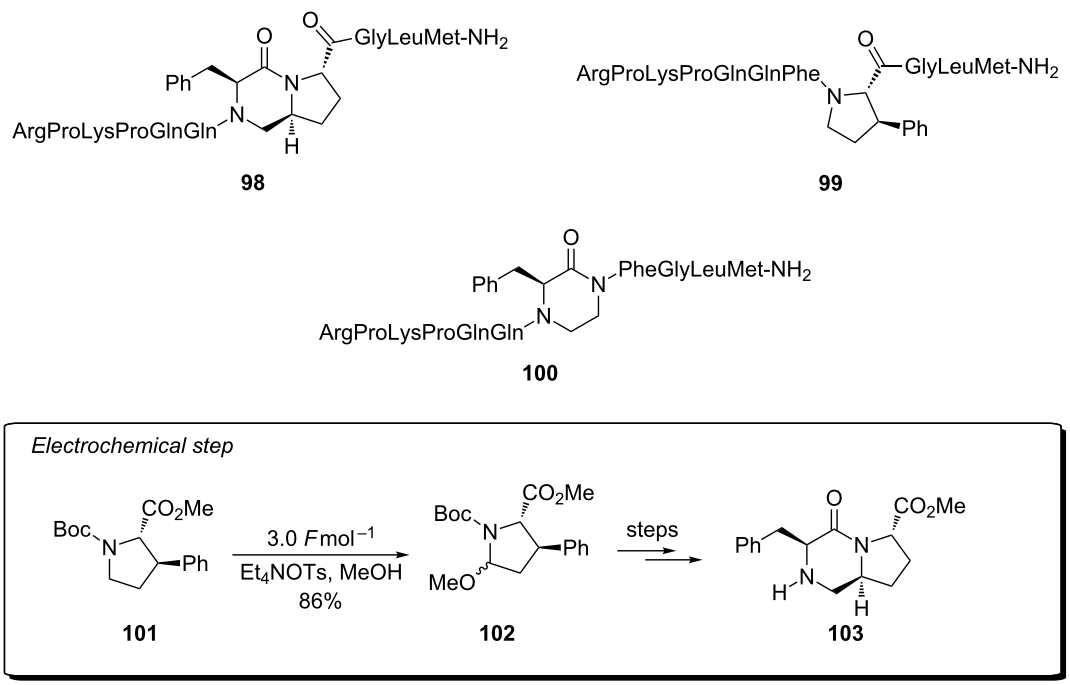

Scheme 23: Examples of Phe[7]–Phe[8] mimics prepared using an electrochemical approach [93].

utilised a strategy of anodic methoxylation to complete the first step in the synthesis of **106** (Scheme 24) [96,97].

The preparation of chiral (up to 99% ee) cyclic amino acids was achieved by Onomura and colleagues (Scheme 25) [20]. In their paper, the authors justify the choice of the anode and cathode material, something not always considered by others working in the field of electrosynthesis, where it was shown that through different combinations of cathode and anodes the product yield was affected and also different amounts of electricity (Fmol^{-1}) was required [20]. The authors also detail a deallylation and a debenzylation deprotection method to **108**. An alternative strategy to chiral amino acids was demonstrated by Kuźnik and colleagues [98] through the electrochemical preparation of 3-triphenylphosphine-2,5-piperazinediones as chiral glycine cation equivalents. Steckhan and co-workers have previously demonstrated the power of electrosynthetic chiral glycine equivalents [99,100].

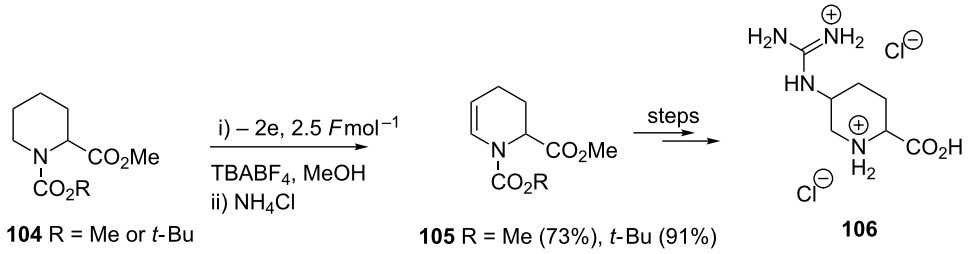

Scheme 24: Preparation of arginine mimics employing an electrooxidation step [96].

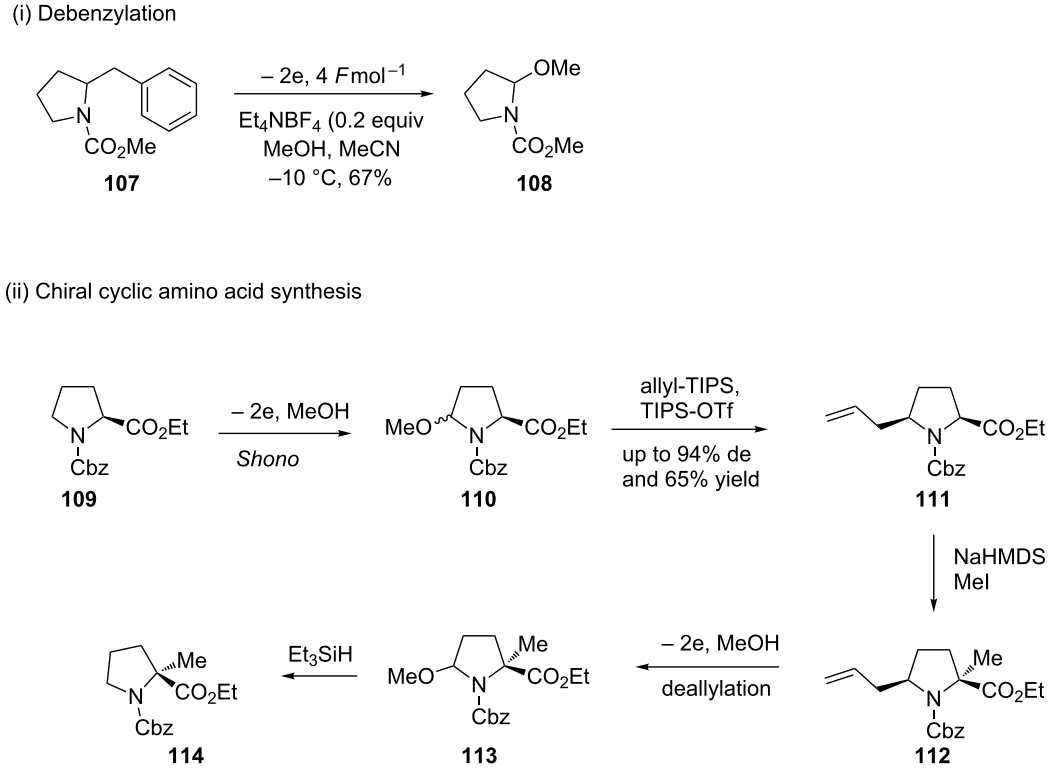

Scheme 25: Preparation of chiral cyclic amino acids [20].

Combination of technology and natural product analogue synthesis

Lastly, Ley and co-workers have recently reported the expedient synthesis of indole alkaloid nazlinine **117** (Scheme 26) using a commercial electrochemical flow cell which allowed the electrolyte loading to be reduced yet still obtained high conversion and product purity [101]. Interestingly, the use of steel or platinum electrode resulted in no conversion to the product and

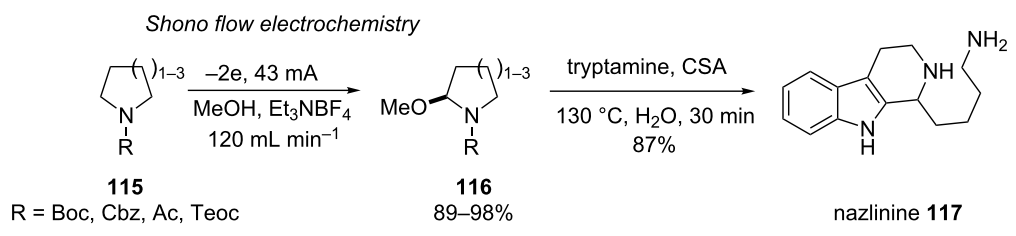

Scheme 26: Two-step preparation of Nazlinine **117** using Shono flow electrochemistry [101].

was only possible using a carbon anode. The reason for this was not eluded to and voltammetry was not performed.

The judicial employment of a Shono electrooxidation coupled to a flow cell led to the preparation of a range of α-methoxy cyclic amines in excellent yield. The Ley group then tested this enabling route to the total synthesis of the natural product, nazlinine **117**. Nazlinine was isolated in 1991 from the plant, *Nitraria schoberi*, and exhibits serotonergic bioactivity. There had been only two previous syntheses of nazlinine and neither was sufficiently modular to prepare not only nazlinine but structurally similar analogues. The α-methoxy cyclic amines were treated with tryptamine (or analogues) and a camphorsulfonic acid (CSA)-mediated Pictet–Spengler reaction afforded the desired Nazlinine and structural variants in one pot.

Conclusion

In this review article we have highlighted the scope of the Shono-type electrooxidation from simple intermediate synthesis to natural product total syntheses and looked at the possibilities of molecularly engineering reaction set-ups to drive the formation of a desired compound electrochemically. We note from the above exciting work that electrochemical parameters and experimental set-ups are in some cases arbitrary with no real consideration or foresight and there remains a great deal further to explore. To quote the namesake of this paper Prof. Tatsuya Shono in his 1984 review "*Since electroorganic chemistry seems rather unfamiliar to those investigating organic synthesis, the purpose of this review is to show that electroorganic chemistry is one of the promising tools for organic synthesis*" [10]. Some excellent progress has been made in the intervening years and still further progress is needed; namely, employing a collaborative approach between synthetic chemists and electrochemists to significantly progress this exciting and burgeoning field.

Acknowledgements

The authors thank Manchester Metropolitan University for seed funding (Research Accelerator Grant D-80005.5.B) and the Dalton Research Institute.

References

1. Mayr, H.; Ofial, A. R.; Würthwein, E.-U.; Aust, N. C. *J. Am. Chem. Soc.* **1997,** *119,* 12727–12733. doi:10.1021/ja972860u
2. Yamamoto, Y.; Nakada, T.; Nemoto, H. *J. Am. Chem. Soc.* **1992,** *114,* 121–125. doi:10.1021/ja00027a017
3. Speckamp, W. N.; Hiemstra, H. *Tetrahedron* **1985,** *41,* 4367–4416. doi:10.1016/S0040-4020(01)82334-6
4. Royer, J.; Bonin, M.; Micouin, L. *Chem. Rev.* **2004,** *104,* 2311–2352. doi:10.1021/cr020083x
5. Yoshida, J.-i.; Kataoaka, K.; Horcajada, R.; Nagaki, A. *Chem. Rev.* **2008,** *108,* 2265–2299. doi:10.1021/cr0680843
6. Sperry, J. B.; Wright, D. L. *Chem. Soc. Rev.* **2006,** *35,* 605–621. doi:10.1039/b512308a
7. Francke, R.; Little, R. D. *Chem. Soc. Rev.* **2014,** *43,* 2492–2521. doi:10.1039/c3cs60464k
8. Utley, J. *Chem. Soc. Rev.* **1997,** *26,* 157–167. doi:10.1039/CS9972600157
9. Frontana-Uribe, B. A.; Little, R. D.; Ibanez, J. G.; Palma, A.; Vaquez-Medrano, R. *Green Chem.* **2010,** *12,* 2099–2119. doi:10.1039/c0gc00382d
10. Shono, T. *Tetrahedron* **1984,** *40,* 811–850. doi:10.1016/S0040-4020(01)91472-3
11. Shono, T.; Matsumura, Y.; Tsubata, K. *J. Am. Chem. Soc.* **1981,** *103,* 1172–1176. doi:10.1021/ja00395a029
12. Ross, S. D.; Finkelstein, M.; Peterson, R. C. *J. Am. Chem. Soc.* **1966,** *88,* 4657–4660. doi:10.1021/ja00972a024
13. Shono, T.; Hamaguchi, H.; Matsumura, Y. *J. Am. Chem. Soc.* **1975,** *97,* 4264–4268. doi:10.1021/ja00848a020
14. Shono, T.; Matsumura, Y.; Tsubata, K. *Org. Synth.* **1985,** *63,* 206. doi:10.15227/orgsyn.063.0206
15. Nyberg, K.; Servin, R. *Acta Chem. Scand., Ser. B* **1976,** *30,* 640–642. doi:10.3891/acta.chem.scand.30b-0640
16. Libendi, S. S.; Demizu, Y.; Matsumura, Y.; Onomura, O. *Tetrahedron* **2008,** *64,* 3935–3942. doi:10.1016/j.tet.2008.02.060
17. Suga, S.; Okajima, M.; Yoshida, J.-i. *Tetrahedron Lett.* **2001,** *42,* 2173–2176. doi:10.1016/S0040-4039(01)00128-9
18. Suga, S.; Kageyama, Y.; Babu, G.; Itami, K.; Yoshida, J.-i. *Org. Lett.* **2004,** *6,* 2709–2711. doi:10.1021/ol049049q
19. Maruyama, T.; Suga, S.; Yoshida, J.-i. *Tetrahedron* **2006,** *62,* 6519–6525. doi:10.1016/j.tet.2006.03.114
20. Kirira, P. G.; Kuriyama, M.; Onomura, O. *Chem. – Eur. J.* **2010,** *16,* 3970–3982. doi:10.1002/chem.200903512
21. Suga, S.; Tsutsui, Y.; Nagaki, A.; Yoshida, J.-i. *Bull. Chem. Soc. Jpn.* **2005,** *78,* 1206–1217. doi:10.1246/bcsj.78.1206
22. Suga, S.; Nishida, T.; Yamada, D.; Nagaki, A.; Yoshida, J.-i. *J. Am. Chem. Soc.* **2004,** *126,* 14338–14339. doi:10.1021/ja0455704
23. Suga, S.; Nagaki, A.; Tsutsui, Y.; Yoshida, J.-i. *Org. Lett.* **2003,** *5,* 945–947. doi:10.1021/ol0341243
24. Suga, S.; Suzuki, S.; Maruyama, T.; Yoshida, J.-i. *Bull. Chem. Soc. Jpn.* **2004,** *77,* 1545–1554. doi:10.1246/bcsj.77.1545
25. Suga, S.; Suzuki, S.; Yoshida, J.-i. *J. Am. Chem. Soc.* **2002,** *124,* 30–31. doi:10.1021/ja0171759
26. Suga, S.; Okajima, M.; Fujiwara, K.; Yoshida, J.-i. *J. Am. Chem. Soc.* **2001,** *123,* 7941–7942. doi:10.1021/ja015823i
27. Maruyama, T.; Mizuno, Y.; Shimizu, I.; Suga, S.; Yoshida, J.-i. *J. Am. Chem. Soc.* **2007,** *129,* 1902–1903. doi:10.1021/ja068589a
28. Maruyama, T.; Suga, S.; Yoshida, J.-i. *J. Am. Chem. Soc.* **2005,** *127,* 7324–7325. doi:10.1021/ja0511218
29. Nagaki, A.; Kawamura, K.; Suga, S.; Ando, T.; Sawamoto, M.; Yoshida, J.-i. *J. Am. Chem. Soc.* **2004,** *126,* 14702–14703. doi:10.1021/ja044879k
30. Suga, S.; Okajima, M.; Fujiwara, K.; Yoshida, J.-i. *QSAR Comb. Sci.* **2005,** *24,* 728–741. doi:10.1002/qsar.200440003
31. Yoshida, J.-i.; Suga, S.; Suzuki, S.; Kinomura, N.; Yamamoto, A.; Fujiwara, K. *J. Am. Chem. Soc.* **1999,** *121,* 9546–9549. doi:10.1021/ja9920112
32. Sugawara, M.; Mori, K.; Yoshida, J.-i. *Electrochim. Acta* **1997,** *42,* 1995–2003. doi:10.1016/S0013-4686(97)85473-4
33. Kim, S.; Hayashi, K.; Kitano, Y.; Tada, M.; Chiba, K. *Org. Lett.* **2002,** *4,* 3735–3737. doi:10.1021/ol026713z

34. Yoshida, J.-i.; Isoe, S. *Tetrahedron Lett.* **1987,** *28,* 6621–6624. doi:10.1016/S0040-4039(00)96929-6
35. Le Gall, E.; Hurvois, J.-P.; Sinbandhit, S. *Eur. J. Org. Chem.* **1999,** 2645–2653. doi:10.1002/(SICI)1099-0690(199910)1999:10<2645::AID-EJOC2645>3.0.CO;2-4
36. Fuchigami, T.; Tetsu, M.; Tajima, T.; Ishii, H. *Synlett* **2001,** 1269–1271. doi:10.1055/s-2001-16063
37. Cao, Y.; Suzuki, K.; Tajima, T.; Fuchigami, T. *Tetrahedron* **2005,** *61,* 6854–6859. doi:10.1016/j.tet.2005.04.057
38. Horii, D.; Fuchigami, T.; Atobe, M. *J. Am. Chem. Soc.* **2007,** *129,* 11692–11693. doi:10.1021/ja075180s
39. Horii, D.; Amemiya, F.; Fuchigami, T.; Atobe, M. *Chem. – Eur. J.* **2008,** *14,* 10382–10387. doi:10.1002/chem.200801511
40. Kuleshova, J.; Hill-Cousins, J. T.; Birkin, P. R.; Brown, R. C. D.; Pletcher, D.; Underwood, T. J. *Electrochim. Acta* **2012,** *69,* 197–202. doi:10.1016/j.electacta.2012.02.093
41. Horcajada, R.; Okajima, M.; Suga, S.; Yoshida, J.-i. *Chem. Commun.* **2005,** 1303–1305. doi:10.1039/b417388k
42. Hayashi, K.; Kim, S.; Chiba, K. *Electrochemistry* **2006,** *74,* 621–624. doi:10.5796/electrochemistry.74.621
43. Suga, S.; Nagaki, A.; Yoshida, J.-i. *Chem. Commun.* **2003,** 354–355. doi:10.1039/b211433j
44. Nagaki, A.; Togai, M.; Suga, S.; Aoki, N.; Mae, K.; Yoshida, J.-i. *J. Am. Chem. Soc.* **2005,** *127,* 11666–11675. doi:10.1021/ja0527424
45. Asami, R.; Fuchigami, T.; Atobe, M. *Chem. Commun.* **2008,** 244–246. doi:10.1039/b713859h
46. Asami, R.; Fuchigami, T.; Atobe, M. *Org. Biomol. Chem.* **2008,** *6,* 1938–1943. doi:10.1039/b802961j
47. Tajima, T.; Fuchigami, T. *Chem. – Eur. J.* **2005,** *11,* 6192–6196. doi:10.1002/chem.200500340
48. Tajima, T.; Fuchigami, T. *J. Am. Chem. Soc.* **2005,** *127,* 2848–2849. doi:10.1021/ja0423062
49. Tajima, T.; Kurihara, H.; Fuchigami, T. *J. Am. Chem. Soc.* **2007,** *129,* 6680–6681. doi:10.1021/ja070283w
50. Tajima, T.; Fuchigami, T. *Angew. Chem., Int. Ed.* **2005,** *44,* 4760–4763. doi:10.1002/anie.200500977
51. Tajima, T.; Nakajima, A. *Chem. Lett.* **2009,** *38,* 160–161. doi:10.1246/cl.2009.160
52. Nad, S.; Breinbauer, R. *Angew. Chem., Int. Ed.* **2004,** *43,* 2297–2299. doi:10.1002/anie.200352674
53. Tajima, T.; Nakajima, A. *J. Am. Chem. Soc.* **2008,** *130,* 10496–10497. doi:10.1021/ja804048a
54. Bornemann, S.; Handy, S. T. *Molecules* **2011,** *16,* 5963–5974. doi:10.3390/molecules16075963
55. Nguyen, B. H.; Redden, A.; Moeller, K. D. *Green Chem.* **2014,** *16,* 69–72. doi:10.1039/c3gc41650j
56. Siu, T.; Li, W.; Yudin, A. K. *J. Comb. Chem.* **2000,** *2,* 545–549. doi:10.1021/cc000035v
57. Reufer, C.; Lehmann, T.; Sanzenbacher, R.; Weckbecker, C. Verfahren zur anodischen alkoxylierung von organischen substraten. WO Pat. Appl. WO2004/085710 A2, Oct 7, 2004.
58. Shiigi, H.; Mori, H.; Tanaka, T.; Demizu, Y.; Onomura, O. *Tetrahedron Lett.* **2008,** *49,* 5247–5251. doi:10.1016/j.tetlet.2008.06.112
59. Demizu, Y.; Shiigi, H.; Oda, T.; Matsumura, Y.; Onomura, O. *Tetrahedron Lett.* **2008,** *49,* 48–52. doi:10.1016/j.tetlet.2007.11.016
60. Adamek, J.; Mazurkiewicz, R.; Październiok-Holewa, A.; Grymel, M.; Kuźnik, A.; Zielińska, K. *J. Org. Chem.* **2014,** *79,* 2765–2770. doi:10.1021/jo500174a
61. Izawa, K.; Nishi, S.; Asada, S. *J. Mol. Catal.* **1987,** *41,* 135–146. doi:10.1016/0304-5102(87)80024-X
62. Myers, E. L.; de Vries, J. G.; Aggarawal, V. K. *Angew. Chem., Int. Ed.* **2007,** *46,* 1893–1896. doi:10.1002/anie.200604715
63. Vink, M. K. S.; Schortinghuis, C. A.; Luten, J.; van Maarseveen, J. H.; Schoemaker, H. E.; Hiemstra, H.; Rutjes, F. P. J. T. *J. Org. Chem.* **2002,** *67,* 7869–7871. doi:10.1021/jo025943o
64. Bartels, M.; Zapico, J.; Gallagher, T. *Synlett* **2004,** 2636–2638. doi:10.1055/s-2004-832846
65. David, M.; Dhimane, H. *Synlett* **2004,** 1029–1033. doi:10.1055/s-2004-820048
66. Golub, T.; Becker, J. Y. *J. Electrochem. Soc.* **2013,** *160,* G3123–G3127. doi:10.1149/2.017307jes
67. Suda, K.; Hotoda, K.; Iemuro, F.; Takanami, T. *J. Chem. Soc., Perkin Trans. 1* **1993,** 1553–1555. doi:10.1039/p19930001553
68. Suda, K.; Hotoda, K.; Watanabe, J.-i.; Shiozawa, K.; Takanami, T. *J. Chem. Soc., Perkin Trans. 1* **1992,** 1283–1284. doi:10.1039/p19920001283
69. D'Oca, M. G. M.; Pilli, R. A.; Pardini, V. L.; Curi, D.; Comninos, F. C. M. *J. Braz. Chem. Soc.* **2001,** *12,* 507–513. doi:10.1590/S0103-50532001000400011
70. Turcaud, S.; Martens, T.; Sierecki, E.; Pérard-Viret, J.; Royer, J. *Tetrahedron Lett.* **2005,** *46,* 5131–5134. doi:10.1016/j.tetlet.2005.05.123
71. Shankaraiah, N.; Pilli, R. A.; Santos, L. S. *Tetrahedron Lett.* **2008,** *49,* 5098–5100. doi:10.1016/j.tetlet.2008.06.028
72. Kanda, Y.; Onomura, O.; Maki, T.; Matsumura, Y. *Chirality* **2003,** *15,* 89–94. doi:10.1002/chir.10151
73. Lennartz, M.; Steckhan, E. *Synlett* **2000,** 319–322. doi:10.1055/s-2000-6527
74. Lee, D.-S. *Tetrahedron: Asymmetry* **2009,** *20,* 2014–2020. doi:10.1016/j.tetasy.2009.08.017
75. Moore, J. C.; Davies, E. S.; Walsh, D. A.; Sharma, P.; Moses, J. E. *Chem. Commun.* **2014,** *50,* 12523–12525. doi:10.1039/C4CC05906A
76. Suga, S.; Watanabe, M.; Yoshida, J.-i. *J. Am. Chem. Soc.* **2002,** *124,* 14824–14825. doi:10.1021/ja028663z
77. Suga, S.; Watanabe, M.; Song, C.-H.; Yoshida, J.-i. *Electrochemistry* **2006,** *74,* 672–679. doi:10.5796/electrochemistry.74.672
78. Vu, V. H.; Louafi, F.; Girard, N.; Marion, R.; Roisnel, T.; Dorcet, V.; Hurvois, J.-P. *J. Org. Chem.* **2014,** *79,* 3358–3373. doi:10.1021/jo500104c
79. Wong, P. L.; Moeller, K. D. *J. Am. Chem. Soc.* **1993,** *115,* 11434–11445. doi:10.1021/ja00077a048
80. Wang, X.; Li, J.; Saporito, R. A.; Toyooka, N. *Tetrahedron* **2013,** *69,* 10311–10315. doi:10.1016/j.tet.2013.10.009
81. Moriyama, N.; Matsumura, Y.; Kuriyama, M.; Onomura, O. *Tetrahedron: Asymmetry* **2009,** *20,* 2677–2687. doi:10.1016/j.tetasy.2009.11.028
82. Furukubo, S.; Moriyama, N.; Onomura, O.; Matsumura, Y. *Tetrahedron Lett.* **2004,** *45,* 8177–8181. doi:10.1016/j.tetlet.2004.09.036
83. Faust, M. R.; Höfner, G.; Pabel, J.; Wanner, K. T. *Eur. J. Med. Chem.* **2010,** *45,* 2453–2466. doi:10.1016/j.ejmech.2010.02.029
84. Saka, T.; Okaki, T.; Ifuku, S.; Yamashita, Y.; Sato, K.; Miyawaki, S.; Kamori, A.; Kato, A.; Adachi, I.; Tezuka, Y.; Kiria, P. G.; Onomura, O.; Minato, D.; Sugimoto, K.; Matsuya, Y.; Toyooka, N. *Tetrahedron* **2013,** *69,* 10653–10661. doi:10.1016/j.tet.2013.10.006

85. Kato, A.; Okaki, T.; Ifuku, S.; Sato, K.; Hirokami, Y.; Iwaki, R.; Kamori, A.; Nakagawa, S.; Adachi, I.; Kiria, P. G.; Onomura, O.; Minato, D.; Sugimoto, K.; Matsuya, Y.; Toyooka, N. *Bioorg. Med. Chem.* **2013,** *21,* 6565–6573. doi:10.1016/j.bmc.2013.08.028
86. Dooms, C.; Laurent, P.; Daloze, D.; Pasteels, J.; Nedved, O.; Braekman, J.-C. *Eur. J. Org. Chem.* **2005,** 1378–1383. doi:10.1002/ejoc.200400804
87. Sunilkumar, G.; Nagamani, D.; Argade, N. P.; Ganesh, K. N. *Synthesis* **2003,** 2304–2306. doi:10.1055/s-2003-41075
88. Kim, S.; Shoji, T.; Kitano, Y.; Chiba, K. *Chem. Commun.* **2013,** *49,* 6525–6527. doi:10.1039/c3cc43273d
89. Hack, V.; Reuter, C.; Opitz, R.; Schmieder, P.; Beyermann, M.; Neudörfl, J.-M.; Kühne, R.; Schmalz, H.-G. *Angew. Chem., Int. Ed.* **2013,** *52,* 9539–9543. doi:10.1002/anie.201302014
90. Reuter, C.; Huy, P.; Neudörfl, J.-M.; Kühne, R.; Schmalz, H.-G. *Chem. – Eur. J.* **2011,** *17,* 12037–12044. doi:10.1002/chem.201101704
91. Sun, H.; Moeller, K. D. *Org. Lett.* **2002,** *4,* 1547–1550. doi:10.1021/ol025776e
92. Sun, H.; Martin, C.; Kesselring, D.; Keller, R.; Moeller, K. D. *J. Am. Chem. Soc.* **2006,** *128,* 13761–13771. doi:10.1021/ja064737l
93. Tong, Y.; Fobian, Y. M.; Wu, M.; Boyd, N. D.; Moeller, K. D. *J. Org. Chem.* **2000,** *65,* 2484–2493. doi:10.1021/jo991649t
94. Slomczynska, U.; Chalmers, D. K.; Cornille, F.; Smythe, M. L.; Beusen, D. D.; Moeller, K. D.; Marshall, G. R. *J. Org. Chem.* **1996,** *61,* 1198–1204. doi:10.1021/jo950898o
95. Cornille, F.; Slomczynska, U.; Smythe, M. L.; Beusen, D. D.; Moeller, K. D.; Marshall, G. R. *J. Am. Chem. Soc.* **1995,** *117,* 909–917. doi:10.1021/ja00108a007
96. Le Corre, L.; Kizirian, J.-C.; Levraud, C.; Boucher, J.-L.; Bonnet, V.; Dhimane, H. *Org. Biomol. Chem.* **2008,** *6,* 3388–3398. doi:10.1039/b805811c
97. Le Corre, L.; Dhimane, H. *Tetrahedron Lett.* **2005,** *46,* 7495–7497. doi:10.1016/j.tetlet.2005.09.008
98. Gorewoda, T.; Mazurkiewicz, R.; Simka, W.; Mlostoń, G.; Schroeder, G.; Kubicki, M.; Kuźnik, N. *Tetrahedron: Asymmetry* **2011,** *22,* 823–833. doi:10.1016/j.tetasy.2011.05.002
99. Kardassis, G.; Brungs, P.; Steckhan, E. *Tetrahedron* **1998,** *54,* 3471–3478. doi:10.1016/S0040-4020(98)00081-7
100. Kardassis, G.; Brungs, P.; Nothhelfer, C.; Steckhan, E. *Tetrahedron* **1998,** *54,* 3479–3488. doi:10.1016/S0040-4020(98)00082-9
101. Kabeshov, M. A.; Musio, B.; Murray, P. R. D.; Browne, D. L.; Ley, S. V. *Org. Lett.* **2014,** *16,* 4618–4621. doi:10.1021/ol502201d

License and Terms

BEILSTEIN JOURNAL OF ORGANIC CHEMISTRY

Redox active dendronized polystyrenes equipped with peripheral triarylamines

Toshiki Nokami§, Naoki Musya, Tatsuya Morofuji, Keiji Takeda, Masahiro Takumi, Akihiro Shimizu and Jun-ichi Yoshida*

Letter

Open Access

Address:
Department of Synthetic Chemistry and Biological Chemistry, Graduate School of Engineering, Kyoto University, Nishikyo-ku, Kyoto 615-8510, Japan

Email:
Jun-ichi Yoshida* - yoshida@sbchem.kyoto-u.ac.jp

* Corresponding author
§ Present address: Department of Chemistry and Biotechnology, Graduate School of Engineering, Tottori University, 4-101 Koyama-chominami, Tottori 680-8552, Japan

Keywords:
carbocation; cross-coupling; dendrimer; dendronized polymer; redox

Beilstein J. Org. Chem. **2014,** *10,* 3097–3103.
doi:10.3762/bjoc.10.326

Received: 30 October 2014
Accepted: 10 December 2014
Published: 22 December 2014

This article is part of the Thematic Series "Electrosynthesis".

Guest Editor: S. R. Waldvogel

Abstract

Dendronized polystyrene having peripheral bromo groups was prepared from the dendronization of unfunctionalized polystyrene with dendritic diarylcarbenium ions bearing peripheral bromo groups using the “cation pool” method. The palladium-catalyzed amination of the peripheral bromo groups with diarylamine gave dendronized polystyrene equipped with peripheral triarylamines, which exhibited two sets of reversible redox peaks in the cyclic voltammetry curves.

Introduction

Assembling small functional molecules using dendrimers [1] and dendronized polymers [2-8] as scaffolds serves as a useful method for synthesizing organic functional materials having nanosize three-dimensional structures. Although there are many examples of redox-active dendrimers, including those equipped with ferrocene [9,10], triarylamines [11-14], and tetrathiafulvalene (TTF) derivatives [15-19], the corresponding dendronized polymers are rare [20]. One of the major reasons for this seems to be the difficulty in making such structures. However, redox-active dendronized polymers should provide more opportunities to form functional organic materials, and therefore, the development of efficient methods for the synthesis of redox-active dendronized polymers is highly desirable. Recently, we have developed a new method [21-26] for the synthesis of dendronized polymers [27] from the dendronization of unfunctionalized polystyrenes with electrogenerated dendritic diarylcarbenium ions. The simplicity and step economy of this method prompted us to synthesize dendronized polymers equipped with peripheral functional groups by the use of this method.

In principle, there are two synthetic approaches for synthesizing peripherally functionalized dendronized polystyrenes: (a) the functionalization of dendronized polystyrene (the "graft from" approach, Figure 1a); and (b) dendronization of polystyrenes with the dendritic carbocation equipped with functional groups (the "graft to" approach, Figure 1b). Both approaches have advantages and disadvantages. In the former case, more dendritic scaffolds can be introduced by functionalization, but structural inhomogeneity can occur from incomplete peripheral functionalization. In the latter approach, direct dendronization by the functionalized diarylcarbenium ions may be difficult, although the dendritic substituents would have a uniform structure. In this paper we report on the synthesis of redox-active dendronized polystyrenes via the peripheral modification of dendronized polystyrene [28].

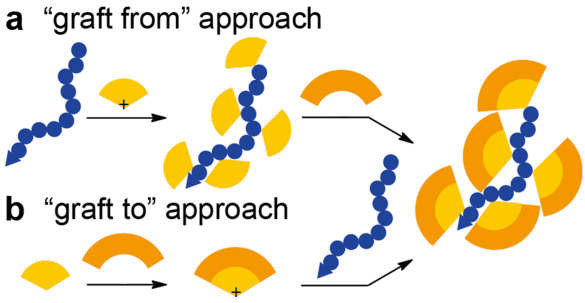

Figure 1: Two synthetic approaches toward the peripherally functionalized dendronized polystyrenes (blue dotted line = polystyrene, orange sector = dendron of the 1st generation, dark orange sector = dendron of the 2nd generation). (a) Peripheral functionalization of the dendronized polystyrene ("graft from" approach). (b) Dendronization with dendritic diarylcarbenium ions equipped with functional groups ("graft to" approach).

Results and Discussion

Dendrimer **4**, having a bromo functionality was prepared on a multigram scale, as shown in Figure 2. Di(*p*-bromophenyl)carbinol (**1**) was treated with $SOCl_2$ to obtain di(*p*-bromophenyl)methyl chloride (**2**) in quantitative yield. A Friedel–Crafts-type alkylation [29] of diphenylsilane **3** with **2** in the presence of boron trifluoride etherate as a Lewis acid gave **4** in 86% yield. The oxidation potential of **4** (E_{ox} = 1.17 V vs SCE) is slightly lower than that of the fluorine analogue (E_{ox} = 1.25 V vs SCE) which was used as a precursor of the dendritic cation in our previous work [25], indicating that bromine analogue **4** can act as a precursor of the dendritic cation.

The functionalization of **4** was examined before studying the functionalization of dendronized polystyrene. Thus, di(*p*-methoxyphenyl)amino groups were introduced to **4** using a

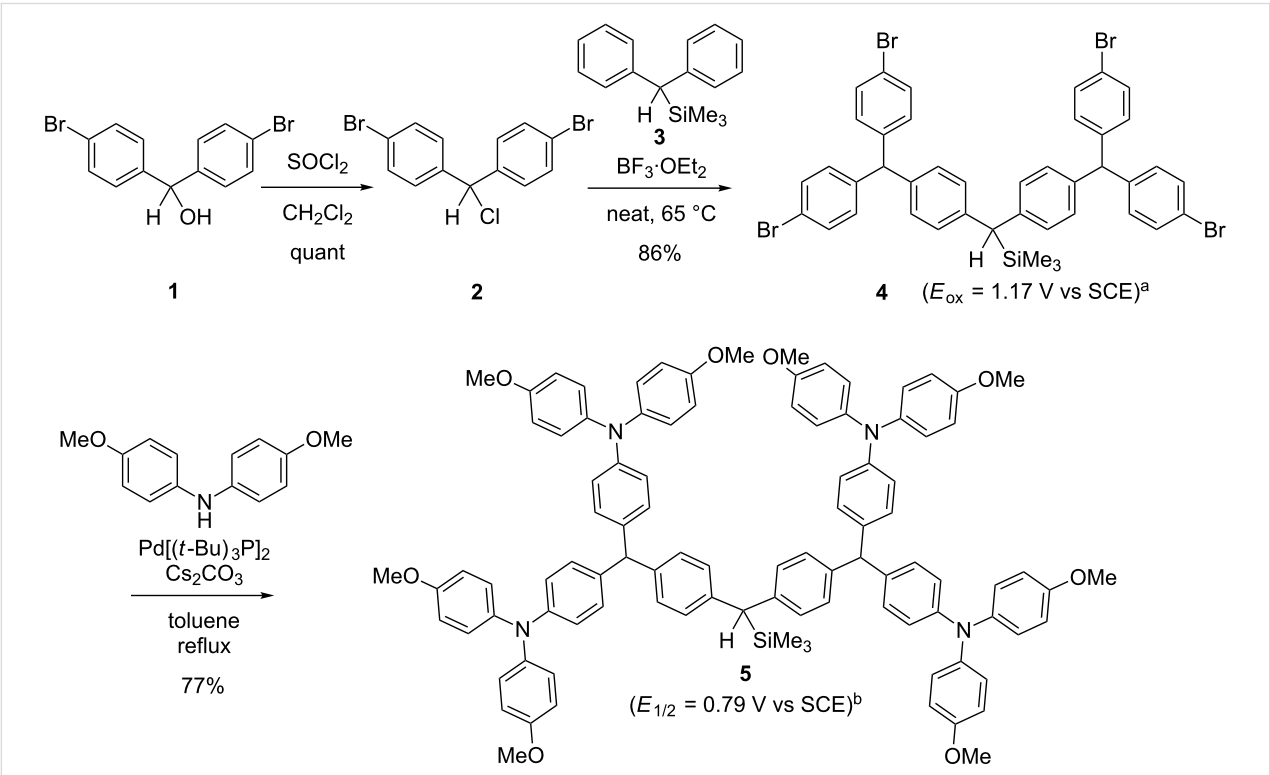

Figure 2: Preparation of the dendrimer having peripheral bromo groups and their conversion to diarylamino groups. [a]Oxdation potential (E_{ox}). [b]Redox potential ($E_{1/2}$).

Buchwald–Hartwig amination [11]. The choice of a base is crucial for this transformation, and the transformation was successfully carried out using Cs_2CO_3 as a base and $Pd[P(t\text{-}Bu)_3]_2$ as a catalyst [30] to obtain the dendrimer **5** having peripheral diarylamino groups in a yield of 77%. Compound **5** can serve as the precursor of dendritic diarylcarbenium ions having peripheral triarylamine structures. However, its redox potential ($E_{1/2}$ = 0.79 V vs SCE) is much lower than the oxidation potential of dendrimer **4**, indicating that the triarylamine moiety is oxidized before the benzylsilane moiety. Using the "graft to" approach to synthesize peripherally functionalized dendronized polystyrene (Figure 1b) employing **5** as a precursor of the dendritic carbocation was unsuccessful. Low-temperature electrochemical oxidation of dendrimer **5** using the "cation pool" method [31-47] did not give the corresponding dendritic diarylcarbenium ion even, when subjected to excess capacitance (up to 5.0 *F*/mol).

Next, we examined the "graft-from" approach (Figure 3). The low-temperature electrochemical oxidation of dendrimer **4** using the "cation pool" method was performed in CD_2Cl_2, and the resulting anodic solution was transferred to NMR tubes.

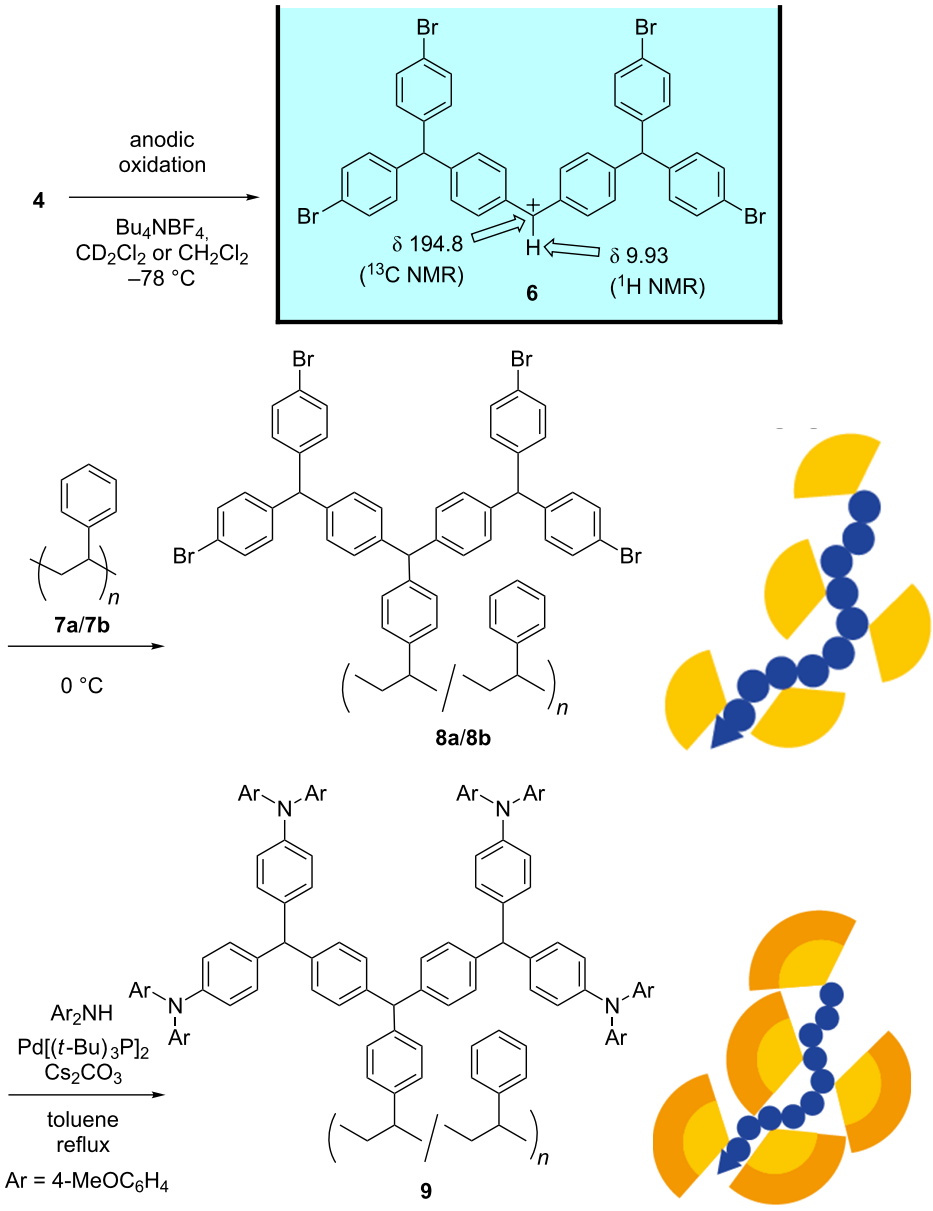

Figure 3: Preparation of dendronized polystyrenes having peripheral diarylamino groups.

Low-temperature NMR analysis indicated that an accumulation of dendritic diarylcarbenium ion **6** in the solution had occurred. The chemical shift of the cationic carbon (^{13}C NMR δ 194.8) and that of the proton attached to the cationic carbon (^{1}H NMR δ 9.93) indicated that there was no interaction between the cationic carbon and peripheral bromo groups, because the chemical shifts were almost identical to those of the fluorine analogue (^{13}C NMR δ 194.4, ^{1}H NMR δ 9.92) [25].

The reaction of **6** (generated on a preparative scale in CH_2Cl_2) with a low-molecular weight polystyrene **7a** (M_n = 1,580, polydispersity index (PDI) = 1.04, 22 mg) was performed at 0 °C (Figure 3). The resulting dendronized polystyrene **8a** was characterized using MALDI–TOF MS analysis. Six peak groups were observed, as shown in Figure 4. The peak occurring at 10,573 Da [M + Ag^+] is derived from 11 dendritic substituents (815 Da × 11), 14 styrene units (103 Da × 11 + 104 Da × 3), and a butyl group (58 Da), which was derived from the initiator at the end of the polystyrene. The broader peaks seem to be attributable to two isotopes of the bromo groups (79 and 81 Da), and the small peak separation 101–103 Da is consistent with the molecular weight of styrene monomer (104 Da). The MS analysis indicated that **6** reacted with about 80% of the phenyl groups on polystyrene **7a**. This ratio is consistent with the implemented rate (77%) calculated from the increase in weight of the polystyrene (22 mg to 150 mg).

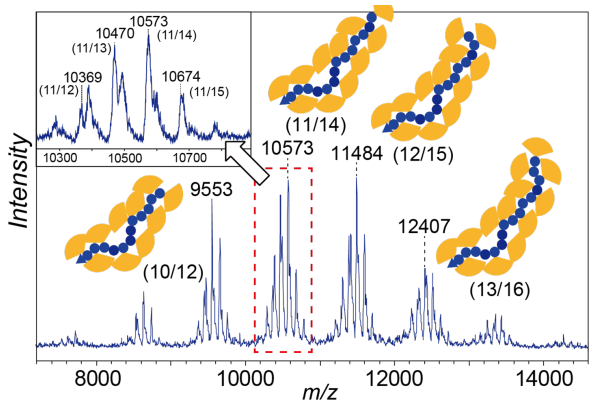

Figure 4: MALDI–TOF MS analysis of the dendronized polystyrene with peripheral bromo groups.

In a similar manner, dendronized polystyrene **8b** was synthesized from polystyrene having a longer chain length **7b** (M_n = 9,300, PDI = 1.02). Using GPC analysis to estimate the molecular weight of the dendronized polymer was not appropriate, because both the M_n and M_w values of the obtained dendronized polystyrene **8b** were only twice that of the starting polystyrene **7b** (Table 1). SEC–MALLS analysis indicated that **6** reacted with about 70% of the phenyl groups on polystyrene **7b**. This ratio is slightly larger than the implemented rate (55%) calculated from the increase in weight of the polystyrene (156 mg to 820 mg).

The peripheral bromo groups of **8b** were converted to diarylamino groups using a Hartwig–Buchwald amination employing $Pd[P(t\text{-}Bu)_3]_2$ (10 mol %) and Cs_2CO_3 (12 equiv) to obtain **9**. Dendronized polystyrene **9** was also analyzed using GPC and SEC–MALLS measurements employing DMF as an eluent. The results are summarized in Table 1. GPC analysis indicated either a slight increase or no increase in molecular weight from the peripheral functionalization, but SEC–MALLS measurements showed an identifiable increase in the molecular weight (M_w = 62,000 to 226,000), which is more than double the theoretical value (M_w = 100,000 after 100% conversion of the peripheral bromo groups to diarylamino groups). Although the PDI did not change appreciably after dendronization (**7b** to **8b**), the PDI increased slightly after peripheral functionalization (**8b** to **9**). Presently, the ratio of methine protons in the focal points of the dendritic structure (δ 5.38–5.00, broad singlet, 3H) and the methyl protons of the peripheral methoxy groups (δ 3.80–3.40, broad singlet, 24H) in the ^{1}H NMR spectra is the only evidence for the conversion of the peripheral bromo groups to diarylamino groups. The observed ratio was 1:8.4 (methane/methyl), which indicates a quantitative conversion (theoretical ratio is 1:8).

The redox behavior of **9** was studied by means of cyclic voltammetry (CV, Figure 5). Compound **9** showed two sets of revers-

Table 1: Molecular weight analyses of the dendronized polystyrenes.

polymer	GPC			SEC-MALLS		
	M_n	M_w	PDI	M_n	M_w	PDI
7b[a]	9,300	9,490	1.02	–	–	–
8b	18,800	19,900	1.06	59,400	62,000	1.04
9	18,200	22,100	1.21	175,800	226,000	1.29

[a]Polymer **7b** was analyzed only by GPC.

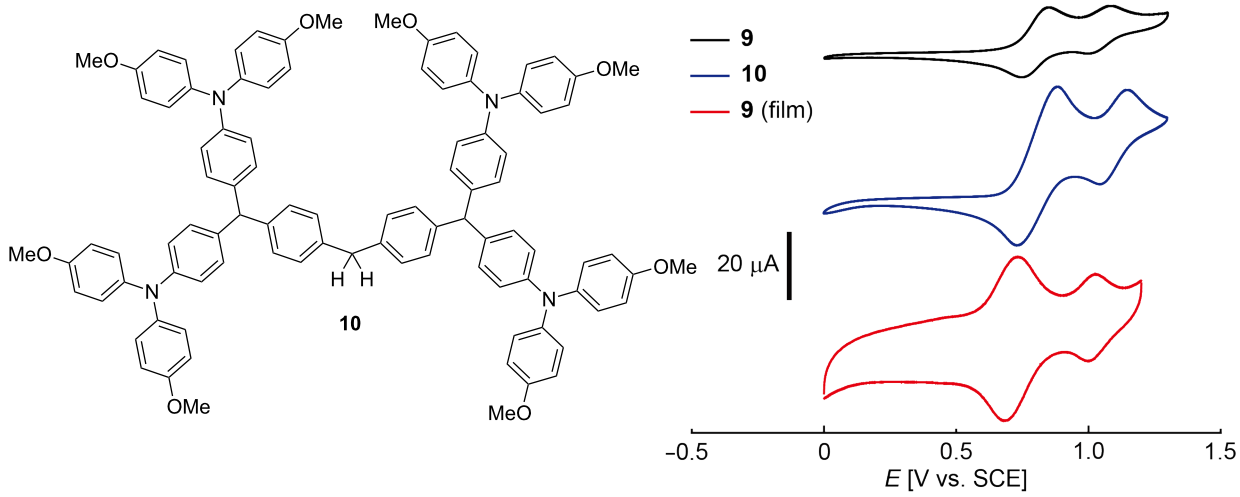

Figure 5: Cyclic voltammograms of dendronized polystyrene **9** (black line), model compound **10** (blue line), and the film of dendronized polystyrene **9** (red line). See the Experimental section for the details.

ible redox peaks ($E_{1/2}$ = 0.80 and 1.04 V vs SCE), although it has been reported that di(*p*-methoxyphenyl)phenylamine shows a single redox peak in its CV curves [48]. Therefore, the two sets of redox peaks of **9** seem to be ascribable to the interaction of the initially formed radical cation from the triarylamine moiety with a neighboring neutral triarylamine moiety, which disfavors the second electron transfer from the latter, although the details of this reaction are not clear as yet [49,50]. This is consistent with the observation that dendrimer **10** prepared by desilylation of **5** followed by amination (see Supporting Information File 1 for preparative details) showed two reversible waves occurring at similar potentials ($E_{1/2}$ = 0.81 and 1.10 V vs SCE) (Figure 5, blue line).

A film of dendronized polystyrene **9** was prepared on a Pt plate electrode as a film by drop casting of a CH_2Cl_2 solution of **9**. The redox behavior of the film of **9** on a Pt electrode was analyzed using CV (Figure 5, red line). Reversible CV cycles ($E_{1/2}$ = 0.76 and 1.01 V vs SCE) were obtained in a mixed solvent (CH_3CN/toluene 1:3) using $Bu_4NB(C_6F_5)_4$ as the electrolyte. The small shifts in the redox peaks from those obtained from solution may be attributable to the changes in solvent and electrolyte. The peak separations for a film of **9** (ΔE ($E_{ox} - E_{red}$) = 52 and 27 mV) are significantly smaller than those observed for a solution of **9** (ΔE = 103 and 87 mV), indicating immobilization of **9** occurred on the surface of the electrode.

Conclusion

In conclusion, redox-active dendronized polystyrene was successfully synthesized by peripheral functionalization of dendronized polystyrene having peripheral bromo groups with diarylamines. Thus, dendronized polystyrene having peripheral bromo groups may serve as a versatile precursor of dendronized polystyrenes equipped with various functional groups. Dendronized polystyrene having peripheral diarylamino groups showed reversible redox behavior in both solution and as a film deposited on an electrode. Further optimization of the present method and applications of peripheral functionalization of dendronized polystyrenes are under investigation in our laboratory.

Experimental

Electrochemical analyses

Electrochemical analysis was performed using an ALS/Chi700DS electrochemical analyzer. A saturated calomel electrode (SCE) (RE-2B, ALS Co. Ltd.) was used as the reference electrode.

The oxidation potential (E_{ox}) of dendrimer **4** was measured using linear sweep voltammetry employing a gassy carbon (GC) rotating disk electrode (diameter = 3.0 mm, ALS Co. Ltd.) and a Pt wire counter electrode at room temperature. CH_2Cl_2 was used as a solvent and Bu_4NBF_4 (0.1 M) was used as a supporting electrolyte. The scan rate was 100 mV/s.

The redox potentials ($E_{1/2}$) of **5** and **10**, and that of dendronized polystyrene **9** were measured by cyclic voltammetry (CV) using a GC working electrode (diameter = 3.0 mm, ALS Co. Ltd.) and a Pt wire counter electrode at room temperature. CH_2Cl_2 was used as a solvent and Bu_4NBF_4 (0.1 M) was used as a supporting electrolyte. The scan rate was 100 mV/s. The GC electrode was polished with alumina powder (0.05 μm) in water using a polishing pad, water-washed, and air-dried before use.

Cyclic voltammetry of a film of **9** deposited on a Pt plate electrode was measured as follows: Dendronized polystyrene **9** was deposited on a Pt plate electrode (1 × 1 cm^2) as a film by drop casting of a CH_2Cl_2 solution of **9**, and the solvent was evaporated under reduced pressure to obtain the film of **9** attached to the Pt plate. The CV measurement was performed using the Pt plate with the film of **9** as the working electrode and a Pt wire counter electrode at room temperature. A mixer of CH_3CN/toluene (1:3) was used a solvent and $Bu_4NB(C_6F_5)_4$ (0.1 M) as a supporting electrolyte. The scan rate was 100 mV/s.

Supporting Information

Supporting Information File 1

Experimental procedures for the synthesis of new compounds and spectral data of new compounds including ^1H NMR, ^{13}C NMR, and HMQC spectra.
[http://www.beilstein-journals.org/bjoc/content/supplementary/1860-5397-10-326-S1.pdf]

Acknowledgements

The authors gratefully acknowledge partial financial supports from Grants-in-Aid for Scientific Research on Innovative Areas (No. 2105) from the MEXT and Young Scientists (B) (No. 23750127) from the JSPS. T. N. thanks the Asahi Glass Foundation for financial support. The authors thank Prof. Mitsuo Sawamoto and Dr. Takaya Terashima of Kyoto University for SCE-MALLS measurements and Dr. Keiko Kuwata of Kyoto University for MS analyses.

References

1. Grayson, S. M.; Fréchet, J. M. J. *Chem. Rev.* **2001,** *101,* 3819–3868. doi:10.1021/cr990116h
2. Schlüter, A. D.; Rabe, J. P. *Angew. Chem., Int. Ed.* **2000,** *39,* 864–883. doi:10.1002/(SICI)1521-3773(20000303)39:5<864::AID-ANIE864>3.0.CO;2-E
3. Schlüter, A. D. *J. Polym. Sci., Part A: Polym. Chem.* **2001,** *39,* 1533–1556. doi:10.1002/pola.1130
4. Zhang, A.; Shu, L.; Bo, Z.; Schlüter, A. D. *Macromol. Chem. Phys.* **2003,** *204,* 328–339. doi:10.1002/macp.200290086
5. Frauenrath, H. *Prog. Polym. Sci.* **2005,** *30,* 325–384. doi:10.1016/j.progpolymsci.2005.01.011
6. Lee, C. C.; MacKay, J. A.; Fréchet, J. M. J.; Szoka, F. C. *Nat. Biotechnol.* **2005,** *23,* 1517–1526. doi:10.1038/nbt1171
7. Rudick, J. G.; Percec, V. *Acc. Chem. Res.* **2008,** *41,* 1641–1652. doi:10.1021/ar800086w
8. Rosen, B. M.; Wilson, C. J.; Wilson, D. A.; Peterca, M.; Imam, M. R.; Percec, V. *Chem. Rev.* **2009,** *109,* 6275–6540. doi:10.1021/cr900157q
9. Valério, C.; Fillaut, J.-L.; Ruiz, J.; Guittard, J.; Blais, J.-C.; Astruc, D. *J. Am. Chem. Soc.* **1997,** *119,* 2588–2589. doi:10.1021/ja964127t
10. Shu, C.-F.; Shen, H.-M. *J. Mater. Chem.* **1997,** *7,* 47–52. doi:10.1039/A604225B
11. Louie, J.; Hartwig, J. F.; Fry, A. J. *J. Am. Chem. Soc.* **1997,** *119,* 11695–11696. doi:10.1021/ja972806d
12. Ranasinghe, M. I.; Varnavski, O. P.; Pawlas, J.; Hauck, S. I.; Louie, J.; Hartwig, J. F.; Goodson, T., III. *J. Am. Chem. Soc.* **2002,** *124,* 6520–6521. doi:10.1021/ja025505z
13. Hagedorn, K. V.; Varnavski, O.; Hartwig, J.; Goodson, T., III. *J. Phys. Chem. C* **2008,** *112,* 2235–2238. doi:10.1021/jp7112076
14. Wong, W. W. H.; Jones, D. J.; Yan, C.; Watkins, S. E.; King, S.; Haque, S. A.; Wen, X.; Ghiggino, K. P.; Holmes, A. B. *Org. Lett.* **2009,** *11,* 975–978. doi:10.1021/ol8029164
15. Bryce, M. R.; Devonport, W.; Goldenberg, L. M.; Wang, C. *Chem. Commun.* **1998,** 945–952. doi:10.1039/A800536B
16. Le Derf, F.; Levillain, E.; Trippé, G.; Gorgues, A.; Sallé, M.; Sebastían, R.-M.; Caminade, A.-M.; Majoral, J.-P. *Angew. Chem., Int. Ed.* **2001,** *40,* 224–227. doi:10.1002/1521-3773(20010105)40:1<224::AID-ANIE224>3.0.CO;2-O
17. Beeby, A.; Bryce, M. R.; Christensen, C. A.; Cooke, G.; Duclairoir, F. M. A.; Rotello, V. M. *Chem. Commun.* **2002,** 2950–2951. doi:10.1039/B209765F
18. Godbert, N.; Bryce, M. R. *J. Mater. Chem.* **2002,** *12,* 27–36. doi:10.1039/B106010B
19. Astruc, D. *Nat. Chem.* **2012,** *4,* 255–267. doi:10.1038/nchem.1304
20. Boisselier, E.; Shun, A. C. K.; Ruiz, J.; Cloutet, E.; Belin, C.; Astruc, D. *New J. Chem.* **2009,** *33,* 246–253. doi:10.1039/B819604D
21. Okajima, M.; Soga, K.; Nokami, T.; Suga, S.; Yoshida, J. *Org. Lett.* **2006,** *8,* 5005–5007. doi:10.1021/ol061647c
22. Nokami, T.; Ohata, K.; Inoue, M.; Tsuyama, H.; Shibuya, A.; Soga, K.; Okajima, M.; Suga, S.; Yoshida, J. *J. Am. Chem. Soc.* **2008,** *130,* 10864–10865. doi:10.1021/ja803487q
23. Okajima, M.; Soga, S.; Watanabe, T.; Terao, K.; Nokami, T.; Suga, S.; Yoshida, J. *Bull. Chem. Soc. Jpn.* **2009,** *82,* 594–599. doi:10.1246/bcsj.82.594
24. Terao, K.; Watanabe, T.; Suehiro, T.; Nokami, T.; Yoshida, J. *Tetrahedron Lett.* **2010,** *51,* 4107–4109. doi:10.1016/j.tetlet.2010.05.140
25. Nokami, T.; Watanabe, T.; Musya, N.; Suehiro, T.; Morofuji, T.; Yoshida, J. *Tetrahedron* **2011,** *67,* 4664–4671. doi:10.1016/j.tet.2011.04.065
26. Nokami, T.; Watanabe, T.; Terao, K.; Soga, K.; Ohata, K.; Yoshida, J. *Electrochemistry* **2013,** *81,* 399–401. doi:10.5796/electrochemistry.81.399
27. Nokami, T.; Watanabe, T.; Musya, N.; Morofuji, T.; Tahara, K.; Tobe, Y.; Yoshida, J. *Chem. Commun.* **2011,** *47,* 5575–5577. doi:10.1039/C1CC10923E
28. Nokami, T.; Musya, N.; Morofuji, T.; Takeda, K.; Yoshida, J. In *Proceedings of the PRiME 2012,* Honolulu, HI, Oct 5–12, 2012; The Electrochemical Society: Pennington, NJ, 2012; Abstract #2079.
29. Olah, G. A.; Krishnamurti, R.; Prakash, G. K. S. Friedel–Crafts Alkylations. In *Comprehensive Organic Synthesis;* Trost, B. M., Ed.; Pergamon Press: Oxford, 1991; Vol. 3, pp 229–339.
30. Littke, A. F.; Fu, G. C. *Angew. Chem., Int. Ed.* **1998,** *37,* 3387–3388. doi:10.1002/(SICI)1521-3773(19981231)37:24<3387::AID-ANIE3387>3.0.CO;2-P
31. Yoshida, J.; Suga, S.; Suzuki, S.; Kinomura, N.; Yamamoto, A.; Fujiwara, K. *J. Am. Chem. Soc.* **1999,** *121,* 9546–9549. doi:10.1021/ja9920112
32. Suga, S.; Suzuki, S.; Yamamoto, A.; Yoshida, J. *J. Am. Chem. Soc.* **2000,** *122,* 10244–10245. doi:10.1021/ja002123p

33. Suga, S.; Okajima, M.; Fujiwara, K.; Yoshida, J. *J. Am. Chem. Soc.* **2001,** *123,* 7941–7942. doi:10.1021/ja015823i
34. Suga, S.; Watanabe, M.; Yoshida, J. *J. Am. Chem. Soc.* **2002,** *124,* 14824–14825. doi:10.1021/ja028663z
35. Yoshida, J.; Suga, S. *Chem. – Eur. J.* **2002,** *8,* 2650–2658. doi:10.1002/1521-3765(20020617)8:12<2650::AID-CHEM2650>3.0.CO;2-S
36. Suga, S.; Nishida, T.; Yamada, D.; Nagaki, A.; Yoshida, J. *J. Am. Chem. Soc.* **2004,** *126,* 14338–14339. doi:10.1021/ja0455704
37. Nagaki, A.; Kawamura, K.; Suga, S.; Ando, T.; Sawamoto, M.; Yoshida, J. *J. Am. Chem. Soc.* **2004,** *126,* 14702–14703. doi:10.1021/ja044879k
38. Okajima, M.; Suga, S.; Itami, K.; Yoshida, J. *J. Am. Chem. Soc.* **2005,** *127,* 6930–6931. doi:10.1021/ja050414y
39. Maruyama, T.; Suga, S.; Yoshida, J. *J. Am. Chem. Soc.* **2005,** *127,* 7324–7325. doi:10.1021/ja0511218
40. Nagaki, A.; Togai, M.; Suga, S.; Aoki, N.; Mae, K.; Yoshida, J. *J. Am. Chem. Soc.* **2005,** *127,* 11666–11675. doi:10.1021/ja0527424
41. Suga, S.; Matsumoto, K.; Ueoka, K.; Yoshida, J. *J. Am. Chem. Soc.* **2006,** *128,* 7710–7711. doi:10.1021/ja0625778
42. Maruyama, T.; Mizuno, Y.; Shimizu, I.; Suga, S.; Yoshida, J. *J. Am. Chem. Soc.* **2007,** *129,* 1902–1903. doi:10.1021/ja068589a
43. Ashikari, Y.; Nokami, T.; Yoshida, J. *J. Am. Chem. Soc.* **2011,** *133,* 11840–11843. doi:10.1021/ja202880n
44. Ashikari, Y.; Nokami, T.; Yoshida, J. *Org. Lett.* **2012,** *14,* 938–941. doi:10.1021/ol203467v
45. Ashikari, Y.; Nokami, T.; Yoshida, J. *Org. Biomol. Chem.* **2013,** *11,* 3322–3331. doi:10.1039/c3ob40315g
46. Ashikari, Y.; Shimizu, A.; Nokami, T.; Yoshida, J. *J. Am. Chem. Soc.* **2013,** *135,* 16070–16073. doi:10.1021/ja4092648
47. Yoshida, J.; Ashikari, Y.; Matsumoto, K.; Nokami, T. *J. Synth. Org. Chem., Jpn.* **2013,** *71,* 1136–1144. doi:10.5059/yukigoseikyokaishi.71.1136
48. Nelson, R. F.; Adams, R. N. *J. Am. Chem. Soc.* **1968,** *90,* 3925–3930. doi:10.1021/ja01017a004
49. Diallo, A. K.; Daran, J.-C.; Varret, F.; Ruiz, J.; Astruc, D. *Angew. Chem., Int. Ed.* **2009,** *48,* 3141–3145. doi:10.1002/anie.200900216
50. Diallo, A. K.; Absalon, S.; Ruiz, J.; Astruc, D. *J. Am. Chem. Soc.* **2011,** *133,* 629–641. doi:10.1021/ja109380u

License and Terms

BEILSTEIN JOURNAL OF ORGANIC CHEMISTRY

Highly selective electrochemical fluorination of dithioacetal derivatives bearing electron-withdrawing substituents at the position α to the sulfur atom using poly(HF) salts

Bin Yin, Shinsuke Inagi and Toshio Fuchigami*

Letter

Open Access

Address:
Department of Electronic Chemistry, Tokyo Institute of Technology, Nagatsuta, Midori-ku, Yokohama 226-8502, Japan

Email:
Toshio Fuchigami* - fuchi@echem.titech.ac.jp

* Corresponding author

Keywords:
anodic fluorination; anodic fluorodesulfurization; electrosynthesis; fluorination product selectivity; poly(HF) salt

Beilstein J. Org. Chem. **2015,** *11,* 85–91.
doi:10.3762/bjoc.11.12

Received: 13 November 2014
Accepted: 08 January 2015
Published: 19 January 2015

This article is part of the Thematic Series "Electrosynthesis".

Guest Editor: S. R. Waldvogel

Abstract

Anodic fluorination of dithioacetals bearing electron-withdrawing ester, acetyl, amide, and nitrile groups at their α-positions was comparatively studied using various supporting poly(HF) salts like $Et_3N{\cdot}nHF$ (n = 3–5) and $Et_4NF{\cdot}nHF$ (n = 3–5). In the former two cases, the corresponding α-fluorination products or fluorodesulfurization products were obtained selectively depending on supporting poly(HF) salts used. In sharp contrast, in the latter two cases, fluorination product selectivity was strongly affected by the electron-withdrawing ability of α-substituents: A dithioacetal bearing a relatively weak electron-withdrawing amide group provided a fluorodesulfurization product selectively while a dithioacetal having a strongly electron-withdrawing nitrile group gave the α-fluorination product predominantly regardless of the poly(HF) salts used.

Introduction

The introduction of fluorine atom(s) into organic molecules very often improves or enhances their desired characteristic physical and biological properties hence organofluorine compounds are highly useful for medicinal, agrochemical, and materials science [1-6]. In order to prepare new fluorine compounds, selective fluorination of organic compounds is becoming significantly important. Although the selective fluorination has been extensively studied, highly efficient and safe fluorination methods are still demanded [7,8]. With these facts in mind, we have developed a selective electrochemical fluorination using ionic liquid poly(HF) salts such as $Et_3N{\cdot}nHF$ and $Et_4NF{\cdot}nHF$ (n = 3–5) as supporting electrolyte and fluorine source [9-11], and we have systematically studied the anodic fluorination of various heteroatom-containing compounds including heterocycles and macromolecules so far [12-20].

More than 20 years ago, we reported the first successful example of the electrochemical selective fluorination of

heteroatom-containing compounds such as α-(phenylthio)ester and its analogues as shown in Scheme 1 [21,22]. Furthermore, anodic fluorodesulfurization of dithioacetals was achieved by direct and indirect anodic oxidation in the presence of the poly(HF) salts [12-16,23-25] or alkali-metal fluorides like KF and CsF with PEG 200 [17]. The anodic fluorination of a dithioacetal derived from an aliphatic aldehyde provided the fluorodesulfurization product while a dithioacetal derived from an aromatic aldehyde provided the α-fluorination product (Scheme 2) [25]. These results suggest that the fluorinated product selectivity seems to be controlled by the easiness of the deprotonation of the cationic intermediate **A**. Namely, since the α-proton of the aromatic dithioacetal is more acidic compared to that of an aliphatic dithioacetal, the deprotonation of the former is faster than it is for the latter. Therefore, it can be stated that the product selectivity is controlled by the kinetic acidity of the cationic intermediate **A** [26,27].

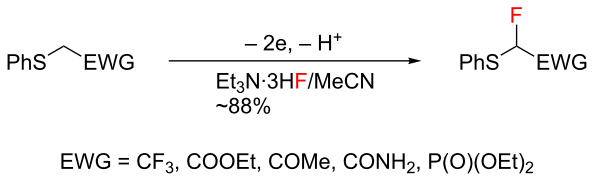

Scheme 1: Anodic fluorination of sulfides having an electron-withdrawing group.

With these facts in mind, we studied comparatively the anodic fluorination of dithioacetal derivatives having various electron-withdrawing groups at their α-positions using various poly(HF) salts [28].

Results and Discussion

Various α-substituted methyl phenyl sulfides, **1a**, **1c**, **1e**, and **1g**, and their α-phenylthio derivatives (dithioacetals) were prepared, and their oxidation potentials (E_p^{ox}) were measured by cyclic voltammetry in an anhydrous acetonitrile (MeCN) solution containing *n*-Bu_4NBF_4 (0.1 M) using a platinum disk working electrode and a saturated calomel electrode (SCE) as the reference electrode. All compounds exhibited irreversible multiple oxidation peaks and the first oxidation peak potentials are summarized in Table 1. It was expected that the introduction of an additional phenylthio group to the α-position of the sulfides would decrease their oxidation potentials. However, unexpectedly they are higher than those of the corresponding sulfides having a single phenylthio group. Although a detailed reason is not clear at present, the additional phenylthio group does not act as an electroauxiliary, but acts as an electron-withdrawing group. As shown in Table 1, the oxidation potentials of sulfide **1g** and dithioacetal **1h** having a stronger electron-withdrawing cyano group (Taft σ* = +1.30) [29] are much higher compared to those of **1a**, **1b** with an ester group (Taft σ* = +0.69) [29] and **1c**, **1d** with an acetyl group (Taft σ* = +0.60) [29], respectively. This indicates that the polar effect, namely electron-withdrawing effect of a substituent greatly affects the electron-transfer step from the substrate to the anode.

Table 1: First oxidation potentials, E_p^{ox} of compounds **1**.

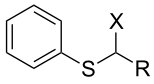

Substrate	X	R (σ* value)[a]	E_p^{ox} (V vs SCE)[b]
1a	H	COOEt (+ 0.69)	1.60
1b	SPh	COOEt (+ 0.69)	1.73
1c	H	COMe (+ 0.60)	1.59
1d	SPh	COMe (+ 0.60)	1.63
1e	H	$CONEt_2$	1.60
1f	SPh	$CONEt_2$	1.64
1g	H	CN (+ 1.30)	1.85
1h	SPh	CN (+ 1.30)	2.04

[a]From [29]. [b]Substrate concentration: 5 mM; sweep rate: 100 mV/s; working electrode: Pt disk (Ø = 1 mm).

At first, anodic fluorination of ethyl α,α-bis(phenylthio)acetate (**1b**) [30,31] was carried out at platinum plate electrodes in an undivided cell using various solvents in the presence of $Et_3N·3HF$ as supporting salt and fluorine source. A constant current was passed until the starting material **1b** was completely consumed (monitored by TLC). As shown in Table 2, the anodic fluorination of **1b** proceeded to give the corresponding

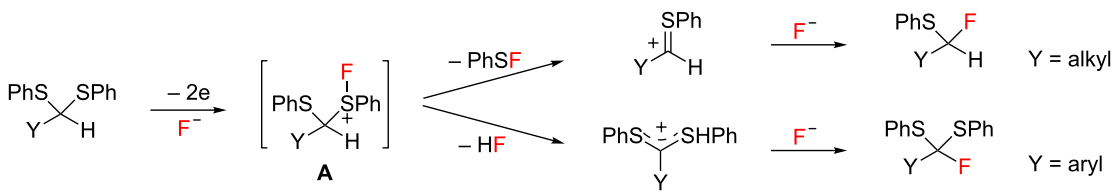

Scheme 2: Anodic fluorination of dithioacetals.

Table 2: Anodic fluorination of **1b** in various solvents containing $Et_3N{\cdot}3HF$[a].

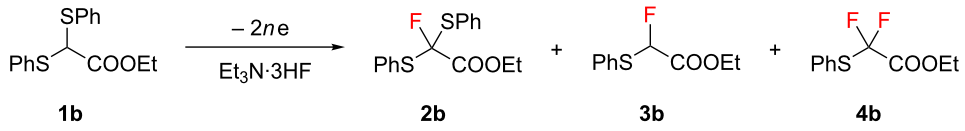

1b **2b** **3b** **4b**

Entry	Solvent	Charge passed (F/mol)	Yield (%)[b,c]			Total yield (%)
			2b	**3b**	**4b**	
1	MeCN	3.0	74 (70)	9	0	83
2	DME	5.0	74	9	0	83
3	CH_2Cl_2	2.5	73	5	4	82
4	$MeNO_2$	2.2	73	7	1	81
5[d]	MeCN	–	–	–	–	–

[a]Constant current (8 mA/cm^2) electrolysis was carried out in 0.3 M $Et_3N{\cdot}3HF$/solvent. [b]Determined by ^{19}F NMR. [c]Isolated yield given in parentheses. [d]Mechanical stirring was performed overnight at ambient temperature without electrolysis.

α-fluoro product **2b** in a good yield regardless of the solvent used. Thus, it was found that the solvents did not affect the yield of **2b** in contrast to the current efficiency. When the reaction was performed in DME as the solvent, anodic decomposition of DME took place simultaneously with the anodic fluorination of **1b**, which resulted in low current efficiency. In all cases, fluorodesulfurization product **3b** [22] was detected in considerable yield. When CH_2Cl_2 and $MeNO_2$ were used, a small amount of ethyl α,α-difluoro-α-(phenylthio)acetate (**4b**) [22] was also detected (Table 2, entries 3 and 4). As a blank test, the electrolytic solution of **1b** was mechanically stirred without electrolysis overnight and **1b** was mostly recovered (Table 2, entry 5). Therefor electrolysis is necessary for the fluorination to take place.

Among the solvents tested for electrolysis, we decided to use MeCN for further studies on the anodic fluorination based on a good current efficiency and the formation of only one byproduct.

Next, anodic fluorination of **1b** was carried out in MeCN using various poly(HF) salts until the substrate was completely consumed and the results are shown in Figure 1. As mentioned earlier, the anodic fluorination of **1b** using $Et_3N{\cdot}3HF$ provided

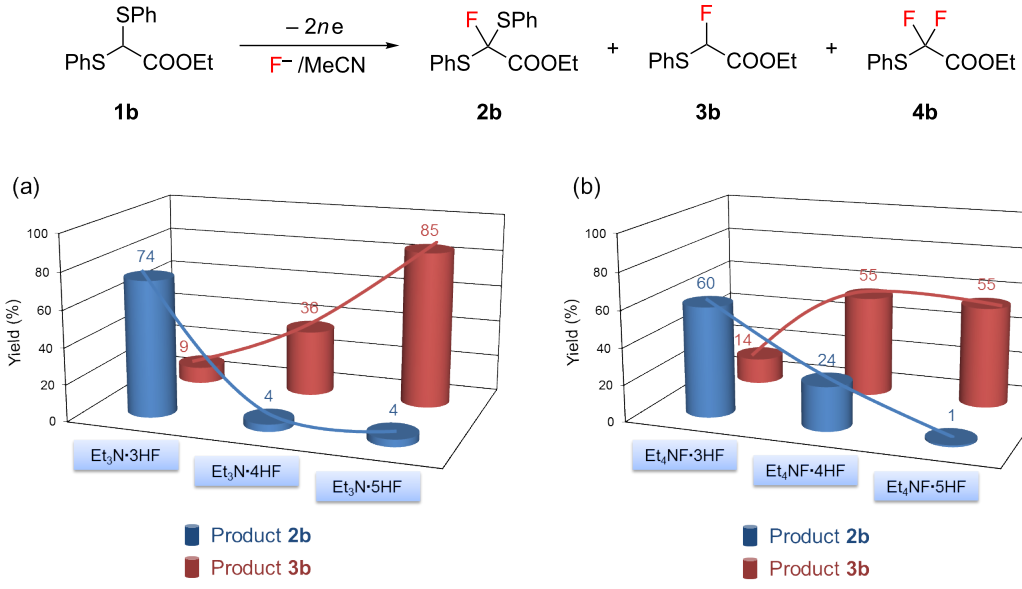

Figure 1: Dependency of fluorinated product selectivity on a series of fluoride salts (a) $Et_3N{\cdot}nHF$ (n = 3–5) and (b) $Et_4NF{\cdot}nHF$ (n = 3–5).

α-fluorinated product **2b** selectively in good yield along with a small amount of fluorodesulfurization product **3b**. In contrast, the fluorodesulfurization reaction was significantly promoted with increasing HF content of the poly(HF) salts; especially the use of $Et_3N·5HF$ gave predominantly the fluorodesulfurization product **3b** in 85% yield (Figure 1a). Previously, we obtained **3b** in 75% yield by constant potential anodic oxidation of ethyl α-(phenylthio)acetate in a similar electrolytic solution [22]. A comparable dependency of product selectivity on supporting poly(HF) salts was also observed in a series of $Et_4NF·nHF$ (n = 3–5) although the product yields are moderate (Figure 1b).

According to these results, we carried out the anodic fluorination of other dithioacetals bearing different electron-withdrawing substituents such as acetyl, amide, and cyano groups under similar conditions. The results are summarized in Table 3. In the case of α,α-bis(phenylthio)acetone (**1d**) [32], the use of $Et_3N·3HF$ and $Et_4NF·3HF$ resulted in predominant α-fluorination to provide the corresponding monofluorinated product **2d** in good to moderate yields (Table 3, entries 1 and 3). On the contrary, when higher HF content salts such as $Et_3N·5HF$ and $Et_4NF·5HF$ were used, fluorodesulfurization product **3d** [22] was obtained almost exclusively in moderate or good yield (Table 3, entries 2 and 4). Regardless of poly(HF) salts, difluorinated product **4d** [33] was always formed due to the further oxidation of products **2d** and **3d**. In contrast, anodic fluorination of *N*,*N*-diethyl-α,α-bis(phenylthio)acetamide (**1f**) with $Et_3N·3HF$ required a large excess amount of electricity to consume the starting substrate **1f**, and fluorodesulfurization took place exclusively to provide the corresponding mono- and difluorinated products **3f** and **4f** [22,34] with the same ratio in rather low yields (Table 3, entry 5). The longer electrolysis caused the formation of complicated products. This result is quite different from the case of **1b** and **1d** (Table 2, entry 1 and Table 3, entry 1). Such different anodic behavior may be attributable to different pK_a values of the α-proton of the substrates. It is known that the acidity of the α-proton of *N*,*N*-diethylacetoamide is 4 to 5 times lower than that of acetone and ethyl acetate [35]. Therefore, the acidity of the α-proton of **1f** having an amide group would be much lower compared to that of **1b** and **1d** having an ester and acetyl group, respectively. Thus, it is reasonable that no deprotonation of the cationic intermediate of **1f** took place. Moreover, when a higher HF content poly(HF) salt like $Et_3N·5HF$ was used, fluorodesulfurization product **3f** was exclusively formed in good yield. This tendency is quite similar to the result of anodic fluorination of **1b** and **1d** (Figure 1a and Table 3, entries 2 and 4). Thus, it was found that due to the low acidity of the α-proton of **1f**, fluorodesulfurization took place prior to α-fluorination even in the presence of $Et_3N·3HF$ containing the free base Et_3N. In sharp contrast to these cases, α,α-bis(phenylthio)acetonitrile (**1h**) [36] bearing a strongly electron-withdrawing cyano group underwent α-fluo-

Table 3: Anodic fluorination of dithioacetal derivative **1** in acetonitrile[a].

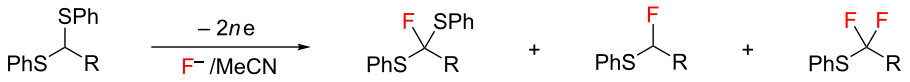

1 **2** **3** **4**

Entry	R	Supporting electrolyte	Charge passed (F/mol)	Yield (%)[b,c]		
				2	**3**	**4**
1	COMe (**1d**)	$Et_3N·3HF$	3.0	80 (66)	–	5
2	COMe (**1d**)	$Et_3N·5HF$	2.5	–	63	3
3	COMe (**1d**)	$Et_4NF·3HF$	2.7	60	–	10
4	COMe (**1d**)	$Et_4NF·5HF$	2.5	6	78 (70)	1
5	$CONEt_2$ (**1f**)	$Et_3N·3HF$	5.0	0	18	17
6	$CONEt_2$ (**1f**)	$Et_3N·5HF$	3.0	0	72 (63)	1
7	CN (**1h**)	$Et_3N·3HF$	3.0	98 (87)	0	0
8	CN (**1h**)	$Et_3N·4HF$	2.8	98	0	0
9	CN (**1h**)	$Et_3N·5HF$	2.5	90	0	0
10	CN (**1h**)	$Et_4NF·3HF$	2.7	94	0	0
11	CN (**1h**)	$Et_4NF·4HF$	2.5	95	0	0
12	CN (**1h**)	$Et_4NF·5HF$	2.5	93	0	0

[a]Constant current (8 mA/cm^2) electrolysis was carried out using 0.3 M supporting fluoride salt. [b]Determined by ^{19}F NMR. [c]Isolated yields are given in parentheses.

rination exclusively to produce α-fluorinated product **2h** in excellent yields regardless of the poly(HF) salts (Table 3, entries 7–12). In case of **1h**, no difluoro product was formed at all, which is probably due to a much higher oxidation potential of **2h** compared to that of the starting substrate **1h**. In support of this, we have already shown that introduction of one fluorine atom to the α-position of α-(phenylthio)acetonitrile increased the oxidation potential by 0.36 V [22].

A plausible mechanism for the anodic fluorination of dithioacetals **1b**, **1d**, and **1f** is shown in Scheme 3. The fluorination reaction is initiated by electron transfer from a sulfur atom of the substrate to generate the corresponding radical cation **B**, which traps a fluoride ion to afford radical **C**. This is followed by a further oxidation to give cationic intermediate **D**. In the cases of **1b** and **1d** having electron-withdrawing ester and acetyl groups, the α-protons are acidic enough and can be cleaved by either base, free Et_3N (from $Et_3N{\cdot}3HF$) [37] or fluoride ions (from $Et_4NF{\cdot}3HF$). The resulting cation **E** reacts with a fluoride ion to form **2b** and **2d**. Further anodic fluorodesulfurization occurs to provide the corresponding difluorinated products **4b** and **4d**, respectively. On the other hand, the desulfurization of intermediate **D** followed by reaction with fluoride provides the corresponding fluorodesulfurization products **3b**, **3d**, and **3f**.

When high HF content salts like $Et_3N{\cdot}5HF$ and $Et_4NF{\cdot}nHF$ (n = 4, 5) are used, the higher concentration of HF in the electrolytic solution would increase the amount of **D** rather than **E** in an equilibrium between them as shown in Scheme 4. Namely, the deprotonation of **D** would be retarded due to high concentration of protons in the solution, and consequently the C–S bond cleavage seems to take place more favorably than a deprotonation. A similar effect on the suppression of defluorination of CF_3-enolate anion in the presence of a large amount of fluoride ions has been reported [38].

On the other hand, it is known that the acidity of α-protons of acetoamides is much lower compared to that of acetate and acetone as mentioned. Therefore, it is understandable that the

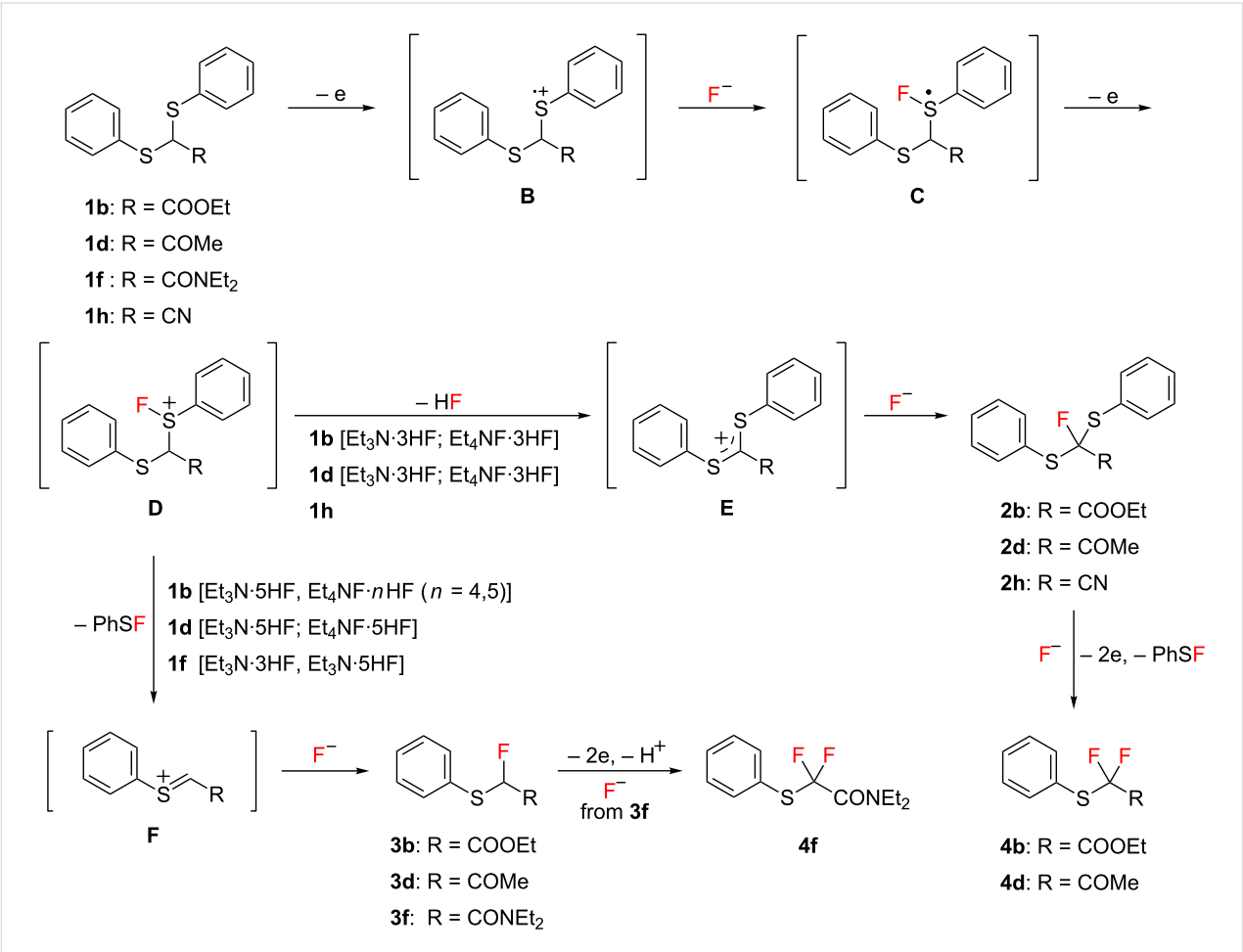

Scheme 3: Plausible reaction mechanism for anodic fluorination of **1b**, **1d**, and **1f**.

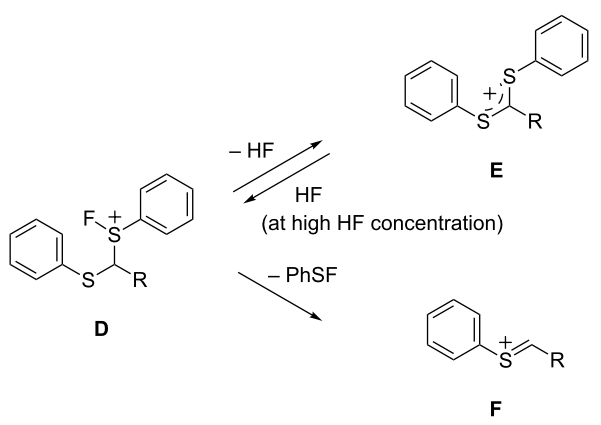

Scheme 4: Mechanism for suppression of the elimination of HF (deprotonation) and preferable desulfurization of **D** at high concentrations of HF in an electrolytic solution.

anodic fluorination of **1f** having a weakly electron-withdrawing amide group resulted in fluorodesulfurization to provide **3f** even when $Et_3N·3HF$ containing free base, Et_3N was used. As mentioned, the yield of monofluorodesulfurization product **3f** increased markedly by using high HF content salt, $Et_3N·5HF$.

In sharp contrast, in the case of substrate **1h** having a cyano group, α-fluorination without desulfurization always took place even when $Et_3N·5HF$ and $Et_4NF·5HF$ were used. This can be explained in terms of fast deprotonation of cationic intermediate **D** promoted by a strongly electron-withdrawing cyano group as shown in Scheme 3.

Conclusion

The regioselective anodic fluorination of ethyl α,α-bis(phenylthio)acetate and its acetone, acetoamide, and acetonitrile analogues was successfully carried out using various poly(HF) salts such as $Et_3N·nHF$ and $Et_4NF·nHF$ (n = 3–5) to provide α-fluoro and/or fluorodesulfurization products. The fluorinated product selectivity was found to depend on substituents and supporting poly(HF) salts. The unique product selectivity was tentatively explained in terms of electron-withdrawing ability (Taft σ*) of substituents and HF content of the used supporting poly(HF) salts.

Supporting Information

Supporting Information File 1

General methods, synthetic procedures, characterzation data of all new compounds including copies of ^{1}H NMR, ^{13}C NMR and ^{19}F NMR spectra.
[http://www.beilstein-journals.org/bjoc/content/supplementary/1860-5397-11-12-S1.pdf]

Acknowledgements

We gratefully acknowledge Morita Chemical Industries Co., Ltd for supplying triethylamine poly(hydrogen fluoride) [$Et_3N·nHF$ (n = 3–5)] and tetraethylammonium fluoride poly(hydrogen fluoride) [$Et_4NF·nHF$ (n = 3–5)] that were used as supporting salt fluorine source. We also thank technical staffs working at Center for Advanced Materials Analysis (Suzukakedai Campus) of Tokyo Institute of Technology for analyzing new compounds. One of the authors (Y. B.) acknowledges Ministry of Education, Culture, Sports, Science & Technology of Japan for awarding national scholarship to conduct this research.

References

1. Ojima, I. *Fluorine in Medicinal Chemistry and Chemical Biology;* Wiley: Chichester, 2009. doi:10.1002/9781444312096
2. Purser, S.; Moore, P. R.; Swallow, S.; Gouverneur, V. *Chem. Soc. Rev.* **2008,** *37,* 320–330. doi:10.1039/b610213c
3. Bégué, J.-P.; Bonnet-Delpon, D. *Bioorganic and Medicinal Chemistry of Fluorine;* John Wiley & Sons, Inc.: Hoboken, 2008. doi:10.1002/9780470281895
4. Uneyama, K. *Organofluorine Chemistry;* Blackwell Publishing: Oxford, 2006. doi:10.1002/9780470988589
5. O'Hagen, D. *J. Fluorine Chem.* **2010,** *131,* 1071–1081. doi:10.1016/j.jfluchem.2010.03.003
6. Hiyama, T., Ed. *Organofluorine Compounds. Chemistry and Applications;* Springer: Berlin, 2000. doi:10.1007/978-3-662-04164-2
7. Umemoto, T.; Singh, R. P.; Xu, Y.; Saito, N. *J. Am. Chem. Soc.* **2010,** *132,* 18199–18205. doi:10.1021/ja106343h
8. Kishi, Y.; Inagi, S.; Fuchigami, T. *Eur. J. Org. Chem.* **2009,** 103–109. doi:10.1002/ejoc.200800872
9. Fuchigami, T.; Atobe, M.; Inagi, S. *Fundamental and Applications of Organic Electrochemistry. Synthesis, Materials, Devices;* Wiley: Chichester, 2014.
10. Fuchigami, T. In *Organic Electrochemistry,* 4th ed.; Lund, H.; Hammerich, O., Eds.; Marcel Dekker: New York, 2001; Chapter 25.
11. Childs, W. V.; Christensen, L.; Klink, F. W. In *Organic Electrochemistry,* 3rd ed.; Lund, H.; Baizer, M. M., Eds.; Marcel Dekker: New York, 1991; Chapter 24.
12. Sawamura, T.; Kuribayashi, S.; Inagi, S.; Fuchigami, T. *Org. Lett.* **2010,** *12,* 644–646. doi:10.1021/ol9028836
13. Sawamura, T.; Kuribayashi, S.; Inagi, S.; Fuchigami, T. *Adv. Synth. Catal.* **2010,** *352,* 2757–2760. doi:10.1002/adsc.201000501
14. Fuchigami, T.; Inagi, S. *Chem. Commun.* **2011,** *47,* 10211–10223. doi:10.1039/C1CC12414E
15. Takahashi, K.; Furusawa, T.; Sawamura, T.; Kuribayashi, S.; Inagi, S.; Fuchigami, T. *Electrochim. Acta* **2012,** *77,* 47–53. doi:10.1016/j.electacta.2012.05.049
16. Takahashi, K.; Inagi, S.; Fuchigami, T. *J. Electrochem. Soc.* **2013,** *160,* G3046–G3052. doi:10.1149/2.005307jes
17. Sawamura, T.; Takahashi, K.; Inagi, S.; Fuchigami, T. *Angew. Chem., Int. Ed.* **2012,** *51,* 4413–4416. doi:10.1002/anie.201200438
18. Inagi, S.; Hayashi, S.; Fuchigami, T. *Chem. Commun.* **2009,** 1718–1720. doi:10.1039/B822510A

19. Hayashi, S.; Inagi, S.; Fuchigami, T. *Macromolecules* **2009,** *42,* 3755–3760. doi:10.1021/ma900358x
20. Shaaban, M. R.; Ishii, H.; Fuchigami, T. *J. Org. Chem.* **2000,** *65,* 8685–8689. doi:10.1021/jo001129u
21. Fuchigami, T.; Shimojo, M.; Konno, A.; Nakagawa, K. *J. Org. Chem.* **1990,** *55,* 6074–6075. doi:10.1021/jo00312a006
22. Fuchigami, T.; Shimojo, M.; Konno, A. *J. Org. Chem.* **1995,** *60,* 3459–3464. doi:10.1021/jo00116a037
23. Fuchigami, T.; Sano, M. *J. Electroanal. Chem.* **1996,** *414,* 81–84. doi:10.1016/0022-0728(96)04642-6
24. Fuchigami, T.; Mitomo, K.; Ishii, H.; Konno, A. *J. Electroanal. Chem.* **2001,** *507,* 30–33. doi:10.1016/S0022-0728(01)00440-5
25. Yoshiyama, T.; Fuchigami, T. *Chem. Lett.* **1992,** *21,* 1995–1998. doi:10.1246/cl.1992.1995
26. Yoon, U. C.; Mariano, P. S. *Acc. Chem. Res.* **1992,** *25,* 233–240. doi:10.1021/ar00017a005
27. Fuchigami, T.; Ichikawa, S. *J. Org. Chem.* **1994,** *59,* 607–615. doi:10.1021/jo00082a018
28. Preliminary results of this work were presented at 225th *ECS Meeting*, 2014, Abstr. No. 820.
29. Hansch, C.; Leo, A.; Taft, R. W. *Chem. Rev.* **1991,** *91,* 165–195. doi:10.1021/cr00002a004
30. Tabti, B.; Gourmala, C.; Bounouara Bouderba, H.; Mulengi, J. K. *J. Soc. Alger. Chim.* **1996,** *6,* 199–206.
31. Ritter, R. H.; Cohen, T. *J. Am. Chem. Soc.* **1986,** *108,* 3718–3725. doi:10.1021/ja00273a028
32. Keiko, N. A.; Funtikova, E. A.; Stepanova, L. G.; Chuvashev, Yu. A.; Larina, L. I. *Russ. J. Org. Chem.* **2002,** *38,* 970–976. doi:10.1023/A:1020893310626
33. Gouault, S.; Guérin, C.; Lemoucheux, L.; Lequeux, T.; Pommelet, J.-C. *Tetrahedron Lett.* **2003,** *44,* 5061–5064. doi:10.1016/S0040-4039(03)01134-1
34. Yagupolski, L.; Korinko, V. A. *Zh. Obshch. Khim.* **1969,** *39,* 1747.
35. McMurry, J. E.; Simanek, E. E. *Fundamentals of Organic Chemistry,* 6th ed.; Brooks–Cole Publishing Co, 2006; Chapter 11.
36. Ishibashi, H.; Okada, M.; Sato, K.; Ikeda, M.; Ishiyama, K.; Tamura, Y. *Chem. Pharm. Bull.* **1985,** *33,* 90–95. doi:10.1248/cpb.33.90
37. Hou, Y.; Higashiya, S.; Fuchigami, T. *J. Org. Chem.* **1999,** *64,* 3346–3349. doi:10.1021/jo981979y
38. Ishikawa, N.; Yokozawa, T. *Bull. Chem. Soc. Jpn.* **1983,** *56,* 724–726. doi:10.1246/bcsj.56.724

License and Terms

BEILSTEIN JOURNAL OF ORGANIC CHEMISTRY

3α,5α-Cyclocholestan-6β-yl ethers as donors of the cholesterol moiety for the electrochemical synthesis of cholesterol glycoconjugates

Aneta M. Tomkiel[1], Adam Biedrzycki[1], Jolanta Płoszyńska[2], Dorota Naróg[2], Andrzej Sobkowiak[2] and Jacek W. Morzycki[*1]

Full Research Paper

Open Access

Address:
[1]Institute of Chemistry, University of Białystok, ul. Ciołkowskiego 1K, 15-245 Białystok, Poland and [2]Faculty of Chemistry, Rzeszów University of Technology, P.O. Box 85, 35-959 Rzeszów, Poland

Email:
Jacek W. Morzycki[*] - morzycki@uwb.edu.pl

* Corresponding author

Keywords:
cholesterol; electrochemical oxidation; glycosylation; i-cholesteryl ethers; i-steroids

Beilstein J. Org. Chem. **2015,** *11,* 162–168.
doi:10.3762/bjoc.11.16

Received: 23 November 2014
Accepted: 13 January 2015
Published: 26 January 2015

This article is part of the Thematic Series "Electrosynthesis".

Guest Editor: S. R. Waldvogel

Abstract

3α,5α-Cyclocholestan-6β-yl alkyl and aryl ethers were proved to be efficient cholesteryl donors in the electrochemical synthesis of glycoconjugates. 3α,5α-Cyclocholestan-6β-ol (i-cholesterol) and its *tert*-butyldimethylsilyl ether can also be used for this purpose. The i-cholesterol derivatives show similar reactivities to those of previously studied 3α,5α-cyclocholestan-6β-thioethers.

Introduction

We have recently elaborated an electrochemical method for the preparation of glycosides and glycoconjugates from 3β-hydroxy-Δ^5-steroids (sterols). The method consists of electrooxidation of a proper cholesterol derivative in the presence of an unactivated sugar with a free hydroxy group at the anomeric position (formation of glycosides) or at any other position (preferentially a primary position) that leads to sterol glycoconjugates. Initially, the reaction of cholesterol (**1**) with various sugars was studied. During anodic oxidation of cholesterol in dichloromethane (the choice of solvent is crucial as the reaction course may be different in other solvents) [1], splitting of the carbon–oxygen bond in an intermediate radical cation occurs, thus leading to a mesomerically stabilized homoallylic carbocation and a hydroxyl radical (Scheme 1) [2]. However, the glycosylation reaction was not very efficient due to competition between the sugar alcohol and cholesterol for the carbocation [3]. If cholesterol wins the competition, the dimer **2** (dicholesteryl ether) is formed. A large excess of sugar was used to avoid this undesired side reaction. In our further study, instead of cholesterol, cholest-5-en-3β-yl and 3α,5α-cyclocholestan-6β-yl thioethers (**3** and **4**) were applied as cholesteryl donors [4]. Of the two, the latter appeared to be much more efficient in cholesteryl transfer to the sugar moiety. The problem, however, with 6β-steroidal thioethers is that they are not easily accessible.

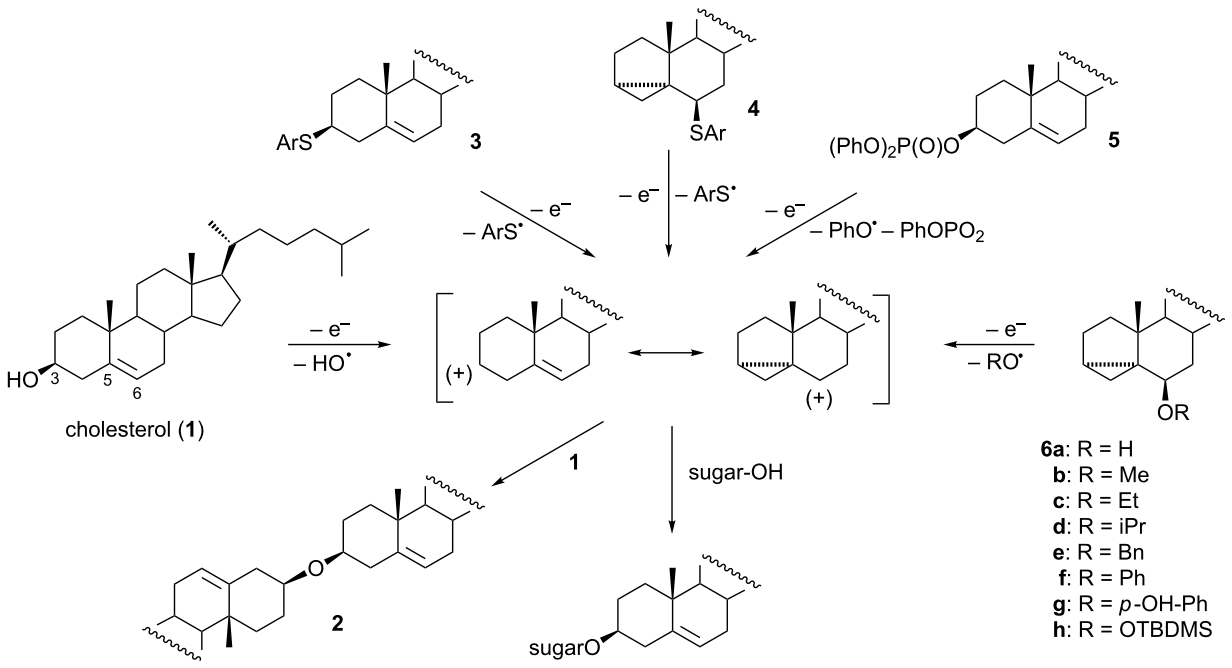

Scheme 1: Synthesis of glycoconjugates from different cholesteryl donors.

Therefore, we searched for the best leaving group at C-3. A series of cholesterol derivatives was tested and, finally, cholesteryl diphenylphosphate (**5**) was selected as the best cholesteryl donor [5]. Apart from these cholesterol derivatives, also simple alkyl or aryl ethers (**6b**–**g**) of 3α,5α-cyclocholestan-6β-ol (**6a**) (i-cholesterol) are readily available by solvolysis of cholesteryl *p*-tosylate in the corresponding alcohol under buffered conditions, while *tert*-butyldimethylsilyl ether **6h** can be prepared by silylation of i-cholesterol **6a** with TBDMSCl. Now we report the results of our study on the application of these ethers as cholesteryl donors in electrochemical glycosylation reactions.

Results and Discussion

The cyclosteroid (i-steroid) rearrangement is a well-known steroid reaction [6]. The solvolysis of cholesteryl *p*-tosylate proceeds via the S_N1 mechanism with the formation of a mesomerically stabilized carbocation. The addition of a nucleophile (alcohol, water, etc.) may occur either to C-3 or C-6, depending on the reaction conditions. In both cases the nucleophile is attached only from the upper side (β) of cholesterol due to stereo-electronic reasons. Under buffered conditions the addition is irreversible and leads to 3α,5α-cyclocholestan-6β-substituted products in excess. The addition to C-6 is faster (the kinetic product is formed) since the mesomeric carbocation is more positively charged in this position than in C-3. However, under acidic conditions the reaction becomes reversible and the 3β-substituted product, which is more stable (the thermodynamic product), is exclusively formed. The i-steroid ethers are frequently prepared for simultaneous protection of both 3β-ol and Δ^5 groups in sterols. The cycloreversion that occurs under acidic conditions allows to recover sterol functions.

We thought that such highly energetic i-steroid ethers would easily generate the mesomeric carbocation during electrochemical oxidation by cleavage of the carbon–oxygen bond in an intermediate radical-cation. For this reason, i-cholesteryl ethers seemed to be suitable donors of the cholesterol moiety for the electrochemical synthesis of cholesterol glycoconjugates.

A series of i-cholesterol derivatives **6b–h** was prepared including alkyl, aryl, and silyl ethers. Most of the compounds were prepared by solvolysis of cholesteryl *p*-tosylate in an appropriate alcohol (neat or mixed with dioxane) in the presence of potassium acetate as a buffer. TBDMS ether **6h** was obtained by silylation of i-cholesterol **6a** with TBDMSCl in DMF in the presence of imidazole and DMAP.

All of these compounds proved to be electrochemically active. Cyclic voltammograms measured in dichloromethane on a platinum electrode indicated that the main oxidation peak for the substances occurred within 1.8–2.0 V (vs $Ag/AgNO_3$ in MeCN). The shapes of the voltammograms are similar (except **6f** and **6g**) to the one for 6β-isopropyloxy-3α,5α-cyclocholestane (**6d**), which is presented in Figure 1 (curve c, blue). The cyclic voltammogram for 6β-phenyloxy-3α,5α-cyclocholestane (**6f**) shows an additional anodic peak at 1.45 V

(curve d, green) and the cyclic voltammogram for 6β-(4-hydroxyphenyloxy)-3α,5α-cyclocholestane (**6g**) shows two additional anodic peaks at 0.88 V and 1.45 V (curve e, brown). The existence of these peaks is probably connected with electrooxidation of the substituents. It is worth to notice that in the case of **6f** and **6g** the oxidation currents are approximately equal to the half of oxidation current of **6d** and also other investigated compounds. This is probably caused by the electrode blocking due to an adsorption of the oxidation products. The fact that the electrochemical oxidation of **6f** and **6g** starts at more negative potentials in comparison to the other investigated compounds supports this explanation. Moreover, during subsequent voltammetric cycles of **6d** the oxidation current is decreased to almost the half of the current registered in the first scan. In addition the second peak for **6d** exhibits the most positive value among ethers investigated. This observation is difficult to explain without further investigations. Figure 1 also presents the voltammogram of a model sugar alcohol – 1,2:3,4-di-*O*-isopropylidene-α-D-galactopyranose (**7**) (curve b, red line), which indicates that the substrate is electrochemically inactive within the applied potential region. The readily available α-D-galactopyranose derivative **7** was chosen as a model sugar since the anomeric and secondary hydroxy groups in this compound are protected as diacetonide and the remaining primary hydroxy group is highly reactive.

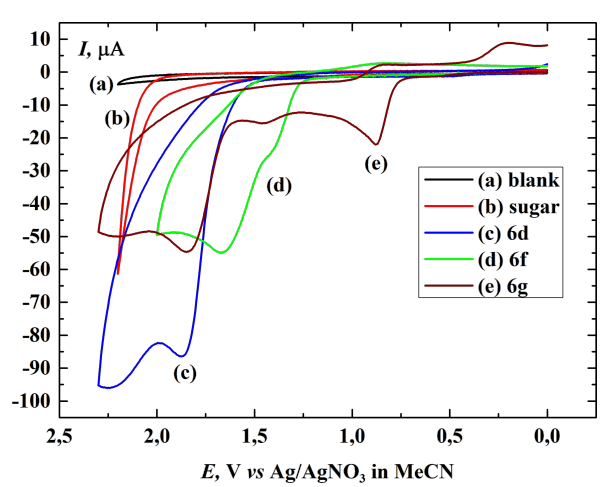

Figure 1: Cyclic voltammograms registered in 0.2 M tetrabutylammonium tetrafluoroborate ($TBABF_4$) in dichloromethane on a platinum electrode (area, 0.008 cm^2) of (a) the supporting electrolyte (black), (b) 1,2:3,4-di-*O*-isopropylidene-α-D-galactopyranose (**7**) (red), (c) 6β-isopropyloxy-3α,5α-cyclocholestane (**6d**), (blue) (d) 6β-phenyloxy-3α,5α-cyclocholestane (**6f**) (green) and (e) 6β-(4-hydroxyphenyloxy)-3α,5α-cyclocholestane (**6g**) (brown). Concentrations of all compounds are equal to 5 mM, scan rate 1 V s^{-1}. Potentials were measured vs Ag/0.1 M $AgNO_3$ in acetonitrile at room temperature.

The results of preparative electrolysis of compounds **6a**–**h** in the presence of 1,2:3,4-di-*O*-isopropylidene-α-D-galactopyranose (**7**) are shown in Scheme 2. In all of the experiments the ratio of sugar:cholesteryl donor was close to 1:1. The electrochemical reaction conditions were the same as those applied in our previous paper for the preparation of cholesterol glycoconjugates by using cholesteryl donors with an activating group at C-3 (such as diphenylphosphate **5**) [5].

The glycosylation reactions leading to **11** were accompanied by isomerization of substrates to analogous cholesterol 3β-deriva-

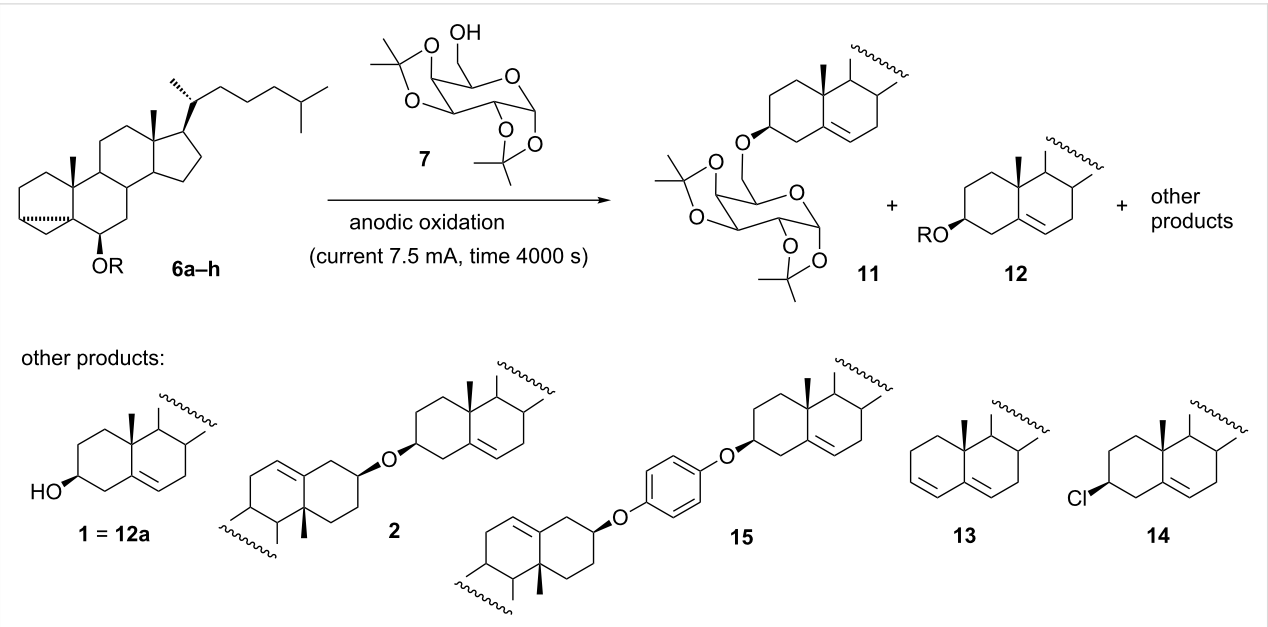

Scheme 2: Electrochemical reaction of 3α,5α-cyclocholestan-6β-yl ethers **6a–h** with 1,2:3,4-di-*O*-isopropylidene-D-galactopyranose (**7**).

tives **12** (Table 1). Compounds **12** proved much less electrochemically active or not active at all.

The electrochemical reaction of i-cholesterol (**6a**) with 1,2:3,4-di-*O*-isopropylidene-α-D-galactopyranose (**7**) afforded product **11** in 47% yield in addition to the product of isomerization (cholesterol (**1**), 8%) and dicholesteryl ether (**2**) (17%). Minor amounts of diene **13** and cholesteryl chloride (**14**) were also formed.

In the reactions of i-cholesterol alkyl ethers (methyl **6b**, ethyl, **6c**, isopropyl **6d**, and benzyl **6e**), cholesterol glycoconjugate **11** was also formed in 40%, 51%, 41%, and 50% yield, respectively. Glycoconjugate **11** was accompanied by substantial amounts of isomerization products **12** (24–45%) and tiny amounts of other products (cholesterol (**1**), dicholesteryl ether (**2**), diene **13**, and cholesteryl chloride **14**).

The best yield (58%) of cholesterol glycoconjugate **11** was achieved with 3α,5α-cyclocholestan-6β-yl phenyl ether (**6f**). The reaction was relatively clean; the isomerization product, i.e., cholesteryl phenyl ether (**12f**), was obtained in 22% yield. It should be emphasized that the yield of **11** was even better than those obtained in analogous reactions of 3α,5α-cyclocholestan-6β-yl phenyl thioether (40%) and 3α,5α-cyclocholestan-6β-yl *p*-tolyl thioether (52%) which we had previously studied [4]. Now it seems to be clear that high efficiency in the generation of the mesomeric carbocation may be attributed to the 3α,5α-cyclocholestan-6β-yl moiety rather than to the presence of an arylthiol group at C-3 or C-6. This conclusion is supported by the fact that cholesteryl phenyl thioether proved to be a rather poor cholesteryl donor for the electrochemical reaction (12% yield).

In contrast to the above, the reaction of 4-hydroxyphenyl i-cholesteryl ether **6g** was messy and afforded only 9% of the desired glycoconjugate **11**. The isomerization product, i.e., 4-hydroxyphenyl cholesteryl ether **12g**, was formed in 12% yield, while the major reaction product (18%) was 1,4-phenylene dicholesteryl diether (**15**).

The difference in reactivity between **6f** and **6g** is rather surprising. Both compounds are oxidized at relatively low potentials, which suggests that the mesomeric carbocation is formed more easily than in the case of the other investigated compounds. Indeed, the best yield of glycosylation obtained for 3α,5α-cyclocholestan-6β-yl phenyl ether (**6f**) as a substrate supports the hypothesis. On the other hand, the reason for the low yield observed for 4-hydroxyphenyl i-cholesteryl ether (**6g**) can be attributed to the electrochemical oxidation of the phenol type substituent, which is responsible for an additional peak at low potentials. The process is usually irreversible, resulting from the fast deprotonation of the primarily generated radical cation [7]. The phenoxy radical formed can be further oxidized to the phenoxenium ion, which reacts with nucleophiles. However, since the phenolic OH group is not sterically shielded here, competitive oligo- and polymerization reactions may also occur. Therefore, despite the low oxidation potential of **6g**, the side reactions account for a low yield of the desired product.

Relatively satisfactory results were obtained with i-cholesterol TBDMS ether **6h**. The glycoconjugate **11** was obtained in 52% yield with only a trace amount of the isomerization product **12h**. The major byproduct in this case was diene **13** (9%).

The occurrence of the isomerization process during electrochemical oxidation of i-cholesterol ethers is rather surprising. We proved that without electrochemical activation the glycosylation or isomerization processes do not take place under the reaction conditions. The likely mechanism of isomerization is shown in Scheme 3. The proposed formation of disteroidal oxonium ions accounts for an alkyl (aryl) group transfer from

Table 1: Electrochemical oxidation[a] of 3α,5α-cyclocholestan-6β-yl ethers **6a–h** in the presence of 1,2:3,4-di-*O*-isopropylidene-α-D-galactopyranose (**7**).

Substrate **6**	3β-*O*-(1',2':3',4'-di-*O*-isopropylidene-D-galactopyranos-6'-yl)-cholest-5-ene (**11**) (yield)	Isomerization product **12** (yield)	Other steroidal product (yield)
6a	47%	8%[b]	**2** (17), **14** (3%), **13** (2%)
6b	40%	24%	**13** (2%), **1** (1%)
6c	51%	45%	**13** (2%), **14** (1%)
6d	41%	34%	**1** (2%), **2** (2%)
6e	50%	40%	**1** (trace)
6f	58%	22%	**1** (4%), **13** (1%), **14** (1%)
6g	9%	12%	**15** (18%)
6h	52%	1%	**13** (9%), **1** (6%), **2** (5%)

[a]Electrochemical reaction conditions given in the Experimental section. [b]Compound **12a = 1** (cholesterol).

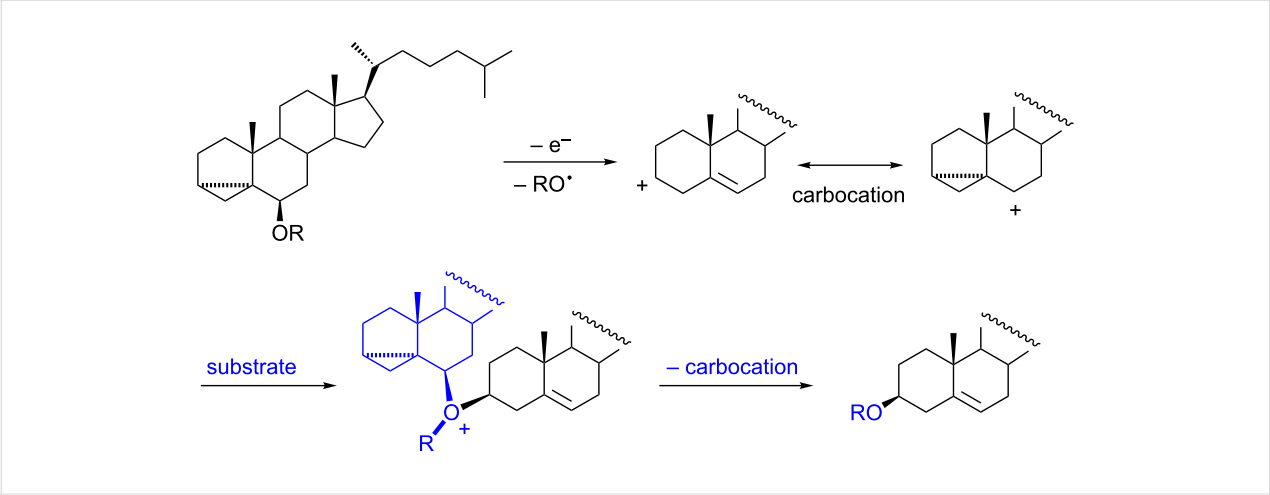

Scheme 3: Plausible mechanism of isomerization.

C-6 to C-3. Interestingly, the isomerization itself is not an electrochemical reaction. Electrooxidation is needed only to initiate the whole process, i.e., to generate the homoallylic carbocation; then the chain process occurs. The blank experiments (electrochemical reactions without the presence of sugar) were carried out to establish the approximate isomerization rates. The concentration of 3α,5α-cyclocholestan-6β-yl alkyl ether (methyl or ethyl) in the reaction mixture has fallen by half in less than 15 minutes, i.e., after that time the 3- and 6-substituted ether concentrations were approximately equal.

Even in the case of i-cholesteryl phenyl ether (**6f**), fast isomerization to **12f** was observed. It is worth noting that no isomerization occurred for i-cholesterol TBDMS ether (**6h**), probably due to steric reasons.

A limitation of the glycosylation process are the consecutive reactions of glycoconjugate **11** at a growing voltage and its limited stability under electrolysis conditions. The major decomposition product is 3β-O-(3',4'-*O*-isopropylidene-α-D-galactopyranos-6'-yl)-cholest-5-ene, i.e., compound **11** loses one of the *O*-isopropylidene groups upon prolonged electrolysis. Although the electrochemical overoxidation of glycoconjugate **11** seems to be a minor problem at the initial steps due to a relatively large difference in the oxidation potentials and concentrations between substrates (sterol donors, sugar alcohol) and the resulting glycoconjugate, the possibility that side processes will occur increases as the anode potential is more positive and the glycoconjugate concentration grows.

A series of blank experiments proved that the electrochemical activation of i-steroidal ethers **6a**–**h** is necessary for their reactions with sugar **7**. No coupling occurred when chemical promoters were attempted.

Conclusion

3α,5α-Cyclocholestan-6β-yl ethers are excellent cholesteryl donors for the electrochemical synthesis of cholesterol glycoconjugates. All of the tested compounds proved efficient in this respect, although the best yields were obtained with ethyl, benzyl, phenyl, and TBDMS ether. The side reaction is isomerization to the much less reactive cholesteryl ethers. This undesired reaction may be partially suppressed by using 3α,5α-cyclocholestan-6β-yl phenyl ether or completely stopped by employing TBDMS ether.

Experimental

Cyclic voltammograms were recorded with iR compensation at 25 °C using a three-electrode potentiostat (Princeton Applied Research, model Parstat 2273). The experiments were conducted in a 3 mL electrochemical cell with an argon-purge system. The working electrode was a Bioanalytical Systems platinum inlay (1 mm in diameter), the auxiliary electrode was a platinum mesh (contained in a glass tube with a medium porosity glass frit), and the reference electrode was Ag/0.1 M $AgNO_3$ in acetonitrile. The potential of the electrode vs the ferrocene/ferricinium ion reference couple is equal to −37 mV [8]. The reference electrode was contained in a Pyrex tube with a cracked softglass tip which was placed inside a Luggin capillary. Before each experiment, the working electrode was polished using Buehler Micropolish Alumina Gamma 3B and a Buehler Microcloth polishing cloth, rinsed with dichloromethane and dried. In all of the measurements, 0.2 M solution of tetrabutylammonium tetrafluoroborate ($TBABF_4$) from Aldrich in dichloromethane was used as a supporting electrolyte.

The preparative electrolyses were performed with a potentiostat/galvanostat (Princeton Applied Research, model Parstat

2273) under galvanostatic conditions using a current that was equal in a typical experiment to 7.5 mA and a reaction time of 4000 s. The current applied was the maximum current available for the electrolysis set-up being used (power supply and ohmic resistance). During the electrolysis the potential of the anode was monitored and the process was stopped when the potential reached the value of +2.3 V vs Ag/0.1 M $AgNO_3$ to avoid the occurrence of undesired oxidation processes. The reactions were also monitored by TLC and stopped when no further increase in the concentration of the glycosylation products was observed. A divided H-cell was used in which the cathodic and anodic compartments (3.5 mL of electrolyte each) were separated by a glass frit. In all measurements, 0.1 M solution of tetrabutylammonium tetrafluoroborate ($TBABF_4$) from Aldrich in dichloromethane was used as a supporting electrolyte. The steroid (0.30 mmol) and sugar (0.36 mmol) substrates were introduced into the anodic compartment together with 0.3 g of 3 Å molecular sieves added to eliminate traces of water, whereas anionite (1.5–2 g, Dowex 2 × 8, 200–400 mesh, perchlorate form) was placed in the cathodic compartment to eliminate chloride ions that are formed by the reduction of dichloromethane. The solutions in both compartments were stirred during electrolysis and, additionally, a continuous flow of argon was applied in the anodic compartment. A platinum mesh was used as a cathode and a platinum plate (2 × 1.5 cm) was used as an anode. All measurements were performed at 25 °C.

The sugar (1,2:3,4-di-*O*-isopropylidene-α-D-galactopyranose; **7**) [9] and steroidal substrates, 3α,5α-cyclocholestan-6β-ol (i-cholesterol; **6a**) [10], 6β-methoxy-3α,5α-cyclocholestane (**6b**) [11], and 6β-ethoxy-3α,5α-cyclocholestane (**6c**) [12], were prepared according to known procedures.

Melting points were determined on a Toledo Mettler-MP70 apparatus. ^1H and ^{13}C NMR (400 and 100 MHz, respectively) spectra were recorded on a Bruker Avance II spectrometer in $CDCl_3$ solutions with TMS as the internal standard (only selected signals in the ^1H NMR spectra are reported in Supporting Information File 1; sugar protons are marked with the 'prime' index). Infrared spectra were recorded on a Nicolet series II Magna-IR 550 FTIR spectrometer in chloroform solutions. Mass spectra were recorded at 70 eV with a time-of-flight (TOF) AMD-604 spectrometer with electrospray ionization (ESI) or AutoSpec Premier (Waters) (EI).

Merck Silica Gel 60, F 256 TLC aluminum sheets were applied for thin-layer chromatographic analysis. For a visualization of the products, a 5% solution of phosphomolybdic acid in ethanol was used. The reaction products were separated by column chromatography performed on a 70–230 mesh silica gel (J. T. Baker).

Typical electrochemical experiment. Anodic oxidation of 6β-phenyloxy-3α,5α-cyclocholestane (6f) in the presence of 1,2:3,4-di-*O*-isopropylidene-D-galactopyranose (7): 6β-Phenyloxy-3α,5α-cyclocholestane (138 mg, 0.30 mmol) and 1,2:3,4-di-*O*-isopropylidene-D-galactopyranose (94 mg, 0.36 mmol) were dissolved in a 0.1 M solution of tetrabutylammonium tetrafluoroborate in dichloromethane (3.5 mL) and introduced into the anodic compartment together with 0.5 g 3 Å molecular sieves to eliminate traces of water. The same supporting electrolyte was placed in the cathodic compartment with an anionite (2 g, Dowex 2 × 8, 200–400 mesh, perchlorate form) added. Preparative electrolysis was carried out in a divided H-cell in which the cathodic and anodic compartments (3.5 mL of electrolytes each) were separated by a glass frit under galvanostatic conditions. A direct current 7.5 mA was run for 4000 s. A platinum mesh was used as a cathode and a platinum plate (2 × 1.5 cm) was used as an anode. Ag/0.1 M $AgNO_3$ in an acetonitrile electrode was used as a reference. When the electrolysis was completed, the solvent was removed from the reaction mixture and the products were separated by silica gel column chromatography. The hexane elution afforded diene **13** (1 mg, 1%) and cholesteryl chloride **14** (1 mg, 1%). With the hexane/ethyl acetate mixture (96:4), cholesteryl phenyl ether **12f** (31 mg, 22%) was eluted. Further elution with hexane/ethyl acetate (93:7) afforded 3β-*O*-(1',2':3',4'-di-*O*-isopropylidene-α-D-galactopyranos-6'-yl)-cholest-5-ene (**11**, 108 mg, 58%), followed by cholesterol **1** (5 mg, 4%) eluted with hexane/ethyl acetate (9:1).

Glycosylation product **11** was described in our previous paper [4]. Also, other products of the electrochemical reactions (compounds **2**, **13**, **14**, and **15**) were described in our previous papers [1-5]. The isomerization products, i.e., 3β-cholesteryl ethers **12b** [13], **12c** [14], **12e** [15], **12f** [14], **12g** [5], and **12h** [16], are known compounds, except for **12d** which was obtained during electrochemical reaction of 3α,5α-cyclocholestan-6β-yl isopropyl ether (**6d**). See the Supporting Information File 1 for full experimental data.

Supporting Information

Supporting Information File 1

Experimental section including ^1H, ^{13}C NMR, and mass spectra for all new compounds.
[http://www.beilstein-journals.org/bjoc/content/supplementary/1860-5397-11-16-S1.pdf]

Acknowledgements

Financial support from the Polish National Science Centre (UMO-2011/01/B/ST5/06046) is gratefully acknowledged.

References

1. Kowalski, J.; Płoszyńska, J.; Sobkowiak, A.; Morzycki, J. W.; Wilczewska, A. Z. *J. Electroanal. Chem.* **2005,** *585,* 275–280. doi:10.1016/j.jelechem.2005.09.003
2. Kowalski, J.; Łotowski, Z.; Morzycki, J. W.; Płoszyńska, J.; Sobkowiak, A.; Wilczewska, A. Z. *Steroids* **2008,** *73,* 543–548. doi:10.1016/j.steroids.2008.01.014
3. Morzycki, J. W.; Łotowski, Z.; Siergiejczyk, L.; Wałejko, P.; Witkowski, S.; Kowalski, J.; Płoszyńska, J.; Sobkowiak, A. *Carbohydr. Res.* **2010,** *345,* 1051–1055. doi:10.1016/j.carres.2010.03.018
4. Tomkiel, A. M.; Brzezinski, K.; Łotowski, Z.; Siergiejczyk, L.; Wałejko, P.; Witkowski, S.; Kowalski, J.; Płoszyńska, J.; Sobkowiak, A.; Morzycki, J. W. *Tetrahedron* **2013,** *69,* 8904–8913. doi:10.1016/j.tet.2013.07.106
5. Tomkiel, A. M.; Kowalski, J.; Płoszyńska, J.; Siergiejczyk, L.; Łotowski, Z.; Sobkowiak, A.; Morzycki, J. W. *Steroids* **2014,** *82,* 60–67. doi:10.1016/j.steroids.2014.01.007
6. Kirk, D. N. *Steroid reaction mechanisms;* Elsevier: Amsterdam, The Netherlands, 1968.
7. Morrow, G. W. Anodic oxidation of oxygen-containing compounds. In *Organic Electrochemistry,* 4th ed.; Lund, H.; Hammerich, O., Eds.; Marcel Dekker: New York, USA, 2001; pp 589–620.
8. Pavlishchuk, V. V.; Addison, A. W. *Inorg. Chim. Acta* **2000,** *298,* 97–102. doi:10.1016/S0020-1693(99)00407-7
9. Calinaud, P.; Gelas, J. Synthesis of isopropylidene, benzylidene, and related acetals. In *Preparative Carbohydrate Chemistry;* Hanessian, S., Ed.; Marcel Dekker: New York, USA, 1997; pp 3–34.
10. Patel, M. S.; Peal, W. J. *J. Chem. Soc.* **1963,** 1544–1546. doi:10.1039/jr9630001544
11. Ford, E. G.; Wallis, E. S. *J. Am. Chem. Soc.* **1937,** *59,* 1415–1416. doi:10.1021/ja01287a001
12. Beynon, J. H.; Heilbron, I. M.; Spring, F. S. *J. Chem. Soc.* **1936,** 907–910. doi:10.1039/jr9360000907
13. Narayanan, C. R.; Iyer, K. N. *J. Org. Chem.* **1965,** *30,* 1734–1736. doi:10.1021/jo01017a007
14. Wang, B.; Du, H.; Zhang, J. *Steroids* **2011,** *76,* 204–209. doi:10.1016/j.steroids.2010.10.011
15. Lu, B.; Li, L.-J.; Li, T.-S.; Li, J.-T. *J. Chem. Res., Synop.* **1998,** 604–605. doi:10.1039/a803050b
16. Bartoszewicz, A.; Kalek, M.; Stawinski, J. *Tetrahedron* **2008,** *64,* 8843–8850. doi:10.1016/j.tet.2008.06.070

License and Terms

BEILSTEIN JOURNAL OF ORGANIC CHEMISTRY

Electrochemical selenium- and iodonium-initiated cyclisation of hydroxy-functionalised 1,4-dienes

Philipp Röse[1], Steffen Emge[1], Jun-ichi Yoshida[2] and Gerhard Hilt[*1]

Full Research Paper

Open Access

Address:
[1]Fachbereich Chemie, Philipps-Universität Marburg, Hans-Meerwein-Str. 4, 35043 Marburg, Germany and [2]Department of Synthetic Chemistry and Biological Chemistry, Graduate School of Engineering, Kyoto University, Nishikyo-ku, Kyoto 615-8510, Japan

Email:
Gerhard Hilt* - hilt@chemie.uni-marburg.de

* Corresponding author

Keywords:
cyclic ethers; cyclisation; 1,4-dienes; electrochemistry; iodonium; selenium

Beilstein J. Org. Chem. **2015,** *11,* 174–183.
doi:10.3762/bjoc.11.18

Received: 27 November 2014
Accepted: 16 January 2015
Published: 28 January 2015

This article is part of the Thematic Series "Electrosynthesis".

Guest Editor: S. R. Waldvogel

Abstract

The cobalt(I)-catalysed 1,4-hydrovinylation reaction of allyloxytrimethylsilane and allyl alcohol with substituted 1,3-dienes leads to hydroxy-functionalised 1,4-dienes in excellent regio- and diastereoselective fashion. Those 1,4-dienols can be converted into tetrahydrofuran and pyran derivatives under indirect electrochemical conditions generating selenium or iodonium cations. The reactions proceed in good yields and regioselectivities for the formation of single diastereomers.

Introduction

The reaction of terminal alkenes with 1,3-dienes under cobalt catalysis results in 1,4-dienes in a 1,4-hydrovinylation reaction. Besides cobalt, also other transition metals were described to undergo such transformations [1-4]. However, only for the cobalt-catalysed reactions a regiodiverse reaction has been described where the carbon–carbon bond formation, either at the terminal carbon of the double bond (C1) or on C2 was formed, depending on the ligand system applied [5,6]. Besides the ozonolysis of the 1,4-dienes for the generation of 1,3-dicarbonyl derivatives [7-9], these 1,4-dienes are in turn potential substrates for the synthesis of functionalised heterocycles. Particularly, we were interested in the synthesis of tetrahydrofuran and pyran derivatives. Those heterocycles are prevalent substructures in many natural compounds, pesticides and drugs with antifungal and antibacterial properties [10-13]. For this purpose, we investigated a protocol for the straight forward synthesis of 1,4-dienols which should be cyclised into the corresponding tetrahydrofuran or pyran derivatives. With our sight set on efficient and atom economic organic reactions electrochemistry seems to be a powerful tool for the transformation of those 1,4-dienols. Although it seems that all possible functional groups have been investigated in organic electrochemistry, reports on electrochemical transformations of 1,4-dienes are rare [14-17]. First attempts of a direct electrochemical conversion were not very successful, so that we turned our attention towards indirect electrochemical methods [18,19]. Among these

we became interested in the electrochemical generation of reactive cations inducing a transformation of the 1,4-diene moiety. As a starting point we put our interest in electrochemical reactions using selenium cations. Several methods applying electrochemically generated selenium cations with alkenes or alkynes including seleno-etherification and lactonisation, epoxidation and oxoselenylation sequences have been reported in the last decades [20-27]. The reactions often proceed in a regio- and stereoselective fashion and tolerate a wide range of functionalities.

Next to selenium cation induced reactions we put our focus on using halonium cations. The advantage of this type of reaction is its lower toxicity and the easy access towards the halonium source. Several reactions using bromonium- and iodonium cations such as iodo-etherification, lactonisation or Friedel–Crafts alkylation reactions can be found in literature. However, these procedures often use expensive or toxic halonium sources like molecular bromine [10,28,29] or organic trihalide salts [30], *N*-bromosuccinimide or *N*-iodosuccinimide and its derivatives [31-36], or more specialised reagents such as bis(pyridinium)iodonium(I) tetrafluoroborate [37-39]. Next to those, the in situ oxidation of halogenide ions with strong oxidants such as oxone, Pb(IV), mCPBA, $FeCl_3$ or H_2O_2 have been reported [40-45]. A more efficient and versatile method is the electrochemical generation of halonium ions. Thereby, it is possible to accumulate the halonium ions in solution and to add those to a substrate in a separated process ("pool" method) [46-51] or to consume the halonium ions in situ in follow-up reactions inside the cell [52].

Accordingly, we envisaged the generation of suitable starting materials via a cobalt-catalysed hydrovinylation reaction and investigated their in situ conversion via electrochemically generated selenium- or iodonium cations.

Results and Discussion

Cobalt-catalysed 1,4-hydrovinylation of allylic alcohols

For the successful application of 1,4-dienes in the electrochemical reactions, 1,4-dienes with additional internal nucleophiles, such as an alcohol group, were envisaged and those 1,4-dienols could be generated from simple 1,3-dienes, such as 1,3-butadiene or 1-aryl-substituted 1,3-dienes **1**, and TMS-protected allylic alcohol (Scheme 1) for the synthesis of 1,4-dienols of type **2**.

The cobalt-catalysed hydrovinylation reaction is highly regiospecific for the carbon–carbon bond formation which takes place exclusively at the internal carbon of the double bond of the terminal alkene (C2) and C4 of the 1-aryl-substituted 1,3-diene. The key intermediate **A** in the reaction mechanism is proposed to be a cobaltacycle which only allows the double bond generated from the 1,3-diene component to adopt a *Z*-configuration. Accordingly, the products of type **2** are formed in high selectivity in terms of regio- and diastereomeric control.

The starting materials of type **1** were generated from the aromatic aldehydes and allyltriphenylphosphonium bromide in a Wittig reaction following a known protocol [53]. The synthesis of the 1,4-dienes was then accomplished utilising the cobalt-catalyst precursor and reducing conditions in the presence of zinc iodide for abstracting the bromide anions at room temperature. The TMS-protected allylic alcohol was applied in the cobalt-catalysed 1,4-hydrovinylation process with aryl-substituted 1,3-dienes **1a–k** because the use of allylic alcohol itself led to significant lower yields (up to 30%). Only in case of buta-1,3-diene, 2,3-dimethyl-1,3-butadiene and isoprene allyl alcohol could be used directly without decreasing the yield (Table 1, entries 12–14). The results of the 1,4-dienol syntheses are summarised in Table 1.

The cobalt-catalysed hydrovinylation tolerates halide, ether, ester, trifluoromethyl and heterocyclic substituents and gave the desired products in acceptable to good yields over a two-step reaction sequence of hydrovinylation and deprotection. Electron-withdrawing and electron-donating groups as well as sterically hindered aryl substituents are also accepted (see Table 1, entries 7 and 9). The use of buta-1,3-diene and 2,3-dimethyl-1,3-butadiene gave the 1,4-dienols in excellent yields (Table 1, entries 12 and 13). When isoprene was used, the regioisomeric products **2n** and **2o** were formed in good yields and acceptable regioselectivity, with the carbon–carbon bond formation taking place predominantly at the lower substituted end of the 1,3-

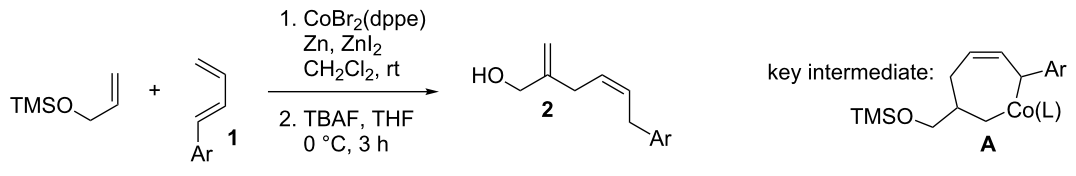

Scheme 1: Cobalt-catalysed 1,4-hydrovinylation.

diene moiety. These results demonstrate that the cobalt-catalysed hydrovinylation reaction is a powerful tool for the straightforward synthesis of various 1,4-dienols of type **2** and the mild reaction conditions made it possible to generate and isolate the products without isomerisation of the double bonds towards undesired side-products.

Transformation of 1,4-dienols via electrogenerated selenium cations

The 1,4-dienols were transformed into cyclic phenylselenoethers by intramolecular cyclisation using selenium cations generated by indirect electrolysis. The reaction was carried out by electrolysing a mixture of the 1,4-dienol, diphenyl disel-

Table 1: Results of the cobalt-catalysed 1,4-hydrovinylation reaction of TMS-protected allylic alcohol with 1,3-dienes of type **1**.

Entry	1,3-Diene (**1**)	1,4-Dienol (**2**)	Yield[a]
1	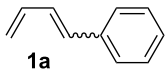 **1a**	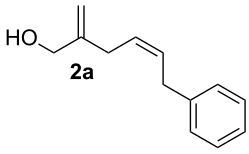 **2a**	60%
2	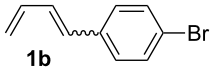 **1b**	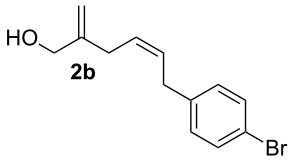 **2b**	71%
3	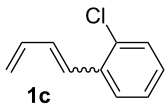 **1c**	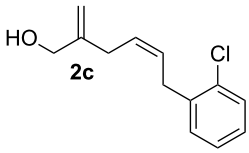 **2c**	81%
4	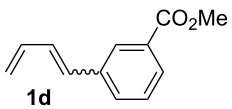 **1d**	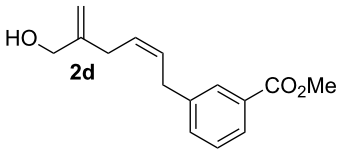 **2d**	51%
5	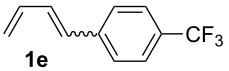 **1e**	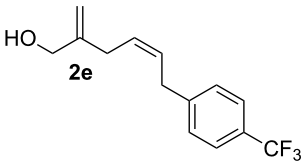 **2e**	69%
6	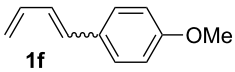 **1f**	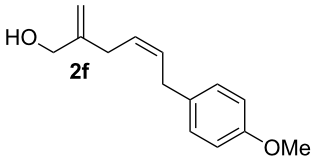 **2f**	87%
7	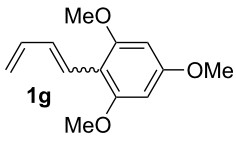 **1g**	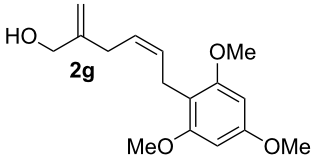 **2g**	64%
8	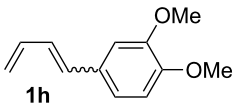 **1h**	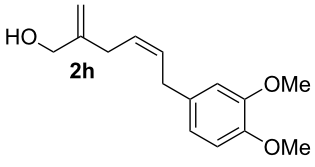 **2h**	67%

Table 1: Results of the cobalt-catalysed 1,4-hydrovinylation reaction of TMS-protected allylic alcohol with 1,3-dienes of type **1**. (continued)

9	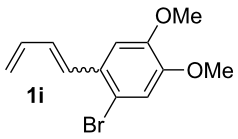 **1i**	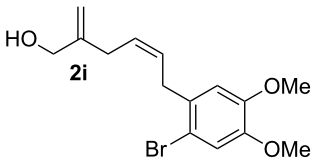 **2i**	60%
10	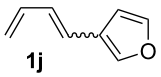 **1j**	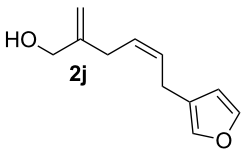 **2j**	59%
11	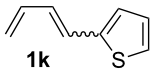 **1k**	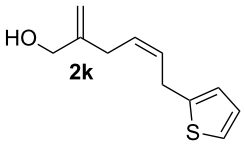 **2k**	87%
12	 **1l**	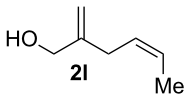 **2l**	92%[b]
13	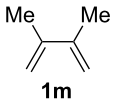 **1m**	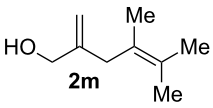 **2m**	90%[b]
14	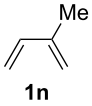 **1n**	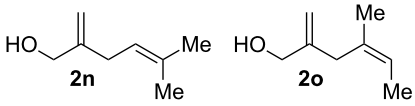 **2n** **2o**	89% (**2n**:**2o** = 79:21)

[a]Reaction conditions: (i) 1,3-diene (1.0 equiv), allyloxytrimethylsilane (1.2 equiv), $CoBr_2$(dppe) (5–10 mol %), Zn powder (10–20 mol %), ZnI_2 (10–20 mol %), CH_2Cl_2 (1 mL/mmol), rt, 12–16 h (ii) TBAF (1.1 equiv), THF, 0 °C, 3 h. [b]Reaction conditions: 1,3-diene (1.0 equiv), allyl alcohol (1.2–2.0 equiv), $CoBr_2$(dppe) (5–10 mol %), Zn powder (10–20 mol %), ZnI_2 (10–20 mol %), CH_2Cl_2 (1 mL/mmol), rt, 12–16 h.

enide and tetraethylammonium bromide in CH_3CN at room temperature in an undivided cell, using platinum foil electrodes (constant current 10 mA). In this investigation only diphenyl diselenide was used as selenium source. These reaction conditions led to the formation of products of type **3** as exclusive diastereomers (Scheme 2).

The cyclisation of **2** could lead to a number of products. The $PhSe^+$ cation could interact with the 1,1-disubstituted double bond and nucleophilic attack could lead to oxiran- or oxetan-type products. On the other hand, the interaction of the $PhSe^+$ ion with the 1,2-disubstituted double bond would lead to the furan-type products **3** or alternatively to pyran-type product **4**. The results of the electrochemical selenoalkoxylation of the 1,4-dienols are summarised in Table 2.

The electrochemical selenoalkoxylation of the aryl-substituted derivatives of type **2** (Table 2, entries 1–7) led exclusively to the tetrahydrofuran derivatives **3** via a 5-*exo*-*tet*-type cyclisation in moderate to good yields. The products were generated in diastereoselective fashion and the configuration of the formed diastereomer could be identified by ^1H NMR experiments

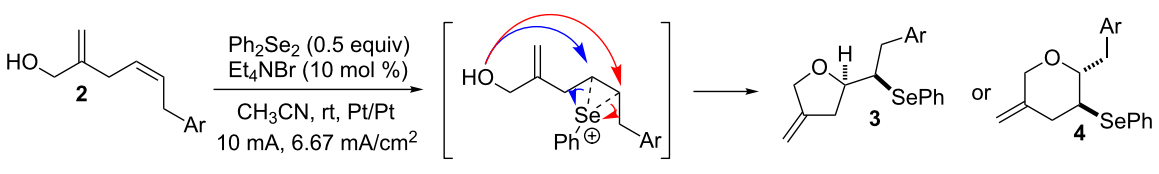

Scheme 2: Electrochemical selenoalkoxylation of **2**.

Table 2: Electrochemical selenoalkoxylation of 1,4-dienols **2**[a].

Entry	1,4-Dienol (**2**)	Furan (**3**) or pyran (**4**)	Yield[b]
1	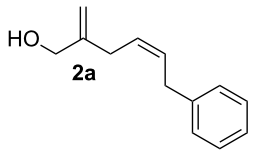 **2a**	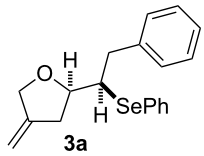 **3a**	50%
2	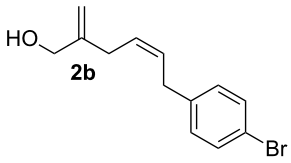 **2b**	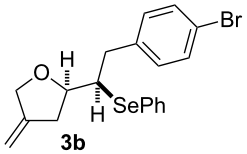 **3b**	82%
3	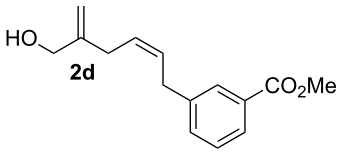 **2d**	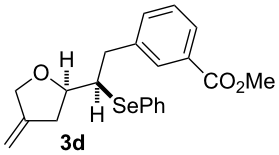 **3d**	58%
4	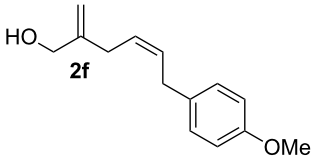 **2f**	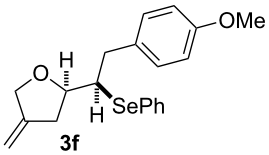 **3f**	68%
5	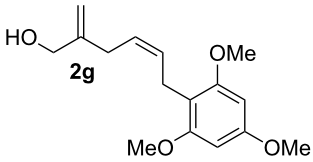 **2g**	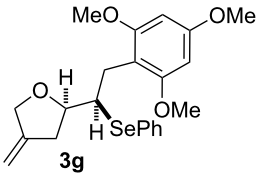 **3g**	42%
6	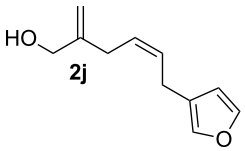 **2j**	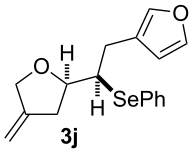 **3j**	90%
7	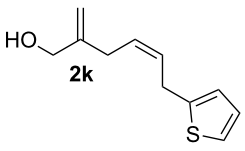 **2k**	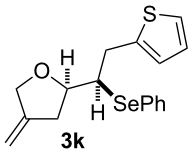 **3k**	62%
8	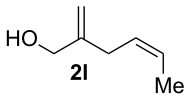 **2l**	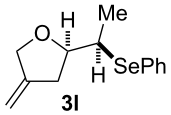 **3l**	86%
9	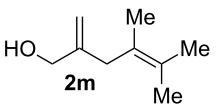 **2m**	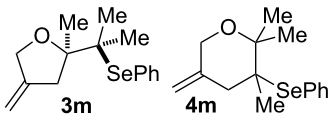 **3m** **4m**	46% (**3m**) 47% (**4m**)
10	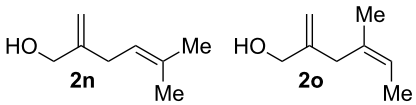 **2n** **2o**	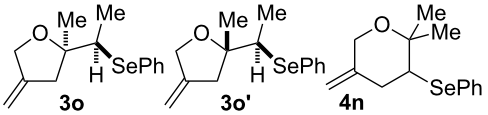 **3o** **3o'** **4n**	10% (**3o**+**3o'**) 58% (**4n**)

Table 2: Electrochemical selenoalkoxylation of 1,4-dienols **2**[a]. (continued)

11	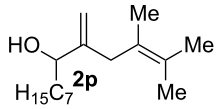	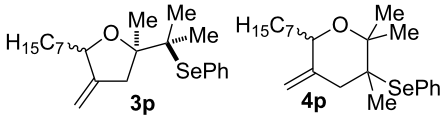	75% (**3p**:**4p** = 1:2.5)
12	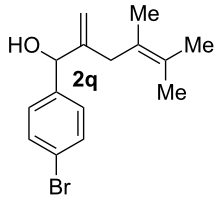	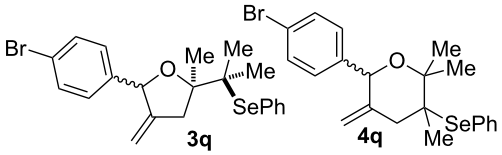	53% (**3q**:**4q** = 1:1.4)

[a]Reaction conditions: 1,4-dienol (0.5 mmol, 1.0 equiv), Ph_2Se_2 (0.5 equiv), Et_4NBr (0.1 equiv), CH_3CN (10 mL), rt, undivided cell, Pt/Pt, 10 mA, 6.67 mA/cm^2. [b]Oxidation of the alcohol could be observed in all reactions (less than 10%).

comparing a mixture of both diastereomers, synthesised by conventional selenoalkoxylation, with the electrochemically generated selenoether (see Supporting Information File 1). As a side reaction the oxidation of the alcohol could be observed in all reactions (less than 10%). Moreover, under electrochemical conditions the simple methyl-substituted derivative **2l** led to the tetrahydrofuran-type product **3l** in 86% yield (Table 2, entry 8) while the reaction using PhSeBr under conventional methods gave the product in 76% yield and a diastereoselectivity of 73:27 (*threo*:*erythro*). When alkyl-substituted 1,4-dienols are used, the formation of tetrahydrofuran or pyran derivatives can be observed (Table 2, entries 9 and 10). Depending on the substitution grade of the internal double bond, the alcohol functionality attacks at the less-substituted carbon of the internal double bond based on better stabilisation of the cationic intermediate. The triple methyl-substituted starting material **2m** gave a 1:1 mixture of tetrahydrofuran and pyran products **3m** and **4m**, the latter product is formed via a 6-*endo*-*tet*-type cyclisation, in an excellent combined yield of 93%. When the mixture of the 1,4-dienols (**2n** and **2o**) was applied, the major regioisomer **2n** gave the pyran exclusively in good yields, while the minor 1,4-dienol **2o** resulted in the formation of two tetrahydrofuran diastereomers which could be separated easily by column chromatography (Table 2, entry 10). Using higher substituted 1,4-dienols (**2p** and **2q)** a preferred formation of the pyran products was observed (Table 2, entries 11 and 12). However, under no circumstances the previously discussed strained epoxy-derivatives could be detected.

Transformation of 1,4-dienols via electrogenerated iodonium cations

In a similar approach we investigated the cyclisation of the 1,4-dienols **2** with in situ electrochemically generated iodonium ions for the desired synthesis of iodoalkoxylated products of type **5** (Scheme 3).

The electrolysis was carried out in an H-type divided cell (4G glass filter) equipped with carbon fiber electrodes (see Supporting Information File 1). Each chamber was charged with 2,6-lutidine and $TBABF_4$ in CH_3CN (0.3 M) and additionally the 1,4-dienol and sodium iodide were placed in the anode chamber. The reaction was performed at constant current electrolysis (10 mA) at 0 °C. It is considerable that the presence of 2,6-lutidine is crucial for a successful reaction. In the absence of 2,6-lutidine only traces of the product can be observed and oxidation of the alcohol functionality takes place. It is mentionable that under the reaction conditions no aromatic iodination could be observed. Next to sodium iodide other iodide sources such as

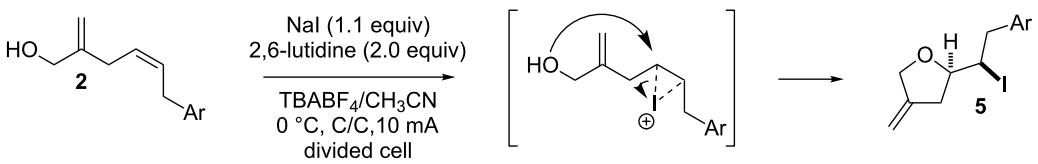

Scheme 3: Electrochemical iodoalkoxylation of **2**.

KI, I_2 or Bu_4NI can be used, whereas applying other halogenides such as NaBr, Et_4NBr or Bu_4NCl led to a complex mixture of products.

In this series of experiments we focussed our attention on the aryl-substituted 1,4-dienes to avoid undesired mixtures of tetrahydrofuran and pyran derivatives as obtained in the selenoalkoxylation for alkyl-substituted dienols. The results of the electrochemical iodoalkoxylation reactions are summarised in Table 3.

The electrochemical iodoalkoxylation of the aryl-substituted 1,4-dienols **2** led to the formation of the tetrahydrofuran derivatives **5** as single regio- and diastereomers. 1,4-Dienols with electron-donating and electron-withdrawing substituents as well as heterocyclic compounds gave the product of type **5** in good yields. It is noteworthy, that under these reaction conditions the electron-rich 1,4-dienols (**2g** and **2h**) gave higher yields than in the selenoalkoxylation (Table 3, entries 7 and 8). For compound **5g** the structure could be verified by X-ray analysis (see Supporting Information File 1). It is also considerable that the 1,4-dienols **2c**, **2e** and **2i** which did not gave the selenoether **3** led to a product formation in at least moderate yields of 40% to 46% (Table 3, entries 3, 5 and 9).

The products of the selenoalkoxylation as well as of the iodoalkoxylation are interesting building blocks for further transformations which are under current investigation.

Conclusion

In conclusion, we have developed the alkoxylation of 1,4-dienols by electrochemically generated selenium and iodonium cations. First, the synthesis of 1,4-dienols via a cobalt-catalysed 1,4-hydrovinylation of substituted 1,3-dienes with allyloxy-

Table 3: Electrochemical iodoalkoxylation of 1,4-dienols **2**.

Entry	1,4-Dienol **2**	Iodofuran **5**	Yield[a]
1	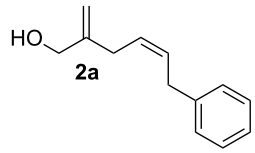 **2a**	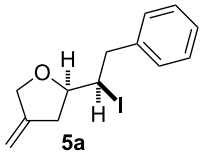 **5a**	66%
2	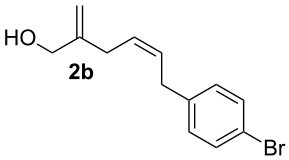 **2b**	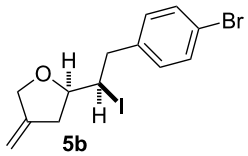 **5b**	60%
3	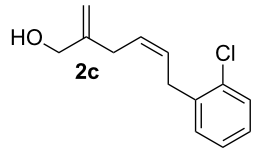 **2c**	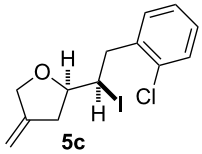 **5c**	40%
4	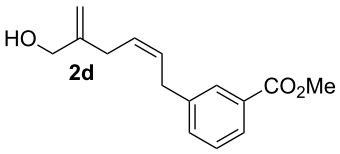 **2d**	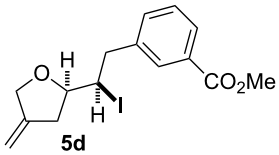 **5d**	68%
5	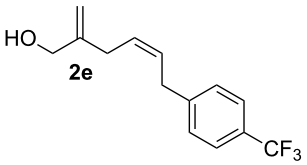 **2e**	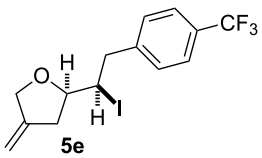 **5e**	46%
6	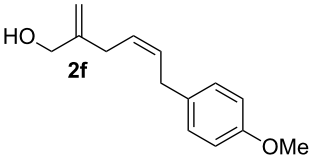 **2f**	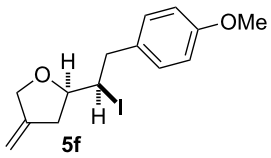 **5f**	68%

Table 3: Electrochemical iodoalkoxylation of 1,4-dienols **2**. (continued)

7	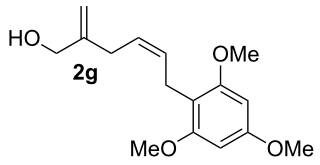 **2g**	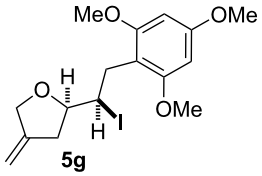 **5g**	70%
8	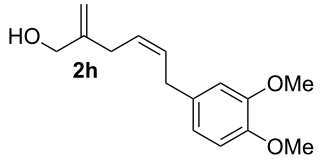 **2h**	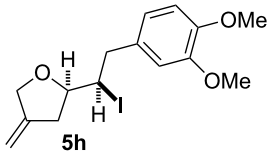 **5h**	67%
9	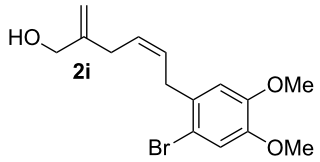 **2i**	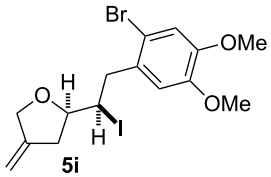 **5i**	46%
10	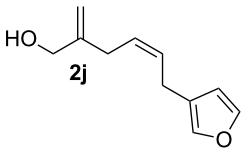 **2j**	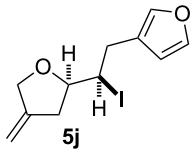 **5j**	82%
11	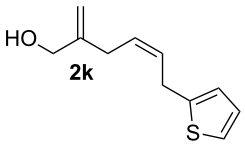 **2k**	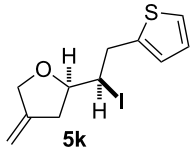 **5k**	66%

[a]Reaction conditions: H-type cell, anodic chamber: 1,4-dienol (0.5 mmol, 1.0 equiv), NaI (1.1 equiv), 2,6-lutidine (2.0 equiv), $TBABF_4/CH_3CN$ (0.3 M, 10 mL); cathode chamber: 2,6-lutidine (2.0 equiv), $TBABF_4/CH_3CN$ (0.3 M, 10 mL); 0 °C, C/C, 10 mA.

trimethylsilane or allyl alcohol has been elaborated. Those 1,4-dienols have been transformed into tetrahydrofuran or pyran derivatives by constant current electrolysis of suitable selenium and iodonium precursors. The reactions proceed in acceptable to good yields in regio- and diasterioselective fashion and tolerate a range of functionalities.

Experimental

General procedure for the cobalt-catalysed 1,4-hydrovinylation of aryl-substituted buta-1,3-dienes with allyloxytrimethylsilane and subsequent desilylation with TBAF

Cobalt dibromo(1,3-bis(diphenylphosphino)ethane) (5–10 mol %), zinc powder (10–20 mol %) and zinc iodide (10–20 mol %) were suspended in dichloromethane and stirred at room temperature for 20 min. Then the 1,3-butadiene (1.0 equiv) and the allyloxytrimethylsilane (1.2–2.0 equiv) were added and the mixture was stirred at room temperature until complete conversion was detected by TLC and GC–MS analysis. *n*-Pentane was added, the mixture was filtered through a short pad of silica and concentrated under reduced pressure. The crude material was dissolved in 5 mL tetrahydrofuran, TBAF (1 M in THF, 1.1 equiv) was added and the mixture was stirred at 0 °C for 3 h. Upon completion of the reaction 15 mL water were added, the mixture was extracted with diethyl ether (three times 15 mL), dried over Na_2SO_4, filtered and concentrated under reduced pressure. The product was obtained after column chromatography (*n*-pentane/diethyl ether).

General procedure for the cobalt-catalysed 1,4-hydrovinylation of buta-1,3-dienes with allyl alcohol

Cobalt dibromo(1,3-bis(diphenylphosphino)ethane) (5 mol %), zinc powder (10 mol %) and zinc iodide (10 mol %) were suspended in dichloromethane and stirred at room temperature for 20 min. Then the 1,3-butadiene (1.0 equiv) and allyl alcohol (1.2–1.5 equiv) were added and stirred at room temperature until complete conversion was detected by TLC and GC–MS analysis. Pentane was added and the mixture was filtered

through a short pad of silica. The solvent was evaporated and the crude product was purified by column chromatography to give the desired 1,4-diene.

General procedure for the electrochemical seleno-alkoxylation of 1,4-dienols

An undivided electrolysis cell was charged with diphenyl diselenide (78 mg, 0.25 mmol, 0.5 equiv), tetraethylammonium bromide (11 mg, 0.05 mmol, 0.1 equiv), the 1,4-diene (0.5 mmol, 1.0 equiv) and 10 mL acetonitrile. Then, the cell was equipped with a platinum plate anode and cathode and electrolysed under a constant current (10 mA, 6.67 mA/cm^2) at 20 °C until completion was detected by TLC and GC–MS analysis. Then, 15 mL water were added, the mixture was extracted with diethyl ether (three times 15 mL), dried over Na_2SO_4 and the solvent was removed under reduced pressure. The product was obtained after column chromatography (*n*-pentane/diethyl ether).

General procedure for the electrochemical iodonium-induced alkoxylation of 1,4-dienols

An H-type divided cell (4G glass filter) was equipped with a carbon fiber anode and carbon fiber cathode. Each chamber was charged with 10 mL $TBABF_4$ solution (0.3 M in acetonitrile) and 2,6-lutidine (2.0 equiv). The anodic chamber was charged with the 1,4-diene (1.0 equiv) and sodium iodide (1.1 equiv). Constant current electrolysis (10 mA) was carried out at 0 °C until completion was detected by TLC and GC–MS analysis. Then, 15 mL $Na_2S_2O_3$ solution (10% in water) were added to both chambers, the mixture was extracted with diethyl ether (three times 15 mL), dried over $MgSO_4$ and the solvent was removed under reduced pressure. The product was obtained after column chromatography (*n*-pentane/diethyl ether).

Supporting Information

Experimental details and detailed spectroscopic data of all compounds are available as Supporting Information. Single crystal data for compound **5g** (CCDC 1030546) has been deposited in the Cambridge Crystallographic Data Center.

Supporting Information File 1

Experimental details and detailed spectroscopic data.
[http://www.beilstein-journals.org/bjoc/content/supplementary/1860-5397-11-18-S1.pdf]

Acknowledgements

GH acknowledges a DAAD/JSPS short-term academic staff exchange fellowship to visit the Yoshida laboratories in Kyoto, Japan, in September 2013.

References

1. Hilt, G. *Eur. J. Org. Chem.* **2012,** 4441–4451. doi:10.1002/ejoc.201200212
2. Hilt, G. *Synlett* **2011,** 1654–1659. doi:10.1055/s-0030-1260800
3. RajanBabu, T. V. *Synlett* **2009,** 853–885. doi:10.1055/s-0028-1088213
4. RajanBabu, T. V. *Chem. Rev.* **2003,** *103,* 2845–2860. doi:10.1021/cr020040g
5. Arndt, M.; Dindaroğlu, M.; Schmalz, H.-G.; Hilt, G. *Org. Lett.* **2011,** *13,* 6236–6239. doi:10.1021/ol202696n
6. Arndt, M.; Dindaroğlu, M.; Schmalz, H.-G.; Hilt, G. *Synthesis* **2012,** 3534–3542. doi:10.1055/s-0032-1316796
7. Hilt, G.; Arndt, M.; Weske, D. F. *Synthesis* **2010,** 1321–1324. doi:10.1055/s-0029-1219278
8. Erver, F.; Kuttner, J. R.; Hilt, G. *J. Org. Chem.* **2012,** *77,* 8375–8385. doi:10.1021/jo301028b
9. Kersten, L.; Roesner, S.; Hilt, G. *Org. Lett.* **2010,** *12,* 4920–4923. doi:10.1021/ol102083v
10. Harmange, J.-C.; Figadère, B. *Tetrahedron: Asymmetry* **1993,** *4,* 1711–1754. doi:10.1016/S0957-4166(00)80408-5
11. Faulkner, D. J. *Nat. Prod. Rep.* **1998,** *15,* 113–158. doi:10.1039/A815113Y
12. Faul, M. M.; Huff, B. E. *Chem. Rev.* **2000,** *100,* 2407–2474. doi:10.1021/cr940210s
13. Lorente, A.; Lamariano-Merketegi, J.; Albericio, F.; Álvarez, M. *Chem. Rev.* **2013,** *113,* 4567–4610. doi:10.1021/cr3004778
14. Lund, H.; Hammerich, O. *Organic Electrochemistry,* 4th ed.; Marcel Dekker, Inc.: New York, 2001. ISBN:0-8247-0430-4.
15. Moeller, K. D. *Tetrahedron* **2000,** *56,* 9527–9554. doi:10.1016/S0040-4020(00)00840-1
16. Sperry, J. B.; Wright, D. L. *Chem. Soc. Rev.* **2006,** *35,* 605–621. doi:10.1039/B512308A
17. Yoshida, J.; Kataoka, K.; Horcajada, R.; Nagaki, A. *Chem. Rev.* **2008,** *108,* 2265–2299. doi:10.1021/cr0680843
18. Steckhan, E. *Angew. Chem., Int. Ed. Engl.* **1986,** *25,* 683–701. doi:10.1002/anie.198606831
19. Suga, S.; Matsumoto, K.; Ueoka, K.; Yoshida, J. *J. Am. Chem. Soc.* **2006,** *128,* 7710–7711. doi:10.1021/ja0625778
20. Uneyama, K.; Fujibayashi, S.; Torii, S. *Tetrahedron Lett.* **1985,** *26,* 4637–4638. doi:10.1016/S0040-4039(00)98772-0
21. Vukićević, R.; Konstantinović, S.; Mihailović, M. L. *Tetrahedron* **1991,** *47,* 859–865. doi:10.1016/S0040-4020(01)87074-5
22. Konstantinović, S.; Vukićević, R.; Mihailović, M. L. *Tetrahedron Lett.* **1987,** *28,* 6511–6512. doi:10.1016/S0040-4039(00)96902-8
23. Torii, S.; Uneyama, K.; Ono, M.; Tazana, H.; Matsunami, S. *Tetrahedron Lett.* **1979,** *20,* 4661–4662. doi:10.1016/S0040-4039(01)86676-4
24. Torii, S.; Uneyama, K.; Ono, M. *Tetrahedron Lett.* **1980,** *21,* 2653–2654. doi:10.1016/S0040-4039(00)92830-2
25. Torii, S.; Uneyama, K.; Ono, M. *Tetrahedron Lett.* **1980,** *21,* 2741–2744. doi:10.1016/S0040-4039(00)78594-7
26. Torii, S.; Uneyama, K.; Ono, M.; Bannou, T. *J. Am. Chem. Soc.* **1981,** *103,* 4606–4608. doi:10.1021/ja00405a064
27. Uneyama, K.; Takano, K.; Torii, S. *Tetrahedron Lett.* **1982,** *23,* 1161–1164. doi:10.1016/S0040-4039(00)87049-5
28. Chamberlin, A. R.; Dezube, M.; Dussault, P.; McMills, M. C. *J. Am. Chem. Soc.* **1983,** *105,* 5819–5825. doi:10.1021/ja00356a020
29. Labelle, M.; Guindon, Y. *J. Am. Chem. Soc.* **1989,** *111,* 2204–2210. doi:10.1021/ja00188a039

30. Still, W. C.; Schneider, M. J. *J. Am. Chem. Soc.* **1977,** *99,* 948–950. doi:10.1021/ja00445a050
31. Hajra, S.; Maji, B.; Karmakar, A. *Tetrahedron Lett.* **2005,** *46,* 8599–8603. doi:10.1016/j.tetlet.2005.09.170
32. Hartung, J.; Kneuer, R.; Laug, S.; Schmidt, P.; Špehar, K.; Svoboda, I.; Fuess, H. *Eur. J. Org. Chem.* **2003,** 4033–4052. doi:10.1002/ejoc.200300107
33. Denmark, S. E.; Burk, M. T. *Proc. Natl. Acad. Sci. U. S. A.* **2010,** *107,* 20655–20660. doi:10.1073/pnas.1005296107
34. Fujioka, H.; Maehata, R.; Wakamatsu, S.; Nakahara, K.; Hayashi, T.; Oki, T. *Org. Lett.* **2012,** *14,* 1054–1057. doi:10.1021/ol203425p
35. Fang, C.; Paull, D. H.; Hethcox, J. C.; Shugrue, C. R.; Martin, S. F. *Org. Lett.* **2012,** *14,* 6290–6293. doi:10.1021/ol3030555
36. Hennecke, U.; Müller, C. H.; Fröhlich, R. *Org. Lett.* **2011,** *13,* 860–863. doi:10.1021/ol1028805
37. Barluenga, J.; González, J. M.; Campos, P. J. *Angew. Chem., Int. Ed. Engl.* **1985,** *24,* 319–320. doi:10.1002/anie.198503191
38. Takaku, K.; Shinokubo, H.; Oshima, K. *Tetrahedron Lett.* **1996,** *37,* 6781–6784. doi:10.1016/S0040-4039(96)01499-2
39. Zhang, H.; Mootoo, D. R. *J. Org. Chem.* **1995,** *60,* 8134–8135. doi:10.1021/jo00130a009
40. Curini, M.; Epifano, F.; Marcotullio, M. C.; Montanari, F. *Synthesis* **2004,** 368–370. doi:10.1055/s-2003-45009
41. Bailey, A. D.; Cherney, S. M.; Anzalone, P. W.; Anderson, E. D.; Ernat, J. J.; Mohan, R. S. *Synlett* **2006,** 215–218. doi:10.1055/s-2005-923586
42. Miller, L. L.; Watkins, B. F. *Tetrahedron Lett.* **1974,** *15,* 4495–4496. doi:10.1016/S0040-4039(01)92201-4
43. Srebnik, M.; Mechoulam, R. *J. Chem. Soc., Chem. Commun.* **1984,** 1070–1071. doi:10.1039/C39840001070
44. Chavan, S. P.; Sharma, A. K. *Tetrahedron Lett.* **2001,** *42,* 4923–4924. doi:10.1016/S0040-4039(01)00876-0
45. Jones, C. C. Application of Hydrogen Peroxide and Derivatives. Clark, J. H., Ed.; RSC Clean Technology Monographs; The Royal Society of Chemistry: Cambridge, U.K., 1999. ISBN:978-0-85404-536-5.
46. Yoshida, J.; Suga, S.; Suzuki, S.; Kinomura, N.; Yamamoto, A.; Fujiwara, K. *J. Am. Chem. Soc.* **1999,** *121,* 9546–9549. doi:10.1021/ja9920112
47. Suga, S.; Suzuki, S.; Yamamoto, A.; Yoshida, J. *J. Am. Chem. Soc.* **2000,** *122,* 10244–10245. doi:10.1021/ja002123p
48. Yoshida, J.; Suga, S. *Chem. – Eur. J.* **2002,** *8,* 2650–2658. doi:10.1002/1521-3765(20020617)8:12<2650::AID-CHEM2650>3.0.CO;2-S
49. Nokami, T.; Ohata, K.; Inoue, M.; Tsuyama, H.; Shibuya, A.; Soga, K.; Okajima, M.; Suga, S.; Yoshida, J. *J. Am. Chem. Soc.* **2008,** *130,* 10864–10865. doi:10.1021/ja803487q
50. Ashikari, Y.; Shimizu, A.; Nokami, T.; Yoshida, J. *J. Am. Chem. Soc.* **2013,** *135,* 16070–16073. doi:10.1021/ja4092648
51. Morofuji, T.; Shimizu, A.; Yoshida, J. *Angew. Chem., Int. Ed.* **2012,** *51,* 7259–7262. doi:10.1002/anie.201202788
52. Torii, S.; Inokuchi, T.; Akahosi, F.; Kubota, M. *Synthesis* **1987,** 242–245. doi:10.1055/s-1987-27901
53. Hilt, G.; Danz, M.; Treutwein, J. *Org. Lett.* **2009,** *11,* 3322–3325. doi:10.1021/ol901064p

License and Terms

BEILSTEIN JOURNAL OF ORGANIC CHEMISTRY

Cathodic reductive coupling of methyl cinnamate on boron-doped diamond electrodes and synthesis of new neolignan-type products

Taiki Kojima[1], Rika Obata[2], Tsuyoshi Saito[3,4], Yasuaki Einaga[*1,4] and Shigeru Nishiyama[*1,4]

Letter

Open Access

Address:
[1]Department of Chemistry, Faculty of Science and Technology, Keio University, Hiyoshi 3-14-1 Kohoku-ku, Yokohama 223-8522, Japan, [2]Research and Education Center for Natural Sciences, Keio University, Hiyoshi 4-1-1 Kohoku-ku, Yokohama 223-8521, Japan, [3]International Institute for Integrative Sleep Medicine, University of Tsukuba, 1-1-1 Tennodai, Tsukuba, Ibaraki 305-8577, Japan and [4]Japan Science and Technology Agency (JST), CREST, Hiyoshi 3-14-1, Yokohama 223-8522, Japan

Email:
Yasuaki Einaga* - einaga@chem.keio.ac.jp; Shigeru Nishiyama* - nisiyama@chem.keio.ac.jp

* Corresponding author

Keywords:
boron-doped diamond (BDD) electrode; cathodic reduction; electrochemistry; electrosynthesis; neolignan

Beilstein J. Org. Chem. **2015,** *11,* 200–203.
doi:10.3762/bjoc.11.21

Received: 23 November 2014
Accepted: 16 January 2015
Published: 03 February 2015

This article is part of the Thematic Series "Electrosynthesis".

Guest Editor: S. R. Waldvogel

Abstract

The electroreduction reaction of methyl cinnamate on a boron-doped diamond (BDD) electrode was investigated. The hydrodimer, dimethyl 3,4-diphenylhexanedioate (racemate/meso = 74:26), was obtained in 85% yield as the major product, along with small amounts of cyclic methyl 5-oxo-2,3-diphenylcyclopentane-1-carboxylate. Two new neolignan-type products were synthesized from the hydrodimer.

Introduction

Numerous lignans and neolignans were found as secondary plant metabolites, and many of them are known to exhibit interesting biological activities [1]. Due to their plausible roles as defense substances of plants, lignans, neolignans, and their congeners are promising candidates for agricultural chemicals, and some of their antioxidant and/or anti-inflammatory properties may be utilized for biological research and as lead structures for chemotherapeutic agents. Despite consisting of two phenylpropane (C_6–C_3) fragments, the variety of carbon frameworks provides a huge library of lignans and neolignans [2-4]. As a result of their structural diversity, they have been targets of synthetic and biological investigations. Several synthetic

approaches, including electrochemical oxidative coupling reactions mimicking biosynthetic pathways, were reported to construct the backbones of these molecules [5]. Recently, boron-doped diamond (BDD) electrodes have attracted a great deal of attention for their wide potential window against evolution of both hydrogen and oxygen and for their high stability which is derived from their diamond carbon structure [6]. Although anodic oxidation reactions mediated by BDD electrodes have been exploited in organic synthesis, there have been only few reports regarding their application in preparative-scale cathodic reduction of organic compounds [7].

During our investigations of phenolic oxidation reactions using BDD electrodes, we observed the generation of solvent-derived methoxy radicals that conducted an oxidation process of the phenol substrate to the corresponding coupling product [8]. In our second investigation on the use of the BDD electrode in organic synthesis, the electrochemical reduction of methyl cinnamate (**1a**) was investigated to assess the applicability of BDD electrodes under cathodic reduction conditions, and to obtain new neolignan-type bioactive substances. As shown in Figure 1, the radical intermediate derived from phenylacrylate through a one-electron reduction (right) differs from that obtained by anodic oxidation of 4-hydroxyphenyl-1-propene (left). Therefore, the reductive dimerization of cinnamic acid derivatives was expected to provide access to unprecedented neolignan-type dimeric compounds.

Results and Discussion

Cathodic reduction on BDD electrode

The ester methyl cinnamate (**1a**) was electrolyzed under constant current electrolysis (CCE) conditions in a divided cell. Solvents used for the reactions played a significant role in providing the desired coupling (Table 1, entries 1–5). Thus, only acetonitrile (Table 1, entry 5) gave the desired coupling product (±)-**2** [9] in 4% yield, recovered educt **1a** and hydrolyzed product **1b**. The undesired hydrolysis could be depressed using a phosphate-buffered solution in the cathodic cell (pH 7, Table 1, entries 7–11), and finally the optimized conditions for the synthesis of **2** (85% yield, racemate/meso = 74:26) were acquired in the case of 2.5 F/mol current (Table 1, entry 11).

To check for a different behavior of the BDD electrode, several electrode materials, including glassy carbon (GC), platinum (Pt), and magnesium (Mg), were examined as cathodes under the optimized electrolytic conditions (Table 1, entry 11). Hydrogen evolution at the electrode was recognized when Pt and Mg electrodes were used, and the educt **1a** was recovered in high yield. The GC electrode provided the coupling product **2** (34%, racemate/meso = 74:26) and *E*-**3** (25%), along with 41% of **1a**. Similar cathodic reductions of cinnamate derivatives were carried out using Hg [10,11], Cu [12,13], Pb [13,14], Zn [13], Sn [13], and Ag [13], and the major products were the cyclic products (type **3**) through Diekmann-type cyclization, whereas the hydrodimer **2** was the predominantly produced product in the present BDD electrode mediated reduction. Despite a different product ratio, the GC electrode gave similar reaction products to that of the BDD electrode.

Synthesis of new neolignans

As shown in Scheme 1, after separation of the diastereomeric mixture, (±)-**2** was submitted to the chemical conversion into the new neolignan-type derivatives *E*-**5** and *E*-**8**. Thus, reduction of (±)-**2** with $LiAlH_4$ gave the alcohol (±)-**4** [15] in quantitative yield, which on oxidation with PCC [16] gave the lactone *E*-**5** in 32% yield. Selective DIBAL reduction of *E*-**5** gave an inseparable mixture of **6** and **7**, which were identified by ^{1}H NMR spectroscopy. Subsequent treatment of the mixture with Et_3SiH in the presence of $BF_3{\cdot}OEt_2$ finally gave *E*-**8**.

Conclusion

The cathodic reduction of **1a** using BDD electrode predominantly gave the dimeric product **2** in 85% yield. A

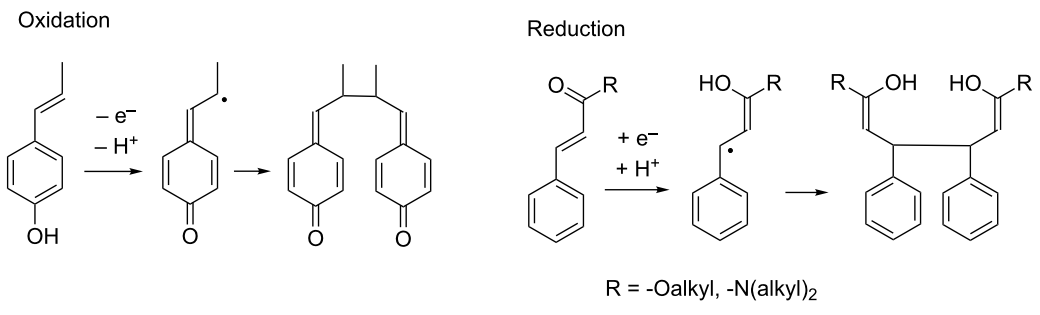

Figure 1: Expected coupling products from one-electron oxidation (left) and one-electron reduction (right) of C_6–C_3 compounds.

Table 1: Cathodic reduction of **1a** on a BDD electrode.

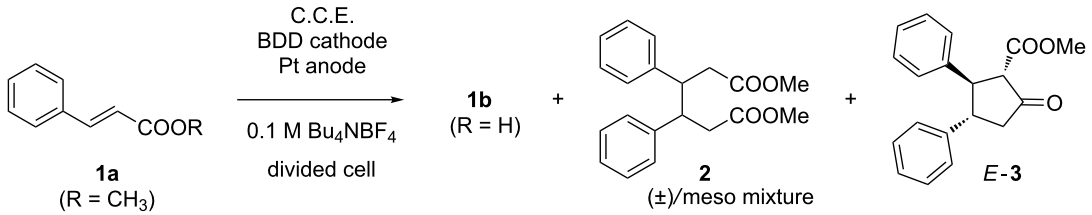

Entry[a]	Solvent	Current density (mA/cm^2)	Potential (V vs SCE)	F/mol	Yield (%)[b]			
					1a	**1b**	**2** [(±)/meso)][c]	**3**[d]
1	DMSO	0.21	−2.08 to −1.93	1	32	51	0	0
2	DMF	0.50	−1.96 to −1.86	1	43	43	0	0
3	TFE[e]	0.53	−2.00 to −1.85	1	100	0	0	0
4	MeOH	1.29	−2.08 to −1.84	1	74	12	0	0
5	MeCN	1.29	−2.00 to −1.88	1	42	46	4 (100/0)	0
6	MeCN[f]	1.29	−2.21 to −1.98	1	10	23	19 (79/21)	3
7	MeCN[g]	1.29	−2.07 to −1.89	1	23	13	33 (85/15)	5
8	MeCN[h]	1.29	−1.91 to −1.83	1	45	0	44 (73/27)	3
9	MeCN[h]	1.29	−2.02 to −1.84	1.5	26	0	67 (73/27)	5
10	MeCN[h]	1.29	−2.00 to −1.82	2.0	15	0	70 (73/27)	5
11	MeCN[h]	1.29	−2.12 to −1.93	2.5	1	0	85 (74/26)	4

[a]Upon using undivided cell systems, the reaction proceeded slower than in the divided cell cases, and lower selectivity of **2** and **3** was observed. [b]Isolated yields. [c]The ratio of (±) and meso forms was determined by ^{1}H NMR spectroscopy. [d]Enantiomeric mixture. [e]2,2,2-Trifluoroethanol. [f]Containing 0.07 M pH 6.0 phosphate buffer. [g]Containing 0.07 M pH 7.0 phosphate buffer. [h]Containing 0.33 M pH 7.0 phosphate buffer.

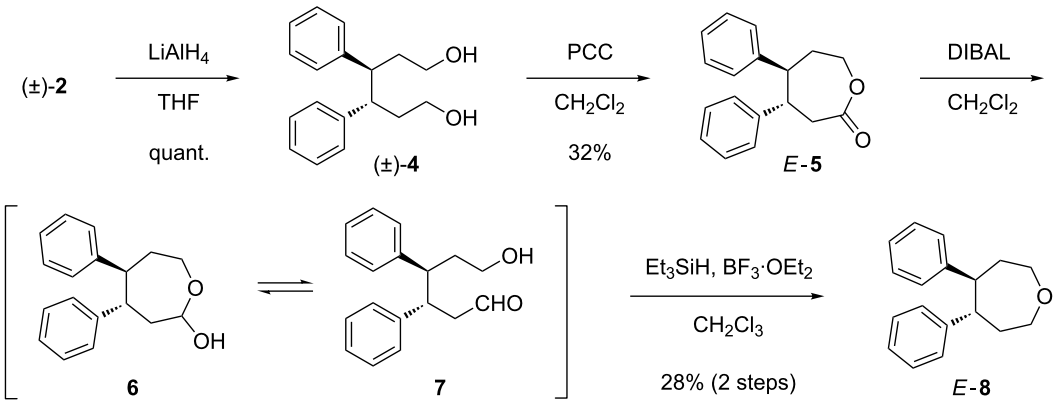

Scheme 1: Chemical conversion of (±)-**2** into *E*-**5** and *E*-**8**.

remarkable solvent effect of MeCN was observed for this dimerization reaction, while stereoselectivity was unaffected among the conditions tested and the racemic form was predominant over the meso form in all cases. Electrochemically prepared (±)-**2** was further converted into *E*-**5** and *E*-**8** as novel unprecedented neolignan-type derivatives. These results provide an example for an electroorganic synthesis using cathodic reductive coupling on a boron-doped diamond electrode.

Supporting Information

Supporting Information File 1

Instrumental setup, general procedure for the electrochemical reaction and physical and spectroscopic data for (±)-**2**, meso-**2**, *E*-**5**, and *E*-**8**.
[http://www.beilstein-journals.org/bjoc/content/supplementary/1860-5397-11-21-S1.pdf]

Acknowledgements

This research was supported by grants from the Science Research Promotion Fund from the Promotion and Mutual Aid Corporation for Private Schools of Japan from MEXT, the Research and Education Center for Natural Sciences Keio University, and Keio Gijuku Academic Development Funds (to RO).

References

1. Zhang, J.; Chen, J.; Liang, Z.; Zhao, C. *Chem. Biodiversity* **2014,** *11,* 1–54. doi:10.1002/cbdv.201100433
2. Apers, S.; Vlietinck, A.; Pieters, L. *Phytochem. Rev.* **2003,** *2,* 201–207. doi:10.1023/B:PHYT.0000045497.90158.d2
3. Ward, R. S. *Nat. Prod. Rep.* **1999,** *16,* 75–96. doi:10.1039/a705992b
4. Ward, R. S. *Nat. Prod. Rep.* **1997,** *14,* 43–74. doi:10.1039/np9971400043
5. Quideau, S.; Pouységu, L.; Duffieux, D. *Curr. Org. Chem.* **2004,** *8,* 113–148. doi:10.2174/1385272043486016
   And related references cited therein.
6. Fuchigami, T.; Atobe, M.; Inagi, S. New Methodology of Organic Electrochemical Synthesis. In *Fundamentals and Applications of Organic Electrochemistry: Synthesis, Materials, Devices;* Fuchigami, T.; Atobe, M.; Inagi, S., Eds.; John Wiley & Sons: Chichester, U.K., 2015; pp 129–186.
7. Waldvogel, S. R.; Mentizi, S.; Kirste, A. *Top. Curr. Chem.* **2012,** *320,* 1–31. doi:10.1007/128_2011_125
8. Sumi, T.; Saitoh, T.; Natsui, K.; Yamamoto, T.; Atobe, M.; Einaga, Y.; Nishiyama, S. *Angew. Chem., Int. Ed.* **2012,** *51,* 5443–5446. doi:10.1002/anie.201200878
9. Curtin, D. Y.; Dayagi, S. *Can. J. Chem.* **1964,** *42,* 867–877. doi:10.1139/v64-129
   See for a separation of the (±)-and meso-forms of **2**.
10. Klemm, L. H.; Olson, D. R. *J. Org. Chem.* **1973,** *38,* 3390–3394. doi:10.1021/jo00959a034
11. Fussing, I.; Güllü, M.; Hammerich, O.; Hussain, A.; Nielsen, M. F.; Utley, J. H. P. *J. Chem. Soc., Perkin Trans. 2* **1996,** 649–658. doi:10.1039/P29960000649
12. Nishiguchi, I.; Hirashima, T. *Angew. Chem., Int. Ed. Engl.* **1983,** *22,* 52–53. doi:10.1002/anie.198300521
13. Kise, N.; Iitaka, S.; Iwasaki, K.; Ueda, N. *J. Org. Chem.* **2002,** *67,* 8305–8315. doi:10.1021/jo026183k
14. Kise, N.; Echigo, M.; Shono, T. *Tetrahedron Lett.* **1994,** *35,* 1897–1900. doi:10.1016/S0040-4039(00)73190-X
15. Brook, A. G.; Cohen, H. L.; Wright, G. F. *J. Org. Chem.* **1953,** *18,* 447–463. doi:10.1021/jo01132a012
16. Ohgiya, T.; Nakamura, K.; Nishiyama, S. *Bull. Chem. Soc. Jpn.* **2005,** *78,* 1549–1554. doi:10.1246/bcsj.78.1549

BEILSTEIN JOURNAL OF ORGANIC CHEMISTRY

Switching the reaction pathways of electrochemically generated β-haloalkoxysulfonium ions – synthesis of halohydrins and epoxides

Akihiro Shimizu, Ryutaro Hayashi, Yosuke Ashikari, Toshiki Nokami[§] and Jun-ichi Yoshida[*]

Full Research Paper

Open Access

Address:
Department of Synthetic Chemistry and Biological Chemistry, Graduate School of Engineering, Kyoto University, Kyotodaigaku-Katsura, Nishikyo-ku, Kyoto 615-8510, Japan

Email:
Jun-ichi Yoshida[*] - yoshida@sbchem.kyoto-u.ac.jp

* Corresponding author
§ Present address: Department of Chemistry and Biotechnology, Graduate School of Engineering, Tottori University, 4-101 Koyama-chominami, Tottori 680-8552, Japan

Keywords:
DMSO; electrosynthesis; epoxides; halohydrins; halogen cations

Beilstein J. Org. Chem. **2015,** *11,* 242–248.
doi:10.3762/bjoc.11.27

Received: 30 November 2014
Accepted: 30 January 2015
Published: 13 February 2015

This article is part of the Thematic Series "Electrosynthesis".

Guest Editor: S. R. Waldvogel

Abstract

β-Haloalkoxysulfonium ions generated by the reaction of electrogenerated Br^+ and I^+ ions stabilized by dimethyl sulfoxide (DMSO) reacted with sodium hydroxide and sodium methoxide to give the corresponding halohydrins and epoxides, respectively, whereas the treatment with triethylamine gave α-halocarbonyl compounds.

Introduction

Alkene difunctionalization through three-membered ring halonium ion intermediates [1] is an important transformation in organic synthesis. Usually the halonium ions such as bromonium or iodonium ions are generated by the reaction of alkenes with Br_2 and I_2 [2]. However, the most straightforward method is the reaction of alkenes with halogen cations such as Br^+ and I^+. The I^+ cation pool exists as reported by Filimonov et al. [3], although the used solvent is concentrated sulfuric acid which is therefore not compatible with most organic compounds.

Electrochemical oxidation [4-11] is a potent technique to generate and accumulate highly reactive cationic species in solution (the "cation pool" method) [12-17]. Although halogen cations are too unstable to accumulate in solution as "cation pools", halogen cations stabilized by an appropriate stabilizing agent that coordinates the cations can be accumulated in the solution. For example, "I^+" cations stabilized by acetonitrile (CH_3CN) [18-20] or by trimethyl orthoformate (TMOF) [21] were reported in the literature. Recently, we reported that dimethyl sulfoxide (DMSO) can also be used to effectively stabilize halogen cations (Scheme 1) [22].

The pools of stabilized halogen cations enable alkene difunctionalization. We previously reported that the reaction of

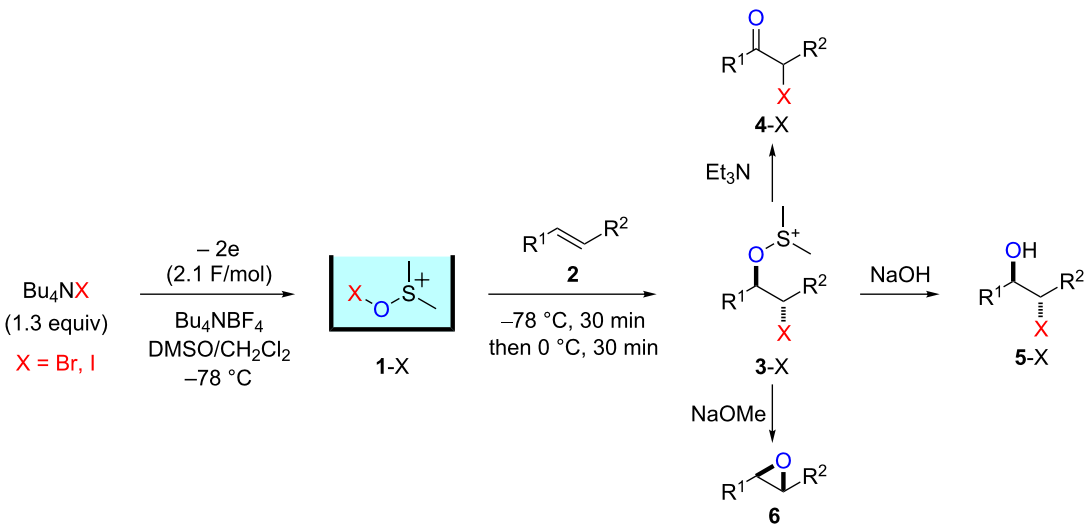

Scheme 1: Synthesis of halohydrins and epoxides through β-haloalkoxysulfonium ions generated by the reaction of alkenes with DMSO-stabilized halogen cations.

alkenes with DMSO-stabilized halogen cations such as Br^+ and I^+ gave β-haloalkoxysulfonium ions and their subsequent treatment with triethylamine gave α-halocarbonyl compounds through Swern–Moffatt-type oxidation [23-27]. Recently reaction integration [28-31] has received significant research interest because it enhances the power and speed of organic syntheses and this is an example of integration of an electrochemical reaction and a chemical reaction using a reactive intermediate. Herein, we report that the reaction pathways of β-haloalkoxysulfonium ions can be switched to give different products by changing the base, thus expanding the utility of the present method. The treatment of β-haloalkoxysulfonium ions **3**-X with sodium hydroxide gave the corresponding halohydrins **5**-X, while the treatment with sodium methoxide gave epoxides **6** (Scheme 1).

Results and Discussion

Reactions of β-bromoalkoxysulfonium ions generated from (*Z*)-5-decene

We first examined the reactions of β-bromoalkoxysulfonium ion **3a**-Br generated by the reaction of (*Z*)-5-decene (**2a**) with Br^+/DMSO (**1**-Br) [21] (Scheme 1, X = Br). Bu_4NBr in DMSO/CH_2Cl_2 (1:9 v/v) was electrochemically oxidized at −78 °C in a divided cell using Bu_4NBF_4 as a supporting electrolyte until 2.1 F/mol of electricity was applied. After addition of **2a** to the solution, the mixture was stirred at 0 °C to give **3a**-Br, which was characterized by NMR spectroscopy [22]. The treatment of **3a**-Br with triethylamine gave α-bromoketone **4a**-Br in 83% yield [22]. However, the treatment of **3a**-Br with NaOH gave bromohydrin **5a**-Br in 89% yield as shown in Table 1. These phenomena can be explained as follows: Due to the steric repulsion, triethylamine cannot attack the sulfur atom in **3a**-Br and acts as base to abstract a proton attached to the carbon adjacent to the sulfur. The formed carbanion part of the resulting sulfur ylide abstracts a proton attached to the carbon adjacent to the oxygen to give α-bromoketone **4a**-Br by the Swern–Moffatt-type oxidation mechanism [23-27]. On the other hand, the hydroxide ion attacks the sulfur atom in **3a**-Br and cleaves the S–O bond to give the alkoxide ion, which is protonated by water to give bromohydrin **5a**-Br (Scheme 2). The stereochemistry determined by NMR (**5a**-Br was synthesized using NBS according to the literature; see Supporting Information File 1) indicated that the addition of Br^+ and DMSO across the C–C double bond was anti-selective, which is consistent with the results reported previously [22].

Treatment of **3a**-Br with NaOMe resulted in a different product, namely epoxide **6a** in 95% yield. In this case, the methoxide ion attacks the sulfur atom and cleaves the S–O bond under formation of an alkoxide ion. The latter intramolecularly attacks the carbon atom bearing the bromine substituent to give epoxide **6a** (Scheme 2). Presumably, the protonation of the alkoxide ion with MeOH is slower than the intramolecular nucleophilic attack. We could not exclude the possibility that a protonated DMSO molecule presumably generated by the reaction of **3a**-Br with the hydroxide ion protonates the alkoxide ion to give **5a**-Br, while a methylated DMSO molecule presumably generated by the reaction of **3a**-Br with the methoxide ion cannot protonate the alkoxide ion, which converts to **6a**. The stereochemistry determined by NMR [32] is consistent with a mechanism involving the back-side attack of the alkoxide ion to form epoxide **6a**.

Table 1: Reaction of **3a**-X (X = Br, I) with different bases.[a]

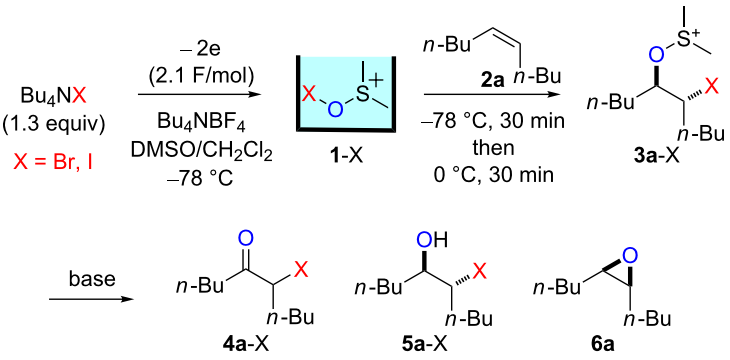

	% Yield of product[b]					
	X = Br			X = I		
Base	**4a**-Br	**5a**-Br	**6a**	**4a**-Ir	**5a**-I	**6a**
Et_3N/CH_2Cl_2	83	ND	ND	85	ND	1
$NaOH/H_2O$	ND	89	2	ND	84	1
NaOMe/MeOH	ND	ND	95	ND	ND	96

[a]The electrolysis was carried out using 1.3 equiv of Bu_4NBr or Bu_4NI (based on the alkene which was added after electrolysis) with 2.1 F/mol of electricity based on Bu_4NBr or Bu_4NI. [b]Yields were determined by GC.

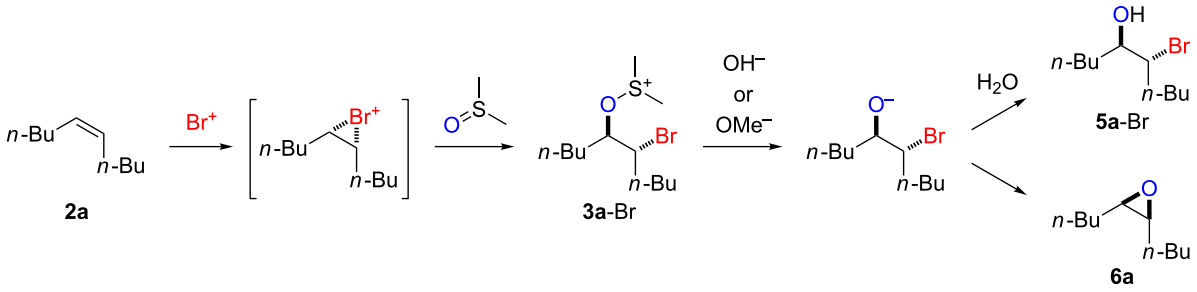

Scheme 2: Proposed reaction mechanisms for the syntheses of bromohydrin **5a**-Br and epoxide **6a**.

Reactions of β-iodoalkoxysulfonium ions generated from (*Z*)-5-decene

We next examined the reactions of β-iodoalkoxysulfonium ion **3a**-I generated by the reaction of (*Z*)-5-decene (**2a**) with I^+/DMSO (**1**-I) cation pool [22] (Scheme 1, X = I). Bu_4NI in $DMSO/CH_2Cl_2$ (1:9 v/v) was electrochemically oxidized at −78 °C in a divided cell using Bu_4NBF_4 as a supporting electrolyte until 2.1 F/mol of electricity was applied. After addition of **2a** to the solution, the mixture was stirred at 0 °C to give **3a**-I, which was characterized by NMR spectroscopy [22]. The treatment of **3a**-I with triethylamine gave α-iodoketone **4a**-I in 85% yield as we reported previously [22]. However, the treatment of **3a**-I with NaOH and NaOMe gave iodohydrin **5a**-I in 84% yield and epoxide **6a** in 96% yield, respectively (Table 1). The stereochemistry as determined by NMR (**5a**-I was synthesized using I_2 and H_2O_2; see Supporting Information File 1) indicated that the addition of I^+ and DMSO across the C–C double bond was anti-selective as anticipated.

Synthesis of halohydrins and epoxides from various alkenes

The present method was successfully applied to the synthesis of halohydrins and epoxides from various alkenes. The reactions of alkenes with **1**-X followed by the treatment with NaOH gave the corresponding halohydrins as shown in Table 2. The reactions of *E* and *Z* isomers of 1-phenyl-1-propene (**2d**) with **1**-Br gave **5d**-Br and **5d'**-Br, respectively (Table 2, entries 7 and 9), indicating the anti-addition of Br^+ and DMSO across the C–C double bond. The reaction with **1**-I also gave the anti-addition products (Table 2, entries 8 and 10). Therefore, the reaction is

Table 2: Synthesis of halohydrins by the reaction of **1**-X with alkenes followed by the treatment with NaOH.[a]

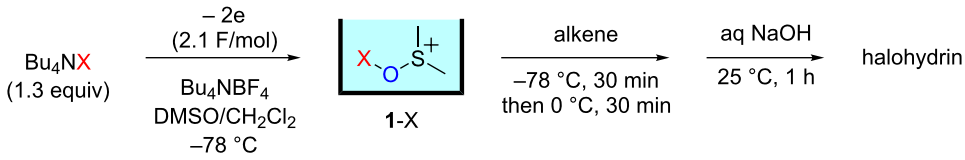

Entry	Alkene	Product	Yield (%)[b]
1 2	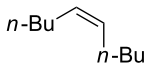 **2a**	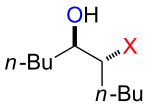 **5a**-Br, **5a**-I	**5a**-Br: 87 **5a**-I: 84[c]
3 4	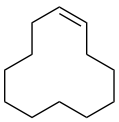 **2b** (*Z*:*E* = 72:28)	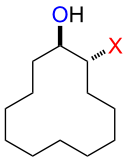 **5b**-Br, **5b**-I	**5b**-Br: 74 (trans:cis = 79:21) **5b**-I: 94 (trans:cis = 71:29)
5 6	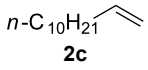 **2c**	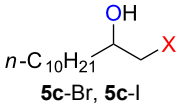 **5c**-Br, **5c**-I	**5c**-Br: 57 **5c**-I: 53
7 8	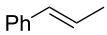 (*E*)-**2d**	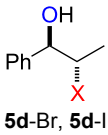 **5d**-Br, **5d**-I	**5d**-Br: 73 **5d**-I: 35
9 10	 (*Z*)-**2d**	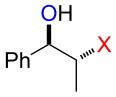 **5d'**-Br, **5d'**-I	**5d'**-Br: 75 **5d'**-I: 51

[a]The electrolysis of Bu_4NBr and Bu_4NI was carried out using 1.3 equiv of Bu_4NX (based on the alkene which was added after the electrolysis) with 2.1 F/mol of electricity based on Bu_4NX. [b]Isolated yield. [c]Yield was determined by GC.

stereospecific, and the stereochemistry is consistent with the proposed reaction mechanism (Scheme 2). The addition of Br^+ or I^+ and DMSO to unsymmetrically substituted olefins **2c** and **2d** regioselectively gave bromohydrins as single regioisomers (Table 2, entries 5–10). The regioselectivity of the products can be explained by the stability of carbocations (benzyl > secondary > primary). In the case of terminal alkene **2c**, Br and I were introduced to a primary carbon atom, whereas OH was introduced to a secondary carbon atom. In the case of styrene derivative **2d**, Br and I were introduced to a secondary carbon, whereas OH was introduced to the benzyl carbon. DMSO seems to attack the more positively charged carbon of the three-membered ring bromonium ion or iodonium ion.

The reaction of **1**-X with alkenes followed by the treatment with NaOMe gave the corresponding epoxides as shown in Table 3. Alkenes having an alkoxycarbonyl group gave the corresponding epoxides in moderate yields (Table 3, entries 11–14). Diene **2f** reacted with **1**-Br and **1**-I to give monoepoxide **6f** in moderate yields (Table 3, entries 13 and 14). Interestingly, **2g** reacted with **1**-Br to give **6g** but not with **1**-I (Table 3, entries 15 and 16), although the reason is not clear at present. The facial selectivity of the reaction is the opposite to that of the epoxidation using conventional reagents such as *m*-chloroperoxybenzoic acid (mCPBA) which epoxidizes alkenes from the less hindered face [33,34]. In this reaction, Br^+ adds to the C–C double bond of **2g** from the less hindered face to form the corresponding three-membered ring bromonium ion intermediate. Subsequently, DMSO attacks the bromonium ion from the more hindered face to form the corresponding β-haloalkoxysulfonium ion. The treatment of the β-haloalkoxysulfonium ion with NaOMe cleaves the O–S bond to generate the alkoxide

Table 3: Synthesis of epoxides by the reaction of **1**-X with alkenes followed by the treatment with NaOMe.[a]

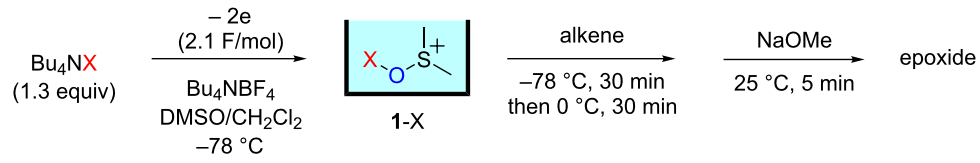

Entry	Alkene	Product	X	Yield (%)[b]
1	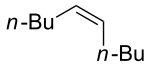 **2a**	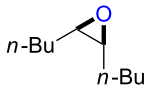 **6a**	Br	95[c]
2			I	96[c]
3	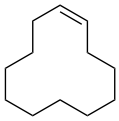 **2b** (*Z*:*E* = 72:28)	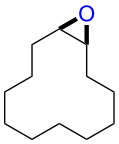 **6b**	Br	68 (*cis*:*trans* = 74:26)
4			I	89 (*cis*:*trans* = 74:26)
5	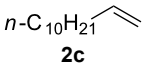 **2c**	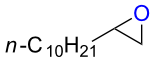 **6c**	Br	73[c]
6			I	86[c]
7	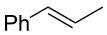 (*E*)-**2d**	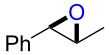 **6d**	Br	53
8			I	38[d]
9	 (*Z*)-**2d**	 **6d'**	Br	60
10			I	67[d]
11	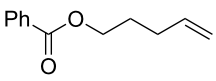 **2e**	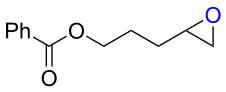 **6e**	Br	52[e]
12			I	57[e]
13	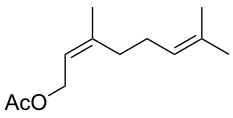 **2f**	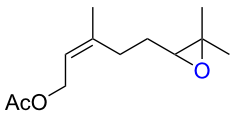 **6f**	Br	49[e]
14			I	47[e]
15	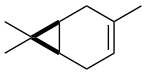 **2g**	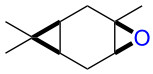 **6g**	Br	69
16			I	0

[a]The electrolysis was carried out using 1.3 equiv of Bu_4NBr or Bu_4NI (based on the alkene which was added after electrolysis) with 2.1 F/mol of electricity based on Bu_4NBr or Bu_4NI. [b]Isolated yield. [c]Yield was determined by GC. [d]2.0 Equiv of Bu_4NI was used. [e]Reacted with 2.5 equiv of NaOMe for 2 h.

ion, which attacks the carbon atom bearing bromine to give epoxide **6g**. Therefore, the installation of the oxygen atom takes place from the more hindered face.

Reaction mechanism

To confirm the mechanism shown in Scheme 2, the experiment was repeated using ^{18}O-labeled DMSO (96% ^{18}O)/CH_2Cl_2 (1:50 v/v). As outlined in Scheme 3, epoxide **6c** containing ^{18}O (94% ^{18}O) was obtained in 81% yield, indicating that the oxygen atom in the product originated from DMSO. Since ^{18}O-labeled DMSO can be easily obtained from $H_2{}^{18}O$ [35], the present transformation serves as a convenient method for synthesizing ^{18}O-labeled epoxides, that can be used for various mechanistic and biological studies.

Conclusion

In conclusion, we found that the reaction pathways of β-haloalkoxysulfonium ions generated by the reaction of elec-

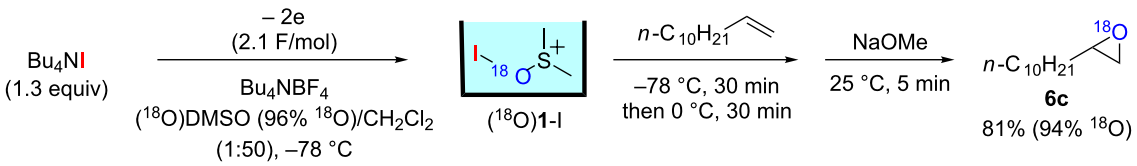

Scheme 3: Mechanistic study using ^{18}O-DMSO.

trogenerated Br^+ and I^+ stabilized by dimethyl sulfoxide (DMSO) can be switched by changing the nature of the base. The present transformation serves as stereospecific route to halohydrins and epoxides from alkenes. The method is also useful for synthesizing ^{18}O-labeled epoxides.

Supporting Information

Supporting Information File 1

Experimental and analytical data.
[http://www.beilstein-journals.org/bjoc/content/supplementary/1860-5397-11-27-S1.pdf]

Acknowledgements

We thank the Ministry of Education, Culture, Sports, Science & Technology, Japan, for a Grant-in-Aid for Scientific Research on Innovative Areas, 2105. We also thank Taiyo Nippon Sanso Corporation for partial support of this work including providing $H_2{}^{18}O$.

References

1. Olah, G. A.; Laali, K. K.; Wang, Q.; Prakash, G. K. S. *Onium ions;* Wiley: New York, 1998; pp 246–268.
2. Rodriguez, J.; Dulcère, J.-P. *Synthesis* **1993,** 1177–1205. doi:10.1055/s-1993-26022
3. Chaikovski, V. K.; Kharlova, T. S.; Filimonov, V. D.; Saryucheva, T. A. *Synthesis* **1999,** 748–750. doi:10.1055/s-1999-3475
4. Moeller, K. D. *Tetrahedron* **2000,** *56,* 9527–9554. doi:10.1016/S0040-4020(00)00840-1
5. Sperry, J. B.; Wright, D. L. *Chem. Soc. Rev.* **2006,** *35,* 605–621. doi:10.1039/b512308a
6. Yoshida, J.; Kataoka, K.; Horcajada, R.; Nagaki, A. *Chem. Rev.* **2008,** *108,* 2265–2299. doi:10.1021/cr0680843
7. Kirste, A.; Elsler, B.; Schnakenburg, G.; Waldvogel, S. R. *J. Am. Chem. Soc.* **2012,** *134,* 3571–3576. doi:10.1021/ja211005g
8. Finney, E. E.; Ogawa, K. A.; Boydston, A. J. *J. Am. Chem. Soc.* **2012,** *134,* 12374–12377. doi:10.1021/ja304716r
9. Sumi, K.; Saitoh, T.; Natsui, K.; Yamamoto, T.; Atobe, M.; Einaga, Y.; Nishiyama, S. *Angew. Chem., Int. Ed.* **2012,** *51,* 5443–5446. doi:10.1002/anie.201200878
10. Morofuji, T.; Shimizu, A.; Yoshida, J. *J. Am. Chem. Soc.* **2013,** *135,* 5000–5003. doi:10.1021/ja402083e
11. Yamaguchi, Y.; Okada, Y.; Chiba, K. *J. Org. Chem.* **2013,** *78,* 2626–2638. doi:10.1021/jo3028246
12. Yoshida, J.; Suga, S.; Suzuki, S.; Kinomura, N.; Yamamoto, A.; Fujiwara, K. *J. Am. Chem. Soc.* **1999,** *121,* 9546–9549. doi:10.1021/ja9920112
13. Suga, S.; Suzuki, S.; Yamamoto, A.; Yoshida, J. *J. Am. Chem. Soc.* **2000,** *122,* 10244–10245. doi:10.1021/ja002123p
14. Yoshida, J.; Suga, S. *Chem. – Eur. J.* **2002,** *8,* 2650–2658. doi:10.1002/1521-3765(20020617)8:12<2650::AID-CHEM2650>3.0.CO;2-S
15. Suzuki, S.; Matsumoto, K.; Kawamura, K.; Suga, S.; Yoshida, J. *Org. Lett.* **2004,** *6,* 3755–3758. doi:10.1021/ol048524h
16. Suga, S.; Matsumoto, K.; Ueoka, K.; Yoshida, J. *J. Am. Chem. Soc.* **2006,** *128,* 7710–7711. doi:10.1021/ja0625778
17. Matsumoto, K.; Sanada, T.; Shimazaki, H.; Shimada, K.; Hagiwara, S.; Fujie, S.; Ashikari, Y.; Suga, S.; Kashimura, S.; Yoshida, J. *Asian J. Org. Chem.* **2013,** *2,* 325–329. doi:10.1002/ajoc.201300017
18. Miller, L. L.; Kujawa, E. P.; Campbell, C. B. *J. Am. Chem. Soc.* **1970,** *92,* 2821–2825. doi:10.1021/ja00712a036
19. Miller, L. L.; Watkins, B. F. *J. Am. Chem. Soc.* **1976,** *98,* 1515–1519. doi:10.1021/ja00422a039
20. Midorikawa, K.; Suga, S.; Yoshida, J. *Chem. Commun.* **2006,** 3794–3796. doi:10.1039/b607284d
21. Shono, T.; Matsumura, Y.; Katoh, S.; Ikeda, K.; Kamada, T. *Tetrahedron Lett.* **1989,** *30,* 1649–1650. doi:10.1016/S0040-4039(00)99543-1
22. Ashikari, Y.; Shimizu, A.; Nokami, T.; Yoshida, J. *J. Am. Chem. Soc.* **2013,** *135,* 16070–16073. doi:10.1021/ja4092648
23. Kornblum, N.; Powers, J. W.; Anderson, G. J.; Jones, W. J.; Larson, H. O.; Levand, O.; Weaver, W. M. *J. Am. Chem. Soc.* **1957,** *79,* 6562. doi:10.1021/ja01581a057
24. Mancuso, A. J.; Swern, D. *Synthesis* **1981,** 165–185. doi:10.1055/s-1981-29377
25. Phan, T. B.; Nolte, C.; Kobayashi, S.; Ofial, A. R.; Mayr, H. *J. Am. Chem. Soc.* **2009,** *131,* 11392–11401. doi:10.1021/ja903207b
26. Ashikari, Y.; Nokami, T.; Yoshida, J. *J. Am. Chem. Soc.* **2011,** *133,* 11840–11843. doi:10.1021/ja202880n
27. Ashikari, Y.; Nokami, T.; Yoshida, J. *Org. Biomol. Chem.* **2013,** *11,* 3322–3331. doi:10.1039/c3ob40315g
28. Schmidt, B. *Pure Appl. Chem.* **2009,** *78,* 469–476. doi:10.1351/pac200678020469
29. Enders, D.; Hüttl, M. R. M.; Grondal, C.; Raabe, G. *Nature* **2006,** *441,* 861–863. doi:10.1038/nature04820
30. Yoshida, J.; Saito, K.; Nokami, T.; Nagaki, A. *Synlett* **2011,** 1189–1194. doi:10.1055/s-0030-1259946
31. Suga, S.; Yamada, D.; Yoshida, J. *Chem. Lett.* **2010,** *39,* 404–406. doi:10.1246/cl.2010.404
32. Brimeyer, M. O.; Mehrota, A.; Quici, S.; Nigam, A.; Regen, S. L. *J. Org. Chem.* **1980,** *45,* 4254–4255. doi:10.1021/jo01309a047
33. Gianini, M.; von Zelewsky, A. *Synthesis* **1996,** 702–706. doi:10.1055/s-1996-4280

34. Majetich, G.; Shimkus, J.; Li, Y. *Tetrahedron Lett.* **2010,** *51,* 6830–6834. doi:10.1016/j.tetlet.2010.10.068
35. Fenselau, A. M.; Moffatt, J. G. *J. Am. Chem. Soc.* **1966,** *88,* 1762–1765. doi:10.1021/ja00960a033

License and Terms

BEILSTEIN JOURNAL OF ORGANIC CHEMISTRY

Photovoltaic-driven organic electrosynthesis and efforts toward more sustainable oxidation reactions

Bichlien H. Nguyen, Robert J. Perkins, Jake A. Smith and Kevin D. Moeller*

Commentary

Open Access

Address:
Washington University in Saint Louis, Saint Louis, Missouri 63130, United States

Email:
Kevin D. Moeller* - moeller@wustl.edu

* Corresponding author

Keywords:
electrochemistry; sustainable oxidation reactions; visible light

Beilstein J. Org. Chem. **2015,** *11,* 280–287.
doi:10.3762/bjoc.11.32

Received: 18 December 2014
Accepted: 09 February 2015
Published: 23 February 2015

This article is part of the Thematic Series "Electrosynthesis".

Guest Editor: S. R. Waldvogel

Abstract

The combination of visible light, photovoltaics, and electrochemistry provides a convenient, inexpensive platform for conducting a wide variety of sustainable oxidation reactions. The approach presented in this article is compatible with both direct and indirect oxidation reactions, avoids the need for a stoichiometric oxidant, and leads to hydrogen gas as the only byproduct from the corresponding reduction reaction.

Introduction

Organic electrochemistry is an extremely versatile tool for conducting a wide variety of chemical reactions [1-3]. This versatility stems from both the gentle, acid/base neutral reaction conditions employed for the reactions and the adjustable potential of the working electrode that enables the oxidation and reduction of substrates that often greatly differ in their electronic structure.

It is particularly easy to take advantage of the opportunities electrochemistry offers when conducting constant current (galvanostatic) electrolysis [4]. When a constant current is passed through an electrolysis cell, the potential at the anode increases until it reaches that of the substrate in solution with the lowest oxidation potential. It then remains constant at that potential until the effective concentration of the substrate at the anode decreases to the point that the rate of substrate oxidation is small relative to the rate of electron transfer. At that point, the potential at the anode begins to increase and the selectivity of the reaction for the initial substrate is lost. When a low current density is used for the reaction, over 90% of the initial substrate can be consumed before this loss of selectivity occurs. Hence, at low current densities a constant current electrolysis reaction automatically adjusts to the potential of the substrate to be oxidized and then remains at that potential for the majority of the reaction. In this way, a series of substrates can be selectively oxidized using the same reaction conditions even if the

substrates have significantly different oxidation potentials. For most of the following cases discussed, reticulated vitreous carbon (RVC) is used as a highly porous anode material to keep current densities low. All of the RVC electrodes used were of 100 pores per inch and approximately 1 × 1 cm in size, and thus the differences in current are directly proportional to the current density from experiment to experiment. An equal but opposite reduction reaction happens at the cathode. For all of the oxidation reactions highlighted in this work, this reduction reaction leads to the formation of hydrogen gas.

In addition to the direct oxidation of a substrate described in the preceding paragraph, indirect electrochemical methods also offer a powerful means of recycling chemical oxidants [5]. In such experiments, the potential at the anode increases to a point where it matches the oxidation potential of the reduced chemical oxidant (Scheme 1). The reduced chemical oxidant is then oxidized in order to generate the active chemical oxidant. The chemical oxidant then performs the desired chemical transformation before returning to the anode as its reduced form. The process converts the chemical oxidant into a catalyst. Since the oxidant is not consumed during the reaction, the potential at the anode remains constant throughout the electrolysis. As in the direct oxidation, the corresponding reduction reaction at the cathode generates hydrogen gas. Hence, the reactions allow for the use of a chemical oxidant together with its inherent selectivity while avoiding the byproducts associated with consumption of the reagent.

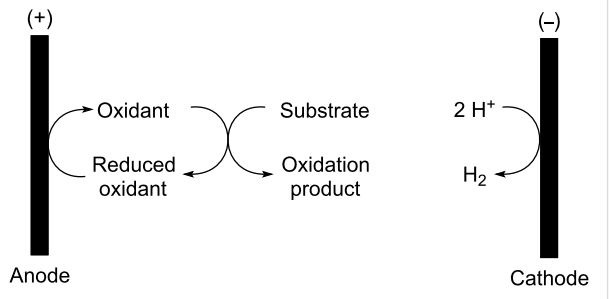

Scheme 1: Electrochemical recycling of a chemical oxidant.

Based on this scenario, it is tempting to suggest electrochemistry is a “green method”. However, any attempt to promote electrochemistry as being environmentally benign must account for both the use of the electrolyte in the reactions and the source of the electricity used.

Most electrochemical reactions require the use of an electrolyte. The electrolyte provides counter ions for the ions generated at the electrodes and serves to reduce the resistance of the cell by making the electron-transfer reaction at the electrodes easier. The presence of this electrolyte, often used in large excess, can render an electrochemical reaction less than sustainable unless the electrolyte is recycled. A number of research groups have addressed this issue by either providing alternative electrolytes that can be easily recycled [6] or conducting the reactions in ionic liquids [7]. An alternative approach takes advantage of flow technology. In these experiments, the electrolysis reaction solution is flowed as a thin film between two closely spaced electrodes. The small separation between the electrodes enables the charged molecules generated at each electrode to interact. This neutralizes the charges, reduces the resistance of the cell, and eliminates the need for an electrolyte [8].

With efforts to address the electrolyte problem already underway in the community, we turned our attention to the source of electricity. Since the potential at the electrodes in a constant current electrolysis automatically adjusts to match that of the substrates, in principle, any source of current can be used to drive the reactions in a selective fashion. With this in mind, it seemed that a photovoltaic system would make an excellent power supply for performing the reactions with minimal environmental impact. There are numerous commercial photovoltaic systems that can be used to convert visible light into electricity, two of which are shown in Figure 1 [9].

The first is a portable photovoltaic device capable of generating a potential large enough to recharge a wide variety of batteries. The second is a much less expensive alternative that is sold for use in connection with science fair projects and the operation of solar-driven toys [10]. Both can be used to power an electrochemical reaction, and both offer the opportunity to perform oxidation reactions that consume only sunlight and generate hydrogen gas as the only byproduct.

The experimental setup for a photochemically driven reaction is trivial. One simply needs to connect the wires originating from the photovoltaic source to the electrodes used for the reaction. One can vary the current passing through the cell by simply changing the amount of photovoltaic that is exposed to light. With a large panel like the one shown in Figure 1a, regions of the array can be covered to generate only a small amount of current. For the smaller units (Figure 1b), the total surface area of photovoltaic can be controlled by varying the number of individual photovoltaic cells connected in series. One is, thus, not limited by the day to day variations in sunlight intensity, as the current through the cell can be adjusted very quickly using these methods.

With an experimental design in place, a series of direct and indirect oxidation reactions were used to determine the viability of the method [11,12].

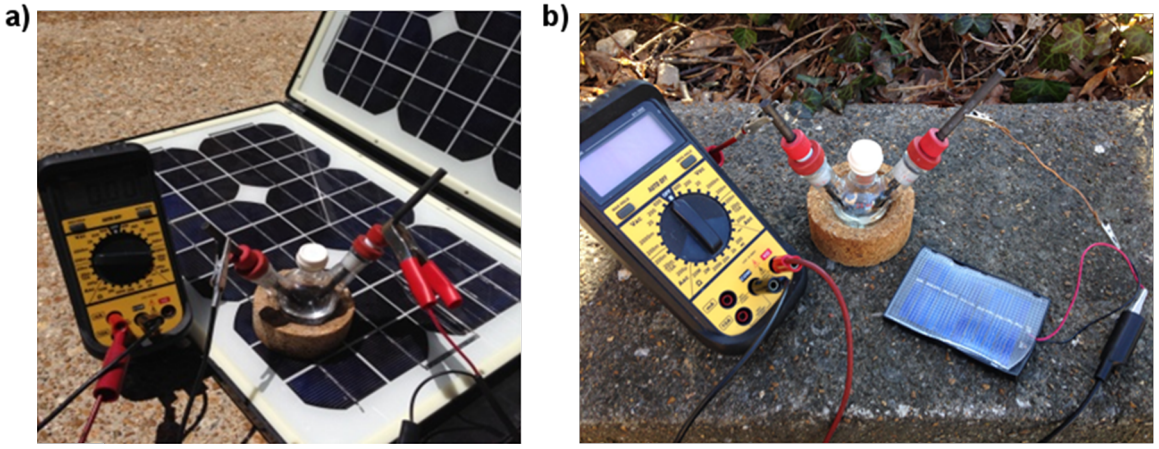

Figure 1: a) Electrolysis setup with a “suitcase” photovoltaic device. b) Electrolysis with a very simple, commercially available, photovoltaic cell.

Discussion

Direct oxidation

Initial efforts began by examining reactions where the substrate to be oxidized underwent the electron-transfer reaction directly at the electrode surface. We have employed reactions of this nature to functionalize amides [13,14] and to conduct umpolung reactions [15,16] that originate from electron-rich olefins [17]. Two examples are given in Scheme 2 [11]. A yield for the reactions is given for an experiment using photovoltaics as the power supply and a comparable reaction using a more traditional electrochemical setup. The photovoltaic-based reactions were conducted by adjusting the area of the photovoltaic cell exposed to the light until the current passing through the reaction was the same as that used with the traditional setup. The two cases in Scheme 2 were selected because the oxidation potential of the substrates differed by more than 0.5 V. However, that difference in potential had little effect on the success of the electrolysis reactions, as the potential at the anode surface adjusted to that of the substrate. In both cases, the reaction using the photovoltaic system led to excellent product yield. In the case of the amide oxidation, a lower current was passed through the cell for the photovoltaic relative to the traditional setup. The lower current was a result of limitations associated with the very simple photovoltaic system employed (Figure 1b). The inexpensive photovoltaic setup did not produce a large enough potential drop to overcome the resistance of an electrolysis reaction with a more difficult-to-oxidize substrate. The use of a larger photovoltaic cell would have afforded a

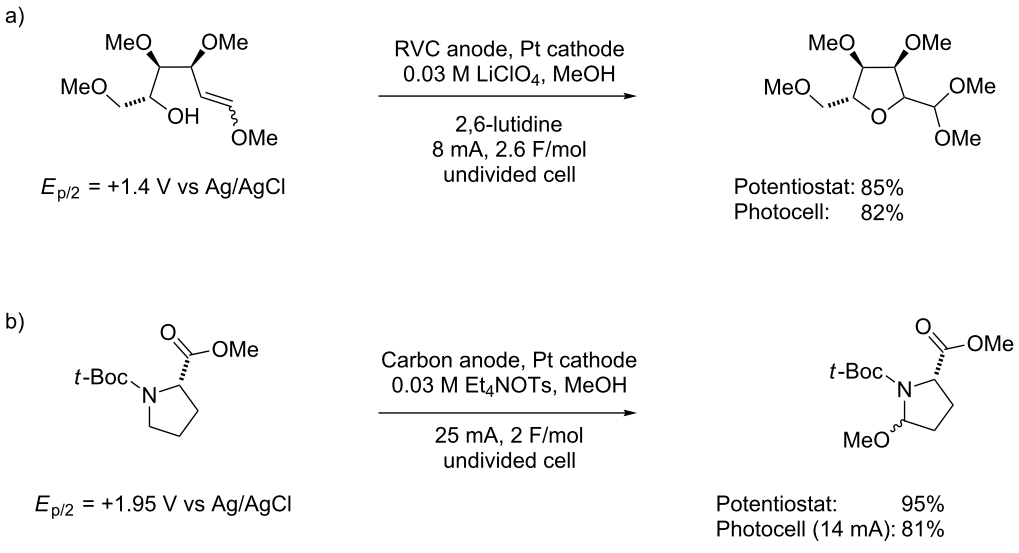

Scheme 2: Examples of solar-driven direct electrochemical oxidations.

larger potential drop across the cell, a scenario that would allow for the passage of more current through the cell. This approach would have been undertaken if further optimization of the reaction had been needed. Another point of interest is related to the choice of the electrolyte for the reaction. The reactions highlighted in Scheme 2 provide an opportunity to address this issue. Typically, the choice of electrolyte is not crucial, and tetraethylammonium tosylate can be employed for the majority of reactions reported. However, this is not always the case. In the first reaction shown, $LiClO_4$ was used as the electrolyte when a reaction utilizing Et_4NOTs failed to afford the product [18]. The change was made because of the polarity of the substrate. In an electrolysis reaction, the electrolyte forms a double layer immediately around the electrode surface that can prevent molecules from reaching the electrode. For example, a "greasy" hydrocarbon-based electrolyte will form a hydrophobic double layer and exclude polar molecules from the region surrounding the electrode. This was the case when Et_4NOTs was used as the electrolyte for the oxidation of the sugar derivative (Scheme 2a). The result was a dramatic reduction in the current efficiency of the process. The switch to $LiClO_4$ as the electrolyte led to a more hydrophilic double layer that no longer excluded the sugar-based substrate, leading to an improved current efficiency and a high product yield.

A number of direct electrolysis reactions were driven by visible light using the same approach shown in Scheme 2. In almost every case, the simple visible-light-driven electrolysis setup appropriately mimicked reactions performed with the significantly more sophisticated electrochemical equipment. The examples where the simple electrolysis setup was not as effective typically required more careful control of the current and hence the working potential of the electrode. The reaction in Scheme 3 provides an example of such a reaction. In this reaction, the initially formed cyclic product has an oxidation potential that is not significantly higher than that of the starting material. As a result, undesired oxidation of the product and cleavage of the dithioketal moiety were observed. When a photovoltaic device was used to conduct the reaction, an increase in this over-oxidation product was observed, presumably due to lessened control of the current being passed through the reaction.

Indirect oxidation

While direct oxidation reactions can be powerful synthetic tools, electrochemical reactions are typically more selective and are based on the relative oxidation potential of the various groups in solution. The group with the lowest oxidation potential is the group that will be oxidized. Chemical oxidations, however, do not have this limitation. They can be selective for one substrate based on steric effects, chirality, or other factors. For this reason, the sunlight-driven oxidation reactions were extended to the recycling of chemical oxidants. Three examples are shown in Scheme 4 [12] where each was chosen for its unique feature related to the indirect electrochemical approach.

In the first reaction (Scheme 4a), an asymmetric dihydroxylation with $K_2OsO_2(OH)_4$ and hydroquinidine 1,4-phthalazinediyl diether ($(DHQD)_2PHAL$) was performed in a catalytic fashion by recycling the ferricyanide cooxidant at the anode [19]. In this case, the use of the chemical oxidation strategy allows for incorporation of an asymmetry-inducing element into the transition state for the oxidation in a manner not possible with a direct electrochemical oxidation.

The oxidation proceeded smoothly in the light-driven electrochemical reaction. The yield and ee of the product was in accordance with that reported in the literature for the reaction using a traditional electrochemical setup. The same electrochemical solar cell developed for the direct oxidation experiments could be utilized to conduct indirect electrolysis.

In the second oxidation illustrated, 2,2,6,6-tetramethylpiperidin-1-oxyl (TEMPO) was recycled at the anode [20]. The bulky oxidant was used to selectively oxidize the primary alcohol of a glucose derivative in the presence of the unprotected secondary alcohols. Once again, this is an example of selectivity that cannot be accomplished with a direct electrochemical oxidation,

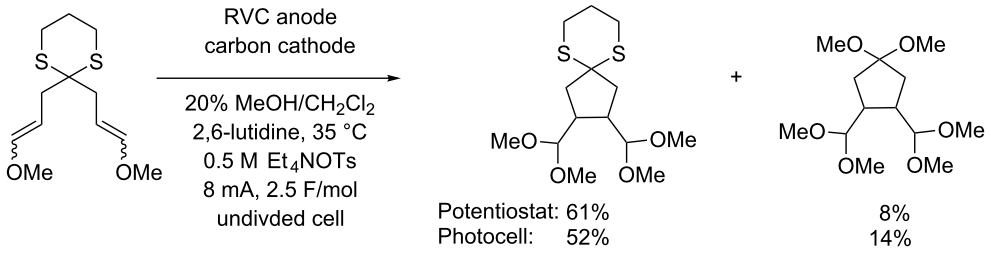

Scheme 3: Overoxidation of dithioketal.

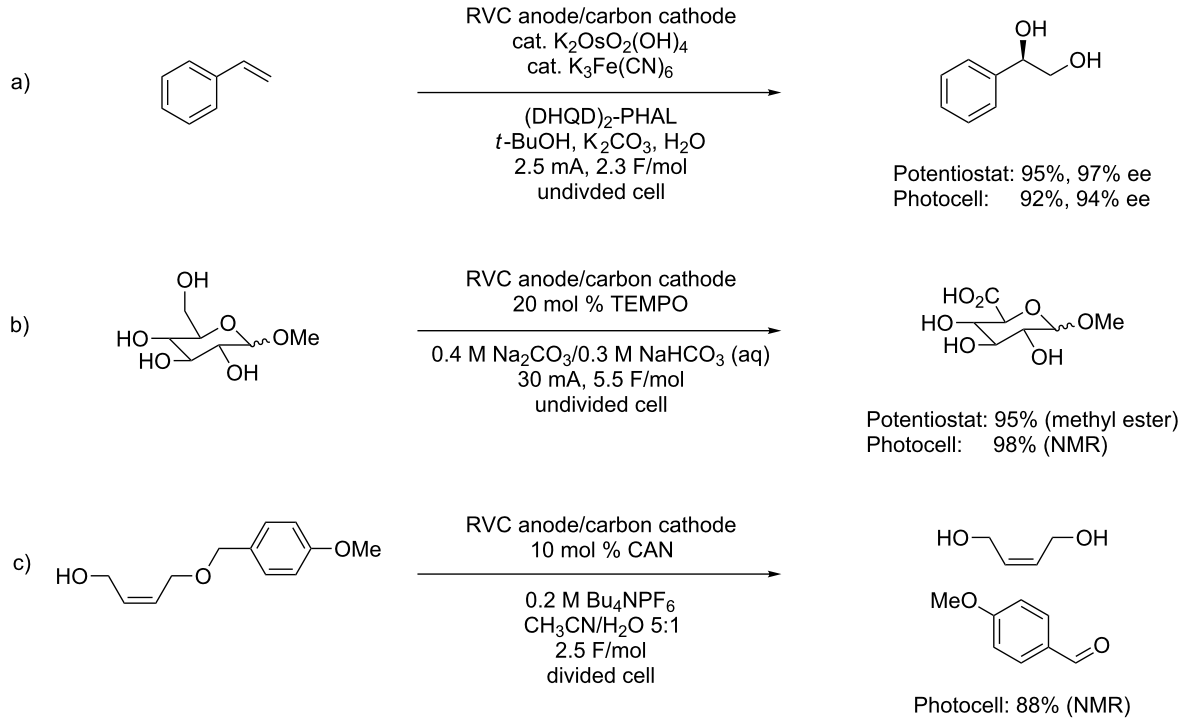

Scheme 4: Examples of solar-driven, indirect electrochemical oxidations.

which would select the oxidation based exclusively on potential. Again, the yield from the light-driven process is comparable to the literature value for the oxidation.

The final oxidation in Scheme 4c illustrates the use of the light-driven electrolysis reaction for recycling ceric ammonium nitrate (CAN) for a *p*-methoxybenzyl deprotection of an alcohol proceeding through oxidation of the aromatic ring. This is a reaction that does not have a direct literature precedent on a preparative scale. Instead, it is an electrochemical reaction that was initially developed in the context of performing site-selective reactions on a microelectrode array [21]. It was selected for discussion here because the reaction serves to both illustrate the range of oxidation reactions that can be performed in a catalytic fashion using a simple photovoltaic and highlight the scalability of the process. In order to perform the reaction on a preparative scale, the array-based method was increased by twelve orders of magnitude without any change in the overall reaction conditions.

Recent advances

The reactions illustrated above are an ideal set. Each was selected to address a key scientific point and because the electrochemical reaction used was straightforward and not particularly complex. The reactions were all easily performed at room temperature and were conducted in simple electrochemical cells and governed by the initial electron-transfer reaction. Given that not all electrochemical oxidation reactions are so straightforward, the compatibility of such a simple photovoltaic power supply with a more challenging electrolysis reaction is a valid concern. In the following section, the use of the visible-light-driven electrolysis setup for three such reactions is illustrated.

The first case stems from the use of an anodic coupling reaction to make *C*-glycoside derivatives from styrenes (Scheme 5) [22]. We have found that the yield of product obtained in these reactions is directly dependent on the efficient removal of a second electron from the system. This requires higher current densities at the electrodes and often the use of more electrolyte. Neither requirement is a problem for the visible-light-driven electrolysis system. The reaction using the photovoltaic power supply provided the same result as the electrolysis using a more advanced electrochemical setup.

The second example (Scheme 6) involves an oxidative condensation reaction between an aromatic aldehyde and a diamine [23-25]. The reaction requires a careful balance between the initial condensation reaction and the oxidative step with either CAN or DDQ serving as the mediator.

In the third reaction (Scheme 7), an intramolecular alcohol nucleophile was added to an olefin coupling reaction [26].

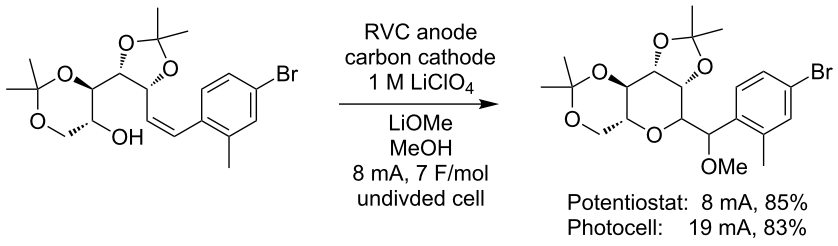

Scheme 5: Solar-driven synthesis of *C*-glycosides.

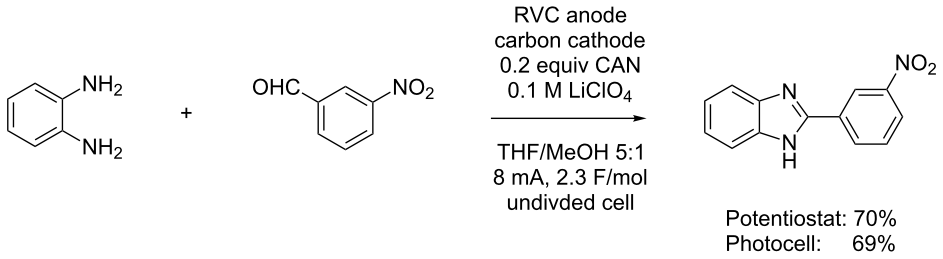

Scheme 6: Solar-driven oxidative condensation.

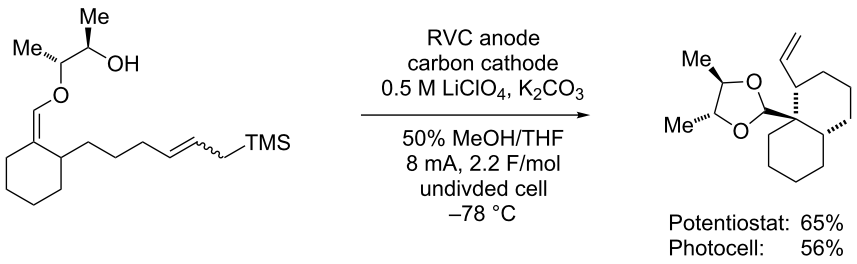

Scheme 7: Solar-driven oxidative cyclization with a second nucleophile.

When a radical cation was generated from the enol ether, it was rapidly trapped by the alcohol nucleophile. This generated a radical that was in turn trapped by an allylsilane. The loss of a second electron and elimination of the silyl group led to the final product. To be successful, the reaction needed to overcome the barriers of quaternary carbon and six-membered ring formation. The use of the second nucleophile and a fast initial trapping reaction reduced the cation character of the radical cation intermediate, slowed competitive elimination reactions, and allowed for the desired quaternary carbon formation. In these reactions, the initial alcohol trapping reaction was found to be both exothermic and reversible. Hence, cooling the reaction to −78 °C helped to maintain the initial cyclization and to keep the cation character of the reactive intermediate low. This significantly increased the yield of the desired cyclization.

As in the previous cases, none of these complications (or the need for the lower reaction temperature) prevented the use of the very simple reaction setup. The use of the photovoltaic system with visible light to generate the electricity needed for the reaction led to product yields only slightly less than those obtained when the overall system was more carefully controlled.

Conclusion

A broad range of electrochemical oxidations can be performed in a fashion that consumes only visible light and generates hydrogen gas as the only byproduct. The reactions include both direct and indirect oxidation strategies, which can be used to generate new carbon–carbon bonds, functionalize amides, and capitalize on the reagent-based selectivity associated with

chemical oxidants. In all cases, the use of constant current electrolysis conditions allows the potential at the anode surface to be adjusted to that of the substrate. Hence, the same experimental protocol can be used for each reaction.

It should be noted, that in many ways, the use of a simple photovoltaic device to directly power an electrochemical reaction as illustrated in Figure 1 is a gimmick. For a more complex system or large-scale electrolysis, a more sophisticated photovoltaic array would be used to harvest enough energy to run a standard potentiostat. This would result in a far more selective electrolysis since the current passed through the reaction could be carefully controlled and the efficiency of the electrochemical process optimized. However, the use of a simple photovoltaic device to drive the reactions does highlight two key points. First, the reactions illustrate how electrochemistry can be used to expand the growing area of visible-light-driven chemistry to include electron-transfer reactions in molecules and reaction systems that have no internal chromophore. Second, the reactions illustrate how simple sustainable electrochemical methods can be employed. This is particularly important since the larger synthetic community is often hesitant to adopt electrochemical reactions. This hesitation frequently has its origins in the perception that electrochemical reactions require the use of sophisticated and expensive equipment. The range of reactions that can be conducted with the very simple reaction setup shown in Figure 1b demonstrates that this perception is not accurate. Any electrochemical reaction in the literature can be mimicked satisfactorily with only a small investment of time and money.

Experimental

General information

Electrolysis reactions were performed using a photovoltaic cell and a light source (direct sunlight or a compact fluorescent bulb (hydrophonic, full spectrum, 60 W, 5500K)) with an ammeter and an optional coulometer connected in series. The output voltage of the photovoltaic cells varied from 6–35 V depending on the light intensity, which was varied to control the current output. For reactions requiring higher current, a Topray solar panel briefcase was connected in series with the reaction flask (Figure 1a). Alternatively, several 6 V solar photovoltaic cells can be connected in series to generate the equivalent amount of current (Figure 1b).

Representative procedure for solar-driven direct electrochemical reactions (Scheme 2a)

The enol ether substrate was dissolved in anhydrous MeOH (0.03 M) with lithium perchlorate (0.03 M, 1.0 equiv) in a flame-dried three-necked round-bottomed flask at room temperature under an argon atmosphere. The flask was equipped with a RVC anode and platinum wire cathode using two of the three necks of the flask. The photovoltaic system was inserted in series with the reaction flask along with an ammeter to monitor the current. The reaction was carried out at a constant current of 8.0 mA until the desired amount of charge was passed. The crude mixture was washed with water and then the organic solution was concentrated under reduced pressure and purified by silica gel chromatography.

Representative procedure for solar-driven indirect electrochemical reactions (Scheme 6)

A flame-dried three-necked round-bottomed flask was charged under argon with 1 equiv of *o*-phenylenediamine (0.31 mmol, 33.8 mg), 1.1 equiv of 3-nitrobenzaldehyde (0.34 mmol, 52 mg), 20 mol % CAN (31 mg), and $LiClO_4$ (0.1 M, 127 mg) in 12 mL of THF/MeOH 5:1. A RVC anode and a carbon rod cathode were inserted into the flask. A constant current of 8 mA was supplied (either via a potentiostat or a photovoltaic cell) until 2.3 F/mol of charge had passed. After the electrolysis, the contents of the flask were extracted with EtOAc, washed with brine, and dried with $MgSO_4$. The product was purified by column chromatography (EtOAc/hexanes 1:1) to give the benzimidazole product.

Specific electrolysis procedures for other substrates may be found in the original publications for the reactions as cited in the main text. The modification of these reactions to the solar-driven versions were carried out according to the general information and example solar-driven procedures provided above.

Acknowledgements

We thank the National Science Foundation (CHE-1151121, CBET-1262176) and (CHE-1240194/CenSURF) for their generous support of our work.

References

1. Sperry, J. B.; Wright, D. L. *Chem. Soc. Rev.* **2006,** *35,* 605. doi:10.1039/b512308a
2. Yoshida, J.; Kataoka, K.; Horcajada, R.; Nagaki, A. *Chem. Rev.* **2008,** *108,* 2265. doi:10.1021/cr0680843
3. Frontana-Uribe, B. A.; Little, R. D.; Ibanez, J. G.; Palma, A.; Vasquez-Medrano, R. *Green Chem.* **2010,** *12,* 2099. doi:10.1039/c0gc00382d
4. Moeller, K. D. *Tetrahedron* **2000,** *56,* 9527. doi:10.1016/S0040-4020(00)00840-1
   See for a description of electrochemical methods specifically targeted to a synthetic audience.
5. Francke, R.; Little, R. D. *Chem. Soc. Rev.* **2014,** *43,* 2492. doi:10.1039/c3cs60464k
   See for a recent review of indirect electrochemical methods.
6. Fuchigami, T.; Tajima, T. *Electrochemistry* **2006,** *74,* 585. doi:10.5796/electrochemistry.74.585

7. Feroci, M.; Orsini, M.; Rossi, L.; Inesi, A. *Curr. Org. Synth.* **2012,** *9,* 40. doi:10.2174/157017912798889206
8. Paddon, C. A.; Atobe, M.; Fuchigami, T.; He, P.; Watts, P.; Haswell, S. J.; Pritchard, G. J.; Bull, S. D.; Marken, F. *J. Appl. Electrochem.* **2006,** *36,* 617. doi:10.1007/s10800-006-9122-2
9. Licht, S.; Wang, B.; Wu, H. *J. Phys. Chem. C* **2011,** *115,* 11803. doi:10.1021/jp111781a
   And references therein for a related approach.
10. The simple photovoltaic-cell shown is available from SolarMade.
11. Anderson, L. A.; Redden, A.; Moeller, K. D. *Green Chem.* **2011,** *13,* 1652. doi:10.1039/c1gc15207f
    See for direct oxidation reactions.
12. Nguyen, B. H.; Redden, A.; Moeller, K. D. *Green Chem.* **2014,** *16,* 69. doi:10.1039/c3gc41650j
    See for indirect oxidation reactions.
13. Sun, H.; Martin, C.; Kesselring, D.; Keller, R.; Moeller, K. D. *J. Am. Chem. Soc.* **2006,** *128,* 13761. doi:10.1021/ja064737l
    And references therein.
14. Moeller, K. D. Electrochemistry of Nitrogen Containing Compounds. In *Encyclopedia of Electrochemistry;* Schäfer, H. J., Ed.; Wiley-VCH: Weinheim, 2004; Vol. 8, pp 277–312.
    See for a review of earlier work.
15. Little, R. D.; Moeller, K. D. *Electrochem. Soc. Interface* **2002,** *11,* 36.
    See for a discussion of electrochemistry and umpolung reactions.
16. Tang, F.; Chen, C.; Moeller, K. D. *Synthesis* **2007,** 3411. doi:10.1055/s-2007-990835
    See for a discussion of electrochemistry and umpolung reactions.
17. Moeller, K. D. *Synlett* **2009,** 1208. doi:10.1055/s-0028-1088126
    See for a review.
18. Xu, G.; Moeller, K. D. *Org. Lett.* **2010,** *12,* 2590. doi:10.1021/ol100800u
19. Torii, S.; Liu, P.; Tanaka, H. *Chem. Lett.* **1995,** *24,* 319. doi:10.1246/cl.1995.319
    See for the original procedure.
20. Schnatbaum, K.; Schäfer, H. J. *Synthesis* **1999,** 864. doi:10.1055/s-1999-3464
21. Nguyen, B. H.; Kesselring, D.; Tesfu, E.; Moeller, K. D. *Langmuir* **2014,** *30,* 2280. doi:10.1021/la404895b
22. Smith, J. A.; Moeller, K. D. *Org. Lett.* **2013,** *15,* 5818. doi:10.1021/ol402826z
23. Vourloumis, D.; Takahashi, M.; Simonsen, K. B.; Ayida, B. K.; Barluenga, S.; Winters, G. C.; Hermann, T. *Tetrahedron Lett.* **2003,** *44,* 2807. doi:10.1016/S0040-4039(03)00453-2
24. Vanden Eynde, J. J.; Delfosse, F.; Lor, P.; Van Haverbeke, Y. *Tetrahedron* **1995,** *51,* 5813. doi:10.1016/0040-4020(95)00252-4
25. For an indirect electrochemical version of the reaction that uses catalytic oxidant on an array see reference [21].
26. Redden, A.; Perkins, R. J.; Moeller, K. D. *Angew. Chem., Int. Ed.* **2013,** *52,* 12865. doi:10.1002/anie.201308739

License and Terms

BEILSTEIN JOURNAL OF ORGANIC CHEMISTRY

Stereoselective cathodic synthesis of 8-substituted (1*R*,3*R*,4*S*)-menthylamines

Carolin Edinger, Jörn Kulisch and Siegfried R. Waldvogel*

Full Research Paper

Open Access

Address:
Institut für Organische Chemie, Johannes Gutenberg-Universität Mainz, Duesbergweg 10-14, 55128 Mainz, Germany

Email:
Siegfried R. Waldvogel* - waldvogel@uni-mainz.de

* Corresponding author

Keywords:
cathodic reduction; chiral amines; electrosynthesis; menthylamines; oximes

Beilstein J. Org. Chem. **2015,** *11,* 294–301.
doi:10.3762/bjoc.11.34

Received: 28 December 2014
Accepted: 11 February 2015
Published: 27 February 2015

This article is part of the Thematic Series "Electrosynthesis".

Associate Editor: J. A. Murphy

Abstract

The electrochemical generation of menthylamines from the corresponding menthone oximes equipped with an additional substituent in position 8 is described. Due to 1,3-diaxial interactions a pronounced diastereoselectivity for the menthylamines is found.

Introduction

Optically active amines serve as powerful and versatile tools in organic synthesis. Among numerous applications they are applied as chiral ligands [1], as catalysts for various asymmetric transformations [2], and as building blocks for alkaloid and pharmaceutical drug synthesis [3,4]. The increasing number of applications leads to a growing interest in the stereoselective preparation of such amines. Throughout the last decades, several strategies [3] such as stereospecific amination via C–H insertion [5-8] or asymmetric olefin hydroamination [9-13] have been investigated in order to obtain access to optically pure amines. However, the major fraction of starting materials for the synthesis of these compounds is still provided by the chiral pool. Usually, optically active alcohols or amino acids serve as starting material for such amine syntheses [14]. Naturally occurring terpenes such as carene [15], limonene [16], pinene [17,18] or camphor [19] are used as precursors for chiral β-amino alcohols. As precursors for α-chiral primary amines, fenchone [20] and camphor [21,22] are typically employed. Furthermore, optically pure dehydroabietylamine is readily available and applicable without further modification [23-25].

Among the terpenoid derived amines, menthylamine and its 8-substituted derivatives **1** represent a particularly interesting candidate. Due to the strong steric influence in the vicinity of the amino functionality, high selectivity can be expected for asymmetric transformations [26,27], since appropriate moieties as substituents R create a molecular U-turn (see Scheme 1).

However, while optically pure menthol derivatives play a significant role in organic synthesis [28], menthylamines have

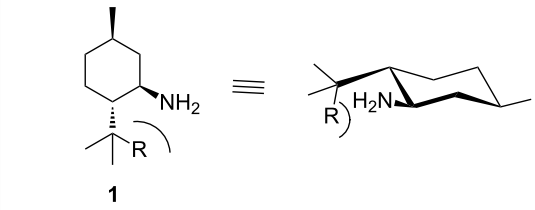

Scheme 1: Structural features of 8-substituted menthylamines **1**.

only been used in a few situations, which is attributable to their rather poor availability in optically pure manner. Among the applications reported so far, are the uses as building blocks in supramolecular receptors [29-34] or the synthesis of high-performance stationary phases for liquid chromatography [35-38]. (−)-Menthone (**2**) can be converted to menthylamine by different methods: A general way to convert naturally occurring terpenoids is the reductive amination under Leuckart–Wallach conditions (see Scheme 2, pathway **I**) [39]. This method was applied to convert **2** to *N*-alkyl substituted menthylamines [40]. However, a significant disadvantage of this method is the lack of stereocontrol and partial inversion of the configuration at position 4 resulting in a complex diastereomeric mixture. Alternatively, reduction of menthone oxime can be achieved, either employing Bouveault–Blanc conditions [41], or via hydrogenolysis at a transition metal catalyst [42]. Both approaches lead to the desired product as a diastereomeric mixture.

In the past, we elaborated straightforward and efficient approaches to optically pure (−)-menthylamine (**3**, see Scheme 2, pathways **II**, **III**, **IV**).

One protocol involves conversion of the inexpensive technical intermediate racemic neomenthol to menthylamine in a three-step sequence, followed by enantiomeric resolution employing tartaric acid (see Scheme 2, pathway **IV**) [43]. By the amount of water in the crystallisation mixture the precipitation of the desired diastereomeric salt can be chosen [44]. Furthermore, we developed a Bouveault–Blanc-type protocol where (−)-menthone oxime is converted to **3** in attractive diastereoselectivity (see Scheme 2, pathway **II**) [45]. However, the necessity for excess amounts of sodium metal constitutes a major drawback. Consequently, we also investigated on electrochemical alternatives for the reduction of (−)-menthone oxime. In this context, we found that it can be efficiently converted to the corresponding diastereomeric amines with an excess of **3a** in a divided cell under galvanostatic conditions employing an Hg pool cathode (see Scheme 2, pathway **III**) [26]. Here, we report a new synthetic route to optically pure 8-substituted menthylamines **1** starting from commercially available (+)-pulegone (**4**, Scheme 3). An important feature of this sequence is the initial introduction of a sterically demanding moiety R in position 8 via cuprate addition. After conversion to menthone oximes **7** within the second step, R is supposed to enhance the stereoselectivity of the following electrochemical reduction process (Scheme 3, step 3). Concomitantly, the resulting amines **1** are expected to have improved properties as catalysts/auxiliaries for

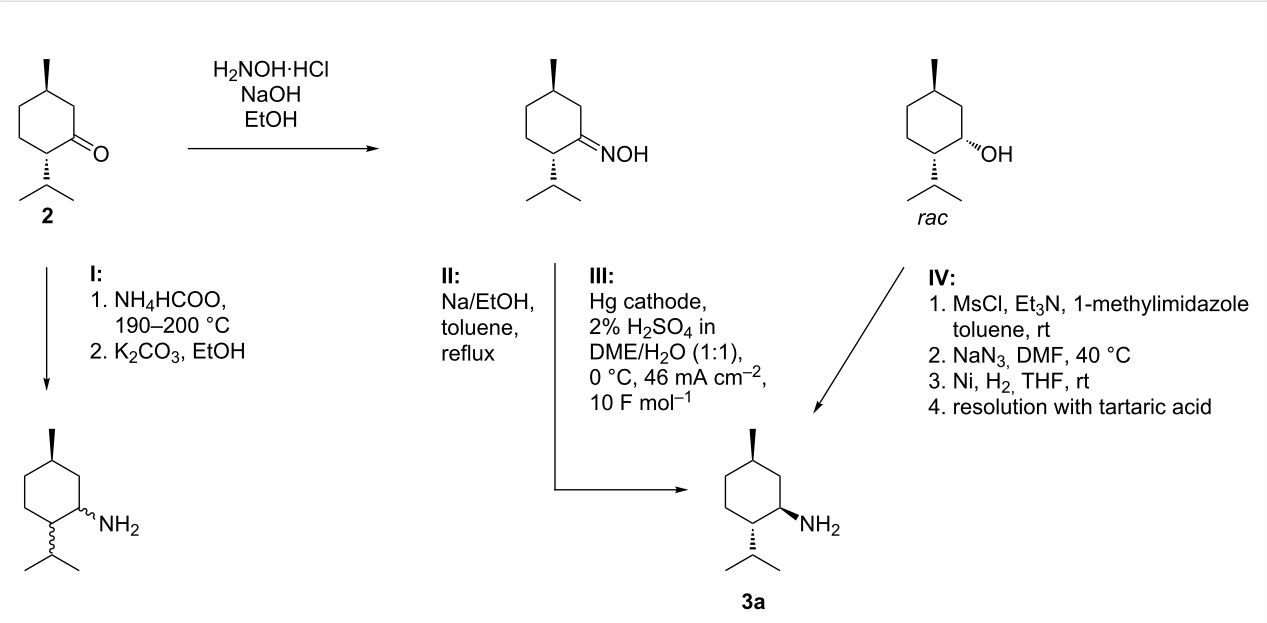

Scheme 2: Synthetic strategies to menthylamines.

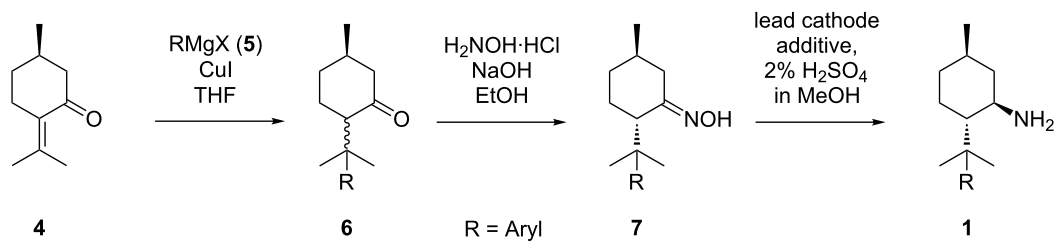

Scheme 3: Stereoselective synthesis of 8-substituted (1*R*,3*R*,4*S*)-menthylamines.

asymmetric transformations due to the increased sterical demand in the vicinity of the amine group.

Results and Discussion

Exploratory work

Our previous studies revealed that menthone oxime can be electrochemically reduced on either mercury pool or lead cathode (see Scheme 4) [26]. Under optimized reaction conditions, the use of a mercury pool cathode renders compound **3** in 86% yield with a diastereomeric ratio (dr) **3a**:**3b** of 2.4. In contrast, using a lead cathode under optimized conditions leads to a reversed diastereomeric ratio of 0.6 in 99% yield. Notably, methyltriethylammonium methylsulfate (MTES) was used as additive in the latter case in order to suppress lead corrosion and to improve the current efficiency [26,46,47]. These promising results prompted us to study the stereoselectivity of the reduction in the presence of a sterically demanding group in position 8 of the substrate molecule.

Synthesis of the menthone oxime substrates

In order to obtain the desired 8-substituted (1*R*,4*S*)-menthone oxime substrates **7** we started from commercially available (+)-pulegone (**4**) in technical grade (92%) (see Scheme 5). First, the desired aryl moiety was installed by cuprate addition generated from aryl bromide **5**, yielding the corresponding menthones **6a–c** in good yields. In all cases, simple distillation is sufficient to isolate **6** in high purity.

Subsequent treatment of epimeric mixtures **6a–c** with NH_2OH·HCl and NaOH provides the corresponding (1*R*,4*S*)-menthone oximes in good yields (68–85%). For both, cuprate addition and oxime formation, conversions of the compounds exhibiting the diphenyl moiety in position 8 (**6c** and **7c**, R^2 = Ph) require prolonged reaction times and render slightly lower yields.

Electrochemical reduction of 8-substituted menthone oximes

The electrolyses were carried out in a divided cell using a Nafion® sheet as separator and platinum as anodic material. Since previous studies revealed that the reduction of the non-substituted menthone oxime was most effective on mercury or lead as cathodic material [26], we were prompted to study the influence of such cathodes onto yield and stereoselectivity in the conversion of **7a** (see Scheme 6).

The results clearly indicate that lead represents the superior cathode for this application. Compared to mercury, the use of a

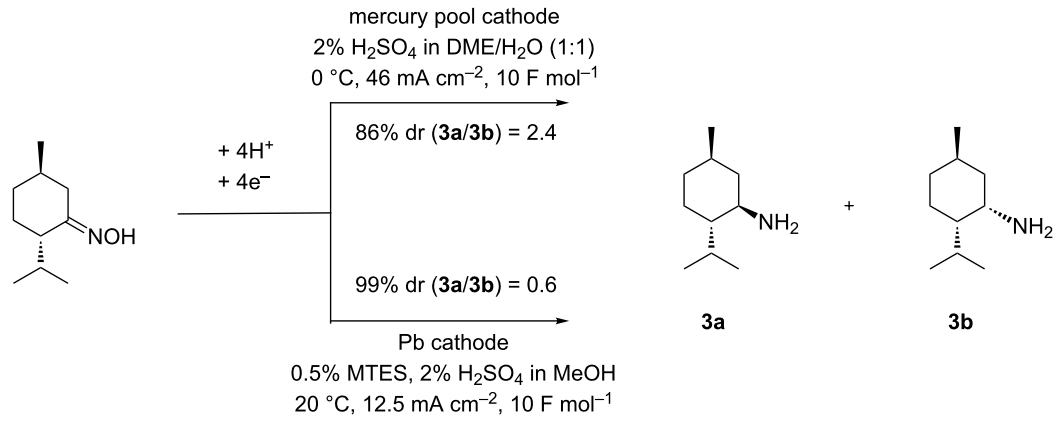

Scheme 4: Influence of the cathode system onto the stereoselectivity of the reduction of (1*R*,4*S*)-menthone oxime.

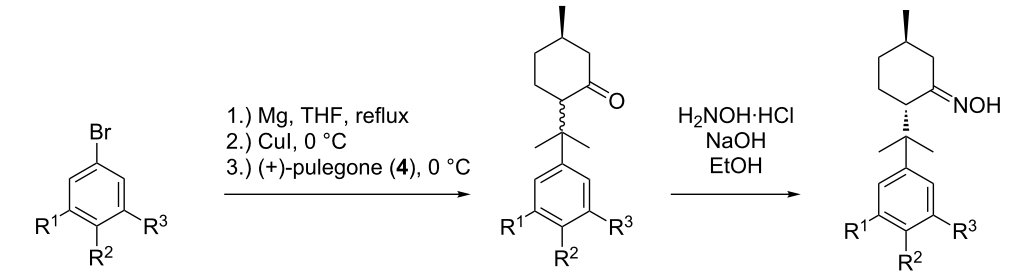

5a $R^1 = R^2 = R^3 = H$
5b $R^1 = R^3 = OMe$ $R^2 = H$
5c $R^1 = R^3 = H$ $R^2 = Ph$

6a 70%
6b 69%
6c 62%

7a 85%
7b 81%
7c 68%

Scheme 5: Preparation of 8-substituted (1*R*)-menthones **6** and the corresponding oximes **7**.

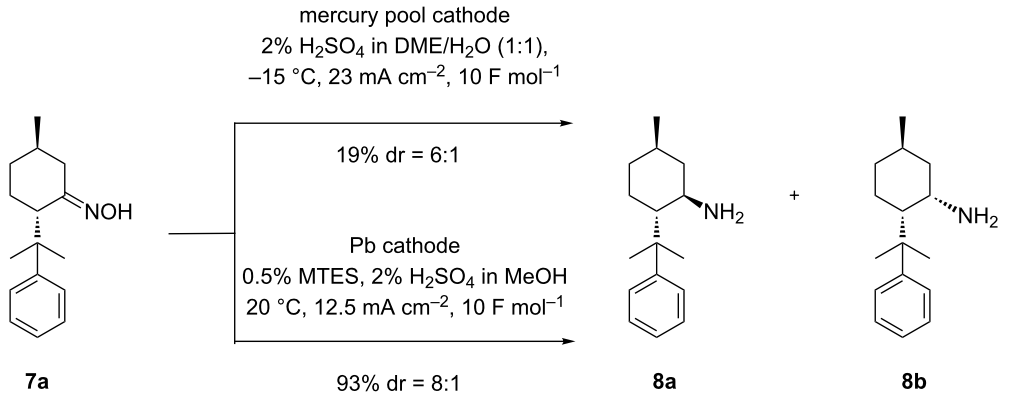

7a **8a** **8b**

Scheme 6: Influence of cathode material on the preparation of (1*R*,3*R*,4*S*)-menthylamine **8a**.

lead cathode renders significantly higher yields (93% vs 19%). Furthermore, an improved dr of 8:1 in favor of the desired isomer **8a** is obtained (compare dr = 6:1 obtained at Hg). Both results clearly demonstrate the positive effect of the substituent in position 8 onto the diastereoselectivity of the reduction (compare Scheme 4, dr = 2.4). Since lead was distinctly the prime cathode material it was used throughout all further investigations. To determine the influence by the temperature onto the selectivity, the reaction was carried out at 20, 40, and 60 °C (see Table 1). Methyltriethylammonium methylsulfate (MTES) serves as additive in order to suppress electrode corrosion due to $PbSO_4$ formation [26,46,47].

With increasing temperature higher diastereoselectivity can be observed, but the product yield strongly decreases. At 60 °C, hydrolysis of the oxime becomes the predominant reaction, yielding large amounts of menthone **6a** and the desired product **8** in only 33% yield (Table 1, entry 1). Moreover, the influence of alkylammonium salt additives on the reaction was studied (see Table 2). Such additives are known to have a positive effect on reductions on lead cathodes due to the formation of an ionic coating on the electrode surface and concomitant inhibition of cathodic corrosion and evolution of molecular hydrogen [46,47].

Table 1: Effect of temperature onto yield and stereoselectivity of the electrochemical reduction of **7a** on a lead cathode.

Entry[a]	*T* [°C]	yield[b] [%]	c.e.[c] [%]	dr[d] [**8a**:**8b**]
1	60	33	13	6.2
2	40	85	34	5.4
3	20	93	38	5.2

[a]Catholyte: 0.5% MTES and 2% H_2SO_4 in MeOH, current density: 12.5 mA cm^{-2}, passed charge: 10 F mol^{-1}, anode: platinum; [b]yield determined by GC (internal standard); [c]c.e. = current efficiency; [d]ratio determined by NMR spectroscopy.

The chosen additives differ in size and number of ammonium groups. The use of additive **11** leads to the highest product yield (Table 2, entry 3) but with a dr of 4.7 the lowest stereoselectivity. However, optimal compromise is given by MTES (additive **10**) as additive with a yield of 93% and a diastereomeric

Table 2: Influence of alkylammonium salts on the electrochemical preparation of **8a**.

Entry[a]	additive	yield[b] [%]	c.e.[c] [%]	dr[d] [**8a**:**8b**]
1	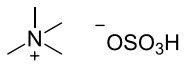 **9**	83	33	7.5
2	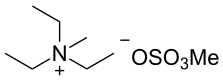 **10**	93	37	6.2
3	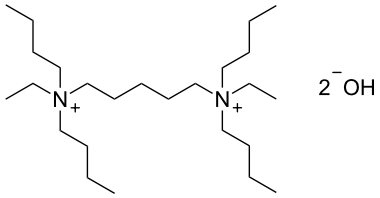 **11**	95	38	4.7

[a]Catholyte: 0.5% additive and 2% H_2SO_4 in MeOH, current density: 12.5 mA cm^{-2}, passed charge: 10 F mol^{-1}, anode: platinum; [b]yield determined by GC (internal standard); [c]c.e. = current efficiency; [d]ratio determined by NMR spectroscopy.

ratio of 6.2 (Table 2, entry 2). The compact cation **9** renders the best result with regard to diastereomeric ratio, but with inferior yield of 83%.

Next, the elaborated conditions were applied to oxime **7b** (Table 3, entry 2). The corresponding menthylamines **12a** and **12b** were obtained in only 42% yield in a diastereomeric ratio of 6:1. However, the yield can be significantly improved using other alkylammonium additives, such as tetramethylammonium salt **9**, BQAOH (**11**) and cyclic alkylammonium salt **13** (see Table 3, entries 1, 3 and 4), whereas **10** and **13** render improved yields along with lower diastereoselectivity, the use of additive **11** provides the highest yield with best stereoselectivity (see Table 3, entry 3). Again, the positive effect of the

Table 3: Electrochemical synthesis of **12a** using different additives.

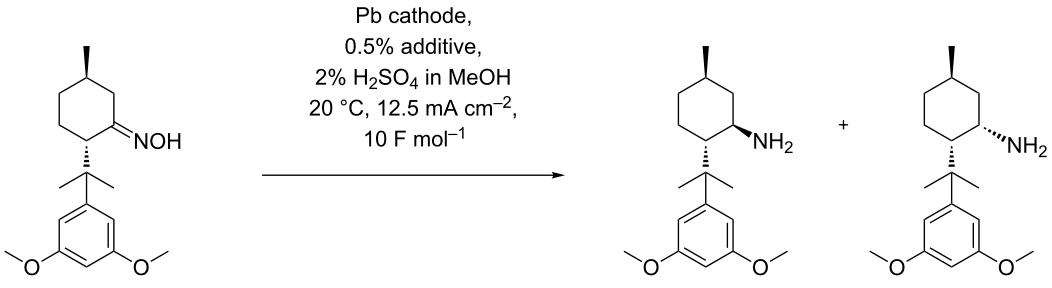

7b **12a** **12b**

Entry[a]	additive	yield[b] [%]	c.e.[c] [%]	dr[d] [**12a**:**12b**]
1	**9**	63	25	6.8
2	**10**	42	17	5.6
3	**11**	78	31	8.6
4	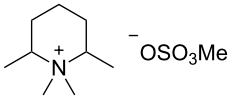 **13**	73	29	4.4

[a]Anode: platinum; [b]yield determined by GC (internal standard); [c]c.e. = current efficiency; [d]ratio determined by NMR spectroscopy.

substituent in position 8 onto the diastereoselectivity of the reduction is clearly demonstrated (compare Scheme 4).

Since the achieved results with additive **11** are very promising (78%, dr 8.6) we were prompted to perform further studies on the effect of the concentration of **11** contained in the electrolyte. The results reveal that a concentration of 1 wt % renders optimum values for product yield, current efficiency and diastereomeric ratio (see Table 4).

Table 4: Influence of the concentration of additive **11** on the electroreduction of **7b**.

Entry[a]	*c* (additive **11**) [%]	yield[b] [%]	c.e.[c] [%]	dr[d] [**12a**:**12b**]
1	0.5	78	13	8.6
2	1	89	36	8.9
3	4	85	37	7.8

[a]Catholyte: 2% H_2SO_4 in MeOH, current density: 12.5 mA cm^{-2}, passed charge: 10 F mol^{-1}, anode: platinum; [b]yield determined by GC (internal standard); [c]c.e. = current efficiency; [d]ratio determined by NMR spectroscopy.

Increasing the additive amount to 4 wt % does not have any further benefit onto the oxime conversion, while simultaneously the stereoselectivity decreases slightly (Table 4, entry 3). Employing oxime **7c** demonstrates the limitations of our methodology. After passing 10 F under the optimized reaction conditions using additive **10**, non-converted oxime **7c** was fully recovered. A possible explanation is a strong decrease of the electron transfer rate due to steric shielding of the oxime functionality (see Scheme 7). Also the low solubility of the substrate is obstructive.

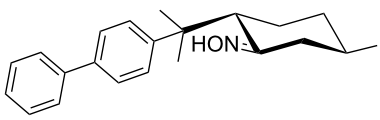

Scheme 7: Protection of the oxime functionality in **7c** due to the sterically demanding diphenyl moiety in 8-position.

Diastereomerically pure 8-substituted menthylamines

To obtain diastereomerically and analytically pure 8-substituted (1*R*,3*R*,4*S*)-menthylamines, each diastereomeric mixture can be transformed to the corresponding hydrochlorides by passing HCl through a solution of **8** or **12** in diethyl ether followed by a selective crystallization of diastereomers **8c** and **12c** from 1,4-dioxane or CH_2Cl_2/heptane, respectively (see Scheme 8). **8c** and **12c** can thus be obtained in 73% and 88% yield.

Conclusion

We presented an efficient strategy to synthesize (1*R*,3*R*,4*S*)-menthylamines with aryl substituents in position 8. Starting from commercially available (+)-pulegone, the desired aryl moiety can be installed in position 8 by cuprate addition. Subsequent treatment with $NH_3OH{\cdot}HCl$ at alkaline conditions provides the enantiomerically pure (1*R*,4*S*)-menthone oximes in good yields. In the final step of the reaction sequence, the oxime is electrochemically reduced. We found that the use of a lead cathode in combination with alkylammonium additives render the desired 8-substituted (1*R*,3*R*,4*S*)-menthylamines in high yields and good diastereoselectivity. Compared to non-substituted (1*R*,3*R*,4*S*)-menthylamine, the diastereoselectivity is significantly improved, owing to the increased steric demand of

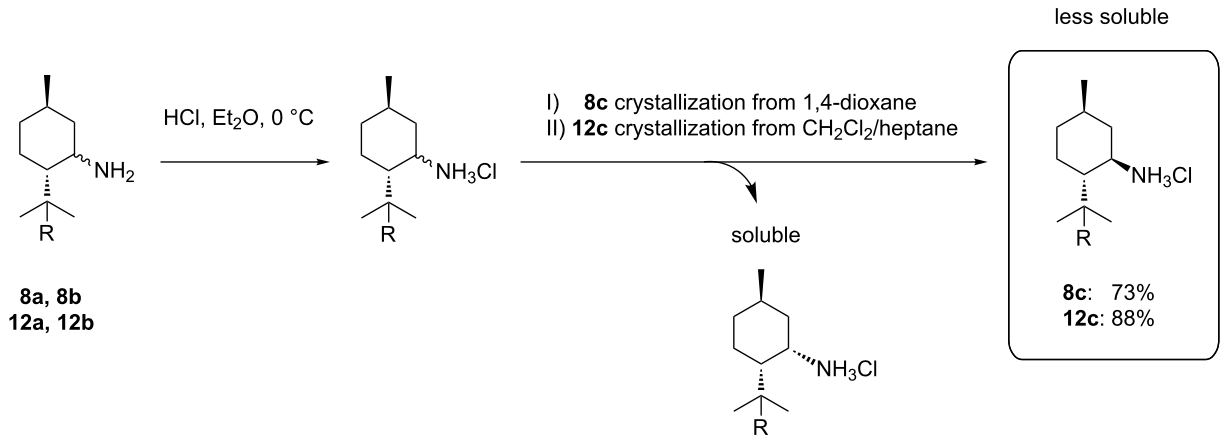

Scheme 8: Separation of the diastereomeric 8-substituted menthylamines by crystallization of their hydrochlorides.

the substituent on the stereocenter in vicinity to the oxime functionality. However, if the size of the substituent is further increased, the electrochemical conversion is significantly impaired.

Supporting Information

Supporting Information File 1

Experimental details and ^{1}H and ^{13}C NMR spectra are provided.
[http://www.beilstein-journals.org/bjoc/content/supplementary/1860-5397-11-34-S1.pdf]

Acknowledgements

Financial support by the BASF SE is highly appreciated.

References

1. Seyden-Penne, J. *Chiral auxiliaries and ligands in asymmetric synthesis;* Wiley Inter-Science: New York, 1995.
2. France, S.; Guerin, D. J.; Miller, S. J.; Lectka, T. *Chem. Rev.* **2003,** *103,* 2985–3012. doi:10.1021/cr020061a
3. Nugent, T. C.; El-Shazly, M. *Adv. Synth. Catal.* **2010,** *352,* 753–819. doi:10.1002/adsc.200900719
4. Newman, D. J.; Cragg, G. M.; Snader, K. M. *J. Nat. Prod.* **2003,** *66,* 1022–1037. doi:10.1021/np030096l
5. Fiori, K. W.; Du Bois, J. *J. Am. Chem. Soc.* **2007,** *129,* 562–568. doi:10.1021/ja0650450
6. Li, Z.; Capretto, D. A.; Rahaman, R.; He, C. *Angew. Chem.* **2007,** *119,* 5276–5278. doi:10.1002/ange.200700760
Angew. Chem., Int. Ed. **2007,** *46,* 5184–5186. doi:10.1002/anie.200700760
7. Milczek, E.; Boudet, N.; Blakey, S. *Angew. Chem.* **2008,** *120,* 6931–6934. doi:10.1002/ange.200801445
Angew. Chem., Int. Ed. **2008,** *47,* 6825–6828. doi:10.1002/anie.200801445
8. Liang, C.; Collet, F.; Robert-Peillard, F.; Müller, P.; Dodd, R. H.; Dauban, P. *J. Am. Chem. Soc.* **2008,** *130,* 343–350. doi:10.1021/ja076519d
9. Gribkov, D. V.; Hultzsch, K. C.; Hampel, F. *J. Am. Chem. Soc.* **2006,** *128,* 3748–3759. doi:10.1021/ja058287t
10. LaLonde, R. L.; Sherry, B. D.; Kang, E. J.; Toste, F. D. *J. Am. Chem. Soc.* **2007,** *129,* 2452–2453. doi:10.1021/ja068819l
11. Zhang, Z.; Bender, C. F.; Widenhoefer, R. A. *J. Am. Chem. Soc.* **2007,** *129,* 14148–14149. doi:10.1021/ja0760731
12. Nishina, N.; Yamamoto, Y. *Angew. Chem.* **2006,** *118,* 3392–3395. doi:10.1002/ange.200600331
Angew. Chem., Int. Ed. **2006,** *45,* 3314–3317. doi:10.1002/anie.200600331
13. Wood, M. C.; Leitch, D. C.; Yeung, C. S.; Kozak, J. A.; Schafer, L. L. *Angew. Chem.* **2007,** *119,* 358–362. doi:10.1002/ange.200603017
Angew. Chem. Int. Ed. **2007,** *47,* 354–358. doi:10.1002/anie.200603017
14. Blaser, H. U. *Chem. Rev.* **1992,** *92,* 935–952. doi:10.1021/cr00013a009
15. Kauffman, G. S.; Harris, G. D.; Dorow, R. L.; Stone, B. R. P.; Parsons, R. L., Jr.; Pesti, J. A.; Magnus, N. A.; Fortunak, J. M.; Confalone, P. N.; Nugent, W. A. *Org. Lett.* **2000,** *2,* 3119–3121. doi:10.1021/ol006321x
16. Chrisman, W.; Camara, J. N.; Marcellini, K.; Singaram, B.; Goralski, C. T.; Hasha, D. L.; Rudolf, P. R.; Nicholson, L. W.; Borodychuk, K. K. *Tetrahedron Lett.* **2001,** *42,* 5805–5807. doi:10.1016/S0040-4039(01)01135-2
17. Goralski, C. T.; Chrisman, W.; Hasha, D. L.; Nicholson, L. W.; Rudolf, P. R.; Zakett, D.; Singaram, B. *Tetrahedron: Asymmetry* **1997,** *8,* 3863–3871. doi:10.1016/S0957-4166(97)00566-1
18. Masui, M.; Shioiri, T. *Tetrahedron* **1995,** *51,* 8363–8370. doi:10.1016/0040-4020(95)00447-G
19. Kitamura, M.; Suga, S.; Kawai, K.; Noyori, R. *J. Am. Chem. Soc.* **1986,** *108,* 6071–6072. doi:10.1021/ja00279a083
20. Rishton, G. M.; Retz, D. M.; Tempest, P. A.; Novotny, J.; Kahn, S.; Treanor, J. J. S.; Lile, J. D.; Citron, M. *J. Med. Chem.* **2000,** *43,* 2297–2299. doi:10.1021/jm990622z
21. Periasamy, M.; Devasagayaraj, A.; Satyanarayana, N.; Narayana, C. *Synth. Commun.* **1989,** *19,* 565–573. doi:10.1080/00397918908050701
22. Yamaguchi, H.; Minoura, Y. *J. Polym. Sci., Part A-1: Polym. Chem.* **1970,** *8,* 929–941. doi:10.1002/pol.1970.150080410
23. Boyle, P. H. *Q. Rev., Chem. Soc.* **1971,** *25,* 323–341. doi:10.1039/QR9712500323
24. Malkowsky, I.; Nieger, M.; Kataeva, O.; Waldvogel, S. R. *Synthesis* **2007,** 773–778. doi:10.1055/s-2007-965895
25. Wilkerson, W. W.; Galbraith, W.; DeLucca, I.; Harris, R. R. *Bioorg. Med. Chem. Lett.* **1993,** *3,* 2087–2092. doi:10.1016/S0960-894X(01)81022-2
26. Kulisch, J.; Nieger, M.; Stecker, F.; Fischer, A.; Waldvogel, S. R. *Angew. Chem.* **2011,** *123,* 5678–5682. doi:10.1002/ange.201101330
Angew. Chem., Int. Ed. **2011,** *50,* 5564–5567. doi:10.1002/anie.201101330
27. Corey, E. J.; Gross, A. W. *J. Org. Chem.* **1985,** *50,* 5391–5393. doi:10.1021/jo00225a082
28. Oertling, H.; Reckziegel, A.; Surburg, H.; Bertram, H.-J. *Chem. Rev.* **2007,** *107,* 2136–2164. doi:10.1021/cr068409f
29. Schopohl, M. C.; Siering, C.; Kataeva, O.; Waldvogel, S. R. *Angew. Chem.* **2003,** *115,* 2724–2727. doi:10.1002/ange.200351102
Angew. Chem., Int. Ed. **2003,** *42,* 2620–2623. doi:10.1002/anie.200351102
30. Siering, C.; Grimme, S.; Waldvogel, S. R. *Chem. – Eur. J.* **2005,** *11,* 1877–1888. doi:10.1002/chem.200401002
31. Schopohl, M. C.; Faust, A.; Mirk, D.; Fröhlich, R.; Kataeva, O.; Waldvogel, S. R. *Eur. J. Org. Chem.* **2005,** 2987–2999. doi:10.1002/ejoc.200500108
32. Bomkamp, M.; Siering, C.; Landrock, K.; Stephan, H.; Fröhlich, R.; Waldvogel, S. R. *Chem. – Eur. J.* **2007,** *13,* 3724–3732. doi:10.1002/chem.200601231
33. Orghici, R.; Willer, U.; Gierszewska, M.; Waldvogel, S. R.; Schade, W. *Appl. Phys. B* **2008,** *90,* 355–360. doi:10.1007/s00340-008-2932-7
34. Börner, S.; Orghici, R.; Waldvogel, S. R.; Willer, U.; Schade, W. *Appl. Opt.* **2009,** *48,* B183–B189. doi:10.1364/AO.48.00B183
35. Arlt, D.; Bömer, B.; Grosser, R.; Lange, W. *Angew. Chem.* **1991,** *103,* 1685–1687. doi:10.1002/ange.19911031223
Angew. Chem., Int. Ed. **1991,** *50,* 1662–1664. doi:10.1002/anie.199116621

36. Schwartz, U.; Großer, R.; Piejko, K.-E.; Arlt, D. Optisch aktive (Meth)-acrylamide, Polymere daraus, Verfahren zu ihrer Herstellung und ihre Verwendung zur Racematspaltung. Ger. Pat. Appl. DE3532356 A1, March 19, 1987.
Chem. Abstr. **1987,** *107,* 40614.
37. Bömer, B.; Großer, R.; Lange, W.; Zweering, U.; Köhler, B.; Sirges, W.; Grosse-Bley, M. Chirale stationäre Phasen für die chromatographische Trennung von optischen Isomeren. Ger. Pat. Appl. DE19546136 A1, June 12, 1997.
Chem. Astr. **1997**, *127*, 96037.
38. Lange, W.; Großer, R.; Michel, S.; Bömer, B.; Zweering, U. Chromatographische Enantiomerentrennung von Lactonen. Ger. Pat. Appl. DE19714343 A1, Oct 15, 1998.
Chem. Abstr. **1998,** *129,* 290016.
39. Wallach, O. *Ber. Dtsch. Chem. Ges.* **1891,** *24,* 3992–3993. doi:10.1002/cber.189102402292
40. Kozlov, N. G.; Pekhk, T. I.; Vyalimyaé, T. K. *Chem. Nat. Compd.* **1981,** *17,* 238–243. doi:10.1007/BF00568510
41. Feltkamp, H.; Koch, F.; Thanh, T. N. *Justus Liebigs Ann. Chem.* **1967,** *707,* 78–86. doi:10.1002/jlac.19677070113
42. Kozlov, N. G. *Chem. Nat. Compd.* **1982,** *18,* 131–143. doi:10.1007/BF00577177
43. Welschoff, N.; Waldvogel, S. R. *Synthesis* **2010,** 3596–3601. doi:10.1055/s-0030-1258295
44. Schmitt, M.; Schollmeyer, D.; Waldvogel, S. R. *Eur. J. Org. Chem.* **2014,** 1007–1012. doi:10.1002/ejoc.201301566
45. Schopohl, M. C.; Bergander, K.; Kataeva, O.; Fröhlich, R.; Waldvogel, S. R. *Synthesis* **2003,** 2689–2694. doi:10.1055/s-2003-42432
46. Edinger, C.; Waldvogel, S. R. *Eur. J. Org. Chem.* **2014,** 5144–5148. doi:10.1002/ejoc.201402714
47. Edinger, C.; Grimaudo, V.; Broekmann, P.; Waldvogel, S. R. *ChemElectroChem* **2014,** *1,* 1018–1022. doi:10.1002/celc.201402050

License and Terms

BEILSTEIN JOURNAL OF ORGANIC CHEMISTRY

Functionalized branched EDOT-terthiophene copolymer films by electropolymerization and post-polymerization "click"-reactions

Miriam Goll[1], Adrian Ruff[1], Erna Muks[1], Felix Goerigk[1], Beatrice Omiecienski[1], Ines Ruff[2,§], Rafael C. González-Cano[3], Juan T. Lopez Navarrete[3], M. Carmen Ruiz Delgado[3] and Sabine Ludwigs[*1]

Full Research Paper

Open Access

Address:
[1]IPOC-Functional Polymers, Institute for Polymer Chemistry, University of Stuttgart, Pfaffenwaldring 55, 70569 Stuttgart, Germany, [2]Thermo Fisher Scientific GmbH, Im Steingrund 4-6, 63303 Dreieich, Germany and [3]Department of Physical Chemistry, University of Málaga, 29071 Málaga, Spain

Email:
Sabine Ludwigs[*] - sabine.ludwigs@ipoc.uni-stuttgart.de

* Corresponding author
§ née Dreiling

Keywords:
band-gap engineering; "click"-chemistry; conducting polymers; electropolymerization; Raman spectroscopy; surface functionalization

Beilstein J. Org. Chem. **2015,** *11,* 335–347.
doi:10.3762/bjoc.11.39

Received: 19 December 2014
Accepted: 18 February 2015
Published: 11 March 2015

This article is part of the Thematic Series "Electrosynthesis".

Guest Editor: S. R. Waldvogel

Abstract

The electrocopolymerization of 3,4-ethylenedioxythiophene (EDOT) with the branched thiophene building block 2,2′:3′,2″-terthiophene (3T) is presented as a versatile route to functional polymer films. Comparisons to blend systems of the respective homopolymers PEDOT and P3T by in situ spectroelectrochemistry and Raman spectroscopy prove the successful copolymer formation and the access to tailored redox properties and energy levels. The use of EDOT-N_3 as co-monomer furthermore allows modifications of the films by polymer analogous reactions. Here, we exemplarily describe the post-functionalization with ionic moieties by 1,3-dipolar cycloaddition ("click"-chemistry) which allows to tune the surface polarity of the copolymer films from water contact angles of 140° down to 40°.

Introduction

The many different applications of conducting polymers demand for tailored properties, especially the position of the HOMO level and the HOMO–LUMO band gap value are crucial for the applicability in different devices such as organic photovoltaics, organic field effect transistors, organic light emitting diodes or organic electrochromic windows [1-6]. There are different ways to tune HOMO–LUMO band gap values, mostly concerning the modification of the used monomers, for example by a rigidification of the conjugated system [7], the introduction of electron-withdrawing [8] or electron-donating groups [9,10] to the monomers or the increase of the quinoid character [11]. One widely used approach is the

introduction of different co-monomers to build up copolymers, e.g., new donor–acceptor low band gap copolymers [12-14]. Among synthetic approaches electropolymerization has gained particular attention, because it allows easy tuning of polymer film properties by modification of the monomers. In addition to electropolymerization of simple conjugated monomers [15] more complex monomers which include different building blocks were presented. Roncali et al. used for example EDOT containing branched thiophene monomers [16,17]. In some of the more complex monomer systems the electropolymerization can be regarded as a crosslinking step [17,18]. Electropolymerization of monomer mixtures is another powerful tool to modify material properties. Among a variety of monomer mixtures including pyrrole and thiophene [19,20], 2,2'-bithiophene and pyrrole [21,22] and dicyanovinylene-substituted cyclopentabithiophene and EDOT [23], we recently presented the copolymerization of EDOT and the branched unit 2,2':3',2''-terthiophene (3T) [24].

Additional functionalities, such as ions, can be introduced either by direct attachment of the functional moieties to the monomers or via precursor monomers which give access to post-polymerization reactions. Ionic groups on conjugated polymers – so-called conjugated polyelectrolytes [25] – are discussed in the context of solubility tuning [26], sensor applications [27], improvement of solar cell performance by usage as hole injection layers [28] or the modification of the surface polarity heading for bio-compatible electrodes [29]. The direct electropolymerization of ionically modified monomers was for example carried out by Reynolds et al. for sulfonic acid functionalized pyrrole [30,31]. The groups of Heeger et al. [32-34], Bäuerle et al. [35] and Visy et al. [36] synthesized sulfonic acid and carboxylic acid functionalized polythiophenes to study the so called "self-doping" effect of conducting polymers [37]. Interwoven polymeric composite materials based on polymer blends were obtained by electrodepositing sulfonic acid modified bithiophene followed by bipyrrole monomers [38].

In some cases the direct polymerization of ionically modified monomers remains problematic: this was for example reported in the case of sulfonic acid modified pyrrole, where film deposition was only possible when a copolymerization with pristine pyrrole was conducted [30].

Post-polymerization processes on the other hand have to provide high yields and mild reaction conditions to keep the formed polymer backbone intact and to reach a considerable degree of conversion of functional groups. The Cu(I)-mediated 1,3-dipolar cycloaddition between azides and alkynes ("click"-reaction) is a commonly used reaction in post-polymerization processes [39,40]. In the case of the azidomethyl-modified EDOT (EDOT-N_3) building block different approaches of modifying the corresponding polymer PEDOT-N_3 have been conducted so far, including the modification of electropolymerized PEDOT-N_3 with different redox functionalities as employed by Bäuerle et al. [41-43]. The PEDOT relative, propargyl-substituted chemically synthesized 3,4-propylenedioxythiophene was used by Kumar et al. to introduce ionic groups by "click"-chemistry to render the solubility of the gained polymers from organic solvents to water solubility [44]. "Electro-click" modifications were used for chemically synthesized PEDOT-N_3 and copolymers of EDOT-N_3 and EDOT with halogens and fluorescent markers [45,46] and of electrochemically synthesized PEDOT-N_3 to introduce fluorinated alkyl chains [47]. In the latter case the water contact angles could be gradually varied.

We here present the electrocopolymerization of EDOT-N_3 with the branched terthiophene 2,2':3',2''-terthiophene and the post-polymerization into an ionically modified copolymer. Only recently, we reported on the copolymerization of 3T and EDOT as a straightforward approach to conducting polymer films with tailored HOMO levels and therefore band gap values by varying the monomer ratio during chemical (with $FeCl_3$ as oxidant) and electrochemical polymerization [24]. Characterization of the chemically polymerized copolymers by ^{1}H DOSY NMR and MALDI–TOF spectroscopy indicated that the EDOT and 3T units are covalently linked. While comparisons with these chemically synthesized polymers support our finding, a real proof of copolymer formation for the electropolymerized films was still missing in our previous publication. Here, we show that by comparison of blend films of the homopolymers with copolymer films obtained by electropolymerizing monomer mixtures the copolymer formation, i.e., the covalent linkage of the two co-monomers can be proven also for the electrochemically synthesized films by means of electrochemical and spectroscopic (in situ and ex situ) techniques.

We further show that the redox properties of the polymers remain identical when EDOT–N_3 is used as a co-monomer instead of EDOT and that "click"-chemistry is a versatile tool to largely modify material properties, e.g., by the introduction of covalently bound ionic groups.

Results and Discussion

Electropolymerization of monomer mixtures does not necessarily lead to copolymers of the two monomers but can also result in polymer blend structures. This is often a difficult task to prove [48]. Case one is that both monomers readily react with each other and the polymerization of a mixture of monomers leads to a copolymer. In case two, both monomers react with themselves but not with each other and the polymerization of

the monomer mixture leads to a mixture of the two homopolymers which can be regarded as a polymer blend. We mimicked the latter case by consecutive electro-deposition of layers of the respective homopolymers on the electrode. We have shown in earlier work [24] that the oxidation potentials of EDOT and 3T at 1.0 V and 1.1 V vs Fc/Fc^+, respectively, do principally allow for copolymer formation. Scheme 1 highlights the different polymer constitutions of the electropolymerized films we discuss in the present article: pure homopolymer films P3T and PEDOT, the blend film containing both P3T and PEDOT layers and the copolymer which represents a random combination of the monomers EDOT and 3T and strongly depends on the ratio of the monomers used during the electropolymerization. The nomenclature of the copolymers is in accordance to our previous publication [24]: P(EDOT-*co*-3T)-1:1 means for example that a 1:1 mixture of 3T and EDOT is used during polymerization.

Figure 1A summarizes representative cyclic voltammograms (CVs) of PEDOT, P3T, a PEDOT/P3T-blend and the copolymer P(EDOT-*co*-3T)-1:1. During the electrochemical oxidation the homopolymers PEDOT and P3T both show chemically reversible behavior, but they differ significantly in their onset potentials of −0.8 V and 0.3 V vs Fc/Fc^+, respectively (blue and red curves). The cyclic voltammogram (CV) of the PEDOT/P3T-blend has two current maxima located at −0.3 and +0.7 V. Both values correspond to the oxidation potentials of the respective homopolymers indicating the combination of the redox properties of PEDOT and P3T. The P(EDOT-*co*-3T)-1:1 film on the other hand shows one broad oxidation wave with an onset potential of −0.6 V. The UV–vis absorption spectra of the neutral electropolymerized films are shown in Figure 1B: while the homopolymers exhibit absorption maxima at 630 nm for PEDOT and 450 nm for P3T, the PEDOT/P3T-blend and the copolymer P(EDOT-*co*-3T)-1:1 film show rather broad spectral shapes with maxima around 530 nm. From the spectra of the neutral compounds a clear distinction between the copolymer and the blend is not possible.

Monitoring the optical properties during the electrochemical oxidation process by in situ spectroelectrochemistry, however, gives further information about the electronic properties of the

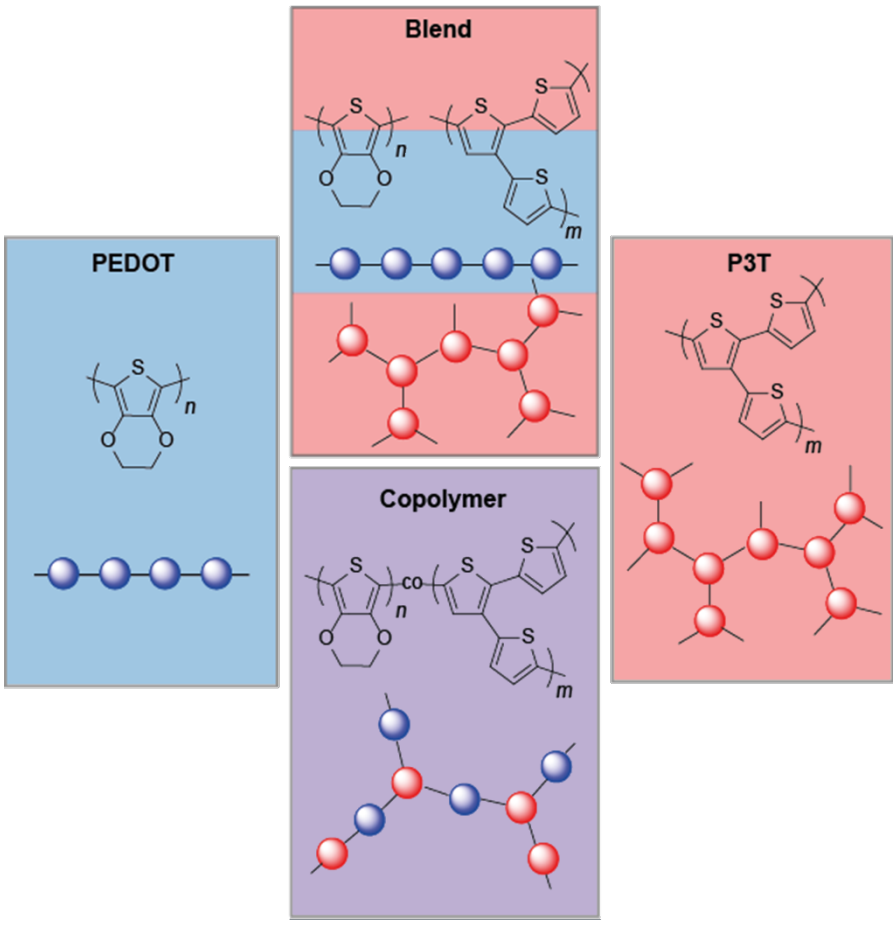

Scheme 1: Polymer constitutions of the electropolymerized films.

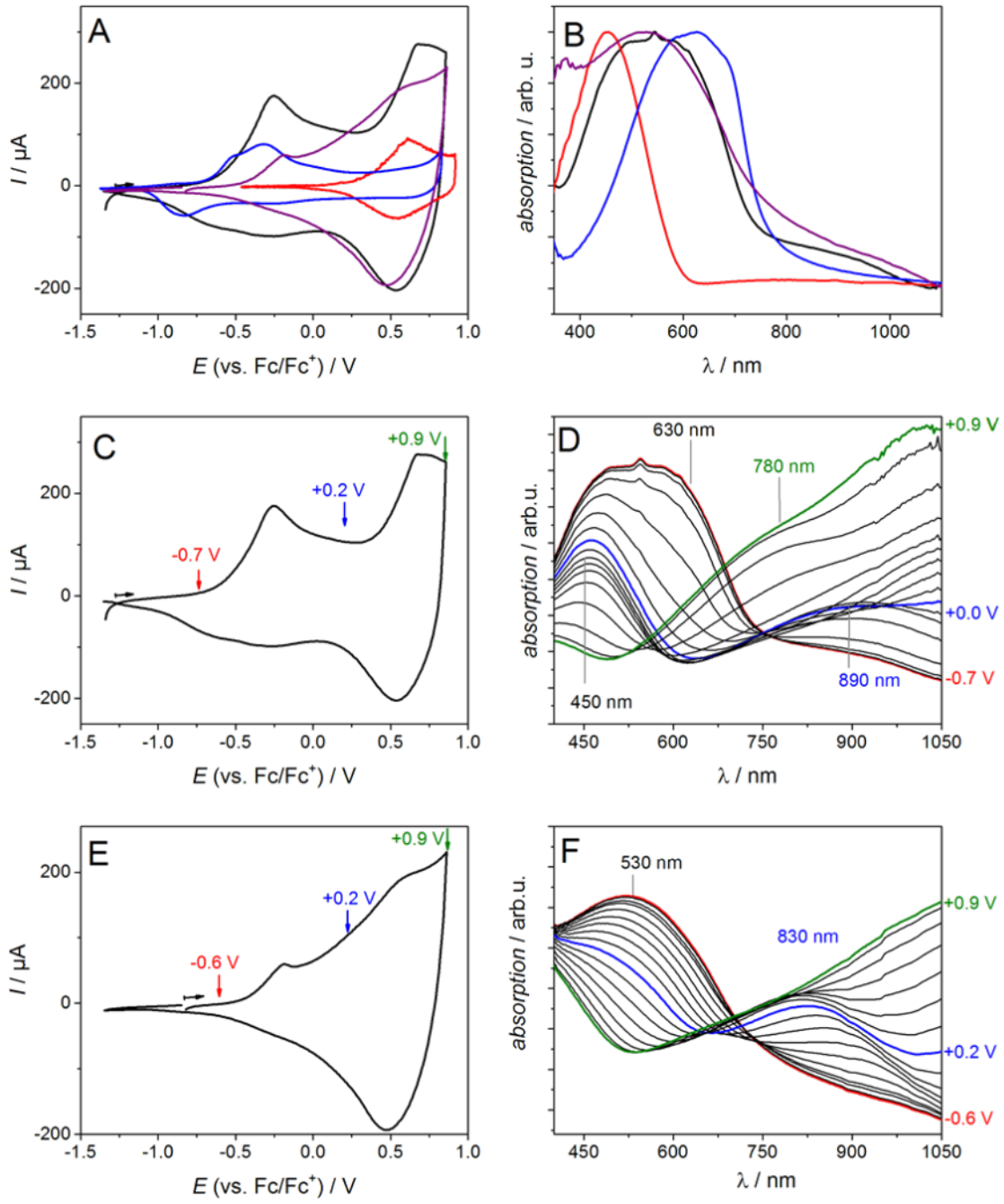

Figure 1: Cyclic voltammograms in 0.1 M NBu_4PF_6/MeCN (A) and vis–NIR spectra (B) of electropolymerized films of PEDOT (blue curve), P3T (red curve), PEDOT/P3T-blend (black curve) and P(EDOT-*co*-3T)-1:1 (purple curve) deposited on ITO-coated glass substrates. C–F: In situ spectroelectrochemistry of films deposited under potentiostatic control on ITO with oxidative cycles at 50 mV s^{-1} in 0.1 M NBu_4PF_6/MeCN (C and E) and vis–NIR spectra (D and F) recorded during the forward scan in the oxidation process of PEDOT/P3T-blend (C and D) and P(EDOT-*co*-3T)-1:1 (E and F). The films were prepared according to [24].

charged species and thus allows to allocate redox states and absorption bands to certain species. The recorded spectra of the blend and the copolymer films reveal remarkable differences. Figure 1C and D show the CVs and the absorption spectra recorded during the forward scan of the PEDOT/P3T-blend film. Following the process of the first oxidation wave in the CV the broad absorption band is decreasing asymmetrically upon potential increase. The loss of the shoulder of the absorption band at around 630 nm suggests that PEDOT is oxidized first yielding the charged PEDOT species with an absorption of

the radical cation around 890 nm. This is in accordance to literature where the PEDOT radical cation is described with an absorption maximum around 880 nm [24]. Only when approaching the second oxidation wave around +0.9 V the absorption band at 450 nm is decreasing, revealing a new absorption at 780 nm which can be attributed to the radical cation formation of P3T matching the literature value [24]. To our knowledge this is one of very few examples [48,49], where a polymer blend provides the separated absorption and redox properties of the homopolymers which allow for the separated addressing of the polymers by CV and monitoring thereof by spectroscopy.

The copolymer P(EDOT-*co*-3T)-1:1 (Figure 1E and F) shows, as described above, one broad oxidation wave in the CV and a broad absorption with a maximum at 530 nm. During the oxidation the 530 nm band is decreasing uniformly and steadily while at 830 nm a single band is ascending, which indicates the formation of the charged radical cation species. This is in agreement with our earlier data where we showed this uniform steady decrease of the band at 830 nm absorption during the oxidation for P(EDOT-*co*-3T) polymer films with different ratios of the monomers EDOT and 3T [24]. This, with respect to the blend films, completely opposite behavior is a reliable argument that indeed a copolymer is formed from the copolymerization of EDOT and 3T. Table 1 summarizes the characteristic values for the neutral and charged polymer films.

As a further analytical tool we employed Raman spectroscopy which addresses the different vibrational modes of the samples. Figure 2A shows the Raman spectra of the homopolymers PEDOT and P3T, the blend film PEDOT/P3T-blend and the copolymer P(EDOT-*co*-3T)-1:1. Note that the spectra are recorded at 532 nm in order to be in resonance with the lowest energy absorption band (HOMO–LUMO transition) of the neutral polymers and therefore out-of-resonance with the absorption bands of the oxidized species. In accordance with earlier work [51], the Raman spectrum of PEDOT exhibits a very intense band at 1428 cm^{-1} which is associated with a symmetric C_α=C_β stretching and two less intense bands at 1519 and 1370 cm^{-1} which arise from asymmetric C_α=C_β and C_β–C_β stretching vibrations, respectively. In the branched P3T polymer, a broadening of the band associated with the collective C_α=C_β stretching mode (at 1459 cm^{-1}) is observed with a shoulder appearing at 1441 cm^{-1} while the two less intense bands appear at 1496 and 1373 cm^{-1}. The broadening of the spectra in P3T is related to its branched architecture with different conjugation paths along their π-conjugated backbones which also results in a lowering of the molecular symmetry and an increase of molecular flexibility when compared to the linear polymers.

On the other hand, the Raman spectrum of the blend is clearly a simple superposition of the homopolymer spectra. Note the very good correlation between the spectral profiles of the experimental blend and the calculated spectrum created by adding the spectra of the two homopolymers PEDOT and P3T in Figure 2A. A direct comparison between the spectra of the blend and copolymer, however, reveals a noticeable downshift of the asymmetric C_α=C_β stretching modes (from 1514 in PEDOT/P3T-blend to 1500 cm^{-1} in P(EDOT-*co*-3T)-1:1) and the C_β–C_β Raman bands (from 1368 in PEDOT/P3T-blend to 1364 cm^{-1} in P(EDOT-*co*-3T)-1:1). This frequency downshift strongly suggests that the copolymer has an improved π-conjugation because of the better π-electron delocalization through the covalently connected 3T and EDOT units. A detailed superposition of the spectra of the blend and the copolymer (see labelled bands in Figure S1 in Supporting Information File 1), evidences the presence of two new bands in the copolymer at 1204 and 1060 cm^{-1} which can be assigned to stretchings of newly formed C_α–C_α bonds [52] between the monomers EDOT and 3T and to C_β–H bending modes [51], respectively. This gives further evidence that the materials formed are copolymers rather than polymer blends.

Table 1: Summary of absorption and electrochemical characteristics of polymer films electrochemically deposited on ITO electrodes under potentiostatic control derived from in situ spectroelectrochemical experiments in 0.1 M NBu_4PF_6/MeCN.

Polymer film	E^{ox}_{onset} [V vs. Fc/Fc^+] (HOMO [eV])[a]	λ_{max} (neutral) [nm][b]	λ_{max} (radical cation) [nm][b,c]
P3T[d]	+0.3 (-5.4)	450	780
PEDOT[d]	−0.8 (−4.3)	630	880
PEDOT/P3T-blend	−0.7 (−4.4)	–	≈780 and ≈890
P(EDOT-*co*-3T)-1:1	−0.6 (−4.5)	530	830

[a]HOMO levels calculated using −5.1 eV as formal potential of the ferrocene/ferrocenium (Fc/Fc^+) redox couple in the Fermi scale [50]; [b]the error is estimated to be ±15 nm; [c]values determined at $E = E^{ox}_{onset}$ +0.5 V as previously described in [24]; [d]from [24].

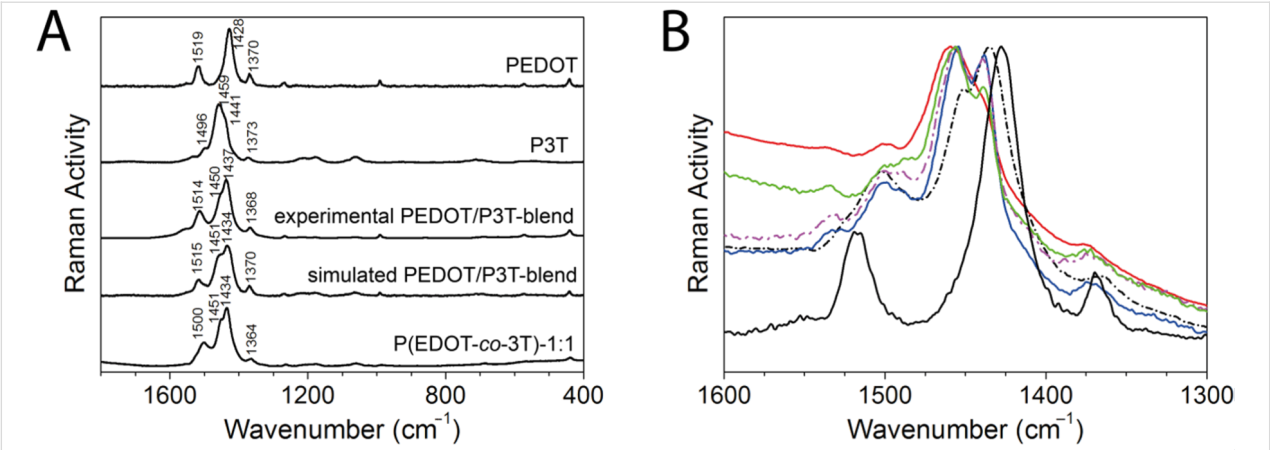

Figure 2: A: Raman spectra of electrodeposited films of the homopolymer P3T and PEDOT, PEDOT/P3T-blend, a simulated spectrum of a blend of PEDOT and P3T (created by adding the spectra of the two homopolymers) and the copolymer P(EDOT-*co*-3T)-1:1, λ_{exc} = 532 nm. B: Comparison of Raman spectra between 1300 and 1600 cm^{-1} for different monomer ratios of the copolymer films (black curve EDOT, broken black curve 1:1, blue 1:3, broken pink curve 1:5, green curve 1:10, red curve P3T), λ_{exc} = 532 nm.

The Raman spectra also give valuable information about different compositions in the copolymers. In a similar manner as described in our earlier work [24] we prepared copolymer films with different compositions (ratio of the monomers EDOT and 3T during polymerization ranging from 1:1 to 1:10). Figure 2B shows the Raman spectra between 1300 and 1600 cm^{-1} of the copolymers as well as of the homopolymers P3T and PEDOT for comparison. The main Raman bands of all copolymers which are associated with the collective symmetric C_α=C_β stretching modes are located between the band maxima in P3T (1459 cm^{-1}) and PEDOT (1428 cm^{-1}) and downshift from 1456 to 1435 cm^{-1} on passing from P(EDOT-*co*-3T)-1:10 to -1:1. It is well established in literature that the frequency of this band shifts downward upon increasing conjugation length or increasing quinoidization [53,54]. Therefore, the shift towards lower frequencies (i.e., lower energies) with increasing EDOT content demonstrates that the incorporation of EDOT in a branched thiophene polymer improves the conjugation length. This can be ascribed to the significant participation of the oxygen atoms in the π-conjugation and a gain in rigidity of the polymer backbone due to intramolecular sulfur–oxygen interactions [55,56]. The asymmetric C_α=C_β stretching modes upshift and increase in intensity with increasing EDOT content while the C_β–C_β mode slightly increases in intensity; this is also in accordance with an improved effective conjugation in going from P(EDOT-*co*-3T)-1:10 to -1:1. Note that a similar spectral evolution is found when the sample is recorded with different excitation wavelengths (see Figure S2 in Supporting Information File 1).

Further functionalization

Summarizing the first part of our manuscript the electropolymerization of monomeric mixtures of 3T and EDOT leads to copolymers and the HOMO levels of these polymers are adjustable by varying the ratio of the monomers during the polymerization process. In a next step we further transferred the copolymerization approach to the azidomethyl-substituted EDOT-N_3 monomer which allows for the straightforward modification with various alkynes by Cu(I)-catalyzed 1,3-dipolar cycloaddition (“click”-reaction) [57].

For the functionalization experiments we chose the copolymer prepared with the highest EDOT-N_3 content namely the 1:1-copolymer. The functionalization was first conducted with 1-hexyne as a model system. The successful modification had been displayed earlier by Bäuerle et al. who could show, that the cycloaddition takes place with high conversion rates both with EDOT-N_3 and when the reaction was performed in electropolymerized films of PEDOT-N_3 [41]. As functional moiety we introduced an ionic alkyne sulfonate (SO_3Na–alkyne). As the cycloaddition-reaction with SO_3Na–alkyne is not known in literature we first made tests on the reaction with the monomer EDOT-N_3 and obtained the product EDOT-clickSO_3Na in high yield. For ^{1}H NMR and IR-spectra we refer to Figure S3 and Figure S4 in Supporting Information File 1. Figure 3A depicts the synthesis of the cycloaddition-reactions of the copolymer films P(EDOT-N_3-*co*-3T)-1:1 with 1-hexyne and SO_3Na-alkyne (yielding a butyl end group or a sulfonate end group, respectively). DMSO was chosen as solvent as the degree of swelling is very high [58] and allows modification of the bulk of the film and not just of the surface.

The modified films were analyzed by IR spectroscopy in a combined reflection/absorption mode (RAS) (Figure 3B). The disappearance of the characteristic azide-band at 2100 cm^{-1} indicates that the cycloaddition-reaction takes place almost

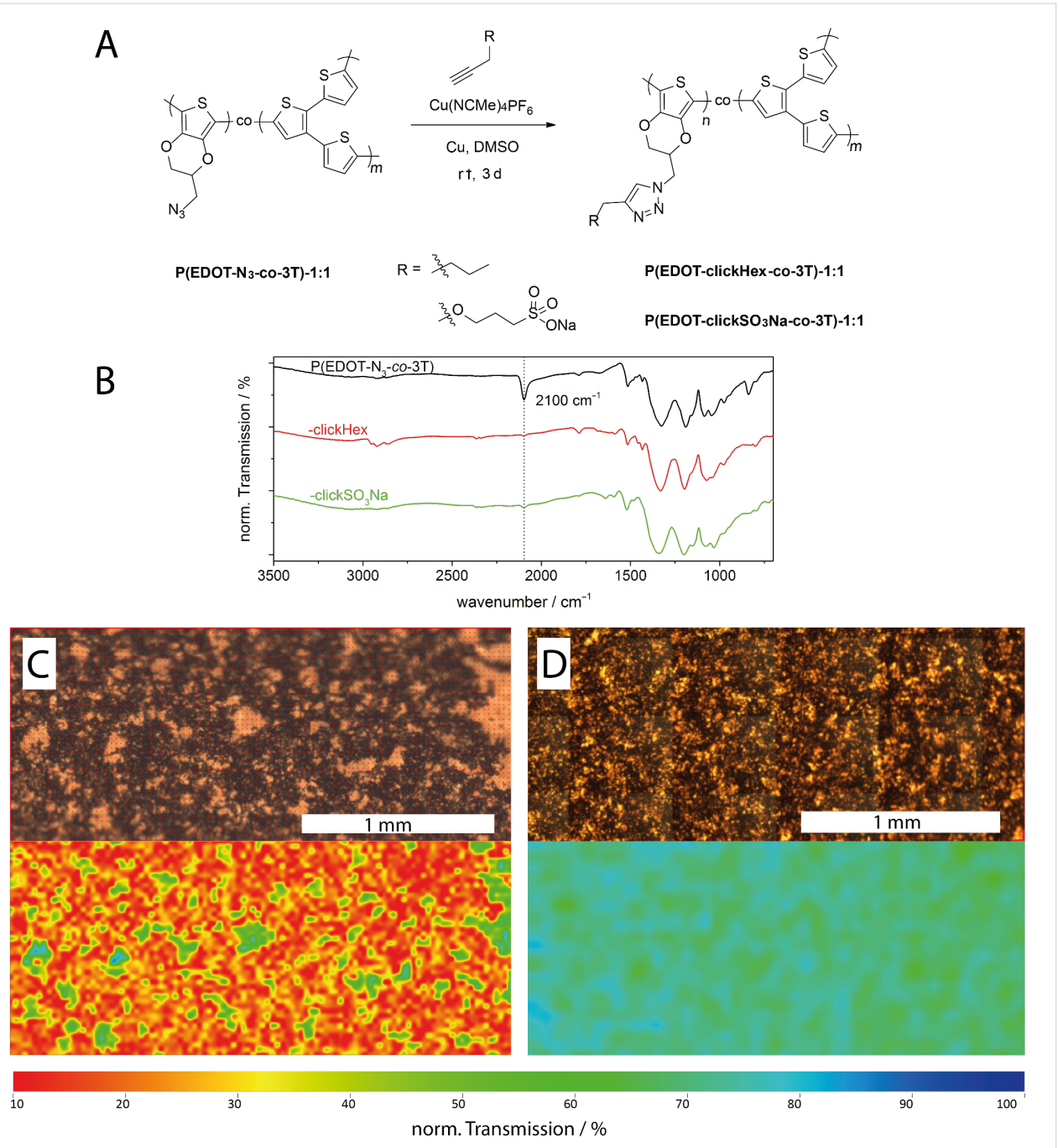

Figure 3: A: Modification of the copolymer films P(EDOT-N_3-*co*-3T) with 1-hexyne and alkyne sulfonate with $[Cu(NCMe)_4]PF_6$ and copper powder as catalyst in DMSO, reaction time 3 days at room temperature (rt). B: IR spectra of copolymer films P(EDOT-N_3-*co*-3T) (black line), P(EDOT-clickHex-*co*-3T)-1:1 (red line, hexyl modification) and P(EDOT-clickSO_3Na-*co*-3T)-1:1 (green line, sulfonate modification); spectra were rescaled (y-offset) for comparison reasons. C, D: Microscope images (top) and IR mappings (bottom) of the azide band intensity at 2100 cm^{-1} of copolymer films deposited under potentiostatic control on gold in 0.1 M NBu_4PF_6/MeCN. P(EDOT-N_3-*co*-3T)-1:1 (C, before modification) and P(EDOT-clickSO_3Na-*co*-3T) (D, after sulfonate modification). Spectra of the IR microscopy were normalized and plotted with identical colour ranges for comparison reasons.

quantitatively (within the detection limit of IR spectroscopy). For the butyl-modified film P(EDOT-clickHex-*co*-3T)-1:1 (red line) one can also observe new sp^3-C–H-vibrations at 2800–3000 cm^{-1}, which also confirm the successful incorporation of the alkyl moieties. The characteristic bands of the sulfonic acid at 1190 and 1030 cm^{-1} (see Figure S4 in Supporting Information File 1) overlap with other bands of the polymer P(EDOT-clickSO_3Na-*co*-3T) (green line) in the fingerprint region and therfore a proper assignment is difficult. Further information was gained by a mapping of the polymer

films with IR-microspectroscopic measurements. Figure 3 shows the microscope images of the polymer films P(EDOT-N_3-*co*-3T)-1:1 (C, top, before modification) and P(EDOT-clickSO_3Na-*co*-3T)-1:1 (D, top, after sulfonate-modification) and the corresponding maps (bottom) of the intensity of the azide-band at 2100 cm^{-1} wherein the highest azide band intensities (transmission of 10%) are displayed in red, and the lowest intensities (transmission of 100%) are displayed in blue. For comparison and to limit the influence of the film thickness all transmission spectra were normalized. While for P(EDOT-N_3-*co*-3T)-1:1 the high intensity and a homogeneous distribution of the azide band is observed for the whole film unless the bare gold electrode is visible (light areas in the microscope images; green and blue spots in the IR map. Note that the background of the single IR spectra is about 70–80%), for the modified P(EDOT-clickSO_3Na-*co*-3T)-1:1 nearly no azide band intensity can be observed. This provides information about the integrity of the modification over the whole film.

The integrity of the redox and optical behavior upon modification of the P(EDOT-N_3-*co*-3T)-1:1 with sulfonic acid with regard to the parent copolymer was further proven by cyclic voltammetry and in situ spectroelectrochemistry. It was recently demonstrated that the azide group does not change the oxidation potentials and that the redox behavior of EDOT-N_3 resembles pristine EDOT [41]. The copolymerization of mixtures of the monomers EDOT-N_3 and 3T in different ratios (1:1, 1:3, 1:5 and 1:10) was performed in analogy to the copolymerization of EDOT and 3T. The cyclic voltammograms of the respective copolymers show broad oxidation waves with onset potentials ranging in between the onset potentials of the homopolymers P3T and PEDOT-N_3 (see Figure 4A). The cathodic cycles of the copolymers reveal identical onset potential values and therefore LUMO levels for P3T and the P3T-rich copolymers (1:3, 1:5 and 1:10), while PEDOT-N_3 and the PEDOT-N_3-rich 1:1 copolymers show a chemically irreversible electron transfer reaction under our conditions. These data are consistent with those obtained for P(EDOT-*co*-3T) films.

The in situ spectroelectrochemistry data in Figure 4B–E reveals that the ionic modification with sulfonic acid has no influence on the oxidation onset and therefore HOMO level of the polymer film. We attribute this finding to the absence of conjugation between the attached N_3 groups and the π-system of the polymer backbone. The absorption development upon electrochemical charging shows the characteristic steady decrease of the neutral band and the increase of the absorption at lower energy accounting for the generation of delocalized charges in both the parent polymer and the ionically modified one. The preparation of a conjugated polyelectrolyte with tunable HOMO level is therefore accessible via this modification process.

While no changes of the electronic properties were detected between P(EDOT-N_3-*co*-3T)-1:1 and P(EDOT-clickSO_3Na-*co*-3T)-1:1, the introduction of ions into the polymers can drastically alter the surface properties. Water contact angle measurements are a convenient tool to study the surface polarity. Interestingly, we found in the context of this study that the water contact angle of as polymerized P(EDOT-N_3-*co*-3T)-1:1 is quite high with a value of 137 ± 2° (Figure 5, left). Similar values were found for P(EDOT-*co*-3T)-1:1 (137 ± 1°). The corresponding homopolymers PEDOT and PEDOT-N_3 have lower values with a contact angle of 71 ± 3° and 91 ± 6°, respectively, whereas P3T gives an even larger value of 147 ± 6° (see Figure S5 in Supporting Information File 1). This highly hydrophobic surface of the polymers containing branched 3T units may be explained by a high porosity based on a 3-dimensional growth of these polymer films during the electropolymerization process [59,60].

After butyl modification the hydrophobic character remains constant (135 ± 2° after modification, Figure 5, middle), while we changed the surface polarity of the polymer from highly hydrophobic to hydrophilic in the case of the sulfonate modification. A water contact angle of 42 ± 4° is obtained for P(EDOT-clickSO_3Na-*co*-3T)-1:1 after modification (Figure 5, right), i.e., 100° lower than in the case of the parent polymer P(EDOT-N_3-*co*-3T)-1:1. In the case of the analogue modification of PEDOT-N_3 similar trends were observed (see Figure S6 in Supporting Information File 1).

Conclusion

We showed that the monomers 3T and EDOT are suited for blend formation by sequential electropolymerization, where both polymers maintain their pristine redox features and are both addressable in electrochemical devices. We used in situ spectroelectrochemistry and Raman spectroscopy to prove that copolymer formation from mixtures of the two monomers takes place and that by variation of the feed ratio polymers with adjustable optical and redox properties are accessible. We successfully transferred the copolymerization route to the functional EDOT derivative EDOT-N_3. As an example we showed the potential of surface polarity adjustment by the introduction of ionic moieties to the hydrophobic polymer films. A decrease of the water contact angle of ≈100° could be achieved which evoked a complete change of the polymer surface nature from hydrophobic to hydrophilic. This opens the way to a library of polymers which carry tailored redox properties as well as additional functionalities through a manifold of different functionalization possibilities by “click”-chemistry by leaving the redox properties unchanged. Such an orthogonal functionalization may further be used to control the properties in new materials for organic photovoltaics where low oxidation potentials are

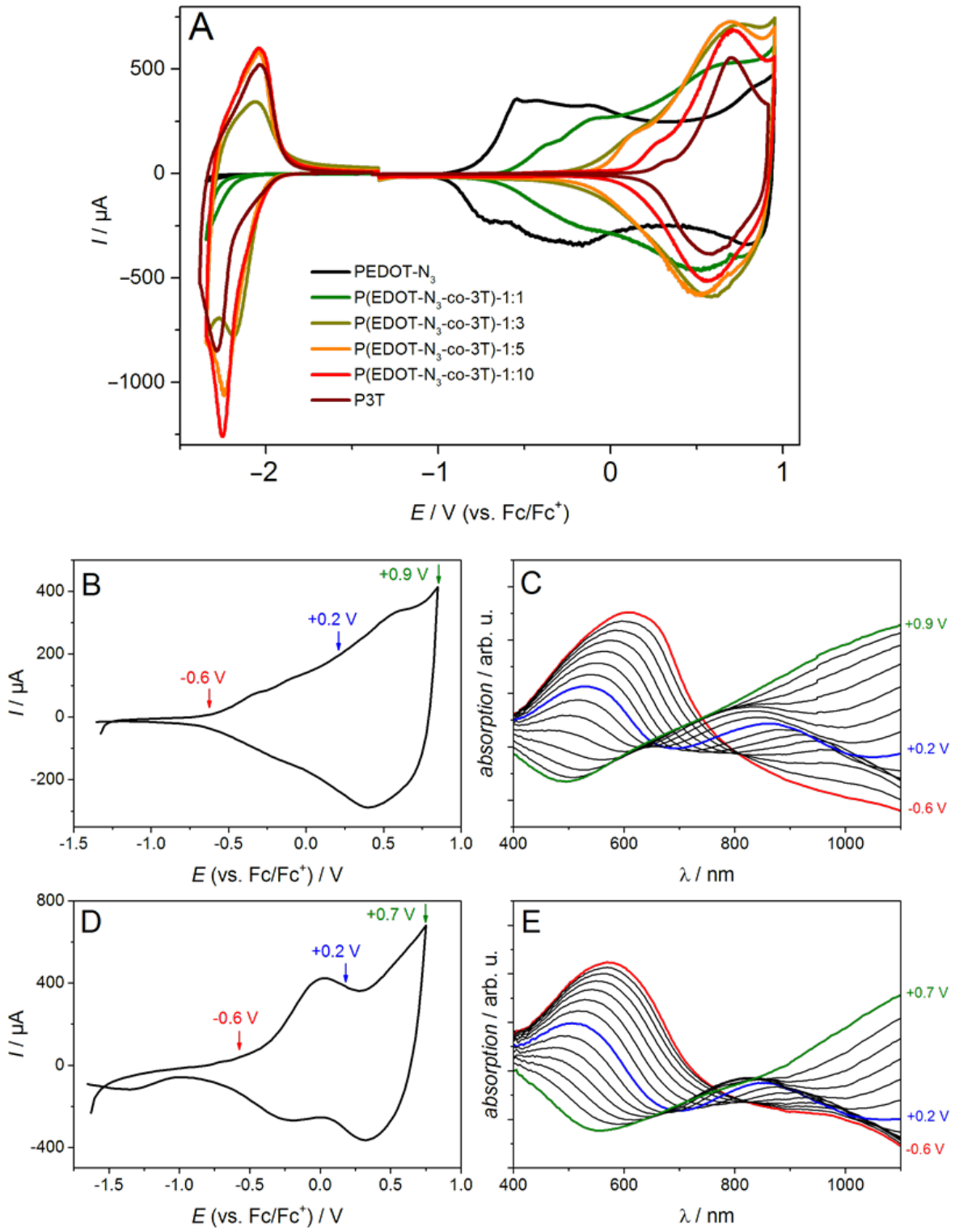

Figure 4: Cyclic voltammograms of films deposited under potentiostatic control on gold-coated glass substrates (1 cm^2) from different monomer mixtures: (A) Ratio of EDOT-N_3:3T = 1:0 (black), 1:1 (dark green), 1:3 (light green), 1:5 (orange), 1:10 (red) and 0:1 (brown curve) recorded in 0.1 M NBu_4PF_6/MeCN, 20 mV/s. B–E: In situ spectroelectrochemistry of films deposited under potentiostatic control on ITO in 0.1 M NBu_4PF_6/MeCN. Cyclic voltammograms (B and D) and corresponding vis–NIR spectra (C and E) recorded during the forward scan of the oxidation of the P(EDOT-N_3-*co*-3T)-1:1 (B and C) and P(EDOT-clickSO_3Na-*co*-3T)-1:1 (D and E) at 50 mV s^{-1}.

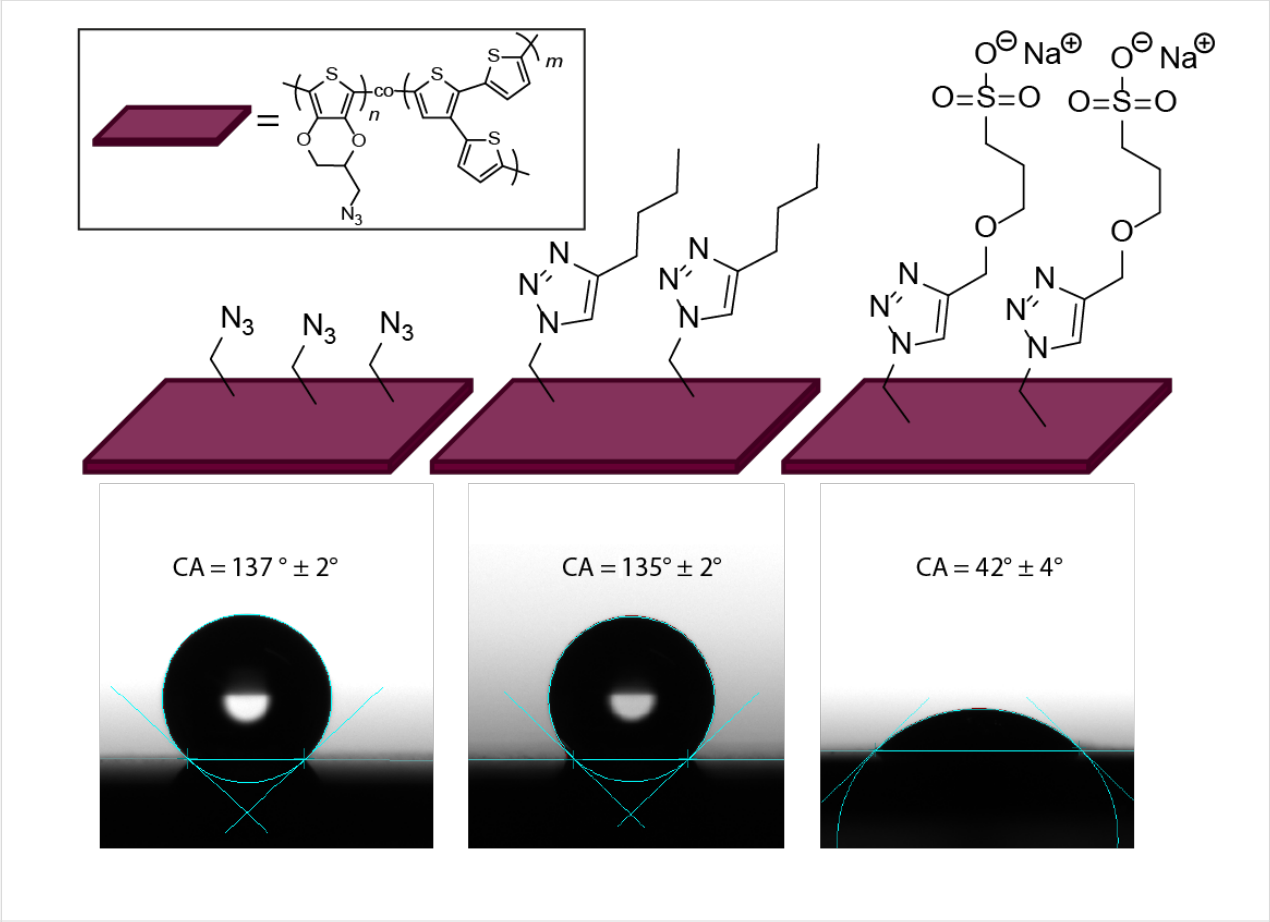

Figure 5: Water contact angle (CA) of the films of P(EDOT-N_3-*co*-3T) (left), P(EDOT-clickHex-*co*-3T)-1:1 (middle) and P(EDOT-clickSO_3Na-*co*-3T)-1:1 (right).

needed (monomer ratio) and a good processability from environmental solvents (e.g., water) is desired (introduction of polar/ionic groups).

Experimental

Materials

All chemicals and solvents were purchased from Sigma-Aldrich or Alfa-Aesar. Solvents were at least of HPLC grade and were used as received except otherwise noted. NBu_4PF_6 (Sigma-Aldrich, electrochemical grade) was stored in a desiccator over silica beads (activated in an oven at 80 °C for several days). Acetonitrile (Alfa Aesar, supergradient HPLC grade (far-UV), +99.9%) was stored over neutral Al_2O_3 (activated under vacuum at 120 °C for 24 h) under an argon atmosphere. DMSO was distilled in vacuum, crystallized at 4 °C and the mother liquor was removed. After melting of the crystals the crystallization procedure was repeated once. DMSO was stored over 3 Å molecular sieves (activated in an oven at 80 °C for several days) under argon atmosphere. All reactions were carried out under argon atmosphere unless otherwise noted. The synthesis of 3T was published elsewhere [61].

Methods

^{1}H (250 MHz) and $^{13}C\{^1H\}$ (63 MHz) NMR spectra were recorded on a Bruker Avance 250 spectrometer. vis-NIR spectra of the polymer films deposited on ITO-coated glass substrates were recorded with a Lambda 35 spectrometer (Bruker).

IR spectroscopy was performed on a Bruker FTIR spectrometer IFS 66/S in a wavelength region of 600–3500 cm^{-1}. Liquids and oils were measured on a diamond-ATR-device (golden gate). Polymer films were measured with a VeeMAX^{TM} II Variable Angle Specular Reflectance Accessory (Pike Technologies) with an incidence angle differing 35° from the orthogonal plane. IR-microscopy experiments (ultra-fast mappings) of deposited films were performed with a Thermo Fisher Scientific Nicolet iN10 MX spectrometer equipped with a nitrogen cooled MCT/A detector. The sampling interval was 0.10 s, with a step size of 25 µm or 50 µm. The spectral resolution was 16 cm^{-1}, the aperture was set to 80 µm or 150 µm. Spectra are corrected for background. Modified electrodes were directly placed under the microscope. Data acquisition was performed with Thermo Fisher Scientific Omnic Picta software. Raman

spectra with 532 laser excitation were recorded using a Bruker Senterra dispersive Raman microscope equipped with a neon lamp and using a Nd:YAG laser with excitation at λ_{exc} = 532 nm. Raman spectra with excitation at λ_{exc} = 488 nm were recorded by using a Microscope Invia ReflexRaman RENISHAW. Fourier Transform (FT) Raman spectra with 1064 nm laser excitation were recorded using a Bruker FRA 106/S instrument and a Nd:YAG laser source with excitation at λ_{exc} = 1064 nm, operating in a back-scattering configuration. Water contact angle measurements were carried out on a Contact Angle System OCA 20 by dataphysics using water droplets of 1–2 µL volume (R > 18.2 MΩ). Calculations of the contact angles were done with the software SCA20 using ellipse fitting. Mean values were calculated using at least 4 different measurements. Deviations given are the mean values of al obtained single deviations.

Electrochemical experiments

All electrochemical experiments were performed with an Autolab PGSTAT101 potentiostat (Metrohm, Germany) in a three-electrode glass cell under argon atmosphere at room temperature. The counter electrode was a Pt plate. The pseudoreference electrode consisted of AgCl-coated silver wire that was directly immersed into the electrolyte. As working electrodes, gold (50 nm layer)-coated Si wafers (with a 5 nm Cr adhesion layer between the Si wafer and the Au layer) or ITO-coated glass (≤50 Ω/sq, PGO, Germany) slides (approximately 1 cm^2) were used. The gold working electrodes were fabricated by the physical vapor deposition of Cr and Au on rotating Si wafers. The gold-coated Si wafers and the ITO substrates were thoroughly washed with acetone prior to use. Additionally, the electrodes were treated with oxygen plasma for at least 5 min before electrodepositions. NBu_4PF_6 was used as the supporting electrolyte at a concentration of 0.1 M. Electrolyte solutions were deaerated by argon bubbling. All potentials are referenced to the formal potential of the Fc/Fc^+ external redox standard [62]. To avoid charge-trapping effects during cyclic voltammetric experiments, the oxidation and reduction cycles were performed separately.

Visible–NIR spectroelectrochemical measurements were made in situ with transparent ITO electrodes (on glass, ≤50 Ω/sq, PGO, Germany) and 0.1 M NBu_4PF_6/MeCN as the electrolyte. The electrodeposited films were used directly for the measurements. The vis–NIR spectra were recorded with a diode array spectrometer from the Zeiss MCS 600 series (equipped with a Zeiss CLH600 halogen lamp and two MCS 611 NIR 2.2 and MCS 621 VIS II spectrometer cassettes).

Electropolymerization of PEDOT, PEDOT-N_3, P3T and copolymers: In a similar manner as described in reference [24] electropolymerization of the monomers 3T, EDOT and EDOT-N_3 on gold or ITO was performed under potentiostatic control (deposition time = 200 s) with an overall monomer or comonomer concentration of 2 mM in 0.1 M NBu_4PF_6/MeCN at 0.9–1.1 V vs Fc/Fc^+, followed by a discharging step (200–205 s, −1.4 V vs Fc/Fc^+). The deposition potentials correspond to the peak potential of the overlapping signal of the oxidation of both comonomers in the corresponding electrolyte. The desired concentrations were achieved by taking appropriate aliquots from stock solutions (c = 10 or 20 mM). For blend formation, four consecutive potentiostatic polymerizations (each for 50 s at 0.9–1.1 V vs Fc/Fc^+, followed by a discharging step of 50 s at −1.4 V vs Fc/Fc^+) were conducted alternating the used monomer in each step. For this purpose, two identical cells, one loaded with EDOT and one with 3T (c = 2 mM) were used. Between the steps, the polymer films were rinsed thoroughly with pure acetonitrile.

Synthesis

2-(Azidomethyl)-2,3-dihydrothieno[3,4-*b*][1,4]dioxine (PEDOT-N_3) [42,63] and sodium 3-(prop-2-yn-1-yloxy)propane-1-sulfonate (SO_3Na–alkyne) [64] were synthesized based on literature.

Synthesis of sodium 3-((1-((2,3-dihydrothieno[3,4-*b*][1,4]dioxin-2-yl)methyl)-1*H*-1,2,3-triazol-4-yl)methoxy)propane-1-sulfonate (EDOT-clickSO_3Na): Sodium 3-(prop-2-yn-1-yloxy)propane-1-sulfonate (SO_3Na–alkyne, 0.1 mmol, 20.0 mg), 2-(azidomethyl)-2,3-dihydrothieno[3,4-*b*][1,4]dioxine (PEDOT-N_3, 0.1 mmol, 19.5 mg) and tetrakis(acetonitrile) copper(I) hexafluorophosphate (0.005 mmol, 2.0 mg) were dissolved in DMSO (2.5 mL). Copper powder (0.1 mmol, 6.9 mg) was added and the reaction mixture was stirred for 3 days at room temperature. The reaction mixture was filtered, the filtrate was concentrated in vacuum and poured in methanol which was then decanted. Residual solvent was removed under reduced pressure to yield the raw product as a greenish highly viscous oil (37 mg, 93%). ^{1}H NMR (250 MHz, DMSO-d_6) δ 8.13 (s, 1H), 6.61 (s, 2H), 4.66 (m, 3H), 4.47 (s, 2H), 4.31 (m, 1H), 3.95 (m, 1H) 3.48 (t, J = 6.6 Hz, 2H), 2.4 (t, J = 7.5 Hz, 2H), 1.78 (m, 2H) ppm; $^{13}C\{^1H\}$ NMR (63 MHz, DMSO-d_6) δ 141.1, 140.8, 125.1, 100.9, 100.6, 72.2, 69.5, 65.7, 63.7, 50.35, 49.6, 26.1 ppm; IR (ATR): 3107, 3006, 2916, 2870, 2484, 2424, 1192, 1035 cm^{-1}.

Synthesis of P(EDOT-clickHex-co-3T) and P(EDOT-clickSO_3Na-co-3T): For the polymer analogue "click"-modification of P(EDOT-N_3-*co*-3T) polymer films on gold or ITO electrodes were placed in flasks containing DMSO (10 mL), tetrakis(acetonitrile) copper(I) hexafluorophosphate (0.005 mmol, 1.9 mg) and copper powder (0.1 mmol, 6.4 mg).

Alkyne (sodium 3-(prop-2-yn-1-yloxy)propane-1-sulfonate, 0.1 mmol, 20.0 mg or 1-hexyne, 0.1 mmol, 8.2 mg) was added. The films were allowed to react for three days, while the solution was gently agitated from time to time. The films were thoroughly rinsed with DMSO (2×) and methanol (3×) and dried in vacuum. The success of the reaction was confirmed by IR spectroscopy.

Supporting Information

Supporting Information File 1

Additional Raman data of PEDOT, P3T, copolymers and blends; ^{1}H NMR and IR spectra of EDOT-ClickSO_3Na; contact angles of P3T; PEDOT-N_3, PEDOT-clickHex and PEDOT-clickSO_3Na.
[http://www.beilstein-journals.org/bjoc/content/supplementary/1860-5397-11-39-S1.pdf]

Acknowledgements

The authors thank K. Dirnberger and M. Scheuble for the helpful discussions. This work was financially supported by the DFG within the Emmy Noether program. The work at the University of Malaga was supported by MINECO project reference CTQ2012-33733 and Junta Andalucía (P09_FQM-4708). R.C.G.C. acknowledges the Junta de Andalucía for a personal doctoral grant. M.C.R.D. thanks the MICINN for a "Ramón y Cajal" research contract.

References

1. Roncali, J. *Macromol. Rapid Commun.* **2007,** *28,* 1761–1775. doi:10.1002/marc.200700345
2. Scharber, M. C.; Mühlbacher, D.; Koppe, M.; Denk, P.; Waldauf, C.; Heeger, A. J.; Brabec, C. J. *Adv. Mater.* **2006,** *18,* 789–794. doi:10.1002/adma.200501717
3. Li, G.; Zhu, R.; Yang, Y. *Nat. Photonics* **2012,** *6,* 153–161. doi:10.1038/nphoton.2012.11
4. Heuer, H. W.; Wehrmann, R.; Kirchmeyer, S. *Adv. Funct. Mater.* **2002,** *12,* 89–94. doi:10.1002/1616-3028(20020201)12:2<89::AID-ADFM89>3.0.CO;2-1
5. Sirringhaus, H. *Adv. Mater.* **2005,** *17,* 2411–2425. doi:10.1002/adma.200501152
6. Gross, M.; Müller, D.; Nothofer, H.-G.; Scherf, U.; Neher, D.; Bräuchle, C.; Meerholz, K. *Nature* **2000,** *405,* 661–665. doi:10.1038/35015037
7. Roncali, J.; Thobie-Gautier, C. *Adv. Mater.* **1994,** *6,* 846–848. doi:10.1002/adma.19940061108
8. Waltman, R. J.; Bargon, J.; Diaz, A. F. *J. Phys. Chem.* **1983,** *87,* 1459–1463. doi:10.1021/j100231a035
9. Sirringhaus, H.; Brown, P. J.; Friend, R. H.; Nielsen, M. M.; Bechgaard, K.; Langeveld-Voss, B. M. W.; Spiering, A. J. H.; Janssen, R. A. J.; Meijer, E. W.; Herwig, P.; de Leeuw, D. M. *Nature* **1999,** *401,* 685–688. doi:10.1038/44359
10. Groenendaal, L.; Jonas, F.; Freitag, D.; Pielartzik, H.; Reynolds, J. R. *Adv. Mater.* **2000,** *12,* 481–494. doi:10.1002/(SICI)1521-4095(200004)12:7<481::AID-ADMA481>3.0.CO;2-C
11. Wudl, F.; Kobayashi, M.; Heeger, A. J. *J. Org. Chem.* **1984,** *49,* 3382–3384. doi:10.1021/jo00192a027
12. Havinga, E. E.; ten Hoeve, W.; Wynberg, H. *Polym. Bull.* **1992,** *29,* 119–126. doi:10.1007/BF00558045
13. Naka, K.; Umeyama, T.; Chujo, Y. *Macromolecules* **2000,** *33,* 7467–7470. doi:10.1021/ma000580k
14. van Duren, J.; Dhanabalan, A.; van Hal, P. A.; Janssen, R. A. J. *Synth. Met.* **2001,** *121,* 1587–1588. doi:10.1016/S0379-6779(00)01307-2
15. Heinze, J.; Frontana-Uribe, B. A.; Ludwigs, S. *Chem. Rev.* **2010,** *110,* 4724–4771. doi:10.1021/cr900226k
16. Piron, F.; Leriche, P.; Mabon, G.; Grosu, I.; Roncali, J. *Electrochem. Commun.* **2008,** *10,* 1427–1430. doi:10.1016/j.elecom.2008.07.014
17. Piron, F.; Leriche, P.; Grosu, I.; Roncali, J. *J. Mater. Chem.* **2010,** *20,* 10260–10268. doi:10.1039/c0jm01873b
18. Benincori, T.; Bonometti, V.; De Angelis, F.; Falciola, L.; Muccini, M.; Mussini, P. R.; Pilati, T.; Rampinini, G.; Rizzo, S.; Toffanin, S.; Sannicolò, F. *Chem. – Eur. J.* **2010,** *16,* 9086–9098. doi:10.1002/chem.200903546
19. Inganäs, O.; Liedberg, B.; Chang-Ru, W.; Wynberg, H. *Synth. Met.* **1985,** *11,* 239–249. doi:10.1016/0379-6779(85)90021-9
20. Kuwabata, S.; Ito, S.; Yoneyama, H. *J. Electrochem. Soc.* **1988,** *135,* 1691–1695. doi:10.1149/1.2096098
21. Funt, B. L.; Peters, E. M.; Van Dyke, J. D. *J. Polym. Sci., Part A: Polym. Chem.* **1986,** *24,* 1529–1537. doi:10.1002/pola.1986.080240711
22. Peters, E. M.; Van Dyke, J. D. *J. Polym. Sci., Part A: Polym. Chem.* **1992,** *30,* 1891–1898. doi:10.1002/pola.1992.080300911
23. Huang, H.; Pickup, P. G. *Chem. Mater.* **1998,** *10,* 2212–2216. doi:10.1021/cm9801439
24. Link, S. M.; Scheuble, M.; Goll, M.; Muks, E.; Ruff, A.; Hoffmann, A.; Richter, T. V.; Lopez Navarrete, J. T.; Ruiz Delgado, M. C.; Ludwigs, S. *Langmuir* **2013,** *29,* 15463–15473. doi:10.1021/la403050c
25. Liu, B.; Bazan, G. C., Eds. *Conjugated Polyelectrolytes: Fundamentals and Applications;* Wiley-VCH: Weinheim, 2013. doi:10.1002/9783527655700
26. Richter, T. V.; Bühler, C.; Ludwigs, S. *J. Am. Chem. Soc.* **2012,** *134,* 43–46. doi:10.1021/ja207458b
27. Skotheim, T. A.; Elsenbaumer, R. L.; Reynolds, J. R., Eds. *Handbook of Conducting Polymers,* 2nd ed.; Marcel Dekker: New York, 1998; pp 977–978.
28. Seo, J. H.; Gutacker, A.; Sun, Y.; Wu, H.; Huang, F.; Cao, Y.; Scherf, U.; Heeger, A. J.; Bazan, G. C. *J. Am. Chem. Soc.* **2011,** *133,* 8416–8419. doi:10.1021/ja2037673
29. Sitter, H.; Draxl, C.; Ramsey, M., Eds. *Small Organic Molecules on Surfaces;* Springer: Berlin, Heidelberg, 2013; pp 311–315. doi:10.1007/978-3-642-33848-9
30. Sundaresan, N. S.; Basak, S.; Pomerantz, M.; Reynolds, J. R. *J. Chem. Soc., Chem. Commun.* **1987,** 621–622. doi:10.1039/C39870000621
31. Reynolds, J. R.; Sundaresan, N. S.; Pomerantz, M.; Basak, S.; Baker, C. K. *J. Electroanal. Chem. Interfacial Electrochem.* **1988,** *250,* 355–371. doi:10.1016/0022-0728(88)85176-3
32. Patil, A. O.; Ikenoue, Y.; Wudl, F.; Heeger, A. J. *J. Am. Chem. Soc.* **1987,** *109,* 1858–1859. doi:10.1021/ja00240a044

33. Patil, A. O.; Ikenoue, Y.; Basescu, N.; Colaneri, N.; Chen, J.; Wudl, F.; Heeger, A. J. *Synth. Met.* **1987,** *20,* 151–159. doi:10.1016/0379-6779(87)90554-6
34. Ikenoue, Y.; Outani, N.; Patil, A. O.; Wudl, F.; Heeger, A. J. *Synth. Met.* **1989,** *30,* 305–319. doi:10.1016/0379-6779(89)90653-X
35. Bäuerle, P.; Gaudl, K.-U.; Würthner, F.; Sariciftci, N. S.; Mehring, M.; Neugebauer, H.; Zhong, C.; Doblhofer, K. *Adv. Mater.* **1990,** *2,* 490–494. doi:10.1002/adma.19900021011
36. Visy, C.; Kankare, J.; Kriván, E. *Electrochim. Acta* **2000,** *45,* 3851–3864. doi:10.1016/S0013-4686(00)00456-4
37. Freund, M. S.; Deore, B. *Self-Doped Conducting Polymers;* John Wiley & Sons, Ltd.: West Sussex, 2007.
38. Zotti, G.; Musiani, M.; Zecchin, S.; Schiavon, G.; Berlin, A.; Pagani, G. *Chem. Mater.* **1998,** *10,* 480–485. doi:10.1021/cm970381o
39. Binder, W. H.; Sachsenhofer, R. *Macromol. Rapid Commun.* **2007,** *28,* 15–54. doi:10.1002/marc.200600625
40. Theato, P.; Klok, H.-A., Eds. *Functional Polymers by Post-Polymerization Modification: Concepts, Guidelines and Applications;* Wiley-VCH: Weinheim, 2012. doi:10.1002/9783527655427
41. Bu, H.-B.; Götz, G.; Reinold, E.; Vogt, A.; Schmid, S.; Blanco, R.; Segura, J. L.; Bäuerle, P. *Chem. Commun.* **2008,** 1320–1322. doi:10.1039/b718077b
42. Bu, H.-B.; Götz, G.; Reinold, E.; Vogt, A.; Schmid, S.; Segura, J. L.; Blanco, R.; Gómez, R.; Bäuerle, P. *Tetrahedron* **2011,** *67,* 1114–1125. doi:10.1016/j.tet.2010.12.022
43. Bu, H.-B.; Götz, G.; Reinold, E.; Vogt, A.; Azumi, R.; Segura, J. L.; Bäuerle, P. *Chem. Commun.* **2012,** *48,* 2677–2679. doi:10.1039/c2cc17374c
44. Sinha, J.; Sahoo, R.; Kumar, A. *Macromolecules* **2009,** *42,* 2015–2022. doi:10.1021/ma802289j
45. Daugaard, A. E.; Hvilsted, S.; Hansen, T. S.; Larsen, N. B. *Macromolecules* **2008,** *41,* 4321–4327. doi:10.1021/ma702731k
46. Hansen, T. S.; Daugaard, A. E.; Hvilsted, S.; Larsen, N. B. *Adv. Mater.* **2009,** *21,* 4483–4486. doi:10.1002/adma.200900980
47. Shida, N.; Ishiguro, Y.; Atobe, M.; Fuchigami, T.; Inagi, S. *ACS Macro Lett.* **2012,** *1,* 656–659. doi:10.1021/mz300210w
48. Holze, R. *Electrochim. Acta* **2011,** *56,* 10479–10492. doi:10.1016/j.electacta.2011.04.013
49. Ak, M.; Cetişli, H.; Toppare, L. *Colloid Polym. Sci.* **2012,** *291,* 767–772. doi:10.1007/s00396-012-2787-7
50. Cardona, C. M.; Li, W.; Kaifer, A. E.; Stockdale, D.; Bazan, G. C. *Adv. Mater.* **2011,** *23,* 2367–2371. doi:10.1002/adma.201004554
51. Garreau, S.; Louarn, G.; Buisson, J. P.; Froyer, G.; Lefrant, S. *Macromolecules* **1999,** *32,* 6807–6812. doi:10.1021/ma9905674
52. Louarn, G.; Buisson, J. P.; Lefrant, S.; Fichou, D. *J. Phys. Chem.* **1995,** *99,* 11399–11404. doi:10.1021/j100029a016
53. Capel Ferrón, C.; Ruiz Delgado, M. C.; Gidron, O.; Sharma, S.; Sheberla, D.; Sheynin, Y.; Bendikov, M.; López Navarrete, J. T.; Hernández, V. *Chem. Commun.* **2012,** *48,* 6732–6734. doi:10.1039/c2cc18144d
54. Casado, J.; Hernández, V.; Hotta, S.; López Navarrete, J. T. *J. Chem. Phys.* **1998,** *109,* 10419–10429. doi:10.1063/1.477697
55. Turbiez, M.; Frère, P.; Roncali, J. *J. Org. Chem.* **2003,** *68,* 5357–5360. doi:10.1021/jo0345493
56. Turbiez, M.; Frère, P.; Allain, M.; Videlot, C.; Ackermann, J.; Roncali, J. *Chem. – Eur. J.* **2005,** *11,* 3742–3752. doi:10.1002/chem.200401058
57. Kolb, H. C.; Finn, M. G.; Sharpless, K. B. *Angew. Chem., Int. Ed.* **2001,** *40,* 2004–2021. doi:10.1002/1521-3773(20010601)40:11<2004::AID-ANIE2004>3.0.CO;2-5
58. Lind, J. U.; Hansen, T. S.; Daugaard, A. E.; Hvilsted, S.; Andresen, T. L.; Larsen, N. B. *Macromolecules* **2011,** *44,* 495–501. doi:10.1021/ma102149u
59. Nicolas, M. *J. Adhes. Sci. Technol.* **2008,** *22,* 365–377. doi:10.1163/156856108X295446
60. Foster, E. L.; De Leon, A. C. C.; Mangadlao, J.; Advincula, R. *J. Mater. Chem.* **2012,** *22,* 11025–11031. doi:10.1039/c2jm31067h
61. Richter, T. V.; Link, S.; Hanselmann, R.; Ludwigs, S. *Macromol. Rapid Commun.* **2009,** *30,* 1323–1327. doi:10.1002/marc.200900186
62. Gritzner, G.; Kůta, J. *Pure Appl. Chem.* **1982,** *54,* 1527–1532. doi:10.1351/pac198254081527
63. Segura, J. L.; Gómez, R.; Reinold, E.; Bäuerle, P. *Org. Lett.* **2005,** *7,* 2345–2348. doi:10.1021/ol050573m
64. Norris, B. C.; Li, W.; Lee, E.; Manthiram, A.; Bielawski, C. W. *Polymer* **2010,** *51,* 5352–5358. doi:10.1016/j.polymer.2010.09.041

License and Terms

BEILSTEIN JOURNAL OF ORGANIC CHEMISTRY

IR and electrochemical synthesis and characterization of thin films of PEDOT grown on platinum single crystal electrodes in [EMMIM]Tf_2N ionic liquid

Andrea P. Sandoval[1,2], Marco F. Suárez-Herrera[1] and Juan M. Feliu[*2]

Full Research Paper

Open Access

Address:
[1]Departamento de Química, Facultad de Ciencias, Universidad Nacional de Colombia, Cra. 30# 45-03, Edificio 451, Bogota, Colombia and [2]Departamento de Química Física e Instituto Universitario de Electroquímica, Universidad de Alicante, Apartado 99, E-03080 Alicante, Spain

Email:
Juan M. Feliu[*] - juan.feliu@ua.es

* Corresponding author

Keywords:
AFM; [EMMIM]Tf_2N ionic liquid; in situ IR; PEDOT; Pt single crystals

Beilstein J. Org. Chem. **2015,** *11,* 348–357.
doi:10.3762/bjoc.11.40

Received: 28 November 2014
Accepted: 18 February 2015
Published: 13 March 2015

This article is part of the Thematic Series "Electrosynthesis".

Guest Editor: S. R. Waldvogel

Abstract

Thin films of PEDOT synthesized on platinum single electrodes in contact with the ionic liquid 1-ethyl-2,3-dimethylimidazolium triflimide ([EMMIM]Tf_2N) were studied by cyclic voltammetry, chronoamperometry, infrared spectroscopy and atomic force microscopy. It was found that the polymer grows faster on Pt(111) than on Pt(110) or Pt(100) and that the redox reactions associated with the PEDOT p-doping process are much more reversible in [EMMIM]Tf_2N than in acetonitrile. Finally, the ion exchange and charge carriers' formation during the p-doping reaction of PEDOT were studied using in situ FTIR spectroscopy.

Introduction

Conducting polymers have been subject of an intense research during the last decades because they exhibit high conductivity and interesting optical properties. These properties allow their use in several electronic devices [1,2]. The poly(3,4-ethylenedioxythiophene) (PEDOT) is one of the most conducting and stable (thermal and chemical) conducting polymer. For these reasons PEDOT thin films have been extensively studied [3].

Special attention has been paid to the use of electrochemical methods to synthesize conducting polymers due to the high degree of control afforded during the polymerization reaction. On the other hand, thin films of conducting polymers are more suitable to explore electrochemical properties such as stability, capacitance, resistance, ionic exchange kinetics and electrocatalysis [4].

Besides the synthesis technique, there are two important factors that can influence the polymer properties: the surface structure of the electrode and the solvent used [2,5]. It has been reported that the nucleation and growth kinetics, and the electrochemical properties, as the ionic resistance or the electrocatalytic activity, of PEDOT are affected by the surface energy state of the electrode [6]. For example, it was found that the ionic resistance of the PEDOT films electrochemically synthesized on platinum

electrodes increases in the order Pt(100) < Pt(110) < Pt(111) [6]. The synthesis of other conducting polymers on well-defined surfaces [7-10] and templates [11] also has shown how the surface affects their adhesion, coverage, morphology and redox kinetics.

On the other hand, the synthesis of conducting polymers in ionic liquids (ILs) has shown an enhancement in stability, organization and electroactivity [12-14]. These characteristics are obtained mainly because of the dry medium, their wide electrochemical window, and their low nucleophilicity. Therefore, during the electrosynthesis of conducting polymers the overoxidation of the polymer is less probable and the average length of the polymer chains is higher in ionic liquids than in molecular solvents [15].

In this work, Pt single crystals electrodes and the moisture stable IL 1-ethyl-2,3-dimethylimidazolium triflimide, [EMMIM]Tf_2N [16], are used to carry out the electrochemical synthesis of PEDOT. The electrochemical properties of thin films of PEDOT are subsequently studied and compared with the behavior obtained in acetonitrile.

Results and Discussion

Cyclic voltammetry

Figure 1 shows the cyclic voltammograms of EDOT in [EMMIM]Tf_2N. The onset of the EDOT oxidation begins at 0.9 V in Pt(111) and Pt(110) while in Pt(100) it starts at 1.0 V. The loop observed during the first scans (Figure 1a – insert) is typical of the electrosynthesis of conducting polymers both in organic media [17] and in ILs [2,18,19]. This characteristic has been well described by Heinze et al. [18]. They associated the loop with an autocatalytic mechanism in which the oligomers formed during the first oxidation cycle react as redox mediators with the monomer, but this kind of loops is also characteristic of a nucleation and growth mechanism. The continuous increase of the current between −1.0 and 1.0 V with the number of cycles clearly indicates that the polymer film is growing. After ten cycles, the currents are higher for the film grown in Pt(111) than in Pt(110) or Pt(100) as it can be observed in Figure 1c. This behavior can be related to the fact that the Pt(111) is more catalytic for the electrodeposition of conducting polymers as it was observed in acetonitrile [6,9].

It is interesting to notice that during the first cycles the voltammograms show one oxidation peak and two negative peaks. In the case of Pt(111) and Pt(110) the oxidation peak appears at 0.37 V and the reduction peaks at 0.31 V and −0.10 V, which rapidly merge to one broad oxidation peak at 0.30 V and two reduction peaks at −0.10 V and −0.50 V. However, in Pt(100) a peak grows at 0.50 V upon potential cycling, while another one

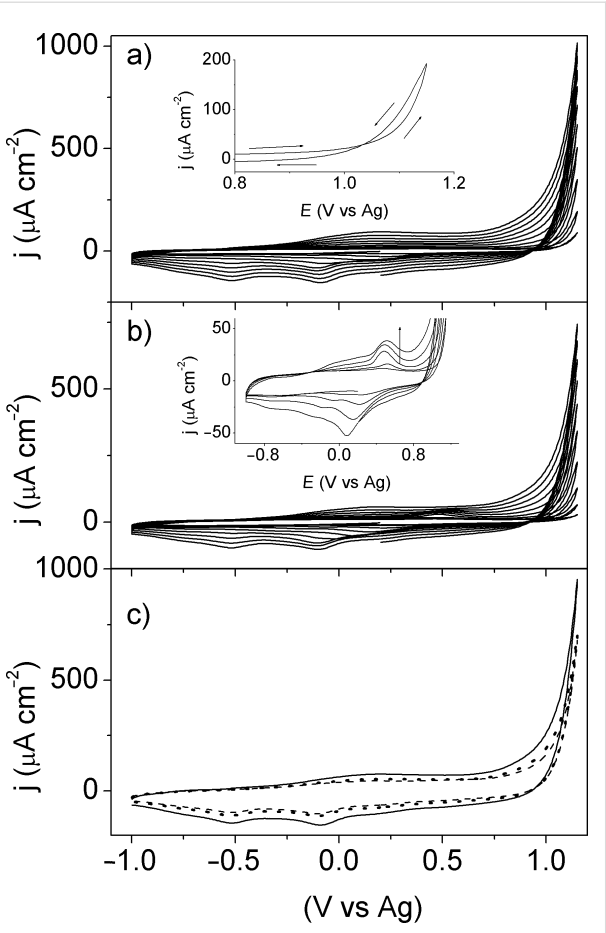

Figure 1: a, b) Cyclic voltammograms of 0.1 M EDOT in [EMMIM]Tf_2N at 100 mV s^{-1}. 10 cycles are shown: a) Pt(111), insert – 2nd cycle; b) Pt(100), Insert – zoom of the cycles from 2 to 6, c) 10th scan of figures "a" and "b" on Pt(111) (solid line), Pt(100) (dashed line) and Pt(110) (dotted line).

appears at 0.30 V, as it can be observed in the Figure 1b (insert graph). On the other hand, the two cathodic peaks at 0.30 V and −0.03 V shift to lower potentials up to the values of −0.10 V and −0.50 V, i.e., the same potentials observed for Pt(111) and Pt(110).

The peaks at 0.50 V and 0.30 V in Pt(100) can be produced by hydrogen oxidation and protons reduction, respectively, because these peaks appear at the same potentials where these reactions take place in [EMMIM]Tf_2N on Pt(100) [20]. Protons can be produced during the oxidation of EDOT and they can be reduced to hydrogen at negative potentials. These hydrogen reactions can inhibit the polymer growth on Pt(100) during the first cycles. Figure 1 clearly shows that the electrochemical polymerization of EDOT on platinum electrodes is a surface sensitive reaction. It was found that Pt(111) has the highest electrocatalytic activity for the EDOT oxidation reaction followed by Pt(110) and finally Pt(100).

Taking into account that more reproducibility during the synthesis of conducting polymers is normally obtained using the galvanostatic method, the following experiments were done using PEDOT films galvanostatically synthesized.

Figure 2 shows the voltammograms of PEDOT in [EMMIM]Tf_2N free of monomer, in the potential range where the p-doping reaction is observed. Two broad oxidation and reduction signals are present after several cycles, as it was previously reported [19,21,22]. Domagala et al. [23] have provided strong experimental evidences that polarons represent the main charge carrier group in p-doped PEDOT. However, it is still unclear if the two oxidation signals in ionic liquids correspond to two different redox states (polarons and bipolarons) or if they are related to different polymer structures [4].

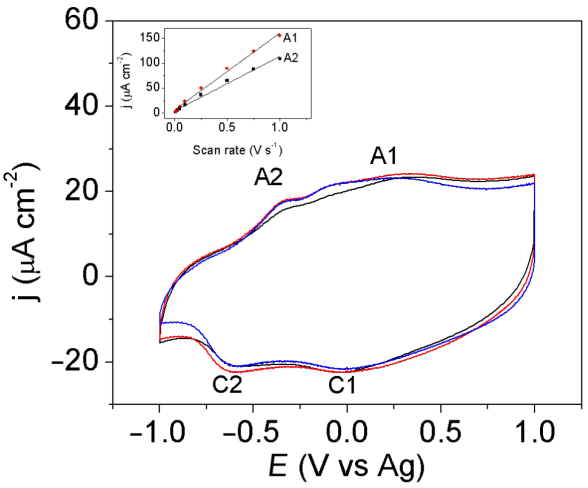

Figure 2: Cyclic voltammograms of PEDOT on Pt(111) (black line), Pt(100) (red line), Pt(110) (blue line) in [EMMIM]Tf_2N Scan rate 100 mV s^{-1}. The films were synthesized applying a charge density of 1.2 mC cm^{-2} during a chronopotentiometry. Insert graph: Current density vs scan rate of PEDOT on Pt(111).

Voltammetric profiles of PEDOT thin films in Figure 2 show that there are no significant differences between the Pt electrodes. On the other hand, the currents measured at 0.35 and −0.30V (A1 and A2) follow an almost linear tendency with the scan rate, which is characteristic of the surface controlled processes (Figure 2 – insert graph). As expected, thicker PEDOT films were obtained when the synthesis time was increased (Figure 3a).

Figure 3b shows the voltammetry of a PEDOT film synthesized as in Figure 2, but transferred into a cell with 0.1 M [EMMIM]Tf_2N in acetonitrile as supporting electrolyte. Many differences are observed between Figure 3a and Figure 3b for the PEDOT films of the same thickness: the ratio between height of the cathodic peaks is different, the separation between

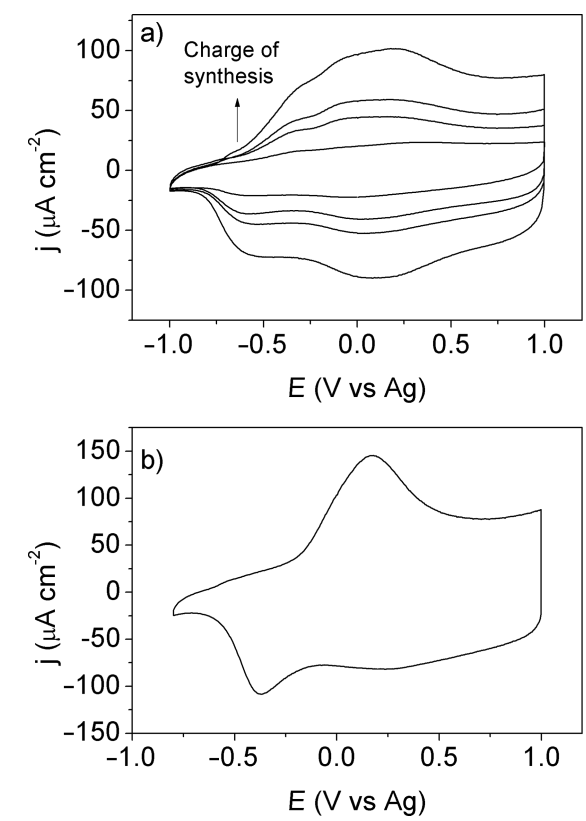

Figure 3: a) Cyclic voltammograms of PEDOT on Pt(111) in [EMMIM]Tf_2N. The total charge densities used for the galvanostatic synthesis were 1.2, 3.0, 4.3 and 6.2 mC cm^{-2}, respectively. The scan rate was 100 mV s^{-1} and the 50th scan is shown. b) Cyclic voltammogram of PEDOT on Pt(111) characterized in 0.1 M [EMMIM]Tf_2N in acetonitrile. The total charge used during the PEDOT synthesis was 6.2 mC cm^{-2}. The scan rate was 100 mV s^{-1}.

the anodic and the cathodic peaks is smaller in pure [EMMIM]Tf_2N and the polymer is oxidized at lower potential in [EMMIM]Tf_2N than in acetonitrile.

Chronoamperometry

In order to maintain electroneutrality, the generation of charges in the conducting polymers must be accompanied with the entrance of counterions from the solution. The chronoamperometric experiments allow the study of the ionic exchange kinetics. Figures 4a–c show the current traces when the potential is switched from −1 V to 1 V and vice versa. It is observed that the transients of PEDOT films on the three Pt surfaces used are characteristic of nucleation kinetics [21].

The insert of Figure 4a shows the integrated charge, Q_i, as a function of the charge of synthesis, Q_{pol}. It can be observed that the charge involved in the current transient increases linearly with increasing polymerization charge. The reduction charge is slightly lower than the oxidation charge. It seems that during the oxidation step the film is slightly overoxidized. No signifi-

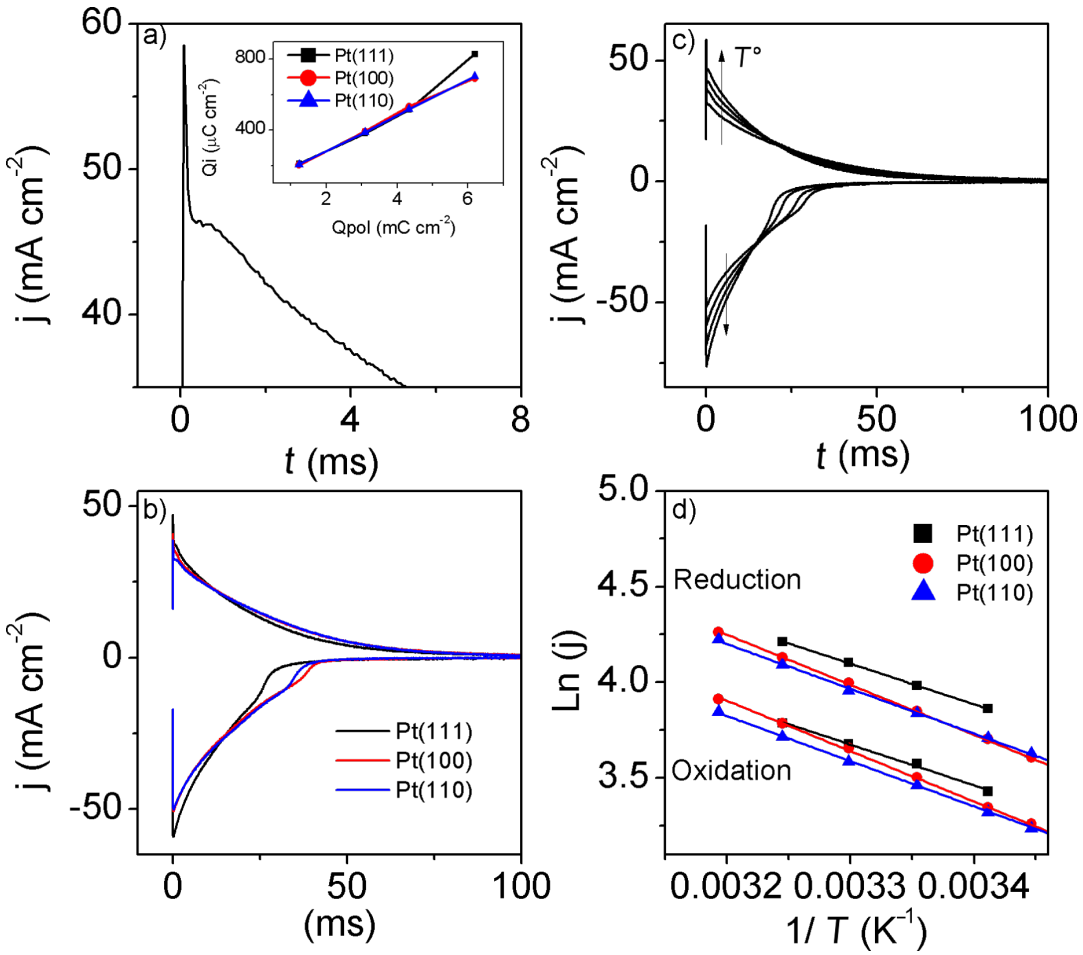

Figure 4: Chronoamperometry of PEDOT films synthesized on platinum single crystals in [EMMIM]Tf_2N. The total synthesis charge was 6.2 mC cm^{-2}. The potential steps were between −1.0 V and 1.0 V. a) Zoom of the first milliseconds for the PEDOT film on Pt(111) at 35 °C. Insert: integrated charge of the chronoamperometry vs the synthesis electric charge for the Pt(hkl) electrodes. b) Chronoamperometry of PEDOT on Pt(hkl) at 25 °C. c) Chronoamperometry of PEDOT on Pt(111) at temperatures of 20, 25, 30, and 35 °C. c) Logarithm of the current at 1.5 ms vs the inverse of temperature for: Pt(111) (black line), Pt(100) (red line) and Pt(110) (blue line).

cant differences were observed in the exchange kinetics for the different Pt surfaces (Figure 4b).

Figure 4c shows the current transients at different temperatures for the oxidation and reduction steps. The increase in temperature favors these processes as it has been observed for other conducting polymers [24,25]. With the value of the current at the very beginning of the transient (1.5 ms) it is possible to establish a relation between the current and the temperature using the “initial rate” approximation and the Arrhenius Equation. Since the logarithm of the current density vs the inverse of the temperature plot showed a linear dependence, Figure 4b, the apparent activation energy were calculated (Table 1).

The values of the activation energy for the oxidation and reduction processes are very similar and very close to the one reported for polythiophene (16 kJ mol^{-1}) [24], which means that the oxidation and reduction of PEDOT (and the corresponding counterion exchange) occurs easily in spite of the fact that the viscosity of the ionic liquid is quite high [16]. It is important to state that the activation energy of the nucleation kinetics related to the ion exchange depends on the overpotential used. Even so, the results shown in Table 1, Figure 3a and Figure 4 show that the kinetics of the redox processes of PEDOT films is faster in [EMMIM]Tf_2N than in acetonitrile [6], which is a relevant characteristic feature for the use of PEDOT thin films to build electrochromic devices or actuators [12,26,27].

Morphology by AFM

Figure 5 shows the AFM images of the polymer synthesized with a charge density of 1.2 mC cm^{-2} on the three Pt basal planes. It can be observed a grain shape with a low root mean square roughness (between 3 nm and 4 nm). These results are in

Table 1: Nucleation activation energies calculated from the linear graphs shown in Figure 4d.

Electrode		Intercept		Slope			Activation energy
		Value	Standard error	Value	Standard error	R^2	kJ mol^{-1}
Pt(111)	Oxidation	10.70	0.35	−2130.27	106.15	0.993	17.71
	Reduction	11.08	0.07	−2116.69	22.11	1.000	17.60
Pt(100)	Oxidation	12.34	0.12	−2636.36	35.68	0.999	21.92
	Reduction	12.64	0.10	−2620.68	29.84	0.999	21.79
Pt(110)	Oxidation	11.39	0.08	−2364.92	22.83	0.999	19.66
	Reduction	11.69	0.10	−2341.47	28.85	0.999	19.47

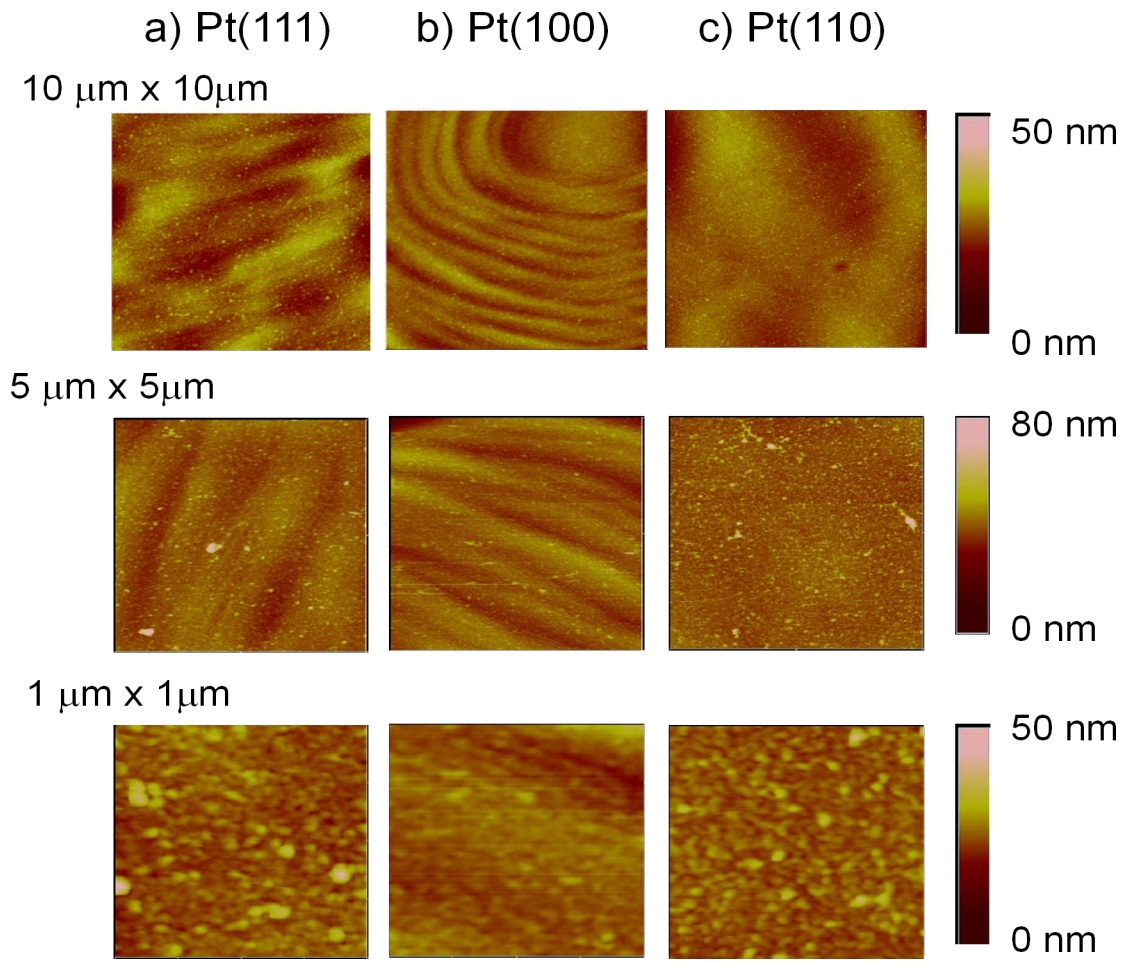

Figure 5: AFM images of PEDOT thin films synthesized on a) Pt(111), b) Pt(100) and c) Pt(110) with a charge density of 1.2 mC cm^{-2}. The film thickness is approximately 10 nm.

agreement with those obtained by MacFarlane et al. [13,28] which also reported very flat polymers in ILs. Opposite to the behavior obtained in aqueous or organic media, the synthesis in ILs generates very flat and homogeneous polymers [29,30]. Specially in the case of Pt(100), the polymer follows the surface and its defects, indicating a two-dimensional growth [31].

In situ FTIR

When the vibrational behavior of PEDOT films is analyzed by in situ infrared spectroscopy, the observed bands depend on the applied potential. The reference potential in this case was −0.9 V in order to start form the neutral form of PEDOT. Therefore, the positive bands correspond to products present in the oxidized form while the negative bands correspond to species consumption at the working potential.

Usually, PEDOT films are studied under attenuated total reflection conditions [17,19,32] because it is difficult to distinguish between the bands coming from solution species and the bands coming from the polymer film. However, we found that it was possible to study the PEDOT behavior under external reflection conditions when very thin layers of polymer are used, as it can be observed in Figure 6 and Figure 7. A comparison between the solution spectrum of the IL and the p- and s-polarized spectra of the polymer is shown in Figure 6. The p-polarized spectrum shows a high absorption between 4000 and 2000 cm^{-1} typical of conducting polymers. This is an electronic absorption related to the formation of charge carriers [3]. However, this feature is not observed with the s-polarized light, which means that the p-polarized spectrum is effectively recording the behavior of the electrode surface. Also, it is important to recognize that there are no water bands, which means that the IL is practically dry.

The bands at 3186 and 3151 cm^{-1} in the p-polarized and ATR spectra, are related to the imidazolium cation. However, the intensity of these bands is very low, hindering their detection. The negative orientation of the bands in the p-spectra means that a considerable amount of cations is being exchanged during the oxidation of the polymer, as it has been reported previously [5].

The zone between 1800 and 1000 cm^{-1} is complex because both polymer and IL bands are detected. The bands at 1334, 1226 cm^{-1}, related to the $[Tf_2N]$ anion, are observed as negative bands both in the p-polarized and the s-polarized spectra which means that the anion is been consumed from the solution. Ispas et al. [33] reported that PEDOT film charge neutralization in ILs proceeds mostly by anion incorporation during the p-doping process, but for $[EMIM]Tf_2N$ at 85 °C and [EMIM][OTf] at 25 °C the charge regulation occurs mainly via cation exchange. Our results show that, upon oxidation of the PEDOT films in $[EMMIM]Tf_2N$ both cations and anions are switched but more cations than anions have to be exchanged in order to keep ion neutrality. In other words, it seems that during PEDOT redox cycling some part of the anions remain within the PEDOT film.

The bands related to the oxidation of the polymer and their assignment, based on the literature [6,17,19,32,34], are listed in

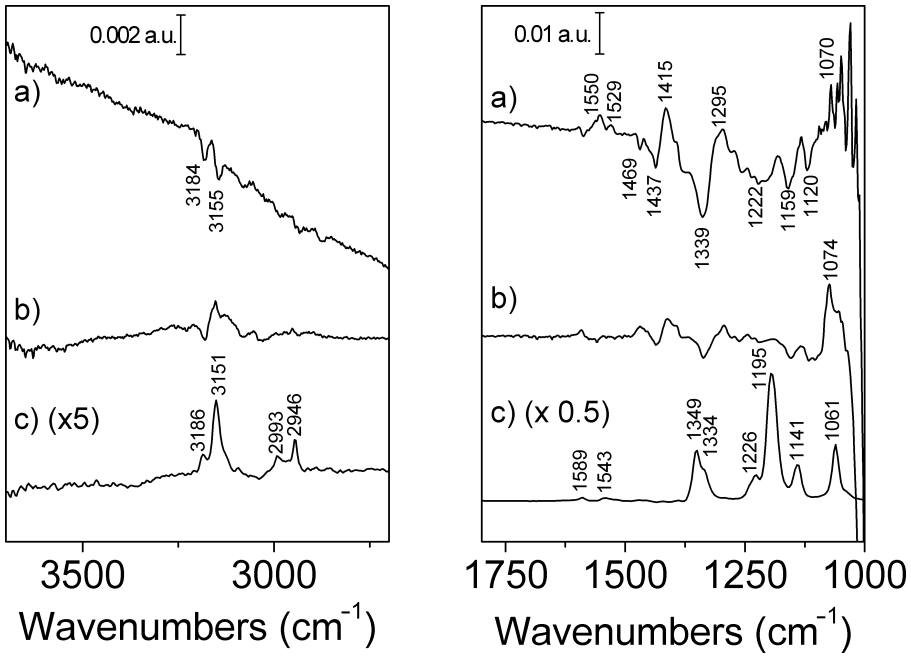

Figure 6: In situ FTIR spectra of a PEDOT thin film synthesized with a charge density of 0.6 mC cm^{-2} on Pt(111). 250 interferograms were recorded per spectrum. The reference potential was −0.90 V. a) p-Polarized spectrum at 0.80 V. b) s-Polarized spectrum at 0.80 V. c) ATR spectrum of 0.1 M $[EMMIM]Tf_2N$ in acetonitrile, obtained as the average of 100 interferograms.

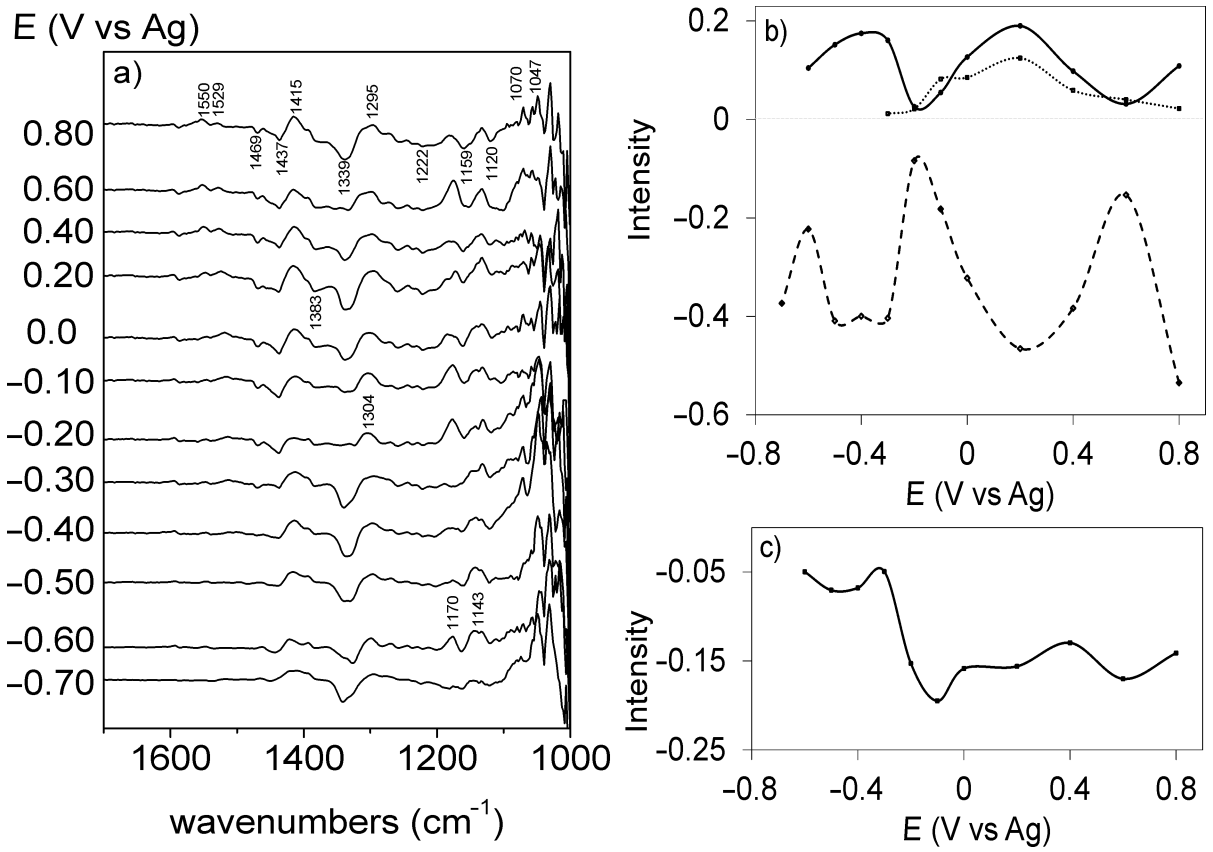

Figure 7: a) In situ FTIR spectra of a PEDOT thin film synthesized with a charge density of 0.6 mC cm^{-2} on Pt(111). 250 interferograms were recorded per spectrum. The reference potential was −0.90 V. Integrated IR intensities of several functional groups vs electrode potential: b) 1415 cm^{-1} (solid line) doping induced band , 1529 cm^{-1} (dotted line) doping induced band; 1339 cm^{-1} (dashed line) $\nu_{as}(SO_2)$; c) 1437 cm^{-1} (solid line) ν(C=C).

Table 2. The absorption bands at 1339 cm^{-1} and 1415 cm^{-1} can be assigned to the asymmetric stretching, ν_{as}, of the SO_2 moiety and the stretching of the thiophene ring in the oxidized state, respectively. Figure 7b shows that there are two potential regions where significant changes of the IR peak intensity are observed, between −0.6 V and −0.2 V and between −0.2 V and 0.6 V. These are the same potential zones where the two reduction signals are observed (Figure 3a). The two potential regions mean that there are two different processes, both related to p-doping, which can be related to two different redox or conformational states. It is important to notice that the intensity of these two signals oscillate out of phase in the potential range studied. Also, the band at 1132 cm^{-1} associated with the symmetric stretching of the SO_2 is positive within the whole potential range showing an adsorption at the surface in which this vibrational mode is active. These features could mean that the consumption of anions (from the IL to inside the polymer) is directly related to the generation of positive charge, which occurs in two regions that correlate well with the peaks A1/C1 and A2/C2 observed in Figure 2.

Also, the bands associated with the C=C bonds in the thiophene ring (1437 and 1469 cm^{-1}) are negative. The trend of the IR intensity at 1437 cm^{-1} (Figure 7c) shows a slight decrease from −0.7 to −0.3V and an abrupt fall at higher potentials. This trend closely resembles the currents observed during the p-doping of PEDOT (Figure 3a), suggesting that the disappearance of the ν(C=C) stretching signal of the thiophene ring upon oxidation can be used to quantify the charge carriers inside the polymer. It seems that with increasing potential, the concentration of charge carriers (polarons) increases between −0.3 V and −0.1 V where a plateau is reached. This IR signal also behaves very similar as the EPR signal intensity upon changing potential reported by Domagala et al. [23].

Finally, it is important to remember that when a weak electric field is applied across a molecule, both the molecular vibrational energy levels and the transition dipoles between the levels change slightly. These changes affect the infrared absorption spectrum of the sample, i.e., the position and the intensity of the bands [36,37]. Taken into account that the IR spectra

Table 2: Comparison between the absorption bands of ATR spectrum of 0.1 M [EMMIM]Tf_2N in acetonitrile and external reflection FTIR spectra of PEDOT in [EMMIM]Tf_2N.

Wavenumber (cm^{-1})		Assignment
[EMIM]Tf_2N]	PEDOT	
3186	3186 (n)	v(C-H) ring [34]
3151	3151 (n)	v(C-H) ring [34]
2993		v(C-H) alkyl
2946		v(C-H) alkyl [34]
1589		v(C=C) ring [35]
1543		v(CH-N) [35]
	1529 (p)	Doping induced band [17]
	1469 (n)	v(C=C) [17,19]
	1437 (n)	v(C=C) [19]
	1415 (p)	Doping induced band
	1381 (n)	v(C-C) [19]
1349		$v_{as}(SO_2)$ [34]
1334	1339 (n)	$v_{as}(SO_2)$ [34]
	1296 (p)	$v_{interring}$ [17,19]
1226	1222 (n)	$v_s(CF_3)$ [34]
1195		$v_{as}(CF_3)$ [34]
	1176 (p)	v(C=C), v(COROC) [19]
1141	1132 (p)	$v_s(SO_2)$ [34]
	1070 (p)	v(COROC) [17,19]
1061		v_{as}(SNS) [34]
	1045 (p)	v(COROC) [17,19]

(n) Negative oriented band; (p) positive oriented band; v: stretching; s; symmetric; as: asymmetric; COROC: ethylenedioxy group.

were recorded at different potentials and that the ion orientation depends on the intensity and direction of the electric field at the interface, some influence of this effect on the spectra shown in Figure 7 is also expected. This effect can explain, in part at least, the complex behavior observed in Figure 7.

Conclusion

PEDOT films were synthesized on platinum single crystal electrode substrates in [EMMIM]Tf_2N. Cyclic voltammetry shows that the polymer grows faster in Pt(111) than in Pt(110) or Pt(100). On the other hand, the chronoamperometric experiments show that the activation energy for the oxidation and reduction processes is very low and that the kinetics of the redox processes of PEDOT films is faster in [EMMIM]Tf_2N than in acetonitrile, which is very useful to build electrochromic devices or actuators.

Pt(111) and Pt(110) show almost the same characteristics in cyclic voltammetry, chronoamperometry and AFM experiments. On the other hand, polymer films grown on Pt(100) present marked differences, which suggests a different nucleation and growth mechanisms in this surface, probably a progressive 2D growth. Finally, the IR and voltammetric experiments show two potential zones where it seems that some changes on the structure and/or on the nature and number of charge carriers take place.

Experimental

The electrochemical experiments were performed in single compartment glass cells. A platinum wire was used as counter electrode, and a silver wire was used as the pseudoreference electrode. Platinum single crystals were used as working electrodes, which were prepared from small single-crystal beads following the Clavilier's method [38].

Prior to each experiment the cell was deareated with Ar (≥99.995% Alphagaz). The electrodes were heated in a gas–oxygen flame, cooled down in a reductive atmosphere (H_2 + Ar) and protected with a droplet of the IL at temperatures low enough to avoid decomposition. Then, the electrode was positioned in contact with the IL using a meniscus configuration.

1-Ethyl-2,3-dimethylimidazolium triflimide ([EMMIM]Tf_2N), >99% purity, was purchased from Iolitec. It was purified prior to use as it has been previously reported [20].

Polymer films were grown under galvanostatic conditions (unless otherwise stated) by applying a current density of 0.124 mA cm^{-2} during 5, 10, 25, 35 or 50 s in a solution of 0.1 M 3,4-ethylenedioxythiophene (EDOT, Sigma-Aldrich 97%). After the electropolymerization, the PEDOT films were rinsed with ionic liquid free of monomer and then positioned in contact with fresh ionic liquid using a meniscus configuration. 50 scans were performed to ensure a stable voltammetric profile. Characterization was also made in a solution of 0.1 M [EMMIM]Tf_2N in acetonitrile (Sigma-Aldrich, anhydrous, 99.8%)

A commercially available potentiostat/galvanostat μ Autolab III (Ecochemie) was used for the electrochemical experiments. The morphology of the polymer was studied with a NanoScope III Multimed contact AFM. Scan rate of 2 Hz. A standard cantilever of Si_3N_4 with piramidal tips (Digital Instruments) were used.

In situ Fourier Transform Infrared spectroscopy (FTIR) experiments were performed with a Nexus 8700 (Thermo Scientific) spectrometer equipped with an MCT detector. The spectroelectrochemical cell was provided with a prismatic CaF_2 window beveled at 60°. Spectra shown are composed of 250 interferograms and were collected with a resolution of 4 cm^{-1}. Unless

otherwise stated, the spectra were collected with p-polarized light. They are presented as absorbance, according to $A = -\log(R/R_0)$, where R and R_0 are the reflectance corresponding to the single-beam spectra obtained at the sample and reference potentials, respectively [39]. The contact of the electrodes with the IL was performed at a potential where the polymer was reduced (−0.90 V). This potential was maintained while the electrode was pressed against the CaF_2 window. After collecting the reference spectrum at this potential, the potential was stepped progressively to higher potentials up to 0.80 V waiting 5 minutes between steps to ensure the stability within the thin layer.

Attenuated total reflection configuration (ATR) was used to obtain the spectra of 0.1 M [EMMIM]Tf_2N in acetonitrile using a ZnSe hemicylindrical window with an incident angle of 45°. The reference spectrum was obtained in acetonitrile. The spectra are composed by 100 interferograms with a resolution of 8 cm^{-1}.

Acknowledgements

APS acknowledges the scholarship “Estudiantes sobresalientes de posgrado” at the “Universidad Nacional de Colombia (UNAL)” and COLCIENCIAS National Doctoral Scholarship (567). MFS acknowledges support of UNAL (Research Project 19030). JMF thanks MINECO (Spain) support through project CTQ2013-44083-P and Generalitat Valenciana (Feder) through project PROMETEOII/2014/013.

References

1. Inzelt, G. *J. Solid State Electrochem.* **2011,** *15,* 1711–1718. doi:10.1007/s10008-011-1338-3
2. Heinze, J.; Frontana-Uribe, B. A.; Ludwigs, S. *Chem. Rev.* **2010,** *110,* 4724–4771. doi:10.1021/cr900226k
3. Elschner, A.; Kirchmeyer, S.; Lövenich, W.; Merker, U.; Reuter, K. *PEDOT: principles and applications of an intrinsically conductive polymer;* CRC Press: Boca Raton, 2011.
4. Inzelt, G. *Conducting Polymers. A New Era in Electrochemistry;* Springer Verlag: Berlin, Heidelberg, 2008. doi:10.1007/978-3-540-75930-0
5. Randriamahazaka, H.; Bonnotte, T.; Noël, V.; Martin, P.; Ghilane, J.; Asaka, K.; Lacroix, J.-C. *J. Phys. Chem. B* **2011,** *115,* 205–216. doi:10.1021/jp1094432
6. Suárez-Herrera, M. F.; Costa-Figueiredo, M.; Feliu, J. M. *Phys. Chem. Chem. Phys.* **2012,** *14,* 14391–14399. doi:10.1039/c2cp42719b
7. Lang, P.; Clavilier, J. *Synth. Met.* **1991,** *45,* 297–308. doi:10.1016/0379-6779(91)91786-A
8. Hidalgo-Acosta, J. C.; Climent, V.; Suárez-Herrera, M. F.; Feliu, J. M. *Electrochem. Commun.* **2011,** *13,* 1304–1308. doi:10.1016/j.elecom.2011.07.021
9. Suárez-Herrera, M. F.; Feliu, J. M. *Phys. Chem. Chem. Phys.* **2008,** *10,* 7022–7030. doi:10.1039/b812323c
10. Suárez-Herrera, M. F.; Feliu, J. M. *J. Phys. Chem. B* **2009,** *113,* 1899–1905. doi:10.1021/jp8089837
11. Jeon, S. S.; Park, J. K.; Yoon, C. S.; Im, S. S. *Langmuir* **2009,** *25,* 11420–11424. doi:10.1021/la901563n
12. Lu, W.; Fadeev, A. G.; Qi, B.; Smela, E.; Mattes, B. R.; Ding, J.; Spinks, G. M.; Mazurkiewicz, J.; Zhou, D.; Wallace, G. G.; MacFarlane, D. R.; Forsyth, S. A.; Forsyth, M. *Science* **2002,** *297,* 983–987. doi:10.1126/science.1072651
13. MacFarlane, D. R.; Pringle, J. M.; Howlett, P. C.; Forsyth, M. *Phys. Chem. Chem. Phys.* **2010,** *12,* 1659–1669. doi:10.1039/b923053j
14. Pringle, J. M.; Efthimiadis, J.; Howlett, P. C.; Efthimiadis, J.; MacFarlane, D. R.; Chaplin, A. B.; Hall, S. B.; Officer, D. L.; Wallace, G. G.; Forsyth, M. *Polymer* **2004,** *45,* 1447–1453. doi:10.1016/j.polymer.2004.01.006
15. Fuchigami, T.; Inagi, S. *Electrolytic Reactions*. In *Electrochemical Aspects of Ionic Liquids,* 2nd ed.; Ohno, H., Ed.; John Wiley & Sons, Inc.: New Jersey, 2011; pp 101–127. doi:10.1002/9781118003350.ch8
16. Galiński, M.; Lewandowski, A.; Stępniak, I. *Electrochim. Acta* **2006,** *51,* 5567–5580. doi:10.1016/j.electacta.2006.03.016
17. Kvarnström, C.; Neugebauer, H.; Blomquist, S.; Ahonen, H. J.; Kankare, J.; Ivaska, A. *Electrochim. Acta* **1999,** *44,* 2739–2750. doi:10.1016/S0013-4686(98)00405-8
18. Heinze, J.; Rasche, A.; Pagels, M.; Geschke, B. *J. Phys. Chem. B* **2007,** *111,* 989–997. doi:10.1021/jp066413p
19. Damlin, P.; Kvarnström, C.; Ivaska, A. *J. Electroanal. Chem.* **2004,** *570,* 113–122. doi:10.1016/j.jelechem.2004.03.023
20. Sandoval, A. P.; Suárez-Herrera, M. F.; Feliu, J. M. *Electrochem. Commun.* **2014,** *46,* 84–86. doi:10.1016/j.elecom.2014.06.016
21. Sandoval, A. P.; Feliu, J. M.; Torresi, R. M.; Suárez-Herrera, M. F. *RSC Adv.* **2014,** *4,* 3383–3391. doi:10.1039/c3ra46028b
22. Randriamahazaka, H.; Plesse, C.; Teyssié, D.; Chevrot, C. *Electrochem. Commun.* **2003,** *5,* 613–617. doi:10.1016/S1388-2481(03)00142-5
23. Domagala, W.; Pilawa, B.; Lapkowski, M. *Electrochim. Acta* **2008,** *53,* 4580–4590. doi:10.1016/j.electacta.2007.12.068
24. Otero, T. F.; Santos, F. *Electrochim. Acta* **2008,** *53,* 3166–3174. doi:10.1016/j.electacta.2007.10.072
25. Otero, T. F.; Grande, H.-J.; Rodriguez, J. *J. Phys. Chem. B* **1997,** *101,* 3688–3697. doi:10.1021/jp9630277
26. Pozo-Gonzalo, C.; Mecerreyes, D.; Pomposo, J. A.; Salsamendi, M.; Marcilla, R.; Grande, H.; Vergaz, R.; Barrios, D.; Sánchez-Pena, J. M. *Sol. Energy Mater. Sol. Cells* **2008,** *92,* 101–106. doi:10.1016/j.solmat.2007.03.031
27. Lu, B.; Zhang, S.; Qin, L.; Chen, S.; Zhen, S.; Xu, J. *Electrochim. Acta* **2013,** *106,* 201–208. doi:10.1016/j.electacta.2013.05.068
28. Pringle, J. M.; Forsyth, M.; MacFarlane, D. R.; Wagner, K.; Hall, S. B.; Officer, D. L. *Polymer* **2005,** *46,* 2047–2058. doi:10.1016/j.polymer.2005.01.034
29. Sekiguchi, K.; Atobe, M.; Fuchigami, T. *J. Electroanal. Chem.* **2003,** *557,* 1–7. doi:10.1016/S0022-0728(03)00344-9
30. Suárez, M. F.; Compton, R. G. *J. Electroanal. Chem.* **1999,** *462,* 211–221. doi:10.1016/S0022-0728(98)00414-8
31. Milchev, A. *Electrocrystalization, Fundamentals of Nucleation And Growth;* Kluwer Academic Publishers: New York, 2002.
32. Kvarnström, C.; Neugebeauer, H.; Ivaska, A.; Sariciftci, S. *J. Mol. Struct.* **2000,** *521,* 271–277. doi:10.1016/S0022-2860(99)00442-1

33. Ispas, A.; Peipmann, R.; Bund, A.; Efimov, I. *Electrochim. Acta* **2009,** *54,* 4668–4675. doi:10.1016/j.electacta.2009.03.056
34. Motobayashi, K.; Minami, K.; Nishi, N.; Sakka, T.; Osawa, M. *J. Phys. Chem. Lett.* **2013,** *4,* 3110–3114. doi:10.1021/jz401645c
35. Moschovi, A. M.; Ntais, S.; Dracopoulos, V.; Nikolakis, V. *Vib. Spectrosc.* **2012,** *63,* 350–359. doi:10.1016/j.vibspec.2012.08.006
36. Boxer, S. G. *J. Phys. Chem. B* **2009,** *113,* 2972–2983. doi:10.1021/jp8067393
37. Hermansson, K. *J. Chem. Phys.* **1993,** *99,* 861–868. doi:10.1063/1.465349
38. Korzeniewski, C.; Climent, V.; Feliu, J. M. Electrochemistry at Platinum Single Crystal Electrodes. In *Electroanalytical Chemistry: A Series of Advances;* Bard, A. J.; Zoski, C. G., Eds.; CRC Press: Boca Raton, 2012; pp 75–166.
39. Osawa, M. In-situ Surface-Enhanced Infrared Spectroscopy of the Electrode/Solution Interface. In *Advances in Electrochemical Science and Engineering: Diffraction and Spectroscopic Methods in Electrochemistry;* Alkire, R. C.; Kolb, D. M.; Lipkowski, J.; Ross, P. N., Eds.; Wiley-VCH Verlag GmbH: Weinheim, 2006. doi:10.1002/9783527616817.ch8

License and Terms

BEILSTEIN JOURNAL OF ORGANIC CHEMISTRY

Electrochemical oxidation of cholesterol

Jacek W. Morzycki*[1] and Andrzej Sobkowiak*[2]

Review

Open Access

Address:
[1]Institute of Chemistry, University of Białystok, ul. Ciołkowskiego 1K, 15-245 Białystok, Poland and [2]Faculty of Chemistry, Rzeszów University of Technology, P.O. Box 85, 35-959 Rzeszów, Poland

Email:
Jacek W. Morzycki* - morzycki@uwb.edu.pl; Andrzej Sobkowiak* - asobkow@prz.edu.pl

* Corresponding author

Keywords:
allylic oxidation; cholesterol; electrochemical halogenation; electrochemical oxidation

Beilstein J. Org. Chem. **2015,** *11,* 392–402.
doi:10.3762/bjoc.11.45

Received: 05 January 2015
Accepted: 03 March 2015
Published: 25 March 2015

This article is part of the Thematic Series "Electrosynthesis".

Guest Editor: S. R. Waldvogel

Abstract

Indirect cholesterol electrochemical oxidation in the presence of various mediators leads to electrophilic addition to the double bond, oxidation at the allylic position, oxidation of the hydroxy group, or functionalization of the side chain. Recent studies have proven that direct electrochemical oxidation of cholesterol is also possible and affords different products depending on the reaction conditions.

Introduction

Cholesterol is the most common steroid in the mammalian body. It is necessary to ensure a proper membrane permeability and fluidity. It also serves as a precursor for the biosynthesis of steroid hormones, bile acids, and vitamin D [1]. The chemical oxidation of cholesterol is a crucial reaction in the synthesis of many compounds that are of pharmaceutical importance [2,3]. At the close of the previous century, special attention started being paid to cholesterol oxidation products [4]. Since then, these compounds have constantly drawn the attention of biochemists and medicinal chemists. Cholesterol that is present in food of animal origin undergoes autoxidation during processing as well as during storage, thus it yields toxic products. These are formed due to oxidation reactions caused by the contact with oxygen, the exposure to sunlight, heating treatments, etc. [5-7]. Furthermore, they can be generated in the human organism through different oxidation processes, some of which require enzymes. Cholesterol oxidation products cause many diseases, coronary heart disease and atherosclerosis being among the most common in modern societies [8-11]. Cholesterol oxidation products have also been proven to exhibit cytotoxicity as well as apoptotic and pro-inflammatory effects [12,13]. Therefore, in-depth studies on cholesterol oxidation may allow for significant advances in cholesterol biology and chemistry.

Review

General remarks

A series of physiological actions in both humans and animals are caused by chemical oxidation, photooxidation or enzymatic oxidation of cholesterol. Despite the importance of these

processes, cholesterol has been regarded as an electrochemically inactive compound [14]. However, during the last two decades the electrochemical oxidation of cholesterol, direct and indirect, was studied intensively. The first reports on cholesterol oxidation concerned indirect electrochemical methods with redox agents as electron mediators [15,16]. In these methods, cholesterol (Chol) forms adducts with the oxidized redox agents and then reacts, affording the products (P). The reduced forms of redox agents also produced in these processes are electrochemically regenerated. The indirect electrochemical reaction can be outlined as follows [17]:

$M_{red} \rightarrow M_{ox} + ne^-$,

$M_{ox} + Chol \rightarrow M_{ox}{\cdot}Chol$,

$M_{ox}{\cdot}Chol \rightarrow M_{red} + P$,

where M_{red} and M_{ox} are the redox agents in the reduced and oxidized states, respectively.

From a chemical point of view, cholesterol (**1**) is a homoallylic alcohol with a relatively large hydrophobic part. The preferential sites of cholesterol electrooxidation are shown in Figure 1. These are the hydroxy group at C3, the C5–C6 double bond, the allylic positions (particularly C7), and the tertiary positions (mainly in the side chain at C25). The multiple potential sites of chemical or electrochemical oxidation of cholesterol lower the reaction yields. The search for highly regio- and stereoselective reactions is a challenging problem. The yields of reactions are also low due to various consecutive reactions. To avoid this problem chemists frequently stop the reactions before completion. In many cases, the yields given in this article are not compensated for a low conversion.

All compounds throughout this review are assigned to Arabic numerals. Sometimes, the only difference between two compounds is the presence of an acetyl group at C3. In that case, the two compounds have the same numeral, but the acetylated derivative is amended by the letter "a", e.g., cholesterol (**1**) and cholesteryl acetate (**1a**).

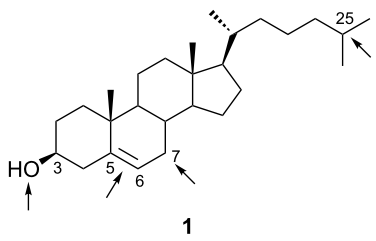

Figure 1: Preferential sites of cholesterol electrooxidation.

Indirect electrochemical oxidation of cholesterol

The selective oxidation of saturated hydrocarbons by dioxygen and hydrogen peroxide remains a challenging problem in chemistry and biology [18-21]. In analogy of the oxidation of cholesterol in the human body the Takayama group [22] has employed the process of dioxygen activation by Tl(II), which was electrochemically generated by the cathodic reduction of the Tl(III) hematoporphyrin (HMP) complex. The system produced activated oxygen species that regioselectively oxidized the tertiary C–H bonds. The reactions were carried out under constant current conditions in aqueous acetonitrile with $Tl(TFA)_3$, HMP, $LiClO_4$ and by bubbling with O_2 gas with platinum electrodes in an undivided cell. The starting cholesterol was transformed to 25-hydroxycholesterol (**2**) in 13% yield (Scheme 1). The statement that the Tl(II)/HMP/O_2 adduct, suggested to be a radical in nature, is responsible for cholesterol oxidation was based on the following observations. The electrolysis performed in the divided cell indicated that the oxidation of cholesterol took place in the cathodic compartment. The oxidation did not occur without the electrochemical reduction of Tl(III), which suggests that Tl(III) cannot activate dioxygen. In addition, the replacement of dioxygen by hydrogen peroxide gave a mixture of oxidation products. This indicates that dioxygen was not electrochemically reduced to hydrogen peroxide, which could act as an oxidant. It was also observed that the replacement of Tl(III) with Fe(III) caused a decrease in the reaction yield and the replacement of HMP with tetraphenylporphyrin or its derivatives resulted in product mixtures.

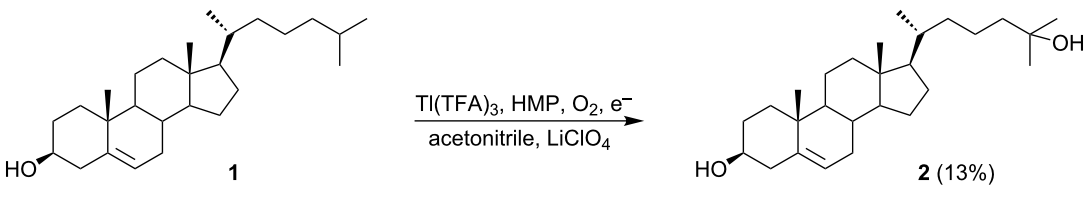

Scheme 1: Functionalization of the cholesterol side chain.

Many investigations on oxygenation reactions have been carried out by using a simple, readily available reagent system mimicking monooxygenase enzymes. An interesting system for the oxidation of aliphatic hydrocarbons, consisting of oxygen, powdered zinc, pyridine, acetic acid, and a catalytic amount of an iron cluster, was described in the 1980s by Barton et al. [23]. The system (Gif system) showed an unusual regioselectivity – the secondary positions were preferentially oxidized. An identical selectivity was also observed in an electrochemical version of the reaction (Gif–Orsay system), in which the reducing agent for oxygen (zinc) was replaced with electroreduction [24,25]. The chemical system was also applied to the oxidation of a side chain (Scheme 2) in protected cholesterol **3** [26], affording the corresponding 20-oxo derivative **4** (4.7%; yields are not corrected for recovered starting material) as the main product in addition to other products (e.g. 15-oxo **5**, 16-oxo **6** and other oxo-steroids). The electrooxidation of cholesterol derivatives also produced ketones but the detailed product analysis was not reported. It seems that the active species for the ketone formation in Gif systems is Fe(V)=O formed by heterolytic O–O-bond cleavage in Fe(III)–O–OH. There is no direct evidence for the existence of such species in Gif-systems and it was not spectroscopically characterized. However, the arguments for the oxoiron(V) species as an active oxidant has been recently summarized by Que [27]. In Gif systems pyridine is not only used as a solvent but it also acts as a ligand on the iron complex [28].

Different Fe(II) or Fe(III) picolinate (PA) and dipicolinate (DPA) complexes as catalysts of oxygenation reactions have been studied by the Sawyer [29-31], Barton [31,32], and Kotani–Takeya [33,34] groups. The oxidation of cholesteryl acetate with hydrogen peroxide or peracetic acid catalyzed by these complexes varied depending on the solvent used and the reaction conditions. To avoid the use of hazardous peroxy reagents, an electrochemical system was invented, which can be considered as analogical to the Gif-system. In this approach, hydrogen peroxide was exchanged for a process of dioxygen activation with electrochemically generated $[Fe^{II}(PA)_3OH_2]^-$ ions. With the system, stereoselective allylic hydroxylation of cholesteryl acetate was carried out [35]. The H-shaped one-compartment glass cell equipped with platinum mesh electrodes (cathode and anode) was filled with a cholesteryl acetate (**1a**) solution in acetonitrile containing ammonium tetrafluoroborate as a supporting electrolyte. The constant potential technique mainly afforded 7-hydroxylated products (**7a** and **8a**; 19–38%), along with the 7-oxo product **9a** (15–19%). In addition to these products, epoxide **10a** (1.5–3%) was also formed under constant current conditions (Scheme 3). Irrespective of the iron complex used, the reactions afforded the 7α-hydroxylated product **7a** in a large excess. The authors postulated the formation of a dimeric Fe(III)–Fe(V) manifold complex, $(H_2O)(PA)_2Fe(III)–O–Fe(V)=O(PA)_2$, as an active intermediate that would work as a monooxygenating species for cholesteryl acetate.

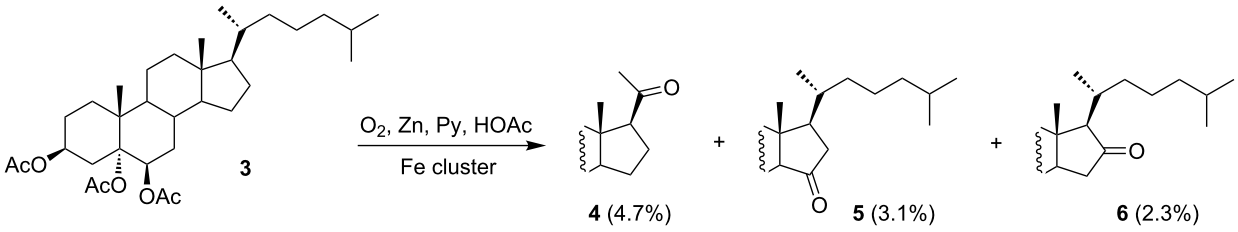

Scheme 2: Oxidation of cholestane-3β,5α,6β-triol triacetate (**3**) with the Gif system.

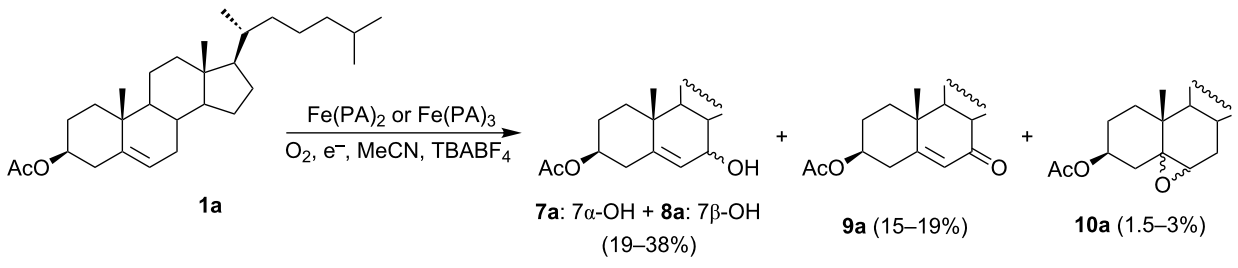

Scheme 3: Electrochemical oxidation of cholesteryl acetate (**1a**) with dioxygen and iron–picolinate complexes.

Indirect electrochemical oxidation of cholesterol was also reported by Wu et al. [36]. The electrolysis was performed under galvanostatic conditions at a platinum electrode in DMF containing 6% water with NaBr as a supporting electrolyte. A mixture of products was formed, among them "3,5,6-trihydroxycholesterol" (probably cholesta-3β,5ξ,6ξ-triol), 7-oxocholesterol (**9**), 5,6-epoxycholesterol (**10**), and 7-ketocholesterol were identified. However, the yields of the products were not reported. Based on cyclic voltammetry and rotating ring-disk electrode measurements the authors suggested that Br^- is electrochemically oxidized through Br to BrO^- and that the latter is the oxidizing agent for cholesterol.

The oxidation of cholesterol by electrochemically generated superoxide radical anion ($O_2^{\bullet-}$) in acetonitrile was described in 1997 [37]. It was established that in dry solution, with water content below 4%, no products were observed. However, cholesterol was oxidized to 7-oxocholesterol (**9**), 7α-hydroxycholesterol (**7**), and 7β-hydroxycholesterol (**8**) when hydrogen peroxide was combined with superoxide solution in water matrix. The authors suggested that under these conditions the rate of the disproportionation reaction of superoxide radical anion is increased, and the formation of more reactive oxygen species such as hydroxyl radical or singlet oxygen is possible.

A stereoselective electrochemical method of the chlorination of steroidal Δ^5-olefins was described by Takayama et al. [38]. The oxidation of cholesterol was carried out in an undivided cell under constant current conditions in CH_2Cl_2/MeCN/H_2O (2:2:1), the cathode and anode being platinum plates. The electrolysis was performed in the presence of $FeCl_3$ and hematoporphyrin (HMP), and dioxygen was constantly delivered to the cell. Three products, 5α,6β-dichlorocholestan-3β-ol (**11**), 6α-chlorocholestane-3β,5ß-diol (**12**), and epoxide (**10**), as a 1:3 mixture of α and β-isomers, were obtained in 32, 31, and 7% yields, respectively (Scheme 4). It is noteworthy that the reaction afforded a single stereoisomer of **11** or **12**.

Several important observations provided in the paper can give an idea on a plausible mechanism of cholesterol oxidation. First, in the absence of HMP and O_2 only compounds **11** (20%) and **12** (43%) were formed. Second, during the reaction with hydrogen peroxide as an oxidant under non-electrochemical conditions no products were detected, which indicates that the role of dioxygen is not the source of electrochemically generated H_2O_2. Furthermore, the epoxide **10** was not converted into chlorohydrin **12** under the reaction conditions, which implies it was not formed through an epoxide intermediate. Finally, no products were formed when the electrolysis was performed in a divided cell. It seems that a chlorine species (e.g. $Cl^{\delta+}\cdots FeCl_4^{\delta-}$), produced from anodically generated chlorine (dichloromethane was the likely source), initiated the sequence of reactions leading to cholesterol oxidation products.

A very similar result was obtained by Kowalski et al. [39]. They carried out the electrolysis of cholesterol in dichloromethane by using a divided cell, the cathode of which was placed in a glass tube with a glass frit. No metal chlorides were added, but again the major products were dichlorides, 5α,6β-dichlorocholestan-3β-ol (**11**, 14%) and its 5β,6α-isomer (9%), as well as chlorohydrin **12** (6%) and 3β-chlorocholest-5-ene (**1c**, 4%). It is clear that dichloromethane was the chlorine source since no additives were employed. The observed results may be explained by assuming a cathodic reduction of dichloromethane to chloride ions, followed by their diffusion to the anodic compartment, and electrooxidation to chlorine which reacted with cholesterol.

An efficient electrochemical chlorination of some Δ^5-steroids (Scheme 5) was reported by Milisavljević and Vukićević [40]. The electrolyses were carried out in dichloromethane under galvanostatic conditions with a graphite anode in an undivided cell. The supporting electrolyte tetraethylamonium chloride was a source of chloride ions, which were anodically oxidized to chlorine. The electrophilic addition of chlorine to the double bond of the investigated compounds cholesteryl acetate (**1a**), cholesteryl benzoate (**1b**), 3β-chloro-5-cholestene (**1c**), and 5-cholestene (**1d**), gave the corresponding 5α,6β-dichloro steroids in good yields (70–73%). However, cholesterol produced a complex mixture of products under the same reaction conditions.

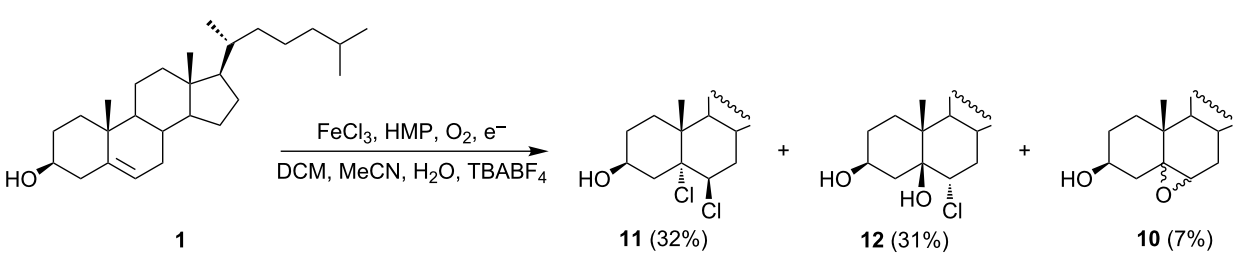

Scheme 4: Electrochemical chlorination of cholesterol catalyzed by $FeCl_3$.

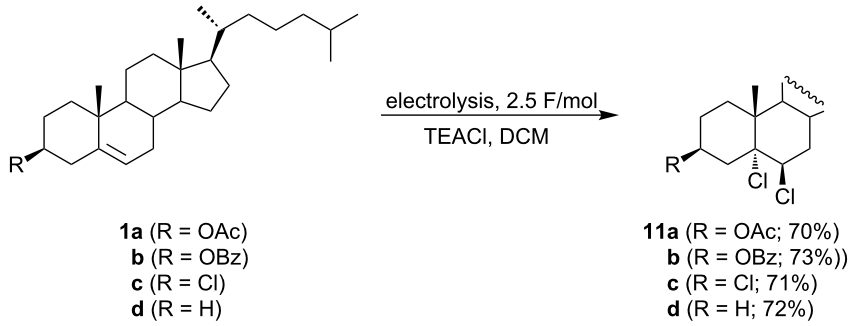

1a (R = OAc)
b (R = OBz)
c (R = Cl)
d (R = H)

11a (R = OAc; 70%)
b (R = OBz; 73%))
c (R = Cl; 71%)
d (R = H; 72%)

Scheme 5: Electrochemical chlorination of Δ^5-steroids.

The same authors also studied the electrochemical bromination of similar cholesterol derivatives **1a**–**c** (Scheme 6) [41]. The electrolyses were performed in a divided cell with a platinum anode in different solvents under constant current conditions. The supporting electrolyte tetraethylammonium bromide was used as a source of bromide ions, which were oxidized to give bromine. In aprotic solvents (dichloromethane, acetonitrile or acetic anhydride) only the corresponding 5α,6β-dibromocholestanes **13a**–**c** were formed in high yields. In methanol, however, in addition to dibromides **13a**–**c**, the corresponding regioisomeric pairs of 5α-bromo-6β-methoxy- and 5α-methoxy-6β-bromocholestanes (**14a**–**c** and **15a**–**c**) in a ratio of 3:1 were produced. The reactions apparently proceeded via a tricentric bromonium ion. Since the subsequent nucleophilic attack on this intermediate must occur from the back, the overall stereochemistry of the addition must be *anti*. It seems that in the first step an electrophilic attack of Br^+ from the α side prevails. The diaxial opening of the bromonium intermediate with bromide yields the same dibromo product **13a**–**c**, irrespective which bromonium ion (α or β) is actually formed. When this intermediate is attacked by methanol, the product structure **14a**–**c** or **15a**–**c** depends on the configuration of the bromonium ion.

Direct electrochemical oxidation of cholesterol

The first direct electrochemical oxidation of cholesterol was reported only in 2005 [42]. The preparative electrolysis was performed in glacial acetic acid on a platinum anode under constant current control in a divided cell. The reaction afforded two major products, 7α-acetoxycholesterol (**16**) and 7β-acetoxycholesterol (**17**), in a ratio of 10:3 (Scheme 7).

However, several byproducts were also formed. Voltammetric measurements indicated that the cholesterol oxidation process is

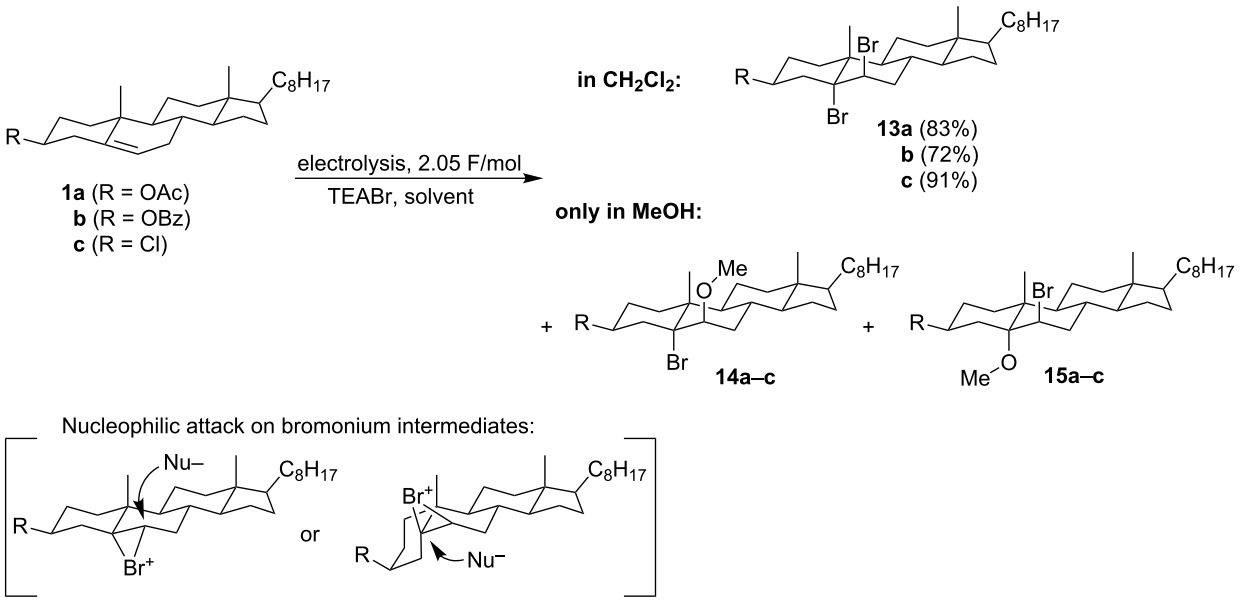

Scheme 6: Electrochemical bromination of Δ^5-steroids in different solvents.

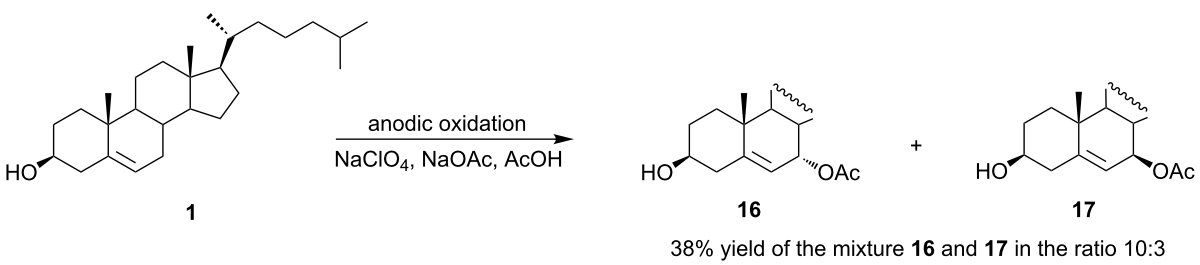

Scheme 7: Direct electrochemical acetoxylation of cholesterol at the allylic position.

controlled by the rate of the electron transfer. It was proven that the oxidation occurs at the allylic position. The C7 carbocation is formed by a two-electron transfer and then a nucleophile (acetate) is added to this intermediate, preferentially from the less sterically hindered α-side.

An interesting product of the electrochemical oxidation of cholesterol [39], i.e. dicholesteryl ether **18**, was obtained in 28% yield during the electrolysis carried out in a divided cell in dichloromethane as a solvent (Scheme 8). Except for the major product, the formation of small amounts of cholesteryl acetate (**1a**, 4%), cholesteryl chloride (**1c**, 3%), and *N*-acetylcholesterylamine (**19**, 4%) were also observed. The formation of cholesteryl chloride (**1c**) was explained by the possibility of cathodic dichloromethane reduction yielding chloride ions, which can migrate to the anodic compartment. To prevent the cathodic reduction of dichloromethane a small amount of glacial acetic acid was added to the cathodic compartment, but its leakage to the anodic part of the cell was responsible for the appearance of cholesteryl acetate (**1a**) among the oxidation products. To avoid this problem the anodic and cathodic parts of the cell were connected with an electrolytic bridge, which contained acetonitrile among other components to increase conductivity. However, its diffusion to the anode can be attributed to the formation of *N*-acetylcholesterylamine (**19**).

All observed products can be formed through a common intermediate. It seems that the first step of the reaction is a one-electron transfer from the oxygen atom of cholesterol to the anode (Scheme 9). The heterolytic cleavage of the C3–O bond in the resulting radical cation leads to the formation of a hydroxyl radical and the steroidal carbocation. Such a mesomerically stabilized homoallylic carbocation can react with any nucleophile present in the reaction mixture. In the absence of better nucleophiles it reacts with cholesterol to give dicholesteryl ether **18**.

Later, the electrochemical system was improved by replacing the functionality of the bridge with a divided H-cell with anionite (Dowex) placed in the cathodic compartment to bind chloride anions which are formed by the reduction of dichloromethane. The formation of byproducts was diminished with this system. The presented system proved suitable for the electrochemical glycosylation of 3β-hydroxy-Δ^5-steroids [43]. In this case, 2,3,4,6-tetra-*O*-acetyl-D-glucopyranose was used as a nucleophile (Scheme 10). The anodic oxidation of cholesterol (**1**) carried out in dichloromethane in the presence of the sugar used in excess afforded glycoside **20** (28%) as a 1:1 mixture of α and β-anomers, accompanied by a number of by-products such as cholesteryl acetate (**1a**, 10%), dicholesteryl ether (**18**, 4%),

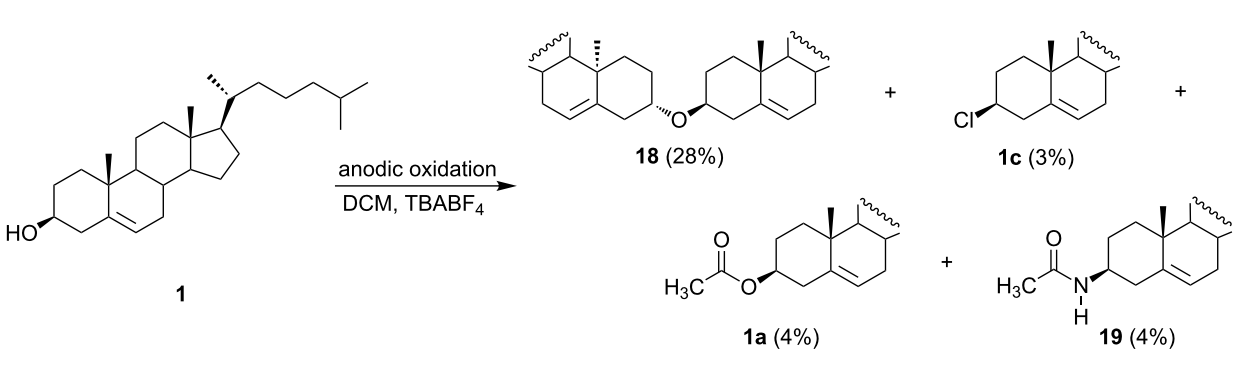

Scheme 8: Direct anodic oxidation of cholesterol in dichloromethane.

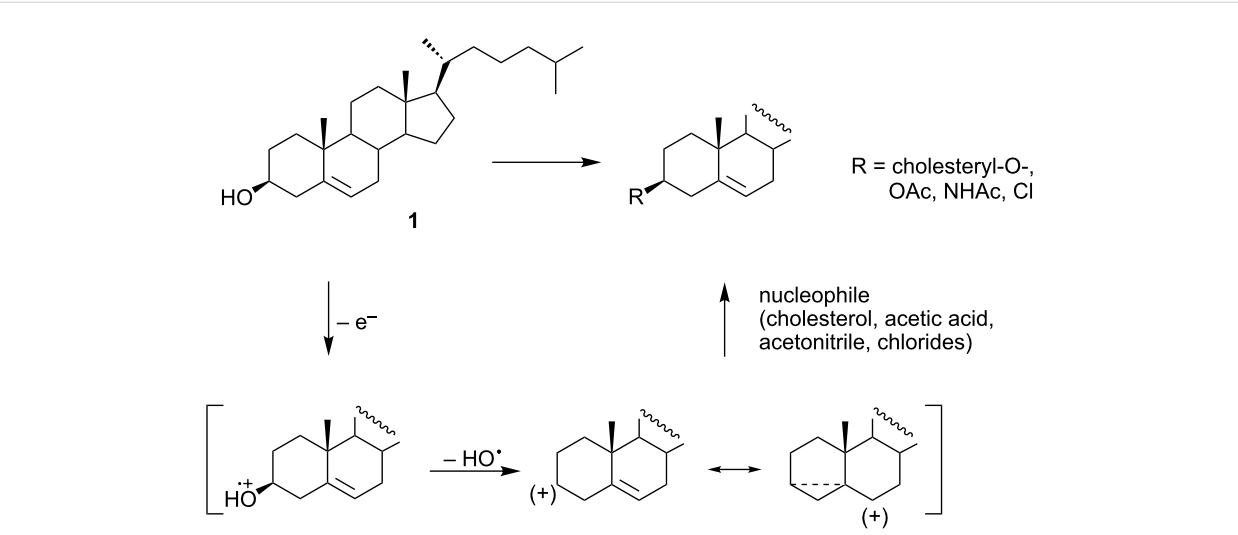

Scheme 9: A plausible mechanism of the electrochemical oxidation of cholesterol in dichloromethane.

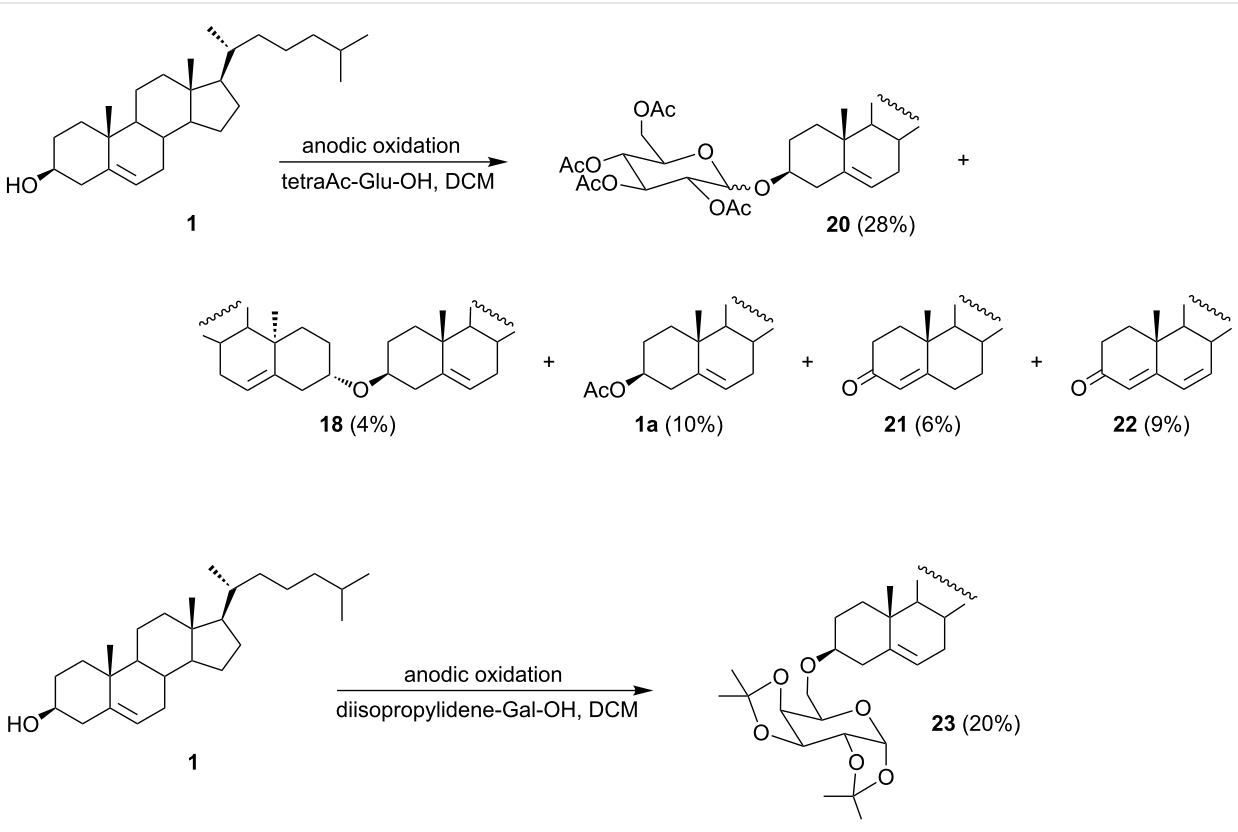

Scheme 10: The electrochemical formation of glycosides and glycoconjugates.

cholest-4-en-3-one (**21**, 6%), and cholesta-4,6-dien-3-one (**22**, 9%).

An analogous reaction carried out with 1,2:3,4-di-*O*-diisopropylidene-α-D-galactopyranose yielded glycoconjugate **23** with an ether bond between the sugar and steroid molecules. In further studies on the preparation of glycoconjugates from 3β-hydroxy-Δ^5-steroids, various derivatives were applied, such as thioethers [44], diphenylphosphates [45], trichloroacetimidates [45], and i-steroids [46].

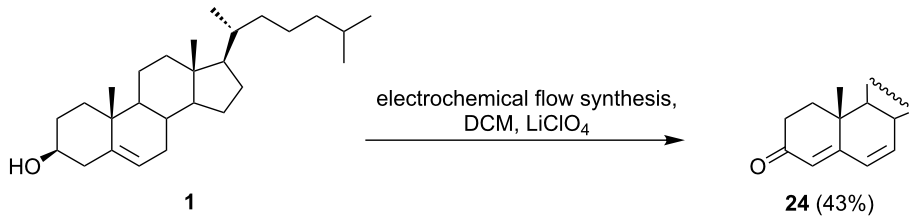

Scheme 11: Efficient electrochemical oxidation of cholesterol to cholesta-4,6-dien-3-one (**24**).

Cholesterol has been shown to be electrochemically oxidized (Scheme 11) in acetonitrile containing $LiClO_4$ at a carbon electrode [47] to give cholesta-4,6-dien-3-one (**24**). The electrolysis conditions were optimized on a laboratory synthetic scale [48]. The use of a flow cell equipped with a carbon fiber working electrode, allowed for the efficient production (43% yield) of cholesta-4,6-dien-3-one (**24**) during electrolysis under potentiostatic conditions at 1.9 V vs Ag/AgCl electrode. This result is rather surprising since cholesta-4,6-dien-3-one was not previously reported as a major product during electrochemical oxidation of cholesterol. The product was formed through a four-electron, four-proton electrochemical process, but no explanation was given for the selectivity observed.

Enzymatic and non-enzymatic methods of cholesterol determination with electrochemical detection

The development of fast and reliable methods of cholesterol determination in the human body and in processed food is still a demanding problem. Since this review article is mainly focused on the electrochemical transformations (direct or indirect) of cholesterol, the analytical aspects of cholesterol oxidation are only briefly mentioned. The cholesterol reactions that lie behind the analytical procedures are frequently unknown or are largely neglected by their authors. To date, many analytical methods have been developed to quantitate cholesterol contents, including spectrophotometry and HPLC, sometimes with electrochemical detection [49].

The majority of cholesterol determination methods however, take advantage of electrochemical biosensors based on cholesterol oxidase immobilized on an electrode surface. Cholesterol oxidase is an enzyme that catalyzes the reaction between cholesterol and dioxygen to produce cholest-4-en-3-one and hydrogen peroxide [50]. Then, the cholesterol level can be determined from an amperometric response, which can either be measured as a decrease in the dioxygen electroreduction current or, more frequently, from the hydrogen peroxide reduction or oxidation current. However, cholesterol in blood is mainly present in form of its fatty acid esters. If the total cholesterol amount is needed, the cholesterol esters must be hydrolyzed prior to analysis by the use of cholesterol esterase [51]. A poor stability of the enzymes and an influence of various factors (e.g., temperature and pH) on their performance limit a practical application of these methods. Therefore, the procedure of an enzyme immobilization on electrode surface is a crucial step for biosensors stability and efficiency.

Enzymatic oxidation of cholesterol with electrochemical detection

There are numerous reports on these methods and their detailed discussion is beyond the scope of the present review. Therefore, we limited ourselves to these publications, which include a comparison of the applied methods and have been published only recently. Up to date the most popular method is the immobilization of an enzyme on the electrode covered with different conducting polymers often embedded with carbon nanotubes and/or metal nanoparticles [52-56]. Chitosan, a naturally occurring biopolymer, has also been utilized for sensor fabrication [57,58]. Cholesterol oxidase has been immobilized on carbon nanotubes [59], metal nanoparticles [60] or graphene [61], and additionally decorated with metal nanoparticles [62] or modified with ionic liquids [63]. The application of composite electrodes, including silica sol–gel matrix with Prussian Blue [64], carbon nanotubes with zinc oxide nanoparticles [65], and zinc oxide nanorods directly grown on silver [66], has also been reported on. The “cholesterol self-powered biosensor” [67], in which the cathodic process is determined by cholesterol oxidase and on an anode phenothiazine-mediated oxidation of cholesterol as well as immobilization of cholesterol oxidase and cholesterol esterase onto thulium oxide [68] have been found as an alternative for biosensors which operate in blood.

Non-enzymatic indirect cholesterol detection with electrochemical techniques

Non-enzymatic approaches toward cholesterol detection exploiting an electrochemical route of sensing, which have a distinct advantage over conventional enzymatic processes, have recently been developed. Some of these methods are based on the indirect electrochemical oxidation of cholesterol by using bromine species in organic media [69,70]. In a recent method,

methylene blue formed an inclusion complex with β-cyclodextrin functionalized graphene and emerged as a cholesterol sensing matrix. Methylene blue was then replaced by the cholesterol molecule and moved out in the buffer solution, where it was detected electrochemically by using the differential pulse voltammetric technique [71]. An interesting technique for non-enzymatic sensors represents molecularly imprinted self-assembled monolayers. In this approach, the layer containing organic compounds together with cholesterol is deposited on an electrode surface. Then, the cholesterol is removed from the layer, and the oxidation current of ferrocyanide is measured. Next, the electrode is placed into a solution containing cholesterol, which is adsorbed in the empty spots and the oxidation current of ferrocyanide is measured again. The difference in the current values is proportional to the concentration of cholesterol [72-74]. These sensors have been proved to be useful for analyzing food samples [74].

Non-enzymatic direct electrochemical oxidation of cholesterol

The third class represents sensors based on the direct electrochemical oxidation of cholesterol. The authors claim that the process occurs on nanoporous electrodes such as Pt [75], Ag [76], Au/Pt [77], and Cu_2S [78]. However, apart from the increase of the registered current, there is no evidence that cholesterol is electrochemically oxidized. The assumption that cholesterol is directly electrooxidized seems surprising, as the observed process occurs at relatively negative potentials (0 to +0.4 V vs SCE). Definitely, the mechanism of the process needs to be established.

There is a worldwide effort toward the development of bioanalytical devices which can be used for the detection, the quantification and the monitoring of specific chemical species. The design of mixed biocatalyst pathways for the comprehensive oxidation of cholesterol, and, at the same time, the acquisition of frequent answers with an individual application for biosensorics is of major interest. Sophisticated sensing arrangements including single and complex selective agents may be expected to contribute to clinical chemistry.

Conclusion

Cholesterol has been regarded as an electrochemically inactive compound for a long time. Since the 1990s several methods have been developed for the indirect oxidation of cholesterol. The active species in these methods were different reactive oxygen species, various hypervalent transition metal–oxo and metal–peroxo species, dihalogens, hypohalites, and enzymes. The first direct electrochemical oxidation was reported only in 2005. The electrochemical oxidation of cholesterol may occur at the C3-hydroxy group, at the C5–C6 double bond, at the allylic position, and at the side chain (particularly at the tertiary position C25). Interestingly, the particular progress of the reaction depends on the reaction conditions, including the solvent, the supporting electrolyte, the mediator, the electrode material, and the potential applied. The yields of cholesterol oxidation products are rather low, often less than 30%. This may be caused by the high oxidation potential of cholesterol and the necessity to operate at a relatively high positive potential. Moreover, due to the hydrophobic properties of cholesterol it is necessary to use non-polar solvents, e.g., dichloromethane, which lowers the conductivity of the supporting electrolyte. Therefore, the galvanostatic regime of electrolyzes is often applied, which favors the occurrence of side reactions. The cholesterol oxidation products are often adsorbed at the electrode surface, which lowers the effectiveness of the electrochemical process. However, in some cases, reasonable yields of products are obtained and these reaction conditions may be of interest in practice.

Acknowledgements

Financial support from the Polish National Science Centre (UMO-2011/01/B/ST5/06046) is gratefully acknowledged.

References

1. Morzycki, J. W. *Steroids* **2014,** *83,* 62–79. doi:10.1016/j.steroids.2014.02.001
2. Djerassi, C. *Steroid Reactions: An Outline for Organic Chemists;* Holden-Day, Inc.: San Francisco, USA, 1963.
3. Fried, J.; Edwards, J. A. *Organic Reactions in Steroid Chemistry;* van Nostrand Reinhold Company: New York, USA, 1972.
4. Schroepfer, G. J., Jr. *Physiol. Rev.* **2000,** *80,* 361–554.
5. Wentworth, P., Jr.; Nieva, J.; Takeuchi, C.; Galve, R.; Wentworth, A. D.; Dilley, R. B.; DeLaria, G. A.; Saven, A.; Babior, B. M.; Janda, K. D.; Albert Eschenmoser, A.; Lerner, R. A. *Science* **2003,** *302,* 1053–1056. doi:10.1126/science.1089525
6. Brinkhorst, J.; Nara, S. J.; Pratt, D. A. *J. Am. Chem. Soc.* **2008,** *130,* 12224–12225. doi:10.1021/ja804162d
7. Derewiaka, D.; Molińska, E. *Food Chem.* **2015,** *171,* 233–240. doi:10.1016/j.foodchem.2014.08.117
8. Umetani, M.; Ghosh, P.; Ishikawa, T.; Umetani, J.; Ahmed, M.; Mineo, C.; Shaul, P. W. *Cell Metab.* **2014,** *20,* 172–182. doi:10.1016/j.cmet.2014.05.013
9. Lim, W. L. F.; Martins, I. J.; Martins, R. N. *J. Genet. Genomics* **2014,** *41,* 261–274. doi:10.1016/j.jgg.2014.04.003
10. Björkhem, I. *Biochimie* **2013,** *95,* 448–454. doi:10.1016/j.biochi.2012.02.029
11. Sottero, B.; Gamba, P.; Gargiulo, S.; Leonarduzzi, G.; Poli, G. *Curr. Med. Chem.* **2009,** *16,* 685–705. doi:10.2174/092986709787458353
12. De Weille, J.; Fabre, C.; Bakalara, N. *Biochem. Pharmacol.* **2013,** *86,* 154–160. doi:10.1016/j.bcp.2013.02.029
13. Miyoshi, N.; Iuliano, L.; Tomono, S.; Ohshima, H. *Biochem. Biophys. Res. Commun.* **2014,** *446,* 702–708. doi:10.1016/j.bbrc.2013.12.107

14. Görög, S. *Quantitative Analysis of Steroids;* Elsevier Scientific Publishing Company, Inc.: Amsterdam, The Netherlands, 1983.
15. Steckhan, E. *Angew. Chem., Int. Ed.* **1986,** *25,* 683–701. doi:10.1002/anie.198606831
16. Shono, T.; Matsumura, Y.; Inoue, K. *J. Am. Chem. Soc.* **1984,** *106,* 6075–6076. doi:10.1021/ja00332a052
17. Simonet, J.; Pilard, J. F. Electrogenerated reagents. In *Organic Electrochemistry;* Lund, H.; Hammerich, O., Eds.; New York, USA: Marcel Dekker, Inc., 2001; pp 1163–1225.
18. Barton, D. H. R.; Doller, D. *Acc. Chem. Res.* **1992,** *25,* 504–512. doi:10.1021/ar00023a004
19. Bovicelli, P.; Lupattelli, P.; Mincione, E.; Prencipe, T.; Curci, R. *J. Org. Chem.* **1992,** *57,* 5052–5054. doi:10.1021/jo00045a004
20. Sawyer, D. T.; Sobkowiak, A.; Matsushita, T. *Acc. Chem. Res.* **1996,** *29,* 409–416. doi:10.1021/ar950031c
21. Barton, D. R. H. *Tetrahedron* **1998,** *54,* 5805–5817. doi:10.1016/S0040-4020(98)00155-0
22. Maki, S.; Konno, K.; Takayama, H. *Tetrahedron Lett.* **1997,** *38,* 7067–7070. doi:10.1016/S0040-4039(97)01650-X
23. Barton, D. H. R.; Boivin, J.; Gastiger, M.; Morzycki, J. W.; Hay-Motherwell, R. S.; Motherwell, W. B.; Ozbalik, N.; Schwartzentruber, K. M. *J. Chem. Soc., Perkin Trans. 1* **1986,** 947–955. doi:10.1039/p19860000947
24. Balavoine, G.; Barton, D. H. R.; Boivin, J.; Gref, A.; Le Coupanec, P.; Ozbalik, N.; Pestana, J. A. X.; Rivière, H. *Tetrahedron* **1988,** *44,* 1091–1106. doi:10.1016/S0040-4020(01)85889-0
25. Barton, D. H. R.; Sobkowiak, A. *New J. Chem.* **1996,** *20,* 929–932.
26. Barton, D. H. R.; Gökturk, A. K.; Morzycki, J. W.; Motherwell, W. B. *J. Chem. Soc., Perkin Trans. 1* **1985,** 583–585. doi:10.1039/p19850000583
27. Oloo, W. N.; Feng, Y.; Iyer, S.; Parmelee, S.; Xue, G.; Que, L. *New J. Chem.* **2013,** *37,* 3411–3415. doi:10.1039/c3nj00524k
28. Barton, D. H. R.; Hu, B.; Li, T.; MacKinnon, J. *Tetrahedron Lett.* **1996,** *37,* 8329–8332. doi:10.1016/0040-4039(96)01904-1
29. Sheu, C.; Richert, S. A.; Cofre, P.; Ross, B., Jr.; Sobkowiak, A.; Sawyer, D. T.; Kanofsky, J. R. *J. Am. Chem. Soc.* **1990,** *112,* 1936–1942. doi:10.1021/ja00161a045
30. Kang, C.; Sobkowiak, A.; Sawyer, D. T. *Inorg. Chem.* **1994,** *33,* 79–82. doi:10.1021/ic00079a015
31. Sheu, C.; Sobkowiak, A.; Zhang, L.; Ozbalik, N.; Barton, D. H. R.; Sawyer, D. T. *J. Am. Chem. Soc.* **1989,** *111,* 8030–8032. doi:10.1021/ja00202a063
32. Barton, D. H. R.; Salgueiro, M. C.; MacKinnon, J. *Tetrahedron* **1997,** *53,* 7417–7428. doi:10.1016/S0040-4020(97)00447-X
33. Takeya, T.; Egawa, H.; Inoue, N.; Miyamoto, A.; Chuma, T.; Kotani, E. *Chem. Pharm. Bull.* **1999,** *47,* 64–70. doi:10.1248/cpb.47.64
34. Okamoto, I.; Funaki, W.; Nobuchika, S.; Sawamura, M.; Kotani, E.; Takeya, T. *Chem. Pharm. Bull.* **2005,** *53,* 248–252. doi:10.1248/cpb.53.248
35. Okamoto, I.; Funaki, W.; Nakaya, K.; Kotani, E.; Takeya, T. *Chem. Pharm. Bull.* **2004,** *52,* 756–759. doi:10.1248/cpb.52.756
36. Wu, X.; Song, C.; Cheng, F.; Zhang, W. *J. Electroanal. Chem.* **1992,** *327,* 321–325. doi:10.1016/0022-0728(92)80156-X
37. Lee, J. H.; Shoeman, D. W.; Kim, S.-S.; Csallany, A. S. *Int. J. Food Sci. Nutr.* **1997,** *48,* 151–159. doi:10.3109/09637489709006975
38. Maki, S.; Konno, K.; Ohba, S.; Takayama, H. *Tetrahedron Lett.* **1998,** *39,* 3541–3542. doi:10.1016/S0040-4039(98)00538-3
39. Kowalski, J.; Łotowski, Z.; Morzycki, J. W.; Płoszyńska, J.; Sobkowiak, A.; Wilczewska, A. Z. *Steroids* **2008,** *73,* 543–548. doi:10.1016/j.steroids.2008.01.014
40. Milisavljević, S.; Vukićević, R. D. *J. Serb. Chem. Soc.* **2004,** *69,* 941–947. doi:10.2298/JSC0411941M
41. Milisavljević, S.; Wurst, K.; Laus, G.; Vukićević, M. D.; Vukićević, R. D. *Steroids* **2005,** *70,* 867–872. doi:10.1016/j.steroids.2005.06.002
42. Kowalski, J.; Płoszyńska, J.; Sobkowiak, A.; Morzycki, J. W.; Wilczewska, A. Z. *J. Electroanal. Chem.* **2005,** *585,* 275–280. doi:10.1016/j.jelechem.2005.09.003
43. Morzycki, J. W.; Łotowski, Z.; Siergiejczyk, L.; Wałejko, P.; Witkowski, S.; Kowalski, J.; Płoszyńska, J.; Sobkowiak, A. *Carbohydr. Res.* **2010,** *345,* 1051–1055. doi:10.1016/j.carres.2010.03.018
44. Tomkiel, A. M.; Brzezinski, K.; Łotowski, Z.; Siergiejczyk, L.; Wałejko, P.; Witkowski, S.; Kowalski, J.; Płoszyńska, J.; Sobkowiak, A.; Morzycki, J. W. *Tetrahedron* **2013,** *69,* 8904–8913. doi:10.1016/j.tet.2013.07.106
45. Tomkiel, A. M.; Kowalski, J.; Płoszyńska, J.; Siergiejczyk, L.; Łotowski, Z.; Sobkowiak, A.; Morzycki, J. W. *Steroids* **2014,** *82,* 60–67. doi:10.1016/j.steroids.2014.01.007
46. Tomkiel, A. M.; Biedrzycki, A.; Płoszyńska, J.; Naróg, D.; Sobkowiak, A.; Morzycki, J. W. *Beilstein J. Org. Chem.* **2015,** *11,* 162–168. doi:10.3762/bjoc.11.16
47. Hosokawa, Y.-Y.; Hakamata, H.; Murakami, T.; Aoyagi, S.; Kuroda, M.; Mimaki, Y.; Ito, A.; Morosawa, S.; Kusu, F. *Electrochim. Acta* **2009,** *54,* 6412–6416. doi:10.1016/j.electacta.2009.06.005
48. Hosokawa, Y.-Y.; Hakamata, H.; Murakami, T.; Kusu, F. *Tetrahedron Lett.* **2010,** *51,* 129–132. doi:10.1016/j.tetlet.2009.10.106
49. Hojo, K.; Hakamata, H.; Ito, A.; Kotani, A.; Furukawa, C.; Hosokawa, Y.-Y.; Kusu, F. *J. Chromatogr., A* **2007,** *1166,* 135–141. doi:10.1016/j.chroma.2007.08.020
50. Pollegioni, L.; Piubelli, L.; Molla, G. *FEBS J.* **2009,** *276,* 6857–6870. doi:10.1111/j.1742-4658.2009.07379.x
51. Stępień, A. E.; Gonchar, M. *Acta Biochim. Pol.* **2013,** *60,* 401–403.
52. Rahman, M. M.; Li, X.; Kim, J.; Lim, B. O.; Ahammad, A. J. S.; Lee, J.-J. *Sens. Actuators, B* **2014,** *202,* 536–542. doi:10.1016/j.snb.2014.05.114
53. Fang, K.-C.; Chu, C.-H.; Hsu, C.-P.; Kang, Y.-W.; Fang, J.-Y.; Hsu, C.-H.; Huang, Y.-F.; Chen, C.-C.; Li, S.-S.; Yeh, J. A.; Yao, D.-J.; Wang, Y.-L. *Appl. Phys. Lett.* **2014,** *105,* 113304. doi:10.1063/1.4896289
54. Cai, X.; Gao, X.; Wang, L.; Wu, Q.; Lin, X. *Sens. Actuators, B* **2013,** *181,* 575–583. doi:10.1016/j.snb.2013.02.050
55. Kakhki, S.; Barsan, M. M.; Shams, E.; Brett, C. M. A. *Anal. Methods* **2013,** *5,* 1199–1204. doi:10.1039/c3ay26409b
56. Prakash, S.; Chakrabarty, T.; Singh, A. K.; Shahi, V. K. *Biosens. Bioelectron.* **2013,** *41,* 43–53. doi:10.1016/j.bios.2012.09.031
57. Srivastava, M.; Srivastava, S. K.; Nirala, N. R.; Prakash, R. *Anal. Methods* **2014,** *6,* 817–824. doi:10.1039/C3AY41812J
58. Charan, C.; Shahi, V. K. *J. Appl. Electrochem.* **2014,** *44,* 953–962. doi:10.1007/s10800-014-0704-0
59. Tong, Y.; Li, H.; Guan, H.; Zhao, J.; Majeed, S.; Anjum, S.; Liang, F.; Xu, G. *Biosens. Bioelectron.* **2013,** *47,* 553–558. doi:10.1016/j.bios.2013.03.072
60. Ahmadalinezhad, A.; Chen, A. *Biosens. Bioelectron.* **2011,** *26,* 4508–4513. doi:10.1016/j.bios.2011.05.011
61. Manjunatha, R.; Suresh, G. S.; Melo, J. S.; D'Souza, S. F.; Venkatesha, T. V. *Talanta* **2012,** *99,* 302–309. doi:10.1016/j.talanta.2012.05.056

62. Cao, S.; Zhang, L.; Chai, Y.; Yuan, R. *Talanta* **2013,** *109,* 167–172. doi:10.1016/j.talanta.2013.02.002
63. Gholivand, M. B.; Khodadadian, M. *Biosens. Bioelectron.* **2014,** *53,* 472–478. doi:10.1016/j.bios.2013.09.074
64. Li, J.; Peng, T.; Peng, Y. *Electroanalysis* **2003,** *15,* 1031–1037. doi:10.1002/elan.200390124
65. Gupta, V. K.; Norouzi, P.; Ganjali, H.; Faridbod, F.; Ganjali, M. R. *Electrochim. Acta* **2013,** *100,* 29–34. doi:10.1016/j.electacta.2013.03.118
66. Israr, M. Q.; Sadaf, J. R.; Asif, M. H.; Nur, O.; Willander, M.; Danielsson, B. *Thin Solid Films* **2010,** *519,* 1106–1109. doi:10.1016/j.tsf.2010.08.052
67. Sekretaryova, A. N.; Beni, V.; Eriksson, M.; Karyakin, A. A.; Turner, A. P. F.; Vagin, M. Y. *Anal. Chem.* **2014,** *86,* 9540–9547. doi:10.1021/ac501699p
68. Singh, J.; Roychoudhury, S.; Srivastava, M.; Solanki, P. R.; Lee, D. W.; Lee, S. H.; Malhotra, B. D. *Nanoscale* **2014,** *6,* 1195–1208. doi:10.1039/C3NR05043B
69. Tsierkezos, N. G.; Ritter, U. *Phys. Chem. Liq.* **2014,** *52,* 601–607. doi:10.1080/00319104.2014.890895
70. Chiang, W.-H.; Chen, P.-Y.; Nien, P.-C.; Ho, K.-C. *Steroids* **2011,** *76,* 1535–1540. doi:10.1016/j.steroids.2011.09.003
71. Agnihotri, N.; Chowdhury, A. D.; De, A. *Biosens. Bioelectron.* **2015,** *63,* 212–217. doi:10.1016/j.bios.2014.07.037
72. Piletsky, S. A.; Piletskaya, E. V.; Sergeyeva, T. A.; Panasyuk, T. L.; El'skaya, A. V. *Sens. Actuators, B* **1999,** *60,* 216–220. doi:10.1016/S0925-4005(99)00273-7
73. Shiigi, H.; Matsumoto, H.; Ota, I.; Nagaoka, T. *J. Flow Injection Anal.* **2008,** *25,* 81–84.
74. Nagaoka, T.; Tokonami, S.; Shiigi, H.; Matsumoto, H.; Takagi, Y.; Takahashi, Y. *Anal. Sci.* **2012,** *28,* 187–191. doi:10.2116/analsci.28.187
75. Lee, Y.-J.; Kim, J.-D.; Park, J.-Y. *J. Korean Phys. Soc.* **2009,** *54,* 1769–1773. doi:10.3938/jkps.54.1769
76. Li, Y.; Bai, H.; Liu, Q.; Bao, J.; Han, M.; Dai, Z. *Biosens. Bioelectron.* **2010,** *25,* 2356–2360. doi:10.1016/j.bios.2010.03.036
77. Lee, Y.-J.; Park, J.-Y. *Biosens. Bioelectron.* **2010,** *26,* 1353–1358. doi:10.1016/j.bios.2010.07.048
78. Ji, R.; Wang, L.; Wang, G.; Zhang, X. *Electrochim. Acta* **2014,** *130,* 239–244. doi:10.1016/j.electacta.2014.02.155

License and Terms

BEILSTEIN JOURNAL OF ORGANIC CHEMISTRY

Highly selective generation of vanillin by anodic degradation of lignin: a combined approach of electrochemistry and product isolation by adsorption

Dominik Schmitt[1], Carolin Regenbrecht[1,2], Marius Hartmer[1], Florian Stecker[2] and Siegfried R. Waldvogel[*1]

Full Research Paper

Open Access

Address:
[1]Institute for Organic Chemistry, Johannes Gutenberg University Mainz, Duesbergweg 10–14, 55128 Mainz, Germany and [2]BASF SE, GCN/ES—M311, 67056 Ludwigshafen, Germany

Email:
Siegfried R. Waldvogel[*] - waldvogel@uni-mainz.de

* Corresponding author

Keywords:
adsorption; electrochemistry; lignin; nickel; renewable resources

Beilstein J. Org. Chem. **2015,** *11,* 473–480.
doi:10.3762/bjoc.11.53

Received: 10 February 2015
Accepted: 24 March 2015
Published: 13 April 2015

This article is part of the Thematic Series "Electrosynthesis".

Associate Editor: J. A. Murphy

Abstract

The oxidative degradation of lignin into a variety of valuable products has been under investigation since the first half of the last century. Especially, the chance to claim this cheap, abundant and renewable source for the production of the important aroma chemical vanillin (**1**) was one of the major driving forces of lignin research. So far most of the developed methods fail in technical application since no viable concept for work-up is included. This work represents a combined approach of electrochemical conversion of Kraft lignin and product recovery by adsorption on a strongly basic anion exchange resin. Electrolysis conditions are optimized regarding reaction temperatures below 100 °C allowing operation of aqueous electrolytes in simple experimental set-up. Employing ion exchange resins gives rise to a selective removal of low molecular weight phenols from the strongly alkaline electrolyte without acidification and precipitation of remaining lignin. The latter represents a significant advantage compared with conventional work-up protocols of lignin solutions.

Introduction

The biopolymer lignin is one of the most abundant and renewable feedstocks in the world [1-3]. Moreover, lignin represents the largest source of aromatic compounds among renewables and can be considered as non-food biomass. It usually occurs as a major waste fraction of the pulping industry on a multimillion ton scale [4]. This source has the potential to be an alternative for petroleum-based production of fuels as well as fine chemicals [5-7]. Since the middle of the last century, the large amount of aromatic structural features making up the polymer led to much effort concerning efficient degradation methods into high value fine chemicals like vanillin (**1**), acetovanillone (**2**) and guaiacol (**3**) (Scheme 1) [8-10]. Different approaches for selec-

tive degradation of lignin, applying catalytic, microbacterial, photochemical, sono-chemical and electrochemical methods were investigated but struggled with several problems [11-17]. The dominating challenges are usually low selectivity resulting in a plethora of products, drastic and technically unreasonable reaction conditions, purification of the resulting crude product mixture, and separation of the desired products from unreacted lignin [18-20]. When using transition metal catalysts they commonly disappear in the unreacted lignin contaminating that particular material which limits further subsequent use. Electrochemistry is one of the most promising approaches for highly sustainable conversions because only electrons serve as reagent [21-27]. Consequently, such conversions are considered as reagent-free and avoid reagent waste [28-30]. We present a highly selective electrochemical approach providing an almost exclusive formation of vanillin (**1**) under very mild reaction conditions. The application of a strongly basic anion exchange resin allows an elegant separation of the formed vanillin (**1**) from remaining lignin directly out of the basic reaction solution.

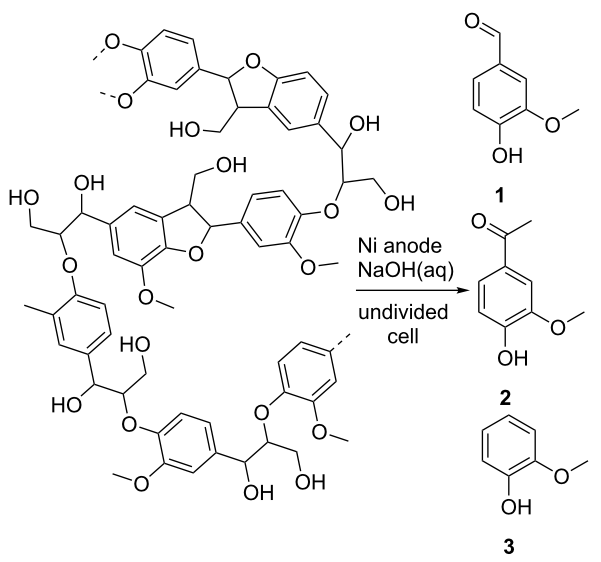

Scheme 1: Direct electrochemical degradation of lignin into low molecular weight phenolic compounds.

Results and Discussion

The electrochemical degradation of lignin in alkaline media is usually performed on nickel anodes. Utley et al. presented a very promising electrochemical approach using Ni anodes which enabled conversion of lignosulfonate in a filter press cell at elevated temperature and pressure. The conversion led to high yields of vanillin (**1**) in the range of 5–7 wt %. The complex experimental set-up as well as evolution of hydrogen are a major drawback of this approach [31]. Nevertheless, the applied Ni electrodes usually exhibit a high stability against corrosion at these conditions due to the formation of an electrocatalytic surface layer which is stable in alkaline electrolytes [32]. Kraft pulping represents the predominant pulping process [33]. Due to this we investigated the electrochemical degradation of Kraft lignin and avoided the use of lignosulfonate which originates from the outbounding sulfite process. The most common mechanistic rationale indicates the formation of an electrocatalytically active NiOOH species at the anodic surface which is regenerated during lignin oxidation [34]. The chemical relation between Ni and Co implies a similar electrocatalytic behaviour. The major focus of this study was to investigate the applicability of a lignin degradation process under technically relevant conditions. This implies an aqueous system due to the limited solubility of Kraft lignin as well as temperatures below 100 °C to avoid pressurized systems. Several electrode materials, based on Ni or Co alloys, were investigated towards their electrocatalytic activity in this particular degradation process. Table 1 displays yields of **1** by electrochemical degradation using the most productive anode materials.

Under the conditions described, the electrochemical process usually resulted in moderate yields of **1** <2.0 wt % per electrolysis run but the selectivity towards vanillin (**1**) formation is outstanding (Figure 1). The only other volatile byproduct formed in much lower yields compared to **1** is acetovanillone (**2**). Information about the quantities of **2** are given in Supporting Information File 2. In general, the application of Co-based materials resulted in higher yields of vanillin (**1**) with a maximum of 1.8 wt %. Unfortunately, all investigated Co-based alloys show some corrosion leading to mass loss and

Table 1: Influence of the anode material on the electrochemical degradation of lignin.[a]

Entry	Anode[b]	UNS-#	Alloy base	Yield of vanillin (**1**) / wt %[c]
1	Ni	–	–	0.7
2	Monel 400k	N04400	Ni	0.7
3	Nichem 1151	–	Ni	1.0
4	Co	–	–	1.4
5	Stellite 21	W73021	Co	1.8

[a]Electrolysis conditions: 80 °C, constant current (1.9 mA·cm^{-2}), undivided cell, 2688 C·g^{-1}, 0.525 g Kraft lignin. [b]Detailed information about the alloys can be found in Supporting Information File 1. [c]Based on used Kraft lignin. UNS = Unified numbering system.

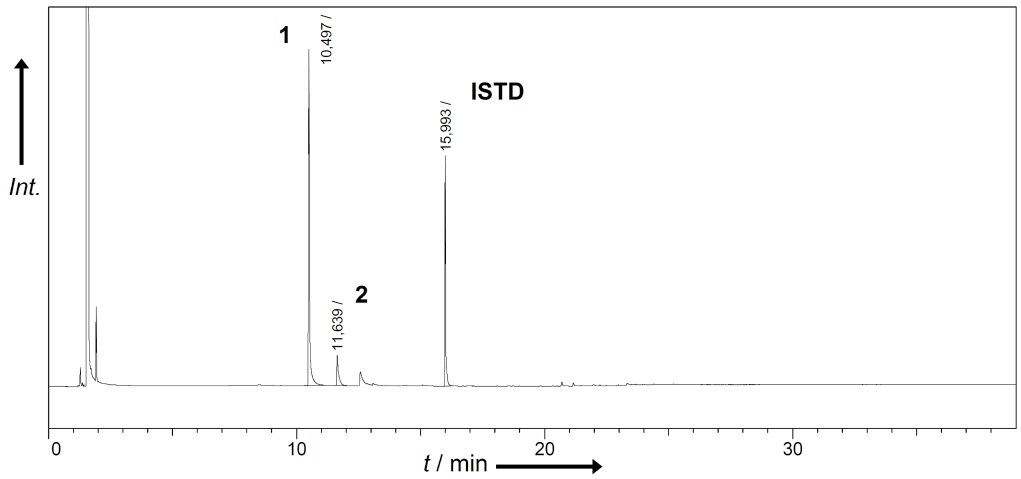

Figure 1: Crude product composition after electrochemical treatment of lignin at Ni-based electrodes by gaschromatography. Retention times: 10.50 min vanillin (**1**), 11.64 min acetovanillone (**2**), 16.00 min dodecylbenzene (ISTD).

the concomitant formation of Co oxides found as dark coating on the electrode surface as well as suspended to a small extent in the electrolyte.

The application of Ni-based materials on the other hand results in lower yields up to 1.0 wt %, but no corrosion is observed. Besides the applied anode materials, the current density has a tremendous influence on the achievable yield. Rather low current densities <2.0 mA·cm^{-2} usually result in the highest yields of vanillin (**1**) independent of the electrode materials. Especially, Co-based materials are very sensitive to this parameter and even a slight increase of the current density leads to a drastic drop in the yield of vanillin (**1**). This effect is displayed in Figure 2 comparing planar electrodes of Ni and the Co base alloy Stellite 21. Low current densities are very unfavourable from a technical point of view due to long electrolysis times. Three-dimensional electrodes are a suitable way to increase the effective anodic area leading to an improved space–time yield. For this reason 3D materials composed of different Ni-based materials were employed as electrode materials for the electrochemical process (Figure 3).

A comparison of 3D and plane Ni-based materials shows that even at low current densities of <2.0 mA·cm^{-2} surface enhanced materials are superior to planar electrodes. Ni foam and stainless steel electrodes, with a Ni content of up to 13%, showed a very similar and promising behaviour especially at elevated current densities. With current densities of up to 38 mA·cm^{-2} (this number corresponds to the geometric surface directly exposed to counter electrode) almost constant yields ≥1.0 wt % of **1** were observed. This application gives rise to increased yields of **1** as well as a decrease of electrolysis time to

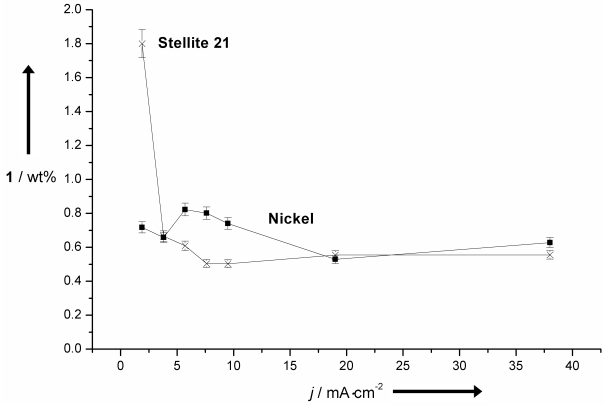

Figure 2: Influence of the current density onto the yield of **1** using Ni or Stellite 21 anodes.

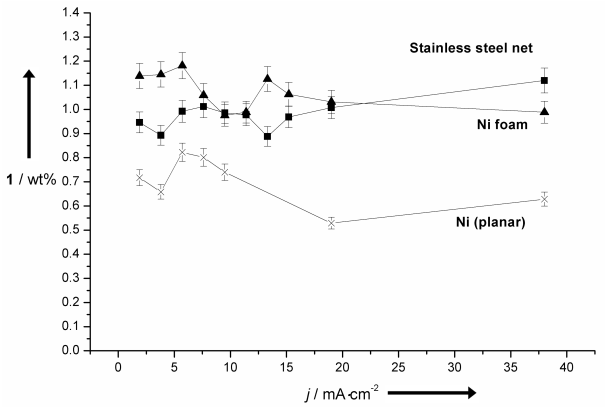

Figure 3: Influence of the current density on the yield of **1** using different geometries of anodic materials.

5% of the initially applied with planar electrodes. Another important factor for the efficiency of the selective degradation to **1** is the reaction temperature. At elevated temperatures usually decoiling or fragmentation takes place in the lignin particles [35,36]. This is very important to improve the accessibility of possible reaction sites located rather inside the lignin particle to the anode surface and high temperatures >100 °C are usually chosen for efficient degradation processes. Due to limited solubility of the commonly used Kraft lignin in aqueous systems, it was necessary to set-up massive autoclaves [37]. This was always a very limiting aspect for technical realizations due to cost and safety issues. It is noteworthy, that on the cathode hydrogen is formed and performing the electrolysis in a closed system is not desired. However, even at rather low reaction temperatures between 20–80 °C the particle behaviour and also the yield of **1** is influenced tremendously (Figure 4). In the past, the use of different mediators and catalysts often led to the formation of over oxidation products, i.e., vanillic acid (**4**) [34]. Our system avoids the formation of these low value products even if an excess of current is applied. As depicted in Figure 5 an almost linear increase of **1** is observed until an applied current of about 1200 $C \cdot g^{-1}$.

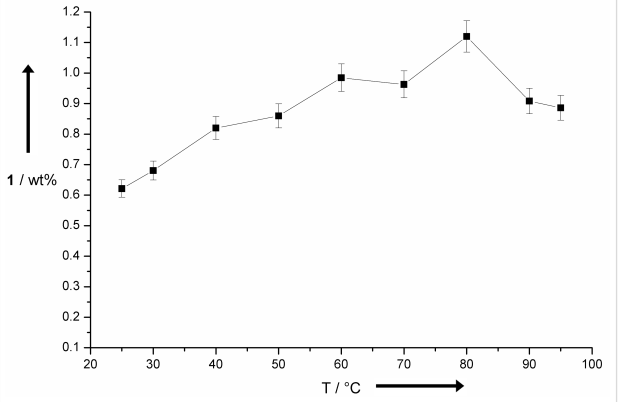

Figure 4: Influence of the reaction temperature onto anodic degradation of lignin using stainless steel electrodes.

Further current does not lead to an increased formation of **1**. But the system tolerates the excess and the formed **1** is not consumed to generate oxidation products like vanillic acid (**4**). Under these conditions the electrochemical oxidation of vanillin (**1**) does not take place. This was proven by a control experiment trying to oxidize vanillin (**1**) in alkaline solution at Ni foam and stainless steel electrodes. In both cases no formation of vanillic acid **4** was observed and the starting material was recovered almost quantitatively which indicates that no oligomer formation took place (see Supporting Information File 2). Screening of different anode materials and reaction

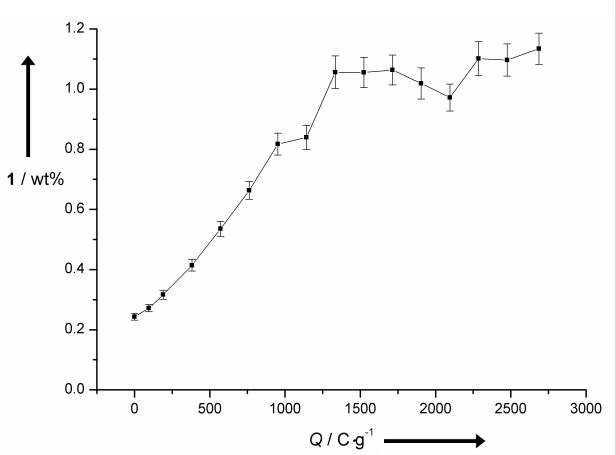

Figure 5: Influence of the applied current onto the yield of **1** by electrochemical degradation of lignin using stainless steel electrodes, applying a current density of 38 $mA \cdot cm^{-2}$.

parameters allowed an optimization of the electrochemical process. Ni foam electrodes enable enhanced current densities of up to 38 $mA \cdot cm^{-2}$ without negative influence on the yield of **1**. A reaction temperature of 80 °C and an applied current of 1500 $C \cdot g^{-1}$ leads to the maximum yield of **1**.

With the ability to selectively generate vanillin (**1**) from lignin in hand, we turned our attention to the development of an isolation strategy for the product. As in the method discussed above, degrees of conversion were usually rather low, but this is compensated by the enormous scope of the feedstock lignin [35]. But selectivity and product recovery are the most challenging aspects. After the electrolysis the electrolyte contains large amounts of unreacted, respectively chemically modified lignin. A conventional approach for product recovery includes acidification of the mixture, which leads to precipitation of lignin. Filtration followed by liquid–liquid extraction results in the clean product **1**. This procedure is rather problematic from a technical point of view. Filtration processes usually are time and maintenance intensive processes but even more disadvantageous is acidification of the whole electrolyte. That approach is expensive comparing the amount of acid necessary to neutralize the solution and the moderate yields of **1** which can be achieved by these processes. Consequently, alternative concepts are necessary to allow product removal without precipitation of lignin and acidification of the whole reaction mixture.

For this purpose the applicability of strongly basic anion exchange resins was tested. It is known from literature that these resins can be utilized for phenol recovery from waste water streams at different pH [38]. These methods usually take advantage of the combined physi- and ionosorptive interactions between the resin and the adsorptive phase. In the case of

phenolate stronger, ionic interactions usually dominate at basic pH [39]. But even under acidic conditions strong interactions between the polymer backbone and the adsorptive phase remain [40]. For this reason several commercially available resins were tested concerning their adsorption and desorption affinity towards **1** in model solutions at two different pH values (Figure 6). The different resins with their functionalities and the individual polymeric backbone are listed in Table 2.

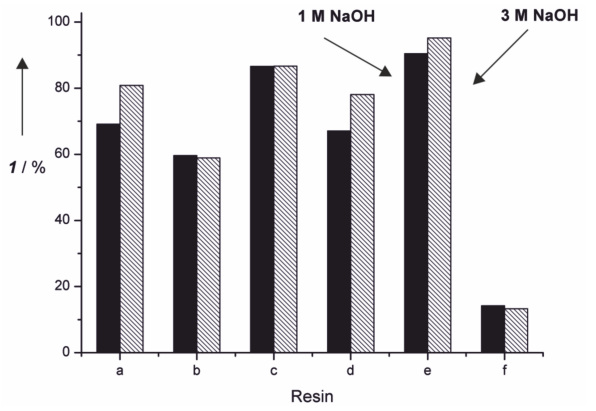

Figure 6: Amount of vanillin (**1**) removed by adsorption in a batch process at different strongly basic anion exchange resins. Experiments were performed at two different NaOH concentrations and desorption was realized by acidic treatment of the loaded resins.

Even in batch processes it was possible to remove more than 90% of dissolved **1** from the model solution which indicates that strong interactions between the resins and the adsorptive phase takes place. Desorption of the product can easily be performed by acidic treatment of the loaded resins. The most promising desorption system so far is a solution of EtOAc and AcOH (ratio 8:2). This treatment leads to protonation of vanillate anions adsorbed at the resin and ionic interactions between the resin and the product vanish. The remaining interactions between vanillin (**1**) and the aromatic backbone are not strong enough to prevent dissolution of **1** in the eluent. The results indicate that besides the ionic function the polymeric backbone has a very important influence on the adsorption behavior (Figure 7).

Table 2: Polymeric backbones and functionalities of the different strongly basic anion exchange resins used for batch adsorption experiments.

Resin[a]	Backbone	Ionic function
a	Polyvinylpyridine divinylbenzene	*N*-Methylpyridinium
b	Polystyrene divinylbenzene	Tetraalkylammonium
c	Polystyrene divinylbenzene	Tetraalkylammonium
d	Polystyrene divinylbenzene	Tetraalkylammonium
e	Polystyrene divinylbenzene	Tetraalkylammonium
f	Polyacrylate divinylbenzene	Tetraalkylammonium

[a]Commercial names of the different resins, corresponding exchange capacities and further information about specifications of the resins are listed in Supporting Information File 1.

The polystyrene backbones appear to be especially well suited for the adsorption of **1** from alkaline solutions. This can be explained by attractive π–π interactions between the backbone and the adsorptive phase. All resins containing an aromatic backbone lead to a loading of **1** >50% based on the total amount of used **1**. Resin **f** is a polyacrylate resin. This resin showed a far inferior loading of **1** <20% which supports the assumption that the polymeric backbone has a major importance for the adsorption process. Control experiments of non-modified polystyrene resin gave no adsorption at all. These batch experiments were optimized regarding the low vanillin (**1**) concentrations in the corresponding reaction solution after electrochemical degradation of lignin. Therefore, experiments were performed applying a high ratio of resin to vanillin (**1**). Further studies regarding the total capacity of this resin were performed showing that a loading of more than 60% is possible. This allows an easy removal of vanillin (**1**) on a gram scale (see

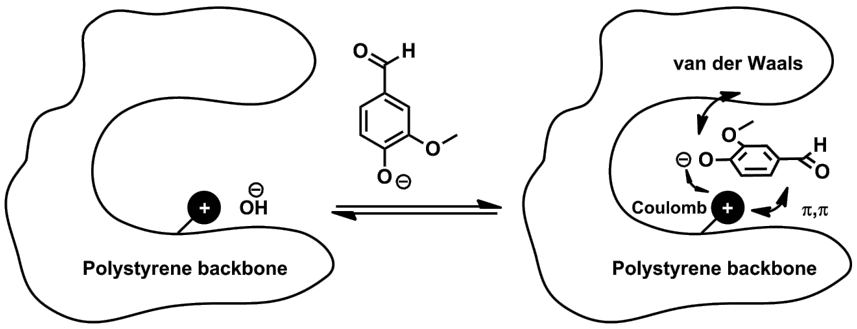

Figure 7: Different attractive interactions between ion exchange resin and the vanillate anion.

Supporting Information File 2). The superior resin **e** was used for the adsorption of **1** from the lignin-containing reaction mixture. Electrochemical degradation reactions of lignin were performed and afterwards various amounts of anion exchange resin were added to perform a batch process for adsorption of **1** (Figure 8).

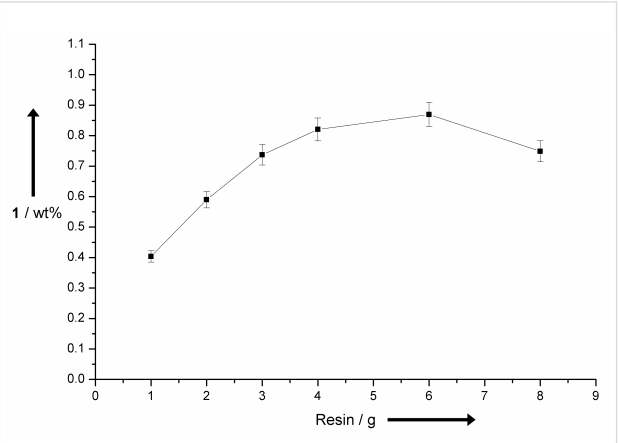

Figure 8: Recovery of vanillin (**1**) by adsorption from lignin containing reaction solutions after electrochemical treatment at Ni foam electrodes. Different amounts of resin were applied in a batch process. Desorption was performed treating the loaded resins with an acidic solution (EtOAc/AcOH, 8:2) in a batch process.

The results indicate that a large excess of resin is necessary to adsorb the maximum amount of **1**. Applying 6 g of resin led to the maximum yield of vanillin (**1**) of 0.9 wt % using this work-up protocol. This is close to the theoretical maximum yield of 1.0 wt % which was observed by conventional work-up of the reaction solution. Addition of more than 6 g of resin does not lead to an enhanced product removal, even lower yields of **1** were observed. This behavior can be rationalized by residual loading of the resin. The concentration of **1** in the reaction solution is about 0.06 mg·mL^{-1} and even under acidic conditions interactions between adsorptive phase and backbone are strong enough to keep a certain amount of formed **1** adsorbed in the equilibrium. This incomplete desorption is a common problem of batch processing [41]. To avoid this process it is necessary to allow a continuous shift of the equilibrium which can be realized by a continuous adsorption and desorption process. This was realized by setting up a column filled with anion exchange resin and the corresponding solutions for adsorption (lignin containing reaction mixture) and desorption (acidic eluent) of **1** were pumped through the column. This set-up allows a continuous enrichment of **1** on the column which avoids acidification of the solution and no precipitation occurs. The performance and applicability of this process was investigated by ten identical electrochemical degradation reactions followed by adsorption of the resulting solutions in a continuous process on the same column. After adsorption the depleted reaction solutions were analyzed for residual amounts of **1** by conventional work-up. No fraction of the depleted solution showed any content of vanillin (**1**) which indicates a complete take up of **1**. Afterwards the loaded resin was treated using an acidic eluent consisting of EtOAc/AcOH (8:2) analogous to the continuous adsorption process. Afterwards the acidic fraction was investigated concerning its content of **1**. It was observed that the expected maximum yield of 1.0 wt %, based on the total amount of used Kraft lignin, was exceeded and an effective yield of 1.3 wt % was found. This surprising observation can be explained by the optimized recovery process which avoids the very disadvantageous precipitation of lignin. The precipitate can include and adsorb certain amounts of **1** which leads to a reduced total yield. The present adsorption process avoids such precipitation and is by far superior to known conventional work-up procedures for alkaline lignin solutions. Using the desorption system EtOAc:AcOH (8:2) is very advantageous from an ecological point of view. Both components are environmental friendly and biocompatible. This is another advantage of this protocol compared with the conventional work-up procedure including acidification and liquid–liquid extraction applying dichloromethane as extracting agent. Excess of EtOAc and AcOH used for desorption can easily be recovered by distillation. Furthermore, the applied resin avoids adsorption of the dissolved lignin particles by size exclusion pictured in Figure 9. The chosen gel type resin is distinguished from macroreticular adsorbents by lower pore diameters [42,43]. Average pore diameters of gel type resins are in the range of 1–2 nm compared with macroreticular diameters up to several hundred nanometer. Lignin particles themselves can have larger diameters up to a few micrometers which allows an exclusion of these particles by application of gel type ion exchange resins [44]. So far no long-term study on the reusability of the resin was performed but the activity of the resin after an adsorption–desorption cycle with high loading of vanillin (**1**) was investigated and no loss of activity was observed. This indicates that adsorption of vanillin (**1**) has no negative influence on

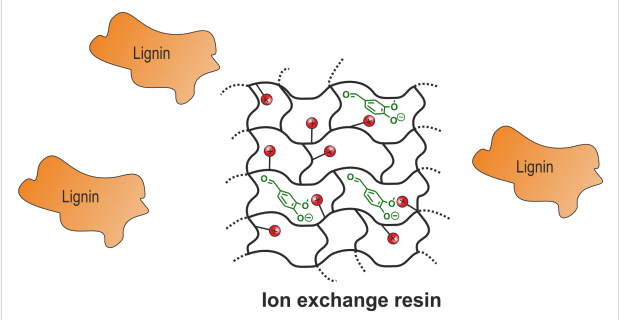

Figure 9: Adsorption of vanillin (**1**) on anion exchange resins and size exclusion of lignin particles by application of gel type resins.

stability of the ion exchange resin (see Supporting Information File 2).

Conclusion

In conclusion, our approach combines a highly selective electrochemical formation of vanillin (**1**) and a novel as well as viable work-up concept exploiting strongly basic anion exchange resins. As renewable feedstock we employed alkaline lignin solutions. Alloys of cobalt and nickel as anodic material are suitable forming in situ electrochemically active MO(OH) coatings. Despite higher yields for **1** using Co based anodes, Ni-based anodes seem to be the electrodes of choice due to their enhanced stability against corrosion. The electrolysis was successfully optimized to a process that can be operated below 100 °C and the application of 3D electrode designs, increased the space–time yield tremendously. To circumvent the common challenges in the work-up of lignin solutions (precipitation of lignin, use of excess acid and subsequent extraction of the low molecular weight products), we developed a novel and viable strategy for direct and selective removal of vanillin (**1**) and related phenols from the alkaline electrolyte. An easy to perform enrichment of the desired product by adsorption at strongly basic anion exchange resins was established. The larger lignin particles were not bound to the gel-type resins because the size exclusion effect does not affect them. Only small amounts of acid will be required to rinse the product from the solid support, which is of significant advantage to the conventional approaches. The resulting lignin-containing waste streams could be incinerated for energy production and base recovery performed, as currently done with waste streams of the pulping process [45]. The combined concepts represent a starting point for vanillin (**1**) production based on renewable resources [46,47].

Supporting Information

Supporting Information File 1

Information about materials.
[http://www.beilstein-journals.org/bjoc/content/supplementary/1860-5397-11-53-S1.pdf]

Supporting Information File 2

Experimental information.
[http://www.beilstein-journals.org/bjoc/content/supplementary/1860-5397-11-53-S2.pdf]

Acknowledgements

The authors want to thank the Federal Ministry of Food and Agriculture (FKZ 22027208), BASF SE, and the Deutsche Telekom Stiftung for financial support.

References

1. Chatel, G.; Rogers, R. D. *ACS Sustainable Chem. Eng.* **2014,** *2,* 322–339. doi:10.1021/sc4004086
2. Hanson, S. K.; Baker, R. T.; Gordon, J. C.; Scott, B. L.; Sutton, A. D.; Thorn, D. L. *J. Am. Chem. Soc.* **2009,** *131,* 428–429. doi:10.1021/ja807522n
3. Türk, O. *Stoffliche Nutzung nachwachsender Rohstoffe;* Springer: Wiesbaden, Germany, 2014. doi:10.1007/978-3-8348-2199-7
4. Chakar, F. S.; Ragauskas, A. J. *Ind. Crops Prod.* **2004,** *20,* 131–141. doi:10.1016/j.indcrop.2004.04.016
5. Yáñez, M.; Rojas, J.; Castro, J.; Ragauskas, A. J.; Baeza, J.; Freer, J. *J. Chem. Technol. Biotechnol.* **2013,** *88,* 39–48. doi:10.1002/jctb.3895
6. Zhang, W.; Chen, J.; Liu, R.; Wang, S.; Chen, L.; Li, K. *ACS Sustainable Chem. Eng.* **2014,** *2,* 683–691. doi:10.1021/sc400401n
7. Lange, H.; Decina, S.; Crestini, C. *Eur. Polym. J.* **2013,** *49,* 1151–1173. doi:10.1016/j.eurpolymj.2013.03.002
8. Creighton, R. H. J.; McCarthy, J. L.; Hibbert, H. *J. Am. Chem. Soc.* **1941,** *63,* 3049–3052. doi:10.1021/ja01856a052
9. Pepper, J. M.; Casselman, B. W.; Karapally, J. C. *Can. J. Chem.* **1967,** *45,* 3009–3012. doi:10.1139/v67-487
10. Forss, K. G.; Talka, E. T.; Fremer, K. E. *Ind. Eng. Chem. Prod. Res. Dev.* **1986,** *25,* 103–108. doi:10.1021/i300021a023
11. Jeon, M.-J.; Jeon, J.-K.; Suh, D. J.; Park, S. H.; Sa, Y. J.; Joo, S. H.; Park, Y.-K. *Catal. Today* **2013,** *204,* 170–178. doi:10.1016/j.cattod.2012.07.039
12. Brown, M. E.; Chang, M. C. Y. *Curr. Opin. Chem. Biol.* **2014,** *19,* 1–7. doi:10.1016/j.cbpa.2013.11.015
13. Rahimi, A.; Azarpira, A.; Kim, H.; Ralph, J.; Stahl, S. S. *J. Am. Chem. Soc.* **2013,** *135,* 6415–6418. doi:10.1021/ja401793n
14. Partenheimer, W. *Adv. Synth. Catal.* **2009,** *351,* 456–466. doi:10.1002/adsc.200800614
15. Nguyen, J. D.; Matsuura, B. S.; Stephenson, C. R. J. *J. Am. Chem. Soc.* **2014,** *136,* 1218–1221. doi:10.1021/ja4113462
16. Ninomiya, K.; Takamatsu, H.; Onishi, A.; Takahashi, K.; Shimizu, N. *Ultrason. Sonochem.* **2013,** *20,* 1092–1097. doi:10.1016/j.ultsonch.2013.01.007
17. Parpot, P.; Bettencourt, A. P.; Carvalho, A. M.; Belgsir, E. M. *J. Appl. Electrochem.* **2000,** *30,* 727–731. doi:10.1023/A:1004003613883
18. Borges de Silva, E. B.; Zabkova, M.; Araújo, J. D.; Cateto, C. A.; Barreiro, M. F.; Belgacem, M. N.; Rodrigues, A. E. *Chem. Eng. Res. Des.* **2009,** *87,* 1276–1292. doi:10.1016/j.cherd.2009.05.008
19. Smith, C.; Utley, J. H. P.; Petrescu, M.; Viertler, H. *J. Appl. Electrochem.* **1989,** *19,* 535–539. doi:10.1007/BF01022110
20. Reichert, E.; Wintringer, R.; Volmer, D. A.; Hempelmann, R. *Phys. Chem. Chem. Phys.* **2012,** *14,* 5214–5221. doi:10.1039/c2cp23596j
21. Steckhan, E. *Angew. Chem., Int. Ed. Engl.* **1986,** *25,* 683–701. doi:10.1002/anie.198606831
22. Yoshida, J.-i.; Kataoka, K.; Horcajada, R.; Nagaki, A. *Chem. Rev.* **2008,** *108,* 2265–2299. doi:10.1021/cr0680843
23. Frontana-Uribe, B. A.; Little, R. D.; Ibanez, J. G.; Palma, A.; Vasquez-Medrano, R. *Green Chem.* **2010,** *12,* 2099–2119. doi:10.1039/C0GC00382D
24. Schäfer, H. J.; Harenbrock, M.; Klocke, E.; Plate, M.; Weiper-Idelmann, A. *Pure Appl. Chem.* **2007,** *79,* 2047–2057. doi:10.1351/pac200779112047

25. Sperry, J. B.; Wright, D. L. *Chem. Soc. Rev.* **2006,** *35,* 605–621. doi:10.1039/B512308A
26. Lund, H.; Hammerich, O., Eds. *Organic Electrochemistry;* Marcel Dekker: New York, NY, USA, 2001.
27. Steckhan, E.; Arns, T.; Heineman, W. R.; Hilt, G.; Hoormann, D.; Jörissen, J.; Kröner, L.; Lewall, B.; Pütter, H. *Chemosphere* **2001,** *43,* 63–73. doi:10.1016/S0045-6535(00)00325-8
28. Elsler, B.; Schollmeyer, D.; Dyballa, K. M.; Franke, R.; Waldvogel, S. R. *Angew. Chem., Int. Ed.* **2014,** *53,* 5210–5213. doi:10.1002/anie.201400627
29. Kulisch, J.; Nieger, M.; Stecker, F.; Fischer, A.; Waldvogel, S. R. *Angew. Chem., Int. Ed.* **2011,** *50,* 5564–5567. doi:10.1002/anie.201101330
30. Morofuji, T.; Shimizu, A.; Yoshida, J.-i. *Angew. Chem., Int. Ed.* **2012,** *51,* 7259–7262. doi:10.1002/anie.201202788
31. Smith, C. Z.; Utley, J. H. P.; Hammond, J. K. *J. Appl. Electrochem.* **2011,** *41,* 363–375. doi:10.1007/s10800-010-0245-0
32. Holleman, A. F.; Wiberg, N. *Lehrbuch der anorganischen Chemie;* Walter de Gruyter: Berlin, Germany, 1995.
33. Santos, R. B.; Hart, P.; Jameel, H.; Chang, H.-m. *BioResources* **2012,** *8,* 1456–1477. doi:10.15376/biores.8.1.1456-1477
34. Pardini, V. L.; Smith, C. Z.; Utley, J. H. P.; Vargas, R. R.; Viertler, H. *J. Org. Chem.* **1991,** *56,* 7305–7313. doi:10.1021/jo00026a022
35. Petridis, L.; Schulz, R.; Smith, J. C. *J. Am. Chem. Soc.* **2011,** *133,* 20277–20287. doi:10.1021/ja206839u
36. Nieminen, K.; Kuitunen, S.; Paananen, M.; Sixta, H. *Ind. Eng. Chem. Res.* **2014,** *53,* 2614–2624. doi:10.1021/ie4028928
37. Zakzeski, J.; Bruijnincx, P. C. A.; Jongerius, A. L.; Weckhuysen, B. M. *Chem. Rev.* **2010,** *110,* 3552–3599. doi:10.1021/cr900354u
38. Carmona, M.; de Lucas, A.; Valverde, J. L.; Velasco, B.; Rodríguez, J. F. *Chem. Eng. J.* **2006,** *117,* 155–160. doi:10.1016/j.cej.2005.12.013
39. Caetano, M.; Valderrama, C.; Farran, A.; Cortina, J. L. *J. Colloid Interface Sci.* **2009,** *338,* 402–409. doi:10.1016/j.jcis.2009.06.062
40. Zhu, L.; Deng, Y.; Zhang, J.; Chen, J. *J. Colloid Interface Sci.* **2011,** *364,* 462–468. doi:10.1016/j.jcis.2011.08.068
41. Dorfner, K. *Ionenaustauscher;* Walter de Gruyter: Berlin, Germany, 1970.
42. Lee, S. C.; Hsiang, C. C.; Huang, H.; Ting, G. *Sep. Sci. Technol.* **1990,** *25,* 1857–1870. doi:10.1080/01496399008050429
43. Tsyurupa, M. P.; Davankov, V. A. *React. Funct. Polym.* **2006,** *66,* 768–779. doi:10.1016/j.reactfunctpolym.2005.11.004
44. Moreva, Yu. L.; Alekseeva, N. S.; Chernoberezhskii, Yu. M. *Russ. J. Appl. Chem.* **2010,** *83,* 1281–1283. doi:10.1134/S1070427210070207
45. Ulber, R.; Sell, D.; Hirth, T., Eds. *Renewable raw materials. New feedstocks for the chemical industry;* Wiley-VCH: Weinheim, Germany, 2011.
46. Stecker, F.; Fischer, A.; Kirste, A.; Waldvogel, S. R.; Regenbrecht, C.; Schmitt, D. Eletrolysis method for producing vanillin. WO 2014006106 A1, 2013.
47. Stecker, F.; Fischer, A.; Kirste, A.; Voitl, A.; Wong, C. H.; Waldvogel, S. R.; Regenbrecht, C.; Schmitt, D.; Hartmer, M. F. Method for obtaining vanillin from aqueous basic compositions containing vanillin. WO 2014006108 A1, 2013.

License and Terms

BEILSTEIN JOURNAL OF ORGANIC CHEMISTRY

Cathodic hydrodimerization of nitroolefins

Michael Weßling and Hans J. Schäfer*

Full Research Paper

Open Access

Address:
Organisch-Chemisches Institut der Westfälischen Wilhelms-Universität, Correns-Straße 40, 48149 Münster, Germany

Email:
Hans J. Schäfer* - schafeh@uni-muenster.de

* Corresponding author

Keywords:
cathodic hydrodimerization; C–C bond formation; 1,4-dinitrocompounds; electrosynthesis; nitroalkene

Beilstein J. Org. Chem. **2015,** *11,* 1163–1174.
doi:10.3762/bjoc.11.131

Received: 17 April 2015
Accepted: 19 June 2015
Published: 14 July 2015

This article is part of the Thematic Series "Electrosynthesis".

Guest Editor: S. R. Waldvogel

Abstract

Nitroalkenes are easily accessible in high variety by condensation of aldehydes with aliphatic nitroalkanes. They belong to the group of activated alkenes that can be hydrodimerized by cathodic reduction. There are many olefins with different electron withdrawing groups used for cathodic hydrodimerization, but not much is known about the behaviour of the nitro group. Synthetic applications of this group could profit from the easy access to nitroolefins in large variety, the C–C bond formation with the introduction of two nitro groups in a 1,4-distance and the conversions of the nitro group by reduction to oximes and amines, the conversion into aldehydes and ketones via the Nef reaction and base catalyzed condensations at the acidic CH bond. Eight 1-aryl-2-nitro-1-propenes have been electrolyzed in an undivided electrolysis cell to afford 2,5-dinitro-3,4-diaryl hexanes in high yield. The 4-methoxy-, 4-trifluoromethyl-, 2-chloro- and 2,6-difluorophenyl group and furthermore the 2-furyl and 2-pyrrolyl group have been applied. The reaction is chemoselective as only the double bond but not the nitro group undergoes reaction, is regioselective as a ß,ß-coupling with regard to the nitro group and forms preferentially two out of six possible diastereomers as major products.

Introduction

Olefins being activated by an electron withdrawing group can be hydrodimerized by cathodic reduction [1,2]. Thereby, the cathode serves as cheap, versatile, immobilized and mostly non-polluting reagent providing economical and ecological advantages compared to chemical reducing agents [3,4]. Alkenes with a large variety of electron withdrawing groups have been explored in cathodic hydrodimerizations (Scheme 1) [1,2]. We were interested in the nitro group as a substituent. It can be easily introduced by addition of a nitroalkyl anion to a carbonyl group followed by elimination of water from the resulting alcohol. The nitroolefin can be reduced at the nitro group, at the double bond and simultaneously at both groups. In acidic medium the nitro group is reduced between −0.25 V to −0.55 V vs SCE to mixtures of *syn*/*anti*-oximes in 85% to 92% yield at a mercury pool cathode and with slightly lower yields at a graphite cathode [5-8]. The current controlled reduction of

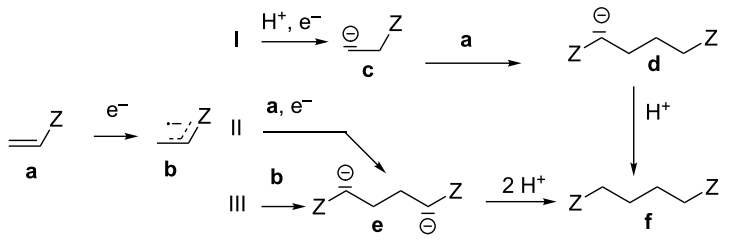

Scheme 1: Proposed mechanisms via pathways (I) to (III) for the cathodic hydrodimerization of olefins with electron attracting substituents.

alkyl- and aryl-substituted nitroalkenes in acidic medium affords mixtures of ketones and oximes in yields of 39% to 72% [9] and 55% to 91% [10], respectively.

Conducting the reduction at the more negative potential of −1.1 V to −1.3 V vs SCE and otherwise comparable conditions amines are obtained in 60% to 69% yield [5]. Thereby, (*E*)-1-(3-cyclohexen-1-yl)-2-nitroethene can be chemoselectively reduced in 69% yield to 1-amino-2-(3-cyclohexen-1-yl)ethane without hydrogenating the C–C double bond.

The hydrodimerization of nitro olefins should lead to 1,4-dinitroalkanes following the regioselectivity found in other hydrodimerizations of activated olefins [1,2]. Thereby, the proton concentration in the electrolyte should be not too high, as otherwise the reduction of the nitro group to oximes would be favoured. On the other side the electrolyte should not be aprotic as protons are required for protonation of the intermediate anions in the reductive dimerization (Scheme 1).

According to the proposed mechanism for the cathodic hydrodimerization the radical anion **b** formed by one electron reduction of the substrate **a**, has three pathways for dimerization [1,2]. In path (I) protonation followed by one-electron reduction leads to anion **c**, which in a Michael addition with substrate **a** forms the anion **d**, which is protonated to hydrodimer **f**. In path (II) **b** undergoes a nucleophilic addition to **a** forming a dimer radical anion that is reduced to **e** that is then protonated to the dimer **f**. In path (III) the radical coupling of two radical anions **b** leads to the dianion **e**, which is protonated to the product.

We first checked the cathodic reduction of (*E*)-2-nitro-1-phenyl-1-propene (**1**) [for chemical formulas see Table 4] whether the dimer 2,5-dinitro-3,4-diphenylhexane (**2**) can be obtained and which would be the optimal conditions for a high selectivity and yield. The optimization and subsequent hydrodimerization of eight nitro olefins has been previously reported in [6-8]. There have been reports on the reductive dimerization of nitro alkenes prior to 1991. 1,4-Dinitro-2,3-diphenylbutane (**3**) has been obtained in less than 20% yield in the catalytic hydrogenation of β-nitrostyrene (**4**) [11]. Hydrodimerization of **4** was observed in enzymatic reduction [12]. Furthermore **3** was found in the reduction of **4** with $TiCl_3$ [13,14]. High dimer yields are reported for the reduction of several nitro olefins with the dianion of cyclooctatetraene [15]. ß-Nitrostyrene (**4**) has been reductively dimerized with organomanganese reagents to **3** in low yield [16]. The electrochemical reduction of 1-nitroalkenes was studied by cyclic voltammetry and controlled potential coulometry. The reduction probably proceeds by initial formation of the radical anion, which subsequently dimerizes [17]. Later conditions were described to achieve selectively either a cathodic ß,ß-coupling (cathodic hydrodimerization) or a α,ß-coupling with aliphatic nitro alkenes having acidic α-protons. ß,ß-Coupling can be achieved in good to high yield (41–95%) at high current densities [18]. In the reduction of 3,3-dimethyl-1-nitrobut-1-ene the intermediate radical anion has been identified by ESR. Nitroalkene **4** is reported to be converted quantitatively to the hydrodimer **3** with SmI_2 [19]. A catalytic reductive β,β-carbon coupling of nitroalkenes catalyzed by a *N*-heterocyclic carbene has been reported recently. Diastereomers are formed, whose dr (*d,l*- over *meso*-ratio) ranges between 66:34 to 90:10. The interesting new reaction proceeds through a radical anion of the nitroalkene generated in a catalytic redox process. For ß-isopropyl-nitroethylene the radical anion has been identified by ESR [20].

Results and Discussion

Investigation of the cathodic hydrodimerization of nitroalkene **1** to hydrodimer **2**

The cathodic hydrodimerization is performed in a divided electrolysis cell by variation of the electrolyte (Table 1, Scheme 2). The working potential was chosen from cyclic voltammetry and current/voltage curves in the cell used for the preparative conversion. The potential in the controlled potential electrolysis was −0.9 V to −0.95 V vs SCE.

Table 1: Hydrodimerization of **1** in dependence on the electrolyte composition.

Nr.	**1** (mmol)	electrolyte	HOAc[a] (mmol)	*T* (°C)	*Q* (F/mol)	yield (%)[b] **2**	**5**	**1**
1	3.06	DMF/H_2O (9:1) 0.2 M $TBABF_4$	0.2 M	20	1.95	24	20	–
2	3.06	DMF/H_2O (25:1) 0.2 M $TBABF_4$	–	20	1.25	[c]	–	–
3	5.09	DMF 0.2 M $TBABF_4$	1 × 5.0	30	1.08	30	7	20
4	7.50	DMF 0.2 M TEA-*p*Tos	2 × 3.7	30	1.5	48	4	–
5	6.13	DMF 0.2 M TEA-*p*Tos	10 × 0.6	30	1.01	60	–	–

[a]0.2 M HOAc in electrolyte (Nr. 1); addition of corresponding fractions of an equivalent of the H^+-donor at the start (Nr. 3, 4, 5) and after throughput of the respective theoretical charge (Nr. 4, 5). [b]Isolated by flash chromatography. [c]Product mixture, about 30% of **2**.

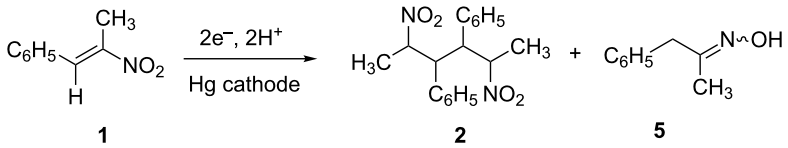

1 **2** **5**

Scheme 2: Cathodic reduction of nitroalkene **1** to hydrodimer **2** and oxime **5**.

The results indicate: an increased acidity favours the formation of oxime **5** (Table 1, Nr. 1), whilst without a proton donor the olefin presumably is polymerized to a large extent (Table 1, Nr. 2). The addition of acetic acid in portions appears to be a good choice as a too high proton concentration is avoided and the necessary amount of protons is continuously provided in the proper amount. TEA-*p*Tos appears to be a better supporting electrolyte than $TBABF_4$: In the latter hydrogen bonds between the fluorine atoms and water possibly increase the water concentration in the double layer and this way reverse partially the hydrophobic effect of the alkyl groups in the tetraethylammonium cation. The dimer yield should increase with increasing radical concentration, which means that at the beginning of the reaction the dimer yield should be higher than towards the end. As olefin **1** and dimer **2** are expected to have a higher oxidation potential than DMF due to the nitro group the advantageous use of an undivided cell appears to be possible. Taking the optimal conditions of electrolysis Nr. 5 in Table 1 the influence of the parameters mentioned above was investigated (Table 2).

Table 2: Hydrodimerization of **1**[a] in dependence of temperature, conversion and cell type.

Nr.	*T* (°C)	*Q* (F/mol)	Yield **2** (%)[b]
5[c]	30	1.01	60
6	50	1.19	63
7	−10	1.27	70
8	0	1.19	81
9	0	0.51	46 (83)[d]
10[e]	30	1.42	44
11[f]	0	0.98	88

[a]5.03 mmol **1** in 25 mL 0.2 M TEA-*p*Tos/DMF. [b]Isolated yield. [c]Nr. 5 in Table 1 is shown for comparison. [d]Yield in parenthesis based on conversion; 45% reisolated **1**. [e]Undivided cell, 0.25 equiv HOAc. [f]Undivided cell without addition of acetic acid.

The influence of the temperature is less significant than expected. The increase of the temperature to 50 °C shows a marginal increase of the yield, whilst a temperature decrease is more successful. Best results could be achieved at 0 °C. The yield after 50% charge consumption based on conversion is insignificantly higher (Table 2, Nr. 9). This indicates that there is no higher yield at higher substrate concentration in the first half of the reaction compared to the second half. However, a remarkable increase of the yield is obtained in an undivided cell without addition of a proton donor. With a quantitative conversion of **1** the dimer **2** is obtained in 88% material yield and 90% current yield. Presumably the protons are generated at the anode by oxidation of residual water and/or the solvent DMF. A major source of residual water could be the very hygroscopic tosylate as one of the reviewers suggested. The conditions of Nr. 11 in Table 2 should be suitable for the conversion of further nitroalkenes.

The cyclovoltammogram (CV) of **1** shows two irreversible reduction peaks at −1.08 V and −1.8 V vs SCE. The second peak can be attributed to the reduction of hydrodimer **2**, as for isolated **2** the reduction peak is found at this potential. The first peak can be assigned to the reduction of **1** forming the radical anion. Addition of acetic acid shows no potential shift but a slight increase of the peak current. This could indicate that the radical anion is fast protonated and the resulting radical is further reduced. Proton addition, however, could also favour the reduction of the nitro group to the oxime, which consumes four electrons. Decreasing hydrodimer yields with increasing temperature could be due to the existence of chemical side reactions of the radical anion, such as oligomerization or protonation, which are more accelerated at higher temperatures compared to the radical dimerization. It should be mentioned that at the cathode deep red species are formed that become colorless upon addition of acetic acid. In an undivided cell and an unstirred electrolyte, which allows diffusion between the electrodes, a red colour appears at the cathode, which disappears at the anode. This indicates the formation of coloured nitroalkyl anions and their decolourization by protonation.

The nitroalkenes were obtained by condensation of aldehydes with nitroalkanes (Scheme 3, Table 3) [21,22].

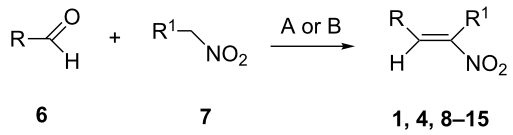

6 **7** **1, 4, 8–15**

A: *n*-BuNH$_2$, abs. EtOH, reflux
B: HOAc, NH$_4$OAc, reflux

Scheme 3: Preparation of the 1-aryl-2-nitroalkenes **1**, **4**, **8–15**.

For work-up unreacted aldehyde was removed by way of the bisulfite adduct, this facilitated the crystallization and improved the yields. The preparation of the nitroalkenes **1**, **4**, **8**, **9** is described in [25]; the IR, ^{1}H NMR, and MS data are provided in the experimental part (Supporting Information File 1). From a comparison of the experimental δ value for the vinylic proton with this from an increment calculation the cis position of the hydrogen atom to the nitro group can be assigned for the nitroalkenes **1**, **8**, **9**, which is the *E*-configuration.

As the trifluoromethyl compound **10** is not accessible by the method A or B it is prepared in two steps from aldehyde **6c** via the *n*-butylazomethine [24]. Particularly difficult was the synthesis of **12**, where a product mixture is formed; additionally **12** decomposes partly during purification by fractional crystallization, furthermore it is air sensitive. All that leads to low yields of **12**. The dinitrodiene **16** was prepared from 1,4-dinitrobutane and two equivalents of benzaldehyde with 1,2-diaminoethane as catalyst in 59% yield [26]; 1,4-dinitrobutane was prepared from 1,4-dibromobutane [27]. The structures of the prepared compounds were secured by comparing the melting points with these from the literature [24-27] and their spectroscopic data. The nitroolefins **10**–**15** exhibit the same spectroscopic features as these of **1**, **4**, **8**, **9**. The C,H,N and C,H,F,N analyses additionally confirm the structures. From the ^{1}H NMR spectra for all nitro olefins the *E*-configuration of the double bond can be derived.

Cyclic voltammetry

The reduction potentials ($E_{p,c}$) of the nitroalkenes were determined by cyclic voltammetry. The values, ordered by decreasing potentials, are shown in Scheme 4.

The reduction potentials $E_{p,c}$ are determined by the conformation of the aryl group, the electron density at the double

Table 3: Preparation of 1-aryl-2-nitroalkenes.

Aldehyde	Nitroalkane	Method	Nitroalkene[a]	Yield (%)[b]
6a, R: phenyl	**7a**, R^1: H	[c]	**4**	50[c]
6a, R: phenyl	**7b**, R^1: Me	A	**1**	54
6a, R: phenyl	**7c**, R^1: Et	A	**8**	62
6b, R: 4-methoxyphenyl	**7b**, R^1: Me	B	**9**	44
6c, R: 4-trifluoromethylphenyl	**7b**, R^1: Me	[d]	**10**	42[d]
6d, R: 2-furyl	**7b**, R^1: Me	A	**11**	75
6e, R: 2-pyrrolyl	**7b**, R^1: Me	A	**12**	10[e]
6f, R: 2-chlorophenyl	**7b**, R^1: Me	A	**13**	58
6g: 2,6-dichlorophenyl	**7b**, R^1: Me	B	**14**	36
6h: 2,6-difluorophenyl	**7b**, R^1: Me	A	**15**	62

[a]For the structures of the nitroalkenes see Scheme 4. [b]Isolated, not optimized yield. [c]Ref. [23]. [d]Ref. [24]. [e]Crude yield higher, product decomposes slowly during recrystallization.

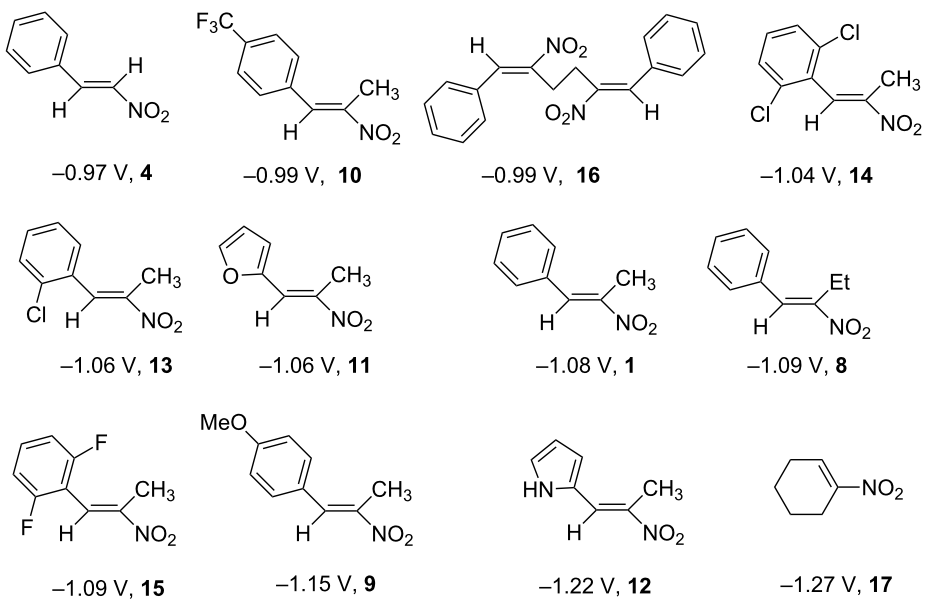

Scheme 4: Reduction potentials ($E_{p,c}$ in Volt) of nitroolefins. Conditions: amalgamated gold wire, v = 0.1 V/s, 0.2 M TEA-*p*Tos in DMF, accuracy of $E_{p,c}$ = +/− 0.02V vs SCE, measured against the Marple electrode and converted to SCE.

bond and the nitro group, the energy of the radical anion and the reactivity of the radical anion. We have not determined these values, but have concentrated ourselves on the preparative aspects of the cathodic hydrodimerization. Certain influences of substituents on the reduction potentials of the nitroolefins can be qualitatively seen. Aryl substituents shift the potentials to more negative values according to their Hammett σ values [28]: **10** (4-CF_3, σ_p = 0.53) > **1** (4-H, σ_p = 0) > **9** (4-CH_3O, σ_p = −0.12). With a Hammett equation for an electrochemical reaction and using the E_p values as E^0-values one obtains from these three values a Hammett reaction constant ρ = 5.34. This is similar to the reaction constant ρ = 6.37 obtained from the Hammett plot for the one-electron reduction of substituted benzo- and naphthoquinones in DMF [29], which have an electrophore being similar to this of the nitroolefins. For the other substituents no σ-values are available to apply the Hammett equation. They are ordered according to decreasing E_p-values in three groups: **11** (2-furyl) > **9** (4-CH_3O) > **12** (2-pyrrolyl); **14** (two *o*-Cl) ≈ **13** (one *o*-Cl) > **15** (two *o*-F); another correlation concerns the vinyl substituents at C2 of the double bond: **4** (2-H) > **1** (2-CH_3) ≈ **8** (2-C_2H_5) > **17** (no aryl group, methylene groups only). These orders are compatible with the electron donating abilities of the substituents, being derived from their σ_m values [28]. The more positive potential of **16** compared to **1** could be due to intramolecular interactions of the nitro groups with the non-conjugated double bonds. The $E_{p,c}$ of **1** and **4** measured at an amalgamated gold-wire electrode in DMF are somewhat more positive than those measured at a Pt-disc in ACN [17].

In the CV of all nitroolefins a second reduction peak appears at a potential being 600–800 mV more cathodic compared to the first one. Possibly this is the reduction of the hydrodimer as the CV of the hydrodimer of nitroolefin **1** indicates. This is different for the nitroolefins **14** and **15**, which are *o*,*o*'-disubstituted at the phenyl ring (Figure 1).

In the CV of **14** and **15** (Figure 1a) already at low scan rates (0.1 V/s) an anodic peak ($E_{p,a}$ = −0.95 V for **14** and $E_{p,a}$ = −0.92 V for **15**) appears in the reverse scan. Reversing the scan after the first peak leads for **15** at a scan rate of 10 V/s to a CV peak with $E_{p,c}$ = −1.084 V, $E_{p,a}$ = −0.904 V and $i_{p,c}/i_{p,a}$ = 1. For **14** higher scan rates were necessary to achieve a similar effect, but there the curve became strongly distorted possibly due an increasing capacitive current and iR-drop. This indicates, that most probably due to the *o*,*o*-substituents in **15** the follow-up reaction of the radical anion is slowed down for steric reasons. For **14** no dimer was found (see below). Further electroanalytic investigations were omitted in favour of the preparative scale hydrodimerizations of the nitroolefins.

Preparative scale electrolyses at the Hg cathode

The preparative scale electrolyses were performed using the following conditions: Hg cathode, undivided cell, 0.2 M TEA-*p*Tos in DMF at 0 °C, cathode potential of −0.90 V to −0.95 V vs SCE. These conditions were optimal for the potential controlled conversion of nitroolefin **1** into dimer **2**. The conversions shown in Table 4 consumed one charge equivalent

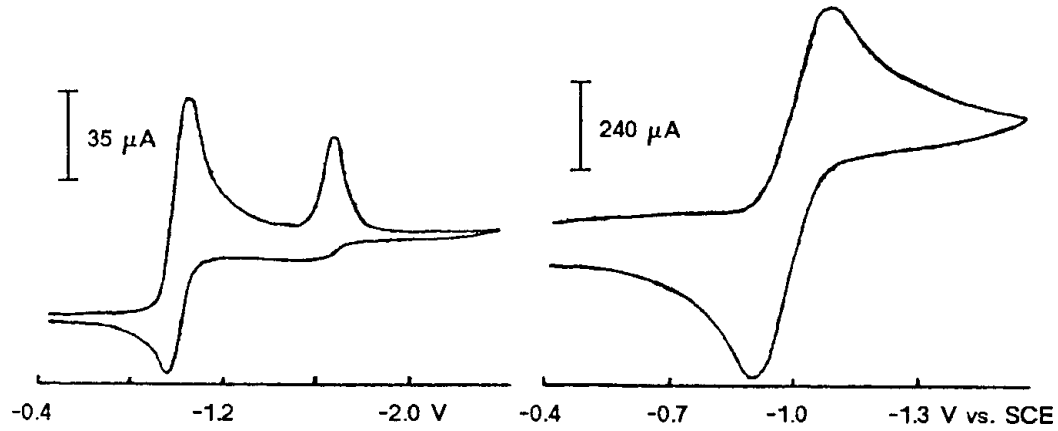

Figure 1: (a) CV of **15**; *v* = 0.1 V/s, (b) CV of **15**; *v* = 10 V/s.

Table 4: Preparative hydrodimerization of nitroalkenes.

Nitroalkene	Hydrodimer[a]	Yield (%)[b]
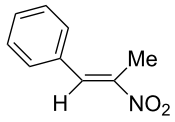 **1**	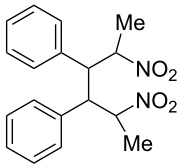 **2**	88
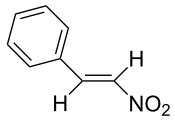 **4**	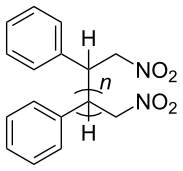 **3**	71[c]
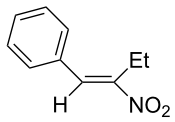 **8**	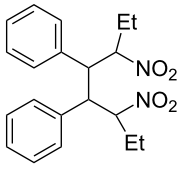 **18**	84
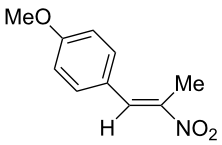 **9**	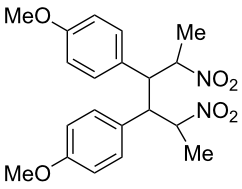 **19**	75
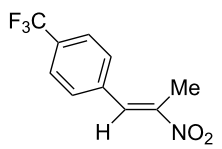 **10**	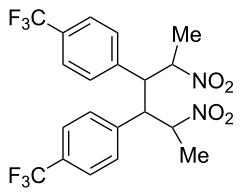 **20**	68

Table 4: Preparative hydrodimerization of nitroalkenes. (continued)

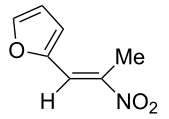 **11**	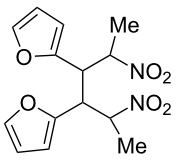 **21**	85
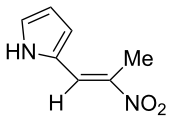 **12**	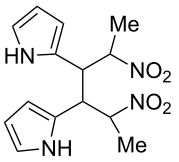 **22**	73[d]
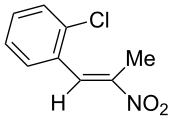 **13**	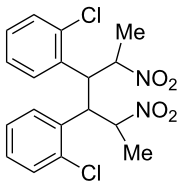 **23**	83

[a]Products are mixtures of diastereomers (see chapter: Structure of the hydrodimers). [b]Isolated yield; material yield corresponds to 95–100% of the current yield. [c]See text following Table 4. [d]Reduction in divided cell, as product is sensitive to anodic oxidation; yield in undivided cell: 60%.

(Q = 1 F mol^{-1}) for completion, then the electrolysis current had decreased to nearly 0 mA. In the work-up following the electrolysis the products in general can be extracted by nonpolar petroleum ether/diethyl ether mixtures from the aqueous emulsions or suspensions, respectively. The insoluble dimer **3** was isolated by filtration and washing the solid with petroleum ether/diethyl ether. The products are obtained after purification by flash chromatography as colourless oils, which are mixtures of diastereomers. They crystallize partially or completely after some time and are in general not sensitive against air and light. An exception is the pyrrole derivative **22**, in the air its light colour deepens quickly to brown. The electrolyses proceed uniformly. The current reaches after a short induction period (1–3 min) depending on the substrate a maximal current of 250–450 mA, which then decreases exponentially to zero.

The dichloro derivative **14** deviates from this behaviour. Applying the usual electrolysis conditions no dimer **26** but only the oxime **24** (37%) and the nitro alcohol **25** (31%) are formed (Scheme 5a). As already indicated in the CV of **14** the dimerization of the intermediate radical anion of **14** is apparently hindered for steric reasons, which can explain the absence of the dimer. This can favour the further reaction of the radical anion of **14** to the oxime **24** and the Michael addition of hydroxy ions to form the nitro alcohol **25**.

The smaller space filling of the fluorine atom compared to the chlorine atom should lead to a sterically less hindered radical anion in the reduction of **15**, which allows the formation of 40% of the dimer **29** and leads to less oxime and nitro alcohol as side products (Scheme 5b).

The dimers **2** and **18**–**23** could be identified by ^{1}H, ^{13}C NMR, MS and elemental analyses (see Structures of the hydrodimers and Experimental part in Supporting Information File 1). Dimer **3** is insoluble in common solvents at rt, thus no ^{1}H and ^{13}C NMR could be obtained. It has a correct elemental analysis and the IR spectrum is similar to this of **2** and the other dimers with regard to the NO_2 group. It melts at 238–242 °C with decomposition, which is similar to the product obtained by hydrogenating dimerization of olefin **4** in [11]. The insolubility and the melting point disagree, however, with compound **3** (n = 1) described in [20]. From the laser desorption ionization (LDI) mass spectrum of **3** it could be presumed that **3** is mainly a trimer (**3**, n = 2). The trimer could arise by a Michael addition of the intermediate dimer radical anion or dimer dianion of **4** to olefin **4**. Indications to greater portions of **3** (n = 1) and **3** (n = 3) were not found in the LDI–MS. Support for this assumption comes from coulometry for **4** in [17], which indicates oligomerization. Oligomerization does not occur if the substituent α to the nitro group is an alkyl group as in olefin **1**, possibly due to steric hindrance.

The dinitrodiene **16** is intramolecularly coupled at the Hg cathode to form the dinitrocyclohexane **30** (Scheme 6a), it also does not show the usual behaviour found in the preceding elec-

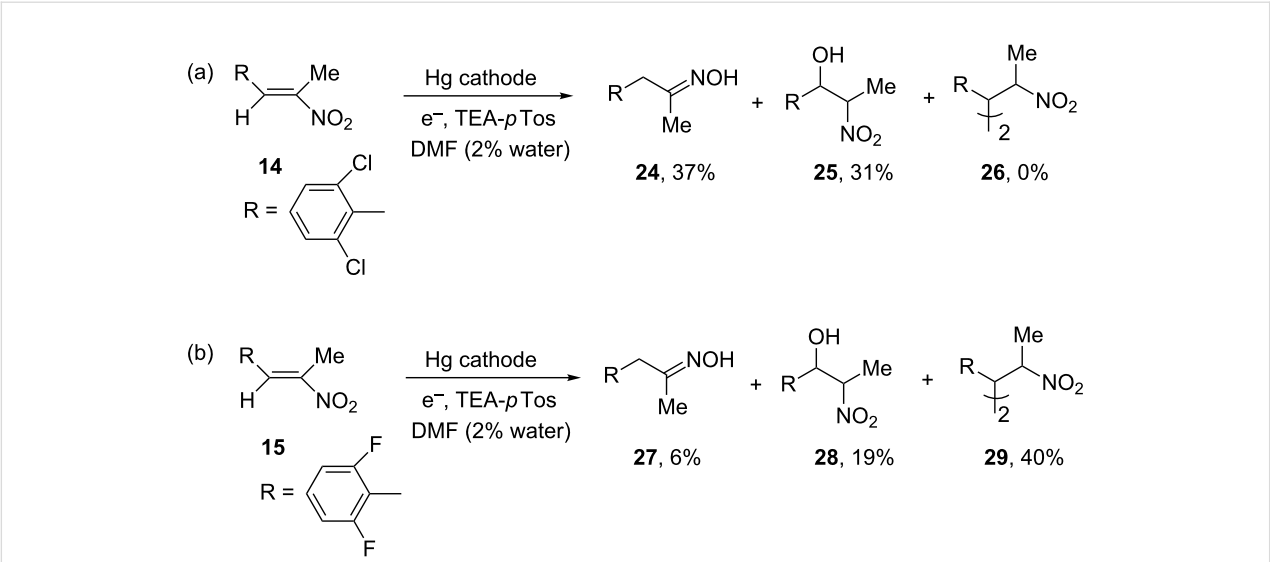

Scheme 5: Hydrodimerization of nitroalkene **14** and **15**.

trolyses. A significant decrease of the current is only found after a current consumption of 2.96 F/mol. Except for benzaldehyde no further side products were detected. **30** is formed as mixture of diastereomers, which could not be separated by flash chromatography.

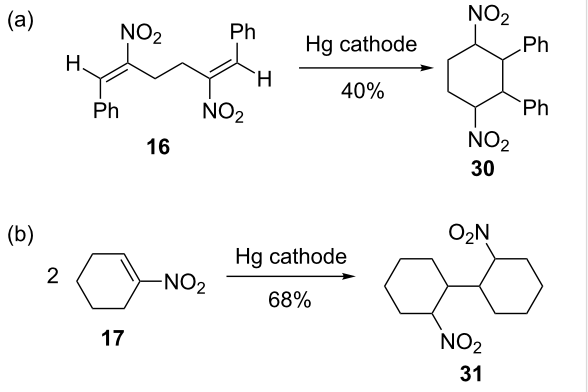

Scheme 6: (a) Intramolecular hydrocoupling of dinitrodiene **16** and (b) hydrodimerization of 1-nitrocyclohexene (**17**).

The aliphatic nitroalkene **17** could be hydrodimerized in 68% yield to the hydrodimer **31**, which is a mixture of diastereomers. Partial separation by flash chromatography and ^{1}H NMR spectroscopy of the fractions indicates four diastereomers in a ratio of about 38:9:14:1.

It is possible to substitute the cathode material mercury against the environmentally benign graphite. At a graphite cathode the nitroolefin **1** could be hydrodimerized to the dimer **2**. With 60% the yield is lower than in the reduction at the Hg cathode, where 88% of the dimer were obtained. Possibly higher yields can be obtained with other graphite varieties or other nontoxic cathode materials. But in principle the mercury cathode can be replaced by a graphite cathode.

Structure of the hydrodimers

All products show for the nitro group characteristic asymmetrical and symmetrical vibrations at 1530–1560 cm^{-1} and 1350–1360 cm^{-1}, which, compared to the educts, are shifted to shorter wavelengths.

The hydrodimers show in the upper masses of the mass spectra few fragments and these have a low intensity. The base peak in all hydrodimers results from breaking of the dibenzyl bond and loss of NO_2 affording the mass = ($M^+/2 - 46$).

The C–C bond formation can lead to α,α-, α,β- and ß,ß-coupled products. The ^{1}H NMR spectra and MS data support in all cases a ß,ß-coupling. A α,β- or a α,α-coupling would lead to the occurrence of methyl singlets or non-coupled benzylic protons. Such signals were not observed in the spectra of the hydrodimers.

The stereochemistry of the hydrodimer results from a β,ß-C–C bond formation and from a α,δ-diprotonation, which creates a dimer with four stereocenters with the exception of dimer **3**, which has only two stereocenters. This means 2^3 diastereomers can be formed, which are decreased to six diastereomers due to the identity of two pairs of enantiomers as shown in Scheme 7.

RRRR diastereomer as pair *SSSS* of enantiomers A/A'	*RRRS* diastereomer as pair *SSSR* of enantiomers B/B'
RRSR diastereomer as pair *SSRS* of enantiomers C/C'	*RSSR* diastereomer as pair *SRRS* of enantiomers D/D'
RRSS meso 1 as pair of *SSRR* identical E/E'	*RSRS* meso 2 as pair of *SRSR* identical F/F'
RSRR G/G' rotation by 180° *SRSS* is identical with C/C'	*SRRR* H/H' rotation by 180° *RSSS* is identical with B/B'

Scheme 7: Possible stereoisomers and their mirror images for the hydrodimers **2** and **18–23**; *R* and *S* are the configurations at the stereogenic centers.

Configurations could not be assigned, as data for comparison are not available in the literature and crystals for X-ray diffraction could not be obtained.

The dimers are obtained as mixtures of diastereomers; as they do not differ significantly in their MS and IR spectra the compounds had to be characterized by their ^{1}H NMR data. For that purpose the diastereomers were purified as good as possible by flash chromatography and/or HPLC. Single diastereomers are denoted alphanumerically (e.g., **2a**, **2b**). The same letter means for two diastereomers of different hydrodimers that they have similar NMR spectra with regard to chemical shift and multiplicity. This corresponds to a similar rate of elution in chromatography.

^{1}H NMR spectra

For the hydrodimers **2** and **18**–**23** five different diastereomers **a**–**e** can be identified. In Table 5 the ^{1}H NMR data of the five diastereomers **2a**–**e** are assembled.

The numbering (determining C-1) is arbitrary, but the remaining positions follow unequivocally from the coupling constants (for example in **2b**: $J_{1,2}$ = 6.64 Hz, $J_{5,6}$ = 6.51 Hz).

The diastereomers show remarkable differences in the chemical shifts. This also holds for significant differences in the chemical shifts for formally identical protons in **2b**/**e**. The considerable differences probably result from the anisotropy effect of the aromatic ring and the nitro group. For the nitro group a similar anisotropic cone as for the carbonyl group is assumed [30]. Due to the presence of two nitro and two phenyl groups conformations are possible, where protons are in shielded and unshielded areas. Also phenyl protons appear as broad, high field shifted signals. For **18c** a ratio of high field and normal signals of 4:6 was found. With decoupling experiments they can be clearly assigned to be phenyl protons. Comparable results, as shown for **2**, were found for the mixtures of diastereomers of the other hydrodimers. Besides decoupling experiments also ^{1}H NMR simulations give valuable support to assign the complex coupling pattern. This is shown for **18b** where the complexity of the spectrum is strongly increased by the diastereotopic methylene protons (Figure 2).

The ratios of diastereomers for the products **2** and **18**–**23** are summarized in Table 6.

The main part of the mixture consists usually of the isomers **a** and **b**. Dimer **22** is an exception being possibly caused by the NH groups of the pyrroles. Their hydrogen bonds could influence the relative energies of the transition states leading to the diastereomers. One of the two *meso*-configurations can be assigned to isomer **22a** because of the missing coupling between the benzylic methine protons.

Table 5: δ-Values and multiplicities of the alkyl protons in **2a**–**e**.

H_3C–CH(NO_2)–CH(Ph)–CH(Ph)–CH(NO_2)–CH_3
1 2 3 4 5 6

Isomer	δ (ppm) and multiplicity for H-atom at carbon-atom Nr.:					
	1	6	2	5	3	4
2a	1.25, d		4.85, dq		3.44, d	
2b	1.28, d	1.90, d	4.91, dq	4.79, dq	3.36 and 3.71, 2 dd	
2c	1.74, d		5.21/5.22, 2 dq[a]		3.64, dd	
2d	1.29, d		4.47–4.56, m		4.13–4.15, m	
2e	1.25, d	1.30, d	4.44, dq	4.62, dq	4.59, dd	3.33, dd

[a]Coupling pattern of the α-nitro protons is verified by NMR-simulation.

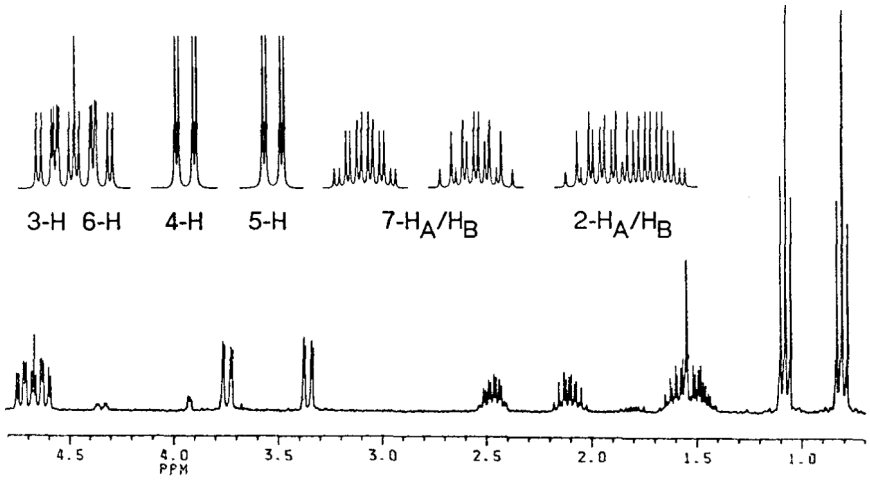

Figure 2: ^{1}H NMR spectrum of **18b** (without aromatic H); below experimental spectrum, above: simulated signals for 2-H to 7-H.

Table 6: Ratio[a] of the diastereomers **a**–**e** from the dimers **2** and **18**–**23**.

Dimer	**a**	**b**	**c**	**d**	**e**
2	10	14	2	1	3
18	11	17	4	1	3
19	12	20	6	1	6
20	7	14	3	1	2
21	11	16	3	1	2
22	1.7	3.2	1.7	1	5.5
23	2	2		Σ 1(for **c**, **d**, **e)**	

[a]Determined by comparing the intensities in the ^{1}H NMR spectra of different mixtures; average values from different electrolyses.

The ^{1}H NMR data obtained for **29**–**31** are compatible with the shown structures.

^{13}C NMR spectra

The proposed structures were confirmed by their ^{13}C NMR spectra. Nearly all diastereomers can be characterized via their ^{13}C signals. The regioselective ß,ß-linkage follows clearly from the multiplicities of the carbon atom resonances. Signals of aliphatic quaternary carbon atoms were not detected. The differences between the signals of single diastereomers of a dimer correlate very well with the results of the proton resonance experiments. The measured values agree quite well with increment calculations (Table 7) [31].

Elemental analyses

The structures could be secured additionally by elemental analyses and in the case of dimer **20** by high resolution MS. They were obtained from the mixtures of isomers taking into account all elements (C, H, N, halogen).

Conclusion

The potential controlled cathodic hydrodimerization of 1-nitroalkenes affords a one step electrochemical C–C bond formation to 1,4-dinitro compounds. Applying optimized conditions the hydrodimers are obtained in good to very good yields. Besides mercury also graphite can be used as cathode material. The scope of the reaction is demonstrated in ten nitroalkenes with different 1-aryl and mostly 2-methyl substituents. Likewise the cathodic cyclization of a dinitrodiene could be realized.

The dimerization is chemoselective: the fairly easy reduction of the nitro group can be suppressed and aryl C–Cl and aryl C–F bonds are not cleaved. Additionally a good regioselectivity is obtained, among the possible three coupling products only the

Table 7: Calculated and experimental ^{13}C shifts for **18**.

Carbon atoms	C-1/-8	C-2/-7	C-3/-6	C-4/-5
δ (ppm) calculated	15.0	22.0	90.4	54.4
δ (ppm) found	9.80–10.81	20.98–26.00	88.92–91.70	48.73–51.31

ß,ß-linked dimer is found. The diastereoselectivity is moderate, one obtains two main diastereomers (about 70–80% of the mixture of isomers) and one of the six possible diastereomers was not found.

The use of an undivided cell facilitates the electrolysis and lowers the energy consumption. For the preparation of dimer **2** in an undivided cell at cell voltages of 10–15 V, one needs 1.8–2.7 kWh/kg of product, which is much below the 8 kWh/kg, where a technical electrolysis becomes favourable with regard to the energy consumption [32,33].

Supporting Information

Supporting Information File 1

Experimental procedures, ^{1}H, ^{13}C NMR and MS spectra and elemental analyses.
[http://www.beilstein-journals.org/bjoc/content/supplementary/1860-5397-11-131-S1.pdf]

Acknowledgements

The authors thank the Arbeitsgemeinschaft Industrieller Forschungsvereinigungen e. V. AIF-Forschungsvorhaben 7543, Kathodische Reduktion ausgewählter funktioneller Gruppen.

References

1. Folmer Nielsen, M.; Utley, J. H. P. Reductive Coupling. In *Organic Electrochemistry,* 4th ed.; Lund, H.; Hammerich, O., Eds.; M. Dekker: New York, 2001.
2. Utley, J. H. P.; Little, R. D.; Folmer Nielsen, M. Reductive Coupling. In *Organic Electrochemistry,* 5th ed.; Speiser, B.; Hammerich, O., Eds.; CRC Press: Boca Raton, 2015.
3. Schäfer, H. J. *C. R. Chim.* **2011,** *14,* 745–765. doi:10.1016/j.crci.2011.01.002
4. Frontana-Uribe, B. A.; Little, R. D.; Ibanez, J. G.; Palma, A.; Vasquez-Medrano, R. *Green Chem.* **2010,** *12,* 2099–2119. doi:10.1039/C0GC00382D
5. Wessling, M.; Schäfer, H. J. *Chem. Ber.* **1991,** *124,* 2303–2306. doi:10.1002/cber.19911241024
6. Weßling, M.; Schäfer, H. J. *Elektrochem. Stoffgewinnung: Grundlagen Verfahrenstech; DECHEMA Monographien*, Vol. 125; Verlag Chemie, 1992; pp 807–813.
7. Weßling, M.; Schäfer, H. J. *Abstr. 16th Sandbjerg Meeting in Organic Electrochemistry*, Sandbjerg, Denmark, June 14–17, 1991.
8. Weßling, M. Elektrochemische Reduktion von 1-Nitroalkenen; C-C Verknüpfung und Funktionsgruppenumwandlung. Ph.D. Thesis, University of Münster, Germany, 1991.
9. Shono, T.; Hamaguchi, H.; Mikami, H.; Nogusa, H.; Kashimura, S. *J. Org. Chem.* **1983,** *48,* 2103–2105. doi:10.1021/jo00160a036
10. Torii, S.; Tanaka, H.; Katoh, T. *Chem. Lett.* **1983,** *12,* 607–610. doi:10.1246/cl.1983.607
11. Sonn, A.; Schellenberg, A. *Ber. Dtsch. Chem. Ges.* **1917,** *50,* 1513–1525. doi:10.1002/cber.19170500251
12. Tatsumi, K.; Yamada, H.; Yoshimura, H.; Kawazoe, Y. *Arch. Biochem. Biophys.* **1982,** *213,* 689–694. doi:10.1016/0003-9861(82)90599-9
13. Sera, A.; Fukumoto, S.; Yoneda, T.; Yamada, H. *Heterocycles* **1986,** *24,* 697–702. doi:10.3987/R-1986-03-0697
14. Sera, A.; Fukumoto, S.; Tamura, M.; Takabatake, K.; Yamada, H.; Itoh, K. *Bull. Chem. Soc. Jpn.* **1991,** *64,* 1787–1791. doi:10.1246/bcsj.64.1787
15. Todres, Z. V.; Tsvetkova, T. M. *Izv. Akad. Nauk SSSR, Ser. Khim.* **1987,** 1553–1556.
16. Namboothiri, I. N. N.; Hassner, A. *J. Organomet. Chem.* **1996,** *518,* 69–77. doi:10.1016/0022-328X(96)06150-5
17. Niazimbetova, Z.; Treimer, S. E.; Evans, D. H.; Guzei, I.; Rheingold, A. L. *J. Electrochem. Soc.* **1998,** *145,* 2768–2774. doi:10.1149/1.1838712
18. Mikesell, P.; Schwaebe, M.; DiMare, M.; Little, R. D. *Acta Chem. Scand.* **1999,** *53,* 792–799. doi:10.3891/acta.chem.scand.53-0792
19. Ankner, T.; Hilmersson, G. *Tetrahedron Lett.* **2007,** *48,* 5707–5710. doi:10.1016/j.tetlet.2007.05.105
20. Du, Y.; Wang, Y.; Li, X.; Shao, Y.; Li, G.; Webster, R. D.; Chi, Y. R. *Org. Lett.* **2014,** *16,* 5678–5681. doi:10.1021/ol5027415
21. Hass, H. B.; Susie, A. G.; Heider, R. L. *J. Org. Chem.* **1950,** *15,* 8–14. doi:10.1021/jo01147a002
22. Gairaud, C. B.; Lappin, G. R. *J. Org. Chem.* **1953,** *18,* 1–3. doi:10.1021/jo01129a001
23. *Organikum,* 15th ed.; VEB Deutscher Verlag der Wissenschaften: Berlin, 1984; p 567.
24. Boberg, F.; Garburg, K. H.; Görlich, K.-J.; Pipereit, E.; Ruhr, M. *Liebigs Ann. Chem.* **1984,** 911–919. doi:10.1002/jlac.198419840510
25. Padeken, H. G.; von Schickh, O.; Segnitz, A. *Methoden Org. Chem. (Houben-Weyl),* 4th ed.; 1971; Vol. X/1, 342, 351, 355.
26. Lipina, E. S.; Perekalin, V. V.; Bobovich, Y. S. *J. Gen. Chem. USSR (Engl. Transl.)* **1964,** *34,* 3683–3687.
27. Stille, J. K.; Vessel, E. D. *J. Org. Chem.* **1960,** *25,* 478–480. doi:10.1021/jo01073a623
28. Exner, O. In *Correlation Analysis in Chemistry;* Chapman, N. B.; Shorter, J., Eds.; Plenum Press: New York, 1978.
29. Heffner, J. E.; Wigal, C. T.; Moe, O. A. *Electroanalysis* **1997,** *9,* 629–632. doi:10.1002/elan.1140090810
30. Wagniere, G. H. In *The chemistry of the nitro and nitroso groups;* Feuer, H., Ed.; J. Wiley: New York, 1969; p 38.
31. Hesse, M.; Meier, H.; Zeeh, B. *Spektroskopische Methoden in der Organischen Chemie,* 2nd ed.; Georg Thieme Verlag: Stuttgart, 1984; p 222.
32. Degner, D. *Top. Curr. Chem.* **1998,** *148,* 82.
33. Pütter, H. Industrial Electroorganic Chemistry. In *Organic Electrochemistry,* 4th ed.; Lund, H.; Hammerich, O., Eds.; M. Dekker: New York, 2001.